EXCHANGES AT THE ROOT-SOIL INTERFACE: RESOURCE TRADING IN THE RHIZOSPHERE THAT DRIVES ECOSYSTEM FUNCTIONING

EDITED BY: Catherine Preece, Erik Verbruggen, Lucia Fuchslueger
and Alberto Canarini
PUBLISHED IN: Frontiers in Plant Science and
Frontiers in Forests and Global Change

frontiers Research Topics

ISSN 1664-8714
ISBN 978-2-88971-490-2
DOI 10.3389/978-2-88971-490-2

About Frontiers

Frontiers is more than just an open-access publisher of scholarly articles: it is a pioneering approach to the world of academia, radically improving the way scholarly research is managed. The grand vision of Frontiers is a world where all people have an equal opportunity to seek, share and generate knowledge. Frontiers provides immediate and permanent online open access to all its publications, but this alone is not enough to realize our grand goals.

Frontiers Journal Series

The Frontiers Journal Series is a multi-tier and interdisciplinary set of open-access, online journals, promising a paradigm shift from the current review, selection and dissemination processes in academic publishing. All Frontiers journals are driven by researchers for researchers; therefore, they constitute a service to the scholarly community. At the same time, the Frontiers Journal Series operates on a revolutionary invention, the tiered publishing system, initially addressing specific communities of scholars, and gradually climbing up to broader public understanding, thus serving the interests of the lay society, too.

Dedication to Quality

Each Frontiers article is a landmark of the highest quality, thanks to genuinely collaborative interactions between authors and review editors, who include some of the world's best academicians. Research must be certified by peers before entering a stream of knowledge that may eventually reach the public - and shape society; therefore, Frontiers only applies the most rigorous and unbiased reviews.
Frontiers revolutionizes research publishing by freely delivering the most outstanding research, evaluated with no bias from both the academic and social point of view. By applying the most advanced information technologies, Frontiers is catapulting scholarly publishing into a new generation.

What are Frontiers Research Topics?

Frontiers Research Topics are very popular trademarks of the Frontiers Journals Series: they are collections of at least ten articles, all centered on a particular subject. With their unique mix of varied contributions from Original Research to Review Articles, Frontiers Research Topics unify the most influential researchers, the latest key findings and historical advances in a hot research area! Find out more on how to host your own Frontiers Research Topic or contribute to one as an author by contacting the Frontiers Editorial Office: frontiersin.org/about/contact

EXCHANGES AT THE ROOT-SOIL INTERFACE: RESOURCE TRADING IN THE RHIZOSPHERE THAT DRIVES ECOSYSTEM FUNCTIONING

Topic Editors:
Catherine Preece, University of Antwerp, Belgium
Erik Verbruggen, University of Antwerp, Belgium
Lucia Fuchslueger, University of Vienna, Austria
Alberto Canarini, Kyoto University, Japan

Citation: Preece, C., Verbruggen, E., Fuchslueger, L., Canarini, A., eds. (2021). Exchanges at the Root-Soil Interface: Resource Trading in the Rhizosphere That Drives Ecosystem Functioning. Lausanne: Frontiers Media SA.
doi: 10.3389/978-2-88971-490-2

Table of Contents

frontiers
in Forests and Global Change

EDITORIAL
published: 25 August 2021
doi: 10.3389/ffgc.2021.747492

Editorial: Exchanges at the Root-Soil Interface: Resource Trading in the Rhizosphere That Drives Ecosystem Functioning

Catherine Preece[1]*, *Alberto Canarini*[2], *Erik Verbruggen*[1] *and Lucia Fuchslueger*[3]

[1] *Research Group PLECO (Plants and Ecosystems), Department of Biology, University of Antwerp, Antwerp, Belgium,* [2] *Center for Ecological Research, Kyoto University, Kyoto, Japan,* [3] *Centre of Microbiology and Environmental Systems Science, University of Vienna, Vienna, Austria*

Keywords: rhizosphere, plant-soil (belowground) feedbacks, volatile organic compound, root exudate, mycorrhiza, soil microorganisms

Editorial on the Research Topic

Exchanges at the Root-Soil Interface: Resource Trading in the Rhizosphere That Drives Ecosystem Functioning

OPEN ACCESS

Edited and reviewed by:
Frank Hagedorn,
Swiss Federal Institute for Forest,
Snow and Landscape Research
(WSL), Switzerland

****Correspondence:***
Catherine Preece
catherine.preece09@gmail.com

Specialty section:
This article was submitted to
Forest Soils,
a section of the journal
Frontiers in Forests and Global
Change

Received: *26 July 2021*
Accepted: *05 August 2021*
Published: *25 August 2021*

Citation:
Preece C, Canarini A, Verbruggen E and Fuchslueger L (2021) Editorial: Exchanges at the Root-Soil Interface: Resource Trading in the Rhizosphere That Drives Ecosystem Functioning. Front. For. Glob. Change 4:747492. doi: 10.3389/ffgc.2021.747492

The interactions between roots, their surrounding soil—the rhizosphere—and soil biota form an intricate web influencing ecosystem functioning. These rhizosphere interactions are not a one-way road but are mostly bi- or multi-directional. For example, roots take up water and nutrients from the soil and deposit carbon (C) used by rhizosphere inhabiting microorganisms for energy and growth. These microorganisms liberate nutrients locked up in soil organic matter, which in turn become available to plants and facilitate plant productivity (Finzi et al., 2015). Hence, tight interactions between plants and soil biota occurring at the rhizosphere scale shape large-scale C and nutrient cycling and can induce feedbacks at the ecosystem level. The chemical complexity of these interactions goes beyond the mere exchange of carbon and nutrients and can involve a large suite of secondary metabolites, including volatile organic compounds (VOCs). These are produced not only by plants to attract or repel microorganisms and soil fauna, but also by microbes themselves to elicit effects on root growth. Classical examples are associations between roots and mycorrhizal fungi that are initiated by strigolactone exudation of roots (Biate et al., 2015), and nitrogen-fixing bacteria that are attracted by flavonoids produced by their legume hosts (Schulz-Bohm et al., 2018).

Through resolving these crucial processes occurring in the vicinity of roots, research in rhizosphere ecology can advance predictions on the responses of plant productivity, species composition, and soil functioning of forests and other terrestrial ecosystems in a future climate. In this collection we highlight studies investigating rhizosphere resource trading in field and laboratory settings, representing a range of terrestrial ecosystems including temperate, dryland, and tropical climates, in both natural and agro-ecosystems. The complexity of the soil-rhizosphere system is brought into focus through the application of a variety of methods, ranging from root trenching and stable isotope analyses, to fingerprint methods to characterize microbial communities, such as phospholipid fatty acid analysis and DNA amplicon sequencing, to quantitative PCR of functional genes followed up by greenhouse gas (GHG) fluxes.

Associations of roots with mycorrhizal fungi play an essential role in forest soils. Mycorrhizal fungi enlarge the surface area of fine roots and enhance or regulate plant nutrient uptake, allowing plants to thrive in nutrient poor soils, emphasizing their role in providing a vital ecosystem service (Smith and Read, 2008). Nevertheless, both tree and mycorrhizal community composition can influence nutrient partitioning in forests. Tatsumi et al. demonstrated that nitrogen (N) uptake of understorey plants growing below different trees in dryland forests in China was linked to their respective mycorrhizal associations. By measuring the natural abundance stable isotopic composition of N (δ15N) they found that the identity of overstory trees determined their root mycorrhizal community, and subsequently controlled the N uptake patterns of understory trees. Mycorrhizal fungi not only transfer nutrients among plants, but also positively or negatively interact with saprotrophic fungi in the breakdown of organic matter (Frey, 2019). In a litter decomposition and root manipulation experiment conducted in a temperate deciduous forest Marañón-Jiménez et al. observed that substrate quality and availability are key factors determining the prevalence of either fungal guild. Ectomycorrhizal fungi were dominant in substrates with low levels of organic matter, whereas saprotrophs were more common at higher levels.

Arbuscular mycorrhizal fungi, in contrast, are considered to play a crucial role for plant phosphorus (P) acquisition (Smith and Smith, 2011). In a tropical lowland forest, Yaffar et al. investigated functional traits, including colonization by mycorrhizal fungi, of fine-roots of trees growing in P-poor soils before and after two consecutive hurricanes. They found that trade-offs between morphological and physiological (phosphatase activity and fungal colonization) root traits related to P acquisition were largely driven by interspecific differences of pioneer vs. non-pioneer species, and that trait distribution was highly stable to hurricane disturbances. These findings highlight the potential of traits related to mycorrhization and nutrient acquisition, as recently advocated by (Bergmann et al., 2020), to shed light on the community assembly of these diverse forest ecosystems.

Carbon released by plant roots not only affects organisms directly interacting with plant roots, but effects propagate to higher trophic levels through the soil food web. Bluhm et al. indeed found that root inputs are shaping the community composition and abundance of different types of soil fauna in Central European forests. The investigated soil macrofauna groups showed high resilience to deprivation of root resources. In contrast, mesofauna (both decomposers and predators) and root feeding microfauna appeared more sensitive than other groups, highlighting their important role for channeling root derived energy through forest soil food webs.

Links and interactions between plant and soil microorganisms are bi-directional. In agricultural systems, fertilizer additions can induce strong changes in the composition, functioning and activity of microbial communities (Geisseler and Scow, 2014), which in turn can feed back on crop yield, as well as greenhouse gas emissions. In such a system, Yoshiura et al. tested the application of plant-growth-promoting-rhizobacteria (PGPR) and different fertilizers on maize yield, rhizosphere microbes and soil greenhouse gas emissions. They found that the best option to balance plant biomass production and reduce GHG mitigation in their system was a combination of maize residue retention, which changed rhizosphere communities, and PGPR inoculation to stimulate plant growth *via* phytohormones. Our knowledge about the array of root inputs to the rhizosphere, in the form of exudates and VOCs produced by rhizosphere microbial communities, continues to expand. Kong et al. investigated VOCs produced by a rhizobacterium which were shown to induce tolerance to iron deficiency stress in Arabidopsis thaliana through changes to a range of root morphological and physiological traits.

This Research Topic highlights the increasing number of studies focusing on exchanges happening at the root-soil interface and their pivotal role in determining numerous ecosystem functions. These exchanges include a multitude of players from plants to soil fauna, and cover a variety of implications from nutrient acquisition to GHGs release. Continuous improvements in experimental manipulations and laboratory analyses are fostering a new understanding of belowground communications and trading, which can translate microscale processes into macroscale ecosystem implications.

AUTHOR CONTRIBUTIONS

CP led the writing of the first draft of this Editorial with comments from the other authors. All authors contributed to the article and approved the submitted version.

FUNDING

CP was funded by an FWO (Research Foundation - Flanders) post-doctoral fellowship. AC received financial support as an International Research Fellow of Japan Society for the Promotion of Science [Postdoctoral Fellowships for Research in Japan (Standard)]. LF acknowledges the European Union's Horizon 2020 research and innovation program under the Marie Sklodovska-Curie grant agreement No 847693 (REWIRE).

REFERENCES

Bergmann, J., Weigelt, A., Van Der Plas, F., Laughlin, D. C., Kuyper, T. W., Guerrero-Ramirez, N., et al. (2020). The fungal collaboration gradient dominates the root economics space in plants. *Sci. Adv.* 6:eaba3756. doi: 10.1126/sciadv.aba3756

Biate, D. L., Kumari, A., Annapurna, K., Kumar, L. V., Ramadoss, D., Reddy, K. K., et al. (2015). "Legume root exudates: their role in symbiotic interactions," in *Plant Microbes Symbiosis: Applied Facets,* ed N. K. Arora (New Delhi: Springer India), 259–271. doi: 10.1007/978-81-322-2068-8_13

Finzi, A. C., Abramoff, R. Z., Spiller, K. S., Brzostek, E. R., Darby, B. A., Kramer, M. A., et al. (2015). Rhizosphere processes are quantitatively important components of terrestrial carbon and nutrient cycles. *Glob. Change Biol.* 21, 2082–2094. doi: 10.1111/gcb.12816

Frey, S. D. (2019). Annual review of ecology, evolution, and systematics. *Ann. Rev.* 50, 237–259. doi: 10.1146/annurev-ecolsys-110617-062331

Geisseler, D., and Scow, K. M. (2014). Long-term effects of mineral fertilizers on soil microorganisms - a review. *Soil Biol. Biochem.* 75, 54–63. doi: 10.1016/j.soilbio.2014.03.023

Schulz-Bohm, K., Gerards, S., Hundscheid, M., Melenhorst, J., De Boer, W., and Garbeva, P. (2018). Calling from distance: attraction of soil bacteria by plant root volatiles. *ISME J.* 12, 1252–1262. doi: 10.1038/s41396-017-0035-3

Smith, S. E., and Read, D. J. (2008). *Mycorrhizal Symbiosis, 3rd Edn.* San Diego and London: Academic Press, 1–769.

Smith, S. E., and Smith, F. A. (2011). Roles of arbuscular mycorrhizas in plant nutrition and growth: new paradigms from cellular to ecosystem scales. *Ann. Rev. Plant Biol.* 62, 227–250. doi: 10.1146/annurev-arplant-042110-103846

Conflict of Interest: The authors declare that the research was conducted in the absence of any commercial or financial relationships that could be construed as a potential conflict of interest.

frontiers in Plant Science

ORIGINAL RESEARCH
published: 14 January 2021
doi: 10.3389/fpls.2020.583585

Arbuscular Mycorrhizal Community in Roots and Nitrogen Uptake Patterns of Understory Trees Beneath Ectomycorrhizal and Non-ectomycorrhizal Overstory Trees

Chikae Tatsumi[1,2,3]*, Fujio Hyodo[4], Takeshi Taniguchi[5], Weiyu Shi[6], Keisuke Koba[7], Keitaro Fukushima[7], Sheng Du[8], Norikazu Yamanaka[5], Pamela Templer[3] and Ryunosuke Tateno[9]

[1] Research Faculty of Agriculture, Hokkaido University, Sapporo, Japan, [2] Graduate School of Agriculture, Kyoto University, Kyoto, Japan, [3] Department of Biology, Boston University, Boston, MA, United States, [4] Research Core for Interdisciplinary Sciences, Okayama University, Okayama, Japan, [5] Arid Land Research Center, Tottori University, Tottori, Japan, [6] School of Geographical Sciences, Southwest University, Chongqing, China, [7] Center for Ecological Research, Kyoto University, Shiga, Japan, [8] State Key Laboratory of Soil Erosion and Dryland Farming on Loess Plateau, Institute of Soil and Water Conservation, Chinese Academy of Sciences, Beijing, China, [9] Field Science Education and Research Center, Kyoto University, Kyoto, Japan

OPEN ACCESS

Edited by:
Erik Verbruggen,
University of Antwerp, Belgium

Reviewed by:
Adriana Corrales,
Del Rosario University, Colombia
Jan Jansa,
Institute of Microbiology, Academy of Sciences of the Czech Republic (ASCR), Czechia

***Correspondence:**
Chikae Tatsumi
chikae@chem.agr.hokudai.ac.jp

Specialty section:
This article was submitted to Plant Symbiotic Interactions, a section of the journal Frontiers in Plant Science

Received: 21 August 2020
Accepted: 07 December 2020
Published: 14 January 2021

Citation:
Tatsumi C, Hyodo F, Taniguchi T, Shi W, Koba K, Fukushima K, Du S, Yamanaka N, Templer P and Tateno R (2021) Arbuscular Mycorrhizal Community in Roots and Nitrogen Uptake Patterns of Understory Trees Beneath Ectomycorrhizal and Non-ectomycorrhizal Overstory Trees. Front. Plant Sci. 11:583585. doi: 10.3389/fpls.2020.583585

Nitrogen (N) is an essential plant nutrient, and plants can take up N from several sources, including via mycorrhizal fungal associations. The N uptake patterns of understory plants may vary beneath different types of overstory trees, especially through the difference in their type of mycorrhizal association (arbuscular mycorrhizal, AM; or ectomycorrhizal, ECM), because soil mycorrhizal community and N availability differ beneath AM (non-ECM) and ECM overstory trees (e.g., relatively low nitrate content beneath ECM overstory trees). To test this hypothesis, we examined six co-existing AM-symbiotic understory tree species common beneath both AM-symbiotic black locust (non-ECM) and ECM-symbiotic oak trees of dryland forests in China. We measured AM fungal community composition of roots and natural abundance stable isotopic composition of N (δ^{15}N) in plant leaves, roots, and soils. The root mycorrhizal community composition of understory trees did not significantly differ between beneath non-ECM and ECM overstory trees, although some OTUs more frequently appeared beneath non-ECM trees. Understory trees beneath non-ECM overstory trees had similar δ^{15}N values in leaves and soil nitrate, suggesting that they took up most of their nitrogen as nitrate. Beneath ECM overstory trees, understory trees had consistently lower leaf than root δ^{15}N, suggesting they depended on mycorrhizal fungi for N acquisition since mycorrhizal fungi transfer isotopically light N to host plants. Additionally, leaf N concentrations in the understory trees were lower beneath ECM than the non-ECM overstory trees. Our results show that, without large differences in root mycorrhizal community, the N uptake patterns of understory trees vary between beneath different overstory trees.

Keywords: ^{15}N natural abundance, arbuscular mycorrhizal fungi, dryland, ectomycorrhizal fungi (ECM fungi), mycorrhizal dependence, nitrate

INTRODUCTION

Soil nitrogen (N) is an essential nutrient for plants and it influences the productivity, composition, and functioning of forests (Tanner et al., 1998; LeBauer and Treseder, 2008; Wright et al., 2011). Plants primarily use soil inorganic N (ammonium and nitrate), but plants can also use organic N as a significant resource in low-N systems (Näsholm et al., 1998; Nordin et al., 2001; Jones and Kielland, 2002). In addition, plants can access various soluble organic compounds such as amino acids and peptides by associating with mycorrhizal fungi (Read and Perez-Moreno, 2003; Smith and Read, 2008; Pellitier and Zak, 2018). The differences in the mycorrhizal association among plants are also an important factor in regulating N uptake in host plants (Veresoglou et al., 2011; Mensah et al., 2015). Thus, plants have many strategies for taking up soil N and can change the form of N taken up in response to soil N availability, although each plant species has uptake preferences (Wei et al., 2015; Andersen et al., 2017; Uscola et al., 2017; Daryanto et al., 2019).

Overstory tree species can play an important role in N uptake of co-existing understory plants by changing the environmental conditions, including soil N availability and mycorrhizal inoculum source. The mycorrhizal type of the dominant tree species has come to be recognized as a potentially large factor controlling soil N availability (Phillips et al., 2013; Averill et al., 2014). Ectomycorrhizal (ECM) fungi can produce many hydrolytic or oxidative extracellular enzymes (Chalot and Brun, 1998; Courty et al., 2010; Averill and Finzi, 2011; Kohler et al., 2015), and obtain small organic N-bearing molecules from soil organic matter (SOM). As a result, ECM fungi are considered to limit the amount of N available for free-living microbes and slow soil decomposition and N transformations (Gadgil and Gadgil, 1971; Averill and Hawkes, 2016; Fernandez and Kennedy, 2016). On the other hand, arbuscular mycorrhizal (AM) fungi lack the ability to produce the extracellular enzymes and therefore are considered to have smaller effects than ECM fungi on soil N cycling (Read and Perez-Moreno, 2003; Smith and Read, 2008; Smith and Smith, 2011; Hodge and Storer, 2014). Accordingly, soil N availability, especially that of nitrate, is reported to be higher in AM than ECM forests (Phillips et al., 2013; Midgley and Phillips, 2016; Tatsumi et al., 2020). It is also possible that the higher nitrate content is caused by higher nitrification rates facilitated by lower acidity and higher ammonium pools in AM forests where decomposition rates are more rapid than ECM forests (Finzi et al., 1998; Phillips et al., 2013). Also, overstory trees associated with N-fixing bacteria can increase soil N availability (Rice et al., 2004; Von Holle et al., 2013), although it is not always the case (Wang et al., 2010).

It has been reported that some plants alter their N uptake patterns, such as slowing their rate of uptake and changing the N source that they take up, in response to changes in soil N availability, sometimes a result of N uptake by competitively superior plants (McKane et al., 2002; Ashton et al., 2010). Root mycorrhizal community also changes with soil N availability (Treseder and Allen, 2002; Porras-Alfaro et al., 2007) and with soil mycorrhizal inoculum sources in some cases (Duponnois et al., 2011; Bittebiere et al., 2019). On the other hand, even when the environmental conditions such as soil N availability changes, some plants do not change root mycorrhizal community composition (Martínez-García and Pugnaire, 2011; Gehring et al., 2017) and the primary source of N that they take up (Ashton et al., 2010; Wang and Macko, 2011). Also, differences in overstory trees may affect the root mycorrhizal community and N uptake pattern of understory trees. It has been reported that the understory tree community varies beneath AM and ECM overstory trees, and this is considered to be partly caused by differences in soil N availability (Jo et al., 2018).

Natural abundance stable isotopic composition of N (δ^{15}N) can reveal plant N use processes (Koba et al., 2003; Templer et al., 2007). The δ^{15}N in plant leaves and roots including mycorrhizal fungi can indicate plant dependence for N acquisition on mycorrhizal fungi, because mycorrhizal fungi transfer N with lower δ^{15}N values to host plants (Kohzu et al., 2000; Emmerton et al., 2001; Hobbie and Colpaert, 2003); that is, mycorrhizal-dependent plants show leaf δ^{15}N values that are lower than δ^{15}N values of their roots including mycorrhizal fungi. Although the transfer of ^{15}N-depleted N from AM fungi to host plants has not clearly been demonstrated compared to ECM fungi (Aguilar et al., 1998; Wheeler et al., 2000), some recent studies based on field observations, greenhouse experiments, and modeling support the idea that AM fungi slightly fractionate N (Schweiger, 2016; Jach-Smith and Jackson, 2020). The δ^{15}N signature of leaves may also indicate the primary source of N that plants take up from soil (Takebayashi et al., 2010; Liu et al., 2018). For example, the δ^{15}N of leaves tend to be low if plants depend on soil nitrate (Falkengren-grerup et al., 2004; Kahmen et al., 2008), because δ^{15}N of soil nitrate is usually much lower than that of ammonium (Choi et al., 2005; Takebayashi et al., 2010). In addition, to determine if soil N availability is high, the measurement of δ^{18}O of soil nitrate is useful because it can indicate whether the nitrate comes mostly from nitrification or atmospheric deposition, as δ^{18}O values of nitrification-derived nitrate can be lower than 10‰ (Kendall et al., 2007; Fang et al., 2012). The δ^{15}N values in the soils are also useful because net mineralization and nitrification rates are typically correlated positively with soil δ^{15}N values (Templer et al., 2007).

Here, we examined root mycorrhizal community and δ^{15}N and N concentrations of leaves and fine roots in co-existing understory plants, as well as the δ^{15}N and soil N forms that plants can take up beneath non-ECM (black locust) and ECM (oak) overstory trees in dryland forests, to determine the effects of overstory trees on N acquisition by understory trees. In dryland forests, competition for N between ECM trees and free-living microbes is strong because N can be more limiting than water for plant production in dryland forests (Ren et al., 2017), which can result in a strong effect of the ECM trees on soil N availability. Black locust and oak are the two dominant species in our study region of dryland forests in China. The non-ECM species in this study (black locust) is associated with N-fixing bacteria, although the trees currently do not have active N-fixation as described below.

In this study, we hypothesized that root mycorrhizal community and N uptake patterns of understory trees vary beneath different overstory trees. We expected (1) the root mycorrhizal communities of understory trees to differ when occurring beneath different overstory trees in response to soil N availability and mycorrhizal inoculum source (derived from root mycorrhizal community in overstory trees), although the hypothesis about mycorrhizal inoculum source should be only in the case that overstory and understory trees are the same mycorrhizal type. We also expected (2) the understory trees beneath non-ECM overstory trees to be less dependent upon mycorrhizal fungi for N acquisition (i.e., leaf $\delta^{15}\text{N} \nless$ root δ^{15}N) and instead to access highly available nitrate (i.e., leaf $\delta^{15}\text{N} \approx$ soil nitrate δ^{15}N). On the other hand, we expected (3) the understory trees beneath ECM overstory trees to be highly dependent upon mycorrhizal fungi for N acquisition (i.e., leaf $\delta^{15}\text{N} <$ root δ^{15}N). We expected the understory tree species to be a stronger driver than the overstory tree species in determining N uptake patterns of understory trees.

MATERIALS AND METHODS

Study Site

This study was conducted in a black locust (*Robinia pseudoacacia*) forest and an oak (*Quercus liaotungensis*) forest in the Loess Plateau of China. Black locust and oak are AM and ECM trees, respectively (Zhang et al., 2013; Yang et al., 2014). Black locust is also a tree with N-fixing symbionts, but there is no active N fixation at this site currently as evidenced by lack of root nodules in the roots and the lower abundance of N-fixing bacteria in soils of the black locust than oak forest (**Supplementary Table 1**). The study site is located near Yan'an city (Mt. Gonglushan, 36° 25 N, 109° 32 E) in Shaanxi Province, China. Black locust trees were widely planted in the 1960s and oak forests are the native climax forests, but most of the natural oak forests were already cut down by human activity (Lü et al., 2003). Thus, they are common forests in this region (Du et al., 2011), but it is difficult to find an oak forest, especially neighboring to a black locust forest. The vegetation type is categorized as a forest-steppe transitional zone (Yamanaka et al., 2014). Mean annual precipitation and mean annual air temperature are 514 mm and 10.2°C, respectively. This area experiences hot summers and cold winters, with heavy rainfall in the summer. According to Tateno et al. (2007), this area was colonized 65–75 years ago by people and was cultivated after native oak forests were cleared. Black locust was planted on abandoned cultivated lands around 45 years ago, and the oak forests comprised 65–70-year-old secondary forest.

Both sites have closed canopies, with more than 90% of the canopy occupied by the dominant species, black locust or oak. Six understory tree species appear commonly and frequently in both forests: *Rosa multiflora* (Rosaceae), *Cotoneaster multiflorus* (Rosaceae), *Platycladus orientalis* (Cupressaceae), *Syringa pekinensis* (Oleaceae), *Acer ginnala* (Sapindaceae), and *Acer stenolobum* (Sapindaceae). All of these species likely have AM associations based on recent plant surveys (Soudzilovskaia et al., 2020). These forests are located on a flat or gentle slope near the ridge at around 1,300 m elevation. The relative photosynthetic photon flux density (rPPFD) of the black locust forest and the oak forest are 7.6 ± 2.7 and 9.7 ± 3.2 (%), respectively.

Sample Collection

We examined five mature individual trees (each 3–5 m height) for each understory tree species in each forest (ca. 50 m × 200 m); the five replications were a minimum of 20–30 m from each other. We also examined five mature individual overstory trees in each forest; the five overstory trees were a minimum of 20–30 m from each other. We sampled healthy leaves and fine roots from each individual. Approximately 10 g of root samples (mostly fine roots but including some coarse roots) were collected from surface soils (0–30 cm depth) where the majority of roots are located. To avoid contamination from the roots of other trees, all root systems were traced from the trunk of the selected trees. Root samples were separated into subsamples for isotopic analysis and DNA analysis. Approximately 10 g of leaf samples were collected randomly from each tree crown and the petiole was included. We also collected mineral soil from 0–10 cm depth around each tree individual to detect whether extractable N content is specifically determined by the tree individual (**Supplementary Figure 1**). Preliminary analyses showed that the effect of overstory tree type (ECM vs. non-ECM) on soil extractable N content was much larger than the effect of tree species, so we measured the δ^{15}N only for each forest representative soils. Collection of leaf, root, and the soils around trees was conducted in mid-September 2015.

For the measurement of δ^{15}N of the soil extractable N associated with the overstory tree species of each forest, additional mineral soil samples (0–10 cm depth) were collected from five locations beneath the overstory trees of each forest. The soil sampling locations were approximately 5 m from each other. These samples were collected in June and September of 2016. Each soil sample was divided into a subsample for water content analysis, and for N extraction to determine δ^{15}N. In order to determine the average value over the growing season, soil inorganic N was captured by ion exchange resin capsules each containing about 1 g of mixed ion exchange resins (IER; PST-2, Unibest, Bozeman, MT, United States). Seven resin capsules were placed at a depth of 10 cm in soil beneath the overstory tree species of each forest beginning in June 2016. The resin capsules were *ca*. 10 m from one another. The resin capsules were collected after 3 months (in September 2016). The collected resin capsules were washed well with distilled water to remove adhering soils.

For additional measurements of δ^{15}N in bulk soil, soil samples (0–10 cm depth and 20–30 cm depth) were collected at four locations (*ca*. >20 m apart) beneath the overstory trees of each forest. At each of the four locations, four samples were collected (>5 m apart) and composited into a single sample. The soil samples (0–10 cm depth) were collected in September of 2016 and October 2017, and the soil samples (20–30 cm depth) were collected in August 2017. Each sample was divided into a sub-sample for water content analysis, and a sub-sample for isotopic analysis of N. Soil water content was determined after samples were dried at 105°C for >3 days.

DNA Extraction From Roots and Amplicon Sequencing

Root samples were carefully washed three times, and 300 root tips were picked up from each root sample and crushed in each 1.5 mL microtube using BioMasher (Nippi. Inc., Tokyo, Japan). To the crushed tissue, 350 μL of CTAB buffer (100 mM Tris; 1.4 M NaCl; 20 mM EDTA; 2% acetyl trimethyl ammonium bromide) was added, and the mixture was incubated for 30 min at 65°C (Sato and Murakami, 2008). After incubation, an equal volume of chloroform was added and centrifuged for 15 min at 12,000 rpm. The supernatant was then transferred to a new microtube. An equal volume of isopropanol and a one-tenth volume of sodium acetate (pH 5) were added to the supernatant and then the mixture was centrifuged for 5 min at 12,000 rpm. After being washed with 70% ethanol, the precipitated DNA was dissolved in 200 μL of TE buffer (10 mM Tris; 1 mM EDTA, pH 8.0). The DNA extracts were kept in a −20°C freezer until sequencing analysis.

We amplified the small subunit of the nuclear ribosomal RNA (SSU rDNA) in the DNA extracts using the primer sets AMV4.5NF/AMDGR (Sato et al., 2005) to reveal AM fungal community in the tree roots. Because all the understory trees are primarily considered as AM trees, AM fungal community was measured. The reaction solution ratio was 20:2:2:3:13 Q5 High-Fidelity DNA Polymerase (New England Biolabs Inc., MA, United States)/10 mM forward primer/10 mM reverse primer/10-fold-diluted DNA sample/sterilized distilled water. Cycling conditions were as follows: initial denaturation at 98°C for 30 s, followed by 35 cycles of 98°C for 10 s, 58°C for 30 s, and 72°C for 30 s, followed by a 2-min final extension at 72°C. Amplification was performed using two replicates from each sample, after which amplification was checked by agarose gel electrophoresis and the replicates were composited to make one solution for purification. Purification was conducted using Agencourt AMPure XP (Beckman Coulter Inc., Brea, CA, United States) following the manufacturer's protocol. After purification, appropriate amounts of samples were combined into one tube and mixed to equalize the DNA quantity in each sample, which was computed using the Qubit dsDNA HS Assay Kit (Thermo Fisher Scientific). The combined samples were separated by the agarose gel electrophoresis, and the gels containing SSU rDNA genes were extracted by QIAquick Gel Extraction Kit (Qiagen, Hilden, Germany) following manufacture's instruction. Based on the size and quality of DNA in the gel extracts, which were checked using the Agilent High Sensitivity DNA Kit and Agilent 2100 Bioanalyzer (Agilent Technologies, Santa Clara, CA, United States), a dilution library of approximately 25 pM was prepared. Using 25 μL of the targeted dilution library, emulsion PCR was conducted using the Ion PGM OT2 400 Kit (Thermo Fisher Scientific) according to the manufacturer's instructions. After recovery of the ion spheres and enrichment, samples were loaded onto an Ion 318 Chip V2 instrument for sequencing using an Ion Personal Genome Machine (PGM) (Thermo Fisher Scientific). After analysis, sequence data with low-quality sequences and polyclonal sequences removed were exported as a FASTQ file from the PGM software. The barcode primer sequence was removed from the sequences, and the SSU rDNA sequences shorter than 250 bp in length were removed, then low-qualify sequences were discarded using a quality-filter of a maximum number of expected errors (E_max) of 0.5 using the FASTX toolkit. Sequences were dereplicated, singletons were removed, and clustering of OTUs at 97% similarity was conducted using USEARCH (Edgar, 2010). Sequences identified as chimeric were eliminated using UCHIME (Edgar et al., 2011), and the taxonomy was assigned with using the Maarj*AM* database (Öpik et al., 2010) and RDP algorithm at an 80% confidence threshold. These computer analyses were conducted using Quantitative Insights Into Microbial Ecology (QIIME) version 1.8.0 (Caporaso et al., 2011). All the OTUs were checked by the BLASTN program, then the OTUs that were not assigned as AM fungi were discarded. Sequence data were deposited in the Sequence Read Archive at NCBI under accession number DRA009209.

OTUs whose relative abundance was <1% were removed. The OTU tables were converted into 1 or 0 binary OTU tables, as >0 and 0 were defined "presence (1)" and "not presence (0)," respectively. AM fungi was categorized by the family level. The frequency was calculated as how many individuals had each AM family. Each understory tree species beneath the overstory trees of each forest have 5 replicates, so the range of frequency is from 0 to 5. We note that the surface of plant roots was carefully washed to avoid the contamination of soils so that the root fungal community could be clearly different from the soil fungal community (**Supplementary Figure 3**). Soil DNA was extracted from 0.25-g soil samples (0–10 cm depth) using the MoBio Powersoil DNA Isolation Kit (Mo Bio, Carlsbad, CA, United States).

Measurement of the δ^{15}N and δ^{18}O and IER-Captured Nitrate Content

Leaf and root samples were washed with distilled water. The leaf, root, and bulk soil samples were oven-dried at 60°C for over 24 h and homogenized into a ground powder. A total of 10 g of bulk soil samples were hydrolyzed using *ca*. 20 ml of 1 M HCl to remove carbonate. Leaf and root samples were loaded into tin capsules for isotope analysis, and total C and N concentration and stable isotope ratios were measured using an isotope ratio mass spectrometer (DELTA V Advantage, Thermo Fisher Scientific Inc., United States) with an elemental analyzer (Flash 2000, Thermo Fisher Scientific Inc., United States). The N stable isotope ratios of bulk soil samples were analyzed with an Elemental Analyser (Eurovector) coupled to an Isotope Ratio Mass Spectrometer (Delta Plus XP, Thermo Fisher Scientific, United States). The precision of the on-line procedure was better than ±0.2‰ for δ^{15}N.

Soil samples for extractable N analysis were extracted with 2 M KCl solution (soil: KCl = 1: 10, w/w). IERs were shaken with 20 ml of 2 M KCL for 20 min three times, making a total extract of 60 ml per one resin. Before preparing 2 M KCl solution, the KCl was muffled at 450°C for 4 h. The extracts were filtered using a precombusted glass-fiber filter (GF/F; Whatman Int. Ltd., Maidstone, United Kingdom, muffled at 450°C for 4 h). The KCl extracts were frozen until analyses of N concentration and isotopic composition. We measured the concentration of ammonium and nitrate in soil and resin extracts, and that of total extractable N in soil extracts, using a microplate reader (Synergy^{TM} HTX, BioTek, United States). For determining the concentration of ammonium and nitrate, the indophenol-blue method and a modified acidic Griess reaction (Miranda et al., 2001) were used, respectively. Total extractable N was oxidized to nitrate, using persulfate oxidization and measured as nitrate (Miyajima et al., 2005). The extractable organic N (EON) is then calculated as [EON] = [Total extractable N] − [Nitrate N] − [Ammonium N]. When [Nitrate N] was below the detection limit, we assigned [Nitrate N] as zero.

The δ^{15}N and δ^{18}O stable isotopes of nitrate were measured using the denitrifier method (Sigman et al., 2001; Casciotti et al., 2002; Thuan et al., 2018). We converted the nitrate into nitrous oxide (N_2O) using a denitrifier (*Pseudomonas aureofacien*) that lacked the enzyme to convert N_2O to N_2. The produced N_2O was introduced into the Isotope Ratio Mass Spectrometer (Sercon 20/22 equipped with Cryoprep and GC; Sercon Ltd., United Kingdom). The δ^{15}N of total extractable N was determined using persulfate oxidation followed by the denitrifier method (Houlton et al., 2007; Koba et al., 2012). The ammonium in the KCl extract was recovered with the diffusion method (Holmes et al., 1998) and the ammonium was captured onto a glass fiber filter (muffled at 450°C for 4 h, GF/D; Whatman Int. Ltd., Maidstone, United Kingdom) during shaking for over 48 h and drying for over 24 h. The captured ammonium was converted into nitrate by persulfate oxidization, then its N isotope ratio was determined by the denitrifier method (Thuan et al., 2018).

The natural abundance of ^{15}N and ^{18}O was expressed in per mil (‰) deviation from international standards: δ^{15}N or δ^{18}O = $[R_{\text{sample}}/R_{\text{standard}} - 1] \times 1000$, where R is ^{15}N/^{14}N or ^{18}O/^{16}O, respectively. Atmospheric N and Vienna standard mean ocean water were used as the international standards for N and O, respectively. Calibrations for these isotopic analyses were carried out using several international and in-house standards [USGS32, 34, 35 and IAEA NO_3^- for nitrate, USGS25, 26 and IAEA N-2 for ammonium and calibrated alanine, glycine, and histidine for total extractable N (Takebayashi et al., 2010)]. Natural abundance δ^{15}N of soil nitrate was measured for nine samples collected from beneath black locust trees, and due to very low nitrate concentration, for only one sample beneath oak trees. For these 10 samples, $\delta^{15}N_{\text{EON}}$ was calculated assigning [Nitrate] as zero. The δ^{15}N of EON was calculated using the following mass and isotopic balance equation: $\delta^{15}N_{\text{EON}} = \{\delta^{15}N_{\text{Total extractable N}} \times [\text{Total extractable N}] - (\delta^{15}N_{\text{nitrate}} \times [\text{Nitrate N}] + \delta^{15}N_{\text{ammonium}} \times [\text{Ammonium N}])\}/[\text{EON}]$. The difference in the δ^{15}N between leaves and roots of the same individual tree was defined as $\delta^{15}N_{\text{root-leaf}} = \delta^{15}N_{\text{root}} - \delta^{15}N_{\text{leaf}}$.

Statistical Analysis

Non-metric multidimensional scaling (NMDS) analysis of AM fungal community structure dissimilarity based on the Bray–Curtis index was performed using the metaMDS function in the vegan package (Oksanen et al., 2016) of R software. The envfit function in the vegan package was used to identify significant correlations between the NMDS values of points and the species of the trees (one tree species = 1, other tree species = 0), and the presence of fungal families and OTUs, to illustrate the vectors on the NMDS ordination plot. To determine the effects of soil environment, the extractable N content, moisture, and pH in soil around each tree individual were illustrated on the ordination. To identify the specific AM fungi that contribute greatly to the N acquisition of the host tree, the vectors of $\delta^{15}N_{\text{root-leaf}}$ (the indicator of mycorrhizal dependence) and leaf N concentration of the host trees were tried to be illustrated on the ordination. Permutational multivariate analysis of variance (PerMANOVA) was performed to test the significance of the effect of overstory tree type and the host tree species on the microbial community of understory trees, using the adonis function in the R vegan package. The 1 or 0 binary OTU tables were used to illustrate NMDS and conduct PerMANOVA. Because three of the oak trees had no AM fungi, and the other oak trees had only one or two AM fungi, oak trees were not included in the NMDS analysis.

We used two-way analysis of variance (ANOVA) to test for significant differences between overstory tree type (black locust [non-ECM] or oak [ECM]) and plant species for the following: the total number of AM fungal OTUs in roots, the leaf N concentration, and the content, δ^{15}N and/or δ^{18}O, of N in soils and captured in IER. We set the difference of sampling occasion (timing) as a random effect. We used generalized mixed model (GLMM) using the binomial family to test for significant differences between overstory tree type and plant species for the presence (1 or 0) of AM family and OTUs in roots. Tukey's multiple comparisons were used to examine potential differences among δ^{15}N of leaves, roots, and soils. We used a paired *t*-test to examine potential differences in δ^{15}N between the leaf and root of the same individual plants. Student's *t*-test was used to test for significant differences in leaf N concentration between the same plant species across beneath the different types of overstory trees. Prior to these tests except for GLMM, we tested for normality and homogeneity of variance in the data using the Kolmogorov–Smirnov and median Levene's tests, respectively. The car package in R software (version 3.1.2; R Core Team, 2014) was used to perform Levene's test (Fox et al., 2014). When the *P*-values of Kolmogorov–Smirnov or Levene's test prior to ANOVA was <0.05, the data were square-root or reciprocally transformed. When the *P*-values of Kolmogorov–Smirnov or Levene's test prior to *t*-test was <0.05, Welch's *t*-test was alternatively used. When the *P*-values of Kolmogorov–Smirnov test was >0.05 but the *P*-values of Levene's test were <0.05 prior to the multiple comparisons, Games–Howell's test was alternatively used. We chose a significance level of $P < 0.05$ for all tests.

RESULTS

AM Fungal Community in the Tree Roots

The total read number we obtained from root samples was 698,455 (the average ± SD was 9,978 ± 3,923 reads per sample). The total read number that was confirmed as AM fungi by the BLASTN was 63,243 (903 ± 558 reads per sample). The total number of AM fungal OTUs was 174, and beneath the black locust trees was 109 OTUs, and beneath the oak trees 91 OTUs. The average ± SD of the number of OTUs was 12 ± 9 per sample.

The AM fungal community structure was not significantly affected by overstory tree type ($F = 1.51$, $R^2 = 0.03$, $P = 0.123$), by the host plant species ($F = 0.893$, $R^2 = 0.07$, $P = 0.696$), or by the interaction between overstory tree type and understory tree species ($F = 1.126$ $R^2 = 0.09$, $P = 0.259$) based on PerMANOVA. NMDS also did not show a difference in the mycorrhizal community composition between beneath the black locust and oak trees (**Figure 1**). The community composition associated with understory trees overlapped with each other. However, when comparing samples from beneath non-ECM and ECM trees to test these differences for each individual species, the significant effect of the overstory tree type was only present in *C. multiflorus* (**Supplementary Figure 3**). The overstory tree type, host tree species, extractable N content, and pH in the soil associated with the trees (**Supplementary Figure 1**) were not significantly correlated with the community composition (**Figure 1**).

The most frequent family of AM fungi was Glomeraceae followed by Acaulosporaceae (**Figure 2**). The presence of all the families was not significantly affected by the overstory tree type or the host tree species (**Figure 2** and **Supplementary Figure 4**). The number of OTUs was also not significantly affected by the overstory tree type or the host tree species. Some of AM fungal OTUs, OTU 37, 544, 265, 622 (Glomeraceae) and OTU 112 (Claroideoglomeraceae), more frequently appeared beneath non-ECM (black locust) trees than beneath ECM (oak) trees (**Supplementary Figure 4**).

The Chemical Properties of the Understory Trees and Soils

Beneath oak trees, leaf δ^{15}N was consistently lower than root δ^{15}N in all understory tree species (**Figure 3B**). On the other hand, beneath black locust trees, the relationship between leaf and root δ^{15}N varied and depended on the understory tree species (**Figure 3A**). Leaf δ^{15}N of *S. pekinensis* and *A. stenolobum* was significantly higher than their root δ^{15}N, although leaf δ^{15}N of *C. multiflorus* was lower than its root δ^{15}N beneath black locust trees (**Figure 3A**). Leaf N concentration was significantly affected by the overstory tree type, and consistently higher beneath black locust than the oak trees in all understory tree species (**Figure 4**).

Beneath black locust trees, the δ^{15}N of understory trees was not significantly different from the δ^{15}N of soil EON, IER-captured nitrate, and that of *P. orientalis* and leaves of *S. pekinensis* and *A. stenolobum* was also not significantly different from that of soil nitrate (**Figure 3A**). However, the δ^{15}N of understory trees was consistently lower than that of soil ammonium beneath black locust trees (**Figure 3A**). The δ^{18}O of nitrate in soils and captured in IER beneath black locust trees was lower than 10‰ (**Table 1**). Beneath oak trees, the δ^{15}N of the leaves and roots of understory trees were significantly lower than δ^{15}N of EON and ammonium (**Figure 3B**). The δ^{15}N of soil nitrate beneath oak trees was measured only in one sample (**Table 1**). The δ^{15}N of IER-captured nitrate was not significantly different with the δ^{15}N of some understory trees (**Figure 3B**), and δ^{18}O of nitrate captured in IER was much higher than 10‰ beneath oak trees (**Table 1**).

In the surface soil (0–10 cm depth), EON and soil ammonium content were not significantly different between different types of overstory trees, but the soil nitrate content was 10 times and significantly higher beneath the black locust than beneath oak trees (**Table 1**, Tatsumi et al., 2020). The content of nitrate captured in IER was higher beneath black locust than oak trees (**Table 1**). The δ^{15}N of bulk surface soil and soil ammonium was also significantly higher beneath black locust than beneath oak trees (**Table 1**).

DISCUSSION

In contrast to our expectation in the first hypothesis, the mycorrhizal community composition associated with roots of understory trees was not significantly different between beneath different types of overstory trees (**Figure 1**). However, some OTUs, especially in Glomeraceae, were more frequent beneath the non-ECM (black locust) trees than the ECM (oak) trees, and the community composition of *C. multiflorus* was significantly different between beneath the non-ECM and ECM trees (**Figure 1** and **Supplementary Figure 3**). The higher frequency of some OTUs in Glomeraceae beneath the non-ECM trees may have been caused by soil N availability, as Glomeraceae is reported to increase under high soil N availability (Treseder and Allen, 2002; Egerton-Warburton et al., 2007), and soil N availability was higher beneath non-ECM than ECM trees (**Table 1**).

In agreement with the second hypothesis that the understory trees beneath the non-ECM overstory trees access nitrate, δ^{15}N of soil nitrate (especially, IER-captured nitrate) was similar to δ^{15}N of the leaves of the understory trees (**Figure 3A**). Further, the understory trees beneath the non-ECM overstory trees did not depend strongly upon mycorrhizal fungi, as shown by the leaf δ^{15}N not being significantly lower than root δ^{15}N, except for *C. multiflorus* (**Figure 3A**). The fact that δ^{15}N of ammonium was higher than δ^{15}N of the understory trees suggests that the understory trees likely did not use ammonium (**Figure 3A**). Although the δ^{15}N of soil EON was also not significantly

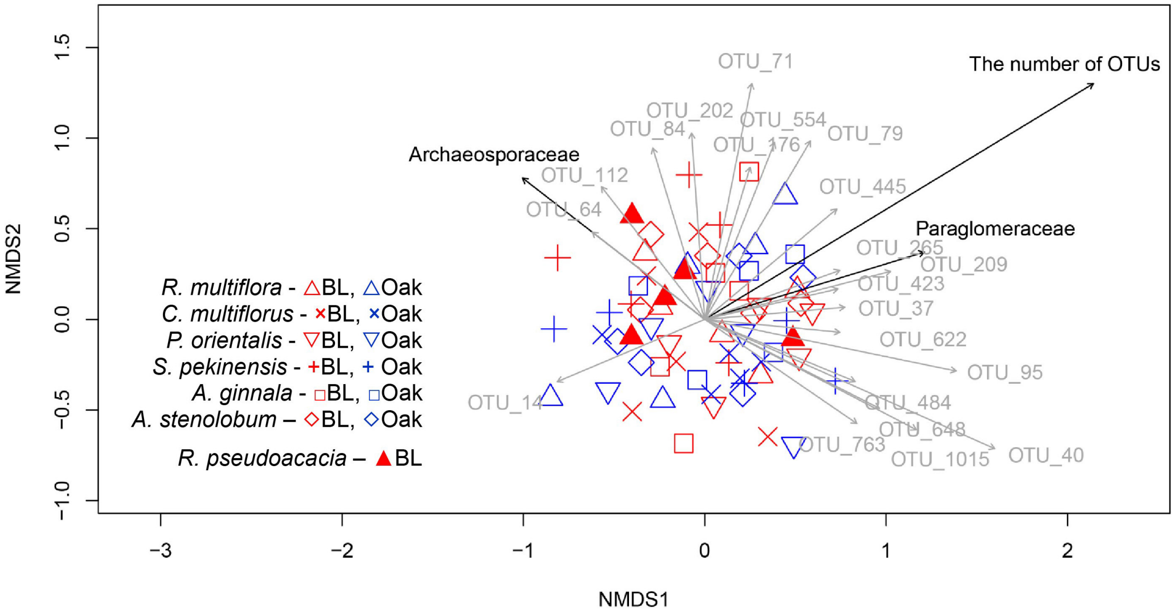

FIGURE 1 | Non-metric multidimensional scaling (NMDS) based on root AM fungal community dissimilarities. Red and blue symbols represent understory trees beneath black locust and oak trees, respectively. The symbols indicate as follows: Δ; *Rosa multiflora*, ×; *Cotoneaster multiflorus*, ∇; *Platycladus orientalis*, +; *Syringa pekinensis*, □; *Acer ginnala*, ⋄; *Acer stenolobum,* ▲; *Robinia pseudoacacia*. The stress value was 0.27. Only significant vectors are plotted on the ordination. Black vectors represent the presence of fungal family and the total number of operational taxonomic units (OTUs). Dark gray vectors represent the presence of frequent OTUs. The experimental design (overstory tree type and host tree species) and soil chemical properties were not plotted.

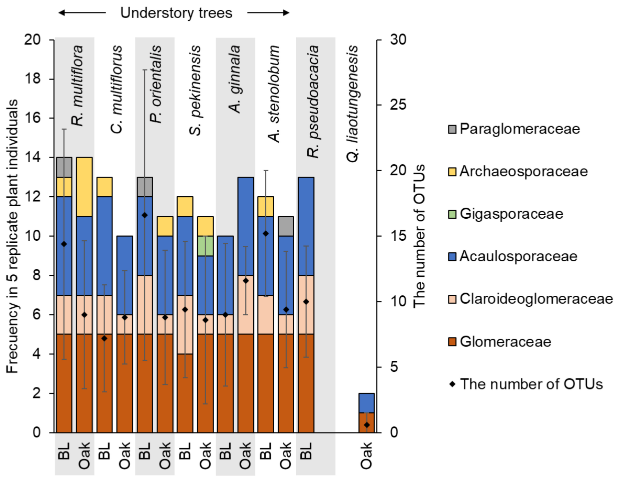

FIGURE 2 | The frequency of AM fungal family and the averaged total number of AM fungal OTUs in 5 replicate plant individual roots collected from beneath black locust (BL) and oak trees. There were no significant effects of overstory tree type and host tree species based on the GLMM (for the frequency) and the two-way ANOVA (for the number of OTUs) with the overstory type and species. The overstory tree samples were not included in the GLMM and two-way ANOVA comparison. Red group belongs to the order Glomerales.

different from the $\delta^{15}N$ of the understory trees, EON might not be major N source because most of the EON is high-molecular-weight and recalcitrant (Jones et al., 2005), and an only small part of EON is possible N source for plants (Takebayashi et al., 2010). Supporting the idea that the understory trees take up nitrate, the $\delta^{15}N$ of leaves was higher than that of roots, especially of *S. pekinensis* and *A. stenolobum*. Nitrate assimilation occurs both in roots and shoots, with lighter nitrate typically assimilated in roots, and then the heavier nitrate is typically transferred to shoots and leaves, leading to greater leaf $\delta^{15}N$ than root $\delta^{15}N$ (Yoneyama and Kaneko, 1989; Evans et al., 1996; Evans, 2001). Further, the active nitrification beneath the non-ECM overstory trees could support the use nitrate by the understory trees. The $\delta^{18}O$ of soil and IER-captured was <10‰ beneath the non-ECM overstory trees, suggesting that nitrate comes primarily from nitrification, although the IER-captured nitrate beneath the ECM overstory trees was likely derived mostly from atmosphere (**Table 1**; Kendall et al., 2007; Fang et al., 2012). Also, the relatively greater $\delta^{15}N$ values in soils beneath the non-ECM than ECM trees support the idea that nitrification rate is higher beneath the non-ECM overstory trees since they are typically positively correlated (Templer et al., 2007), although the soil $\delta^{15}N$ values might be caused by the probably greater $\delta^{15}N$ values of litter input under the non-ECM than ECM overstory trees (**Figure 3A**). Thus, the understory trees beneath the non-ECM overstory trees likely take up a rich nitrate pool, which is derived from active nitrification, being consistent with our second hypothesis. However, it is still not clear from our experimental design, which trait of black locust, AM species or N-fixers presence/activity, caused the rich nitrate pool.

In support of our third hypothesis, all plant species beneath the ECM overstory trees likely took up N via mycorrhizal fungi,

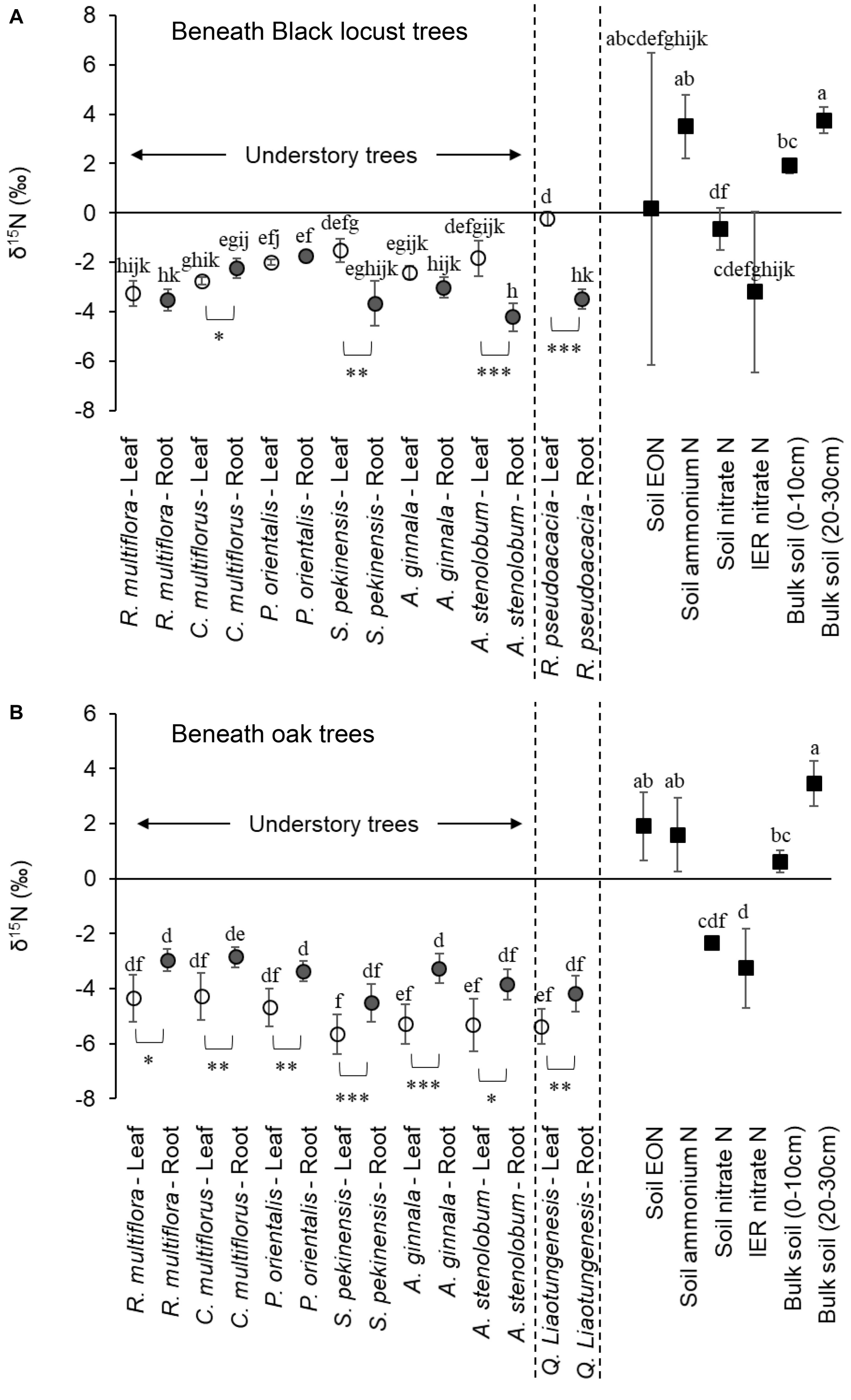

FIGURE 3 | The δ^{15}N of leaves and roots of the six understory trees and the overstory trees, and the δ^{15}N of soil N sources (soil extractable N and bulk soil) beneath **(A)** black locust and **(B)** oak trees (mean ± SD). The results of the paired *t*-test between δ^{15}N of leaves and roots from the same individual trees were shown below of the plots. $^{*}P < 0.05$, $^{**}P < 0.01$, $^{***}P < 0.001$. Different lowercase letters above the plots indicate significant pairwise differences (Tukey–Kramer or Games–Howell test).

as indicated by the fact that leaf δ^{15}N was lower than root δ^{15}N (**Figure 3B**), which suggests mycorrhizal fungi in roots transferred lighter N to leaves (Kohzu et al., 2000; Emmerton et al., 2001; Hobbie and Colpaert, 2003). We could not separate the roots and mycorrhizal fungi for isotope analysis, so the high root δ^{15}N may have come from the N remaining in

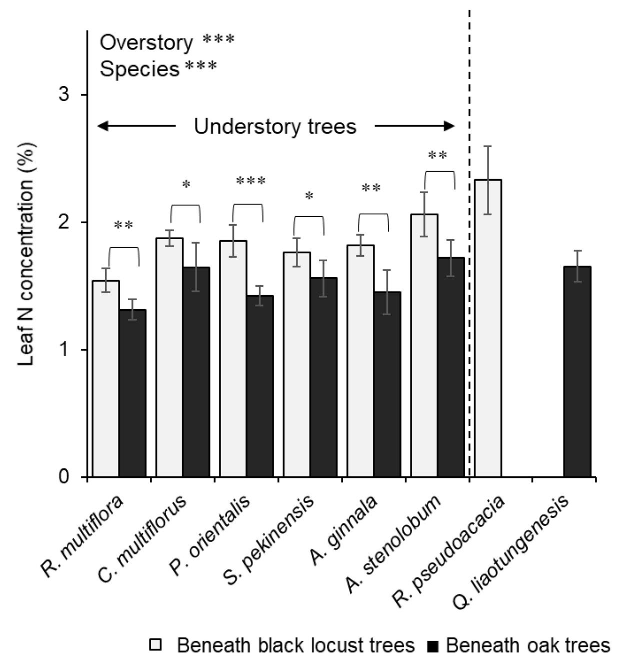

FIGURE 4 | Leaf N concentrations of the six understory trees and the overstory trees beneath the black locust overstory and oak overstory trees. Values are means ± S.D. Significant differences between different overstory tree types in each species (identified by Student's or Welch's *T*-test) are indicated on the bar. The results of two-way ANOVA with the overstory tree type (Overstory) and the tree species (Species) are shown at the top. The overstory tree samples were not included into the two-way ANOVA comparison. *$P < 0.05$, **$P < 0.01$, ***$P < 0.001$.

the fungal root component (Schweiger, 2016). Although the transfer of ^{15}N-depleted N from AM fungi to host plants has not clearly been demonstrated compared to ECM fungi (Aguilar et al., 1998; Wheeler et al., 2000), AM plants are more ^{15}N-depleted than non-mycorrhizal plants (Craine et al., 2015; Schweiger, 2016), or rarely as much ^{15}N-depleted as co-occurring ECM plants, which may indicate AM fungi also fractionate against ^{15}N (Hobbie and Hobbie, 2008). Besides, a study using calculation models and field sampling suggested there is a 2–4‰ fractionation of N in AM transfer to plants (Jach-Smith and Jackson, 2020), and another study also supported the fractionation of AM fungi based on the fact that leaf ^{15}N depletion coincided with root ^{15}N enrichment (Schweiger, 2016). In contrast, it is still possible that understory trees beneath the ECM overstory trees directly take up nitrate without mycorrhizal association as indicated by δ^{15}N of soil nitrate being similar to δ^{15}N of the leaves of the understory trees, and that the internal fractionation within plants is considered to cause 2‰ difference in δ^{15}N between leaf and root (Dawson et al., 2002; Houlton et al., 2007). However, the slow nitrification process beneath the ECM overstory trees, demonstrated by our previous study (Tatsumi et al., 2020) and the total soil δ^{15}N and δ^{18}O values of nitrate as mentioned above, suggest that direct uptake without mycorrhizal fungi was not major N source for understory trees. Besides, the internal fractionation cannot explain why the consistently lower leaf than root δ^{15}N was only observed beneath the ECM overstory trees. Thus, the understory trees beneath the ECM overstory trees likely more depended upon mycorrhizal fungi for N acquisition, following our third hypothesis. As AM fungal community composition was similar between beneath the non-ECM and ECM trees, the dependence on the same AM fungi should largely change between beneath the non-ECM and ECM trees. However, we did not measure rates of root colonization, so more detailed research is needed to determine the mycorrhizal dependency of plants in these dry forests.

We also found that the patterns of N uptake of the understory trees were affected by the understory tree species. For example,

TABLE 1 | The content and δ^{15}N of soil extractable N in soil (0–10 cm depth), nitrate N in ion-exchanged resin (IER) and bulk soil (0–10 cm depth and 20–30 cm depth), and the δ^{18}O of nitrate N in soil (0–10 cm depth) and captured in IER (mean ± SD).

		Black locust trees	**(*n*)**	**Oak trees**	**(*n*)**	***F*-value**
Content (mg kg^{-1}) or (mg cap^{-1})	Soil EON	18.6 ± 10.8	(36)	39.5 ± 18.9	(36)	**59.3 *****
	Soil ammonium N	9.1 ± 3.3	(36)	12.3 ± 3.3	(36)	**66.5 *****
	Soil nitrate N	7.2 ± 3.5	(36)	0.7 ± 0.6	(36)	**238.4 *****
	IER nitrate N	0.24 ± 0.18	(7)	0.03 ± 0.02	(7)	**18.1 ****
	Soil total N (0–10 cm depth)	2312 ± 434	(36)	3234 ± 571	(36)	**68.4 *****
	Soil total N (20–30 cm depth)	544 ± 44	(4)	629 ± 76	(4)	3.8
δ^{15}N (‰)	Soil EON	0.2 ± 6.3	(10)	1.9 ± 1.2	(10)	0.7
	Soil ammonium N	3.5 ± 1.3	(10)	1.6 ± 1.3	(10)	**10.1 ****
	Soil nitrate N	−0.7 ± 0.9	(9)	−2.4	(1)	3.8
	IER nitrate N	−3.2 ± 3.2	(7)	−3.3 ± 1.4	(7)	0.0
	Soil total N (0–10 cm depth)	1.9 ± 0.3	(8)	0.6 ± 0.4	(8)	**54.4 *****
	Soil total N (20–30 cm depth)	3.8 ± 0.5	(4)	3.5 ± 0.8	(4)	0.4
δ^{18}O (‰)	Soil nitrate N	1.5 ± 2.3	(9)	−3.1	(1)	**9.8 ***
	IER nitrate N	4.1 ± 2.3	(7)	38.7 ± 16.2	(7)	**31.6 *****

(n) shows the number of samples. Right side shows F-values and P-values ($P < 0.05$, **$P < 0.01$, ***$P < 0.001$) based on one-way ANOVA with the overstory tree type (beneath black locust or oak trees). The models were performed with sampling occasions as a random variable. The data of soil extractable N content and total N content was from Tatsumi et al. (2019, 2020).*

C. multiflorus had significantly lower δ^{15}N in leaves than roots beneath the non-ECM overstory trees, while other understory tree species had higher or similar δ^{15}N in leaves than roots (**Figure 3A**). The Genus *Cotoneaster* was reported to show lower growth when fertilized with nitrate than with ammonium (Kraus et al., 2002). *C. multiflorus* may not actively access the rich nitrate pool beneath the non-ECM overstory trees.

We conclude that while tree species is an important factor for describing patterns of N uptake by understory trees, we found that differences in understory N utilization also depends on the type of overstory trees present. We suggest that the N uptake patterns of co-existing understory trees vary beneath different types of overstory trees, although it is necessary to compare other non-ECM and ECM overstory tree species. With greater sampling, we may be able to separate the effects of mycorrhizal type vs. the effects of the presence of N fixers on the ability for understory trees to take up N. However, black locust and oak are the most common species in this region, so our findings should be at least important for understanding the reforestation and succession process in this region. Furthermore, the higher N concentrations of understory trees beneath the non-ECM than ECM overstory trees (**Figure 4**) may contribute to further acceleration of N cycling as a positive feedback, because high N concentrations of litter increase rates of decomposition (Cotrufo et al., 1995; Sun et al., 2018), although more research about N in litterfall of understory trees is needed.

DATA AVAILABILITY STATEMENT

The datasets generated for this study can be found in online repositories. The names of the repository/repositories and accession number(s) can be found in the article/**Supplementary Material**.

AUTHOR CONTRIBUTIONS

CT and RT designed the research. CT, FH, TT, SD, NY, and RT conducted the fieldwork. CT, FH, TT, WS, KK, and KF conducted the laboratory work. CT, FH, TT, KK, PT, and RT critically contributed to interpreting the data. CT and RT led the writing of the manuscript. All authors reviewed the manuscript and gave final approval for publication.

FUNDING

This study was financially supported in part by JSPS-KAKENHI (Grant No. 15H05113), Grant-in-Aid for JSPS Research Fellow (Grant No. 17J07686), Oversea Challenge Program for Young Researcher (Grant No. 201980107), JSPS-NSFC Bilateral Joint Research Projects (Nos. 41411140035 and 41171419), and Fund of Joint Research Program of Arid Land Research Center, Tottori University. This work was also supported by Joint Usage/Research Grant of Center for Ecological Research, Kyoto University.

ACKNOWLEDGMENTS

We greatly thank to members of the Institute of Soil and Water Conservation of Chinese Academy of Sciences (CAS), the Arid Land Research Center (ALRC) of Tottori University, the Field Science, Education and Research Center (FSERC) of Kyoto University, the Center for Ecological Research, Kyoto University for cooperation and logistics in both of field survey and laboratory analysis. We also greatly thank Dr. Komei Kadowaki and Dr. Yoshioka Takahito for helpful comments. We also deeply appreciate Mr. Masataka Nakayama for helping laboratory works.

SUPPLEMENTARY MATERIAL

The Supplementary Material for this article can be found online at: https://www.frontiersin.org/articles/10.3389/fpls.2020.583585/full#supplementary-material

REFERENCES

Aguilar, R. A.-G., Handley, L. L., and Scrimgeour, C. M. (1998). The δ^{15}N of lettuce and barley are affected by AM status and external concentration of N. *N. Phytol.* 138, 19–26. doi: 10.1046/j.1469-8137.1998.00883.x

Andersen, K. M., Mayor, J. R., and Turner, B. L. (2017). Plasticity in nitrogen uptake among plant species with contrasting nutrient acquisition strategies in a tropical forest. *Ecology* 98, 1388–1398. doi: 10.1002/ecy.1793

Ashton, I. W., Miller, A. E., Bowman, W. D., and Suding, K. N. (2010). Niche complementarity due to plasticity in resource use: Plant partitioning of chemical N forms. *Ecology* 91, 3252–3260. doi: 10.1890/09-1849.1

Averill, C., and Finzi, A. (2011). Increasing plant use of organic nitrogen with elevation is reflected in nitrogen uptake rates and ecosystem δ^{15}N. *Ecology* 92, 883–891. doi: 10.1890/10-0746.1

Averill, C., and Hawkes, C. V. (2016). Ectomycorrhizal fungi slow carbon cycling. *Ecol. Lett.* 53, 1689–1699. doi: 10.1017/CBO9781107415324.004

Averill, C., Turner, B. L., and Finzi, A. C. (2014). Mycorrhiza-mediated competition between plants and decomposers drives soil carbon storage. *Nature* 505, 543–545. doi: 10.1038/nature12901

Bittebiere, A. K., Vandenkoornhuyse, P., Maluenda, E., Gareil, A., Dheilly, A., Coudouel, S., et al. (2019). Past spatial structure of plant communities determines arbuscular mycorrhizal fungal community assembly. *J. Ecol.* 108, 546–560. doi: 10.1111/1365-2745.13279

Caporaso, J. G., Kuczynski, J., Stombaugh, J., Bittinger, K., Bushman, F. D., Costello, E. K., et al. (2011). QIIME allows analysis of high-throughput community sequencing data. *Nat. Methods* 7, 335–336. doi: 10.1038/nmeth.f.303.QIIME

Casciotti, K. L., Sigman, D. M., Hastings, M. G., Böhlke, J. K., and Hilkert, A. (2002). Measurement of the oxygen isotopic composition of nitrate seawater and freshwater using the dentirifier method. *Anal. Chem.* 74, 4905–4912. doi: 10.1021/ac020113w

Chalot, M., and Brun, A. (1998). Physiology of organic nitrogen acquisition by ectomycorrhizal fungi and ectomycorrhizas. *FEMS Microbiol. Rev.* 22, 21–44. doi: 10.1111/j.1574-6976.1998.tb00359.x

Choi, W. J., Chang, S. X., Allen, H. L., Kelting, D. L., and Ro, H. M. (2005). Irrigation and fertilization effects on foliar and soil carbon and nitrogen isotope ratios in a loblolly pine stand. *For. Ecol. Manage.* 213, 90–101. doi: 10.1016/j.foreco.2005.03.016

Cotrufo, F., Ineson, P., Roberts, J., and derek. (1995). Decomposition of birch leaf litter with varying C to N ratios. *Soil Biol. Biochem.* 27, 1219–1221. doi: 10.1016/0038-0717(95)00043-E

Courty, P. E., Buee, M., Diedhiou, A. G., Frey-Klett, P., Tacon, F., le Rineau, F., et al. (2010). The role of ectomycorrhizal communities in forest ecosystem processes: New perspectives and emerging concepts. *Soil Biol. Biochem.* 42, 679–698. doi: 10.1016/J.Soilbio.2009.12.006

Craine, J. M., Brookshire, E. N. J., Cramer, M. D., Hasselquist, N. J., Koba, K., Marin-Spiotta, E., et al. (2015). Ecological interpretations of nitrogen isotope ratios of terrestrial plants and soils. *Plant Soil* 396, 1–26. doi: 10.1007/s11104-015-2542-1

Daryanto, S., Wang, L., Gilhooly, W. P. III, and Jacinthe, P.-A. (2019). Nitrogen preference across generations under changing ammonium nitrate ratios. *J. Plant Ecol.* 12, 235–244. doi: 10.1093/jpe/rty014

Dawson, T. E., Mambelli, S., Plamboeck, A. H., Templer, P. H., and Tu, K. P. (2002). Stable isotopes in plant ecology. *Annu. Rev. Ecol. Syst.* 33, 507–559. doi: 10.1146/annurev.ecolsys.33.020602.095451

Du, S., Wang, Y. L., Kume, T., Zhang, J. G., Otsuki, K., Yamanaka, N., et al. (2011). Sapflow characteristics and climatic responses in three forest species in the semiarid Loess Plateau region of China. *Agric. For. Meteorol.* 151, 1–10. doi: 10.1016/j.agrformet.2010.08.011

Duponnois, R., Ouahmane, L., Kane, A., Thioulouse, J., Hafidi, M., Boumezzough, A., et al. (2011). Nurse shrubs increased the early growth of Cupressus seedlings by enhancing belowground mutualism and soil microbial activity. *Soil Biol. Biochem.* 43, 2160–2168. doi: 10.1016/j.soilbio.2011.06.020

Edgar, R. C. (2010). Search and clustering orders of magnitude faster than BLAST. *Bioinformatics* 26, 2460–2461. doi: 10.1093/bioinformatics/btq461

Edgar, R. C., Haas, B. J., Clemente, J. C., Quince, C., and Knight, R. (2011). UCHIME improves sensitivity and speed of chimera detection. *Bioinformatics* 27, 2194–2200. doi: 10.1093/bioinformatics/btr381

Egerton-Warburton, L. M., Johnson, N. C., and Allen, E. B. (2007). Mycorrhizal community dynamics following nitrogen fertilization: a cross−site test in five grasslands. *Ecol. Monogr.* 77, 527–544.

Emmerton, K. S., Callaghan, T. V., Jones, H. E., Leake, J. R., Michelsen, A., and Read, D. J. (2001). Assimilation and isotopic fractionation of nitrogen by mycorrhizal fungi. *N. Phytol.* 151, 503–511. doi: 10.1046/j.1469-8137.2001.00178.x

Evans, D. R. (2001). Physiological mechanisms influencing plant nitrogen isotope composition. *Trends Plant Sci.* 6, 121–126. doi: 10.1016/S1360-1385(01)01889-1

Evans, D. R., Bloom, A. J., Sukrapanna, S. S., and Ehleringer, J. R. (1996). Nitrogen isotope composition of tomato (*Lycopersicon esculentum* Mill. cv. T-5) grown under ammonium or nitrate nutrition. *Plant Cell Environ.* 19, 1317–1323. doi: 10.1111/j.1365-3040.1996.tb00010.x

Falkengren-grerup, U., Michelsen, A., Olsson, M. O., Quarmby, C., and Sleep, D. (2004). Plant nitrate use in deciduous woodland: the relationship between leaf N, ^{15}N natural abundance of forbs and soil N mineralisation. *Soil Biol. Biochem.* 36, 1885–1891. doi: 10.1016/j.soilbio.2004.05.009

Fang, Y., Koba, K., Makabe, A., Zhu, F., Fan, S., Liu, X., et al. (2012). Low δ^{18}O values of nitrate produced from nitrification in temperate forest soils. *Environ. Sci. Technol.* 46, 8723–8730. doi: 10.1021/es300510r

Fernandez, C. W., and Kennedy, P. G. (2016). Revisiting the "Gadgil effect": Do interguild fungal interactions control carbon cycling in forest soils? *N. Phytol.* 209, 1382–1394. doi: 10.1111/nph.13648

Finzi, A. C., Canham, C. D., and Van Breemen, N. (1998). Canopy tree soil interactions within temperate forests: Species effects on pH and cations. *Ecol. Appl.* 8, 447–454. doi: 10.2307/2641084

Fox, J., Weisberg, S., Adler, D., Price, B., Bates, D., Bolker, B., et al. (2014). *Package 'car' (Version 2.1-3).*

Gadgil, R. L., and Gadgil, P. D. (1971). Mycorrhiza and litter decomposition. *Nature* 233, 133.

Gehring, C. A., Sthultz, C. M., Flores-rentería, L., and Whipple, A. V. (2017). Tree genetics defines fungal partner communities that may confer drought tolerance. *Proc. Natl. Acad. Sci.* 114, 11169–11174. doi: 10.1073/pnas.1704022114

Hobbie, E. A., and Colpaert, J. V. (2003). Nitrogen availability and colonization by mycorrhizal fungi correlate with nitrogen isotope patterns in plants. *N. Phytol.* 157, 115–126. doi: 10.1046/j.1469-8137.2003.00657.x

Hobbie, E. A., and Hobbie, J. E. (2008). Natural abundance of ^{15}N in nitrogen-limited forests and Tundra can estimate nitrogen cycling through mycorrhizal fungi: A review. *Ecosystems* 11, 815–830. doi: 10.1007/s10021-008-9159-7

Hodge, A., and Storer, K. (2014). Arbuscular mycorrhiza and nitrogen: Implications for individual plants through to ecosystems. *Plant Soil* 386, 1–19. doi: 10.1007/s11104-014-2162-1

Holmes, R. M., McClelland, J. W., Sigman, D., Fry, B., and Peterson, B. J. (1998). Measuring ^{15}N-NH$_4$ in marine, estuarine, and freshwaters: An adaptation of the ammonia diffusion method for samples with low ammonium concentrations. *Mar. Chem.* 60, 235–243. doi: 10.1016/S0304-4203(97)00099-6

Houlton, B. Z., Sigman, D. M., Schuur, E. A. G., and Hedin, L. O. (2007). A climate-driven switch in plant nitrogen acquisition within tropical forest communities. *Proc. Natl. Acad. Sci.* 104, 8902–8906. doi: 10.1073/pnas.0609935104

Jach-Smith, L. C., and Jackson, R. D. (2020). Inorganic N addition replaces N supplied to switchgrass (*Panicum virgatum*) by arbuscular mycorrhizal fungi. *Ecol. Appl.* 30:2047. doi: 10.1002/eap.2047

Jo, I., Potter, K. M., Domke, G. M., and Fei, S. (2018). Dominant forest tree mycorrhizal type mediates understory plant invasions. *Ecol. Lett.* 21, 217–224. doi: 10.1111/ele.12884

Jones, D. L., and Kielland, K. (2002). Soil amino acid turnover dominates the nitrogen flux in permafrost-dominated taiga forest soils. *Soil Biol. Biochem.* 34, 209–219. doi: 10.1016/S0038-0717(01)00175-4

Jones, D. L., Healey, J. R., Willett, V. B., Farrar, J. F., and Hodge, A. (2005). Dissolved organic nitrogen uptake by plants - An important N uptake pathway? *Soil Biol. Biochem.* 37, 413–423. doi: 10.1016/j.soilbio.2004.08.008

Kahmen, A., Wanek, W., and Buchmann, N. (2008). Foliar d^{15}N values characterize soil N cycling and reflect nitrate or ammonium preference of plants along a temperate grassland gradient. *Oecologia* 156, 861–870. doi: 10.1007/s00442-008-1028-8

Kendall, C., Elliott, E. M., and Wankel, S. D. (2007). "Tracing anthropogenic inputs of nitrogen to ecosystems," in *Stable Isotopes in Ecology and Environmental Science*, 2nd Edn, eds R. H. Michener and K. E. Lajtha (New Jersey: Blackwell Publishing), 375–449.

Koba, K., Fang, Y., Mo, J., Zhang, W., Lu, X., Liu, L., et al. (2012). The ^{15}N natural abundance of the N lost from an N-saturated subtropical forest in southern China. *J. Geophys. Res. Biogeosci.* 117, 1–13. doi: 10.1029/2010JG001615

Koba, K., Hirobe, M., Koyama, L., Kohzu, A., Tokuchi, N., Nadelhoffer, K., et al. (2003). Natural ^{15}N abundance of plants and soil N in a temperate coniferous forest. *Ecosystems* 6, 457–469. doi: 10.1007/s10021-002-0132-6

Kohler, A., Kuo, A., Nagy, L. G., Morin, E., Barry, K., Buscot, F., et al. (2015). Convergent losses of decay mechanisms and rapid turnover of symbiosis genes in mycorrhizal mutualists. *Nat. Genet.* 47, 410–415. doi: 10.1038/ng.3223

Kohzu, A., Tateishi, T., Yamada, A., and Koba, K. (2000). Nitrogen isotope fractionation during nitrogen transport from ectomycorrhizal fungi, *Suillus granulatus*, to the host plant, Pinus densiflora. *Soil Sci. Plant Nutr.* 46, 733–739. doi: 10.1080/00380768.2000.10409138

Kraus, H. T., Warren, S. L., and Anderson, C. E. (2002). Nitrogen form affects growth, mineral nutrient content, and root anatomy of Cotoneaster and Rudbeckia. *HortScience* 37, 126–129. doi: 10.21273/HORTSCI.37.1.126

LeBauer, D. S., and Treseder, K. K. (2008). Nitrogen limitation of net primary productivity in terrestrial ecosystems is globally distributed. *Ecology* 89, 371–379. doi: 10.1890/06-2057.1

Liu, X., Koba, K., Koyama, L. A., Hobbie, S., Weiss, M., Inagaki, Y., et al. (2018). Nitrate is an important nitrogen source for Arctic tundra plants. *Proc. Natl. Acad. Sci. U S A.* 115, 3398–3403. doi: 10.1073/pnas.1715382115

Lü, H., Liu, D., and Guo, Z. (2003). Natural vegetation of geological and historical periods in Loess Plateau. *Chin. Sci. Bull.* 48, 7–9. doi: 10.1007/BF03183240

Martínez-García, L. B., and Pugnaire, F. I. (2011). Arbuscular mycorrhizal fungi host preference and site effects in two plant species in a semiarid environment. *Appl. Soil Ecol.* 48, 313–317. doi: 10.1016/j.apsoil.2011.04.003

McKane, R. B., Johnson, L. C., Shaver, G. R., Nadelhoffer, K. J., Rastetter, E. B., Fry, B., et al. (2002). Resource-based niches provide a basis for plant species diversity and dominance in arctic tundra. *Nature* 415, 3–6. doi: 10.1038/415068a

Mensah, J. A., Koch, A. M., Antunes, P. M., Kiers, E. T., Hart, M., and Bücking, H. (2015). High functional diversity within species of arbuscular mycorrhizal fungi is associated with differences in phosphate and nitrogen uptake and fungal phosphate metabolism. *Mycorrhiza* 25, 533–546. doi: 10.1007/s00572-015-0631-x

Midgley, M. G., and Phillips, R. P. (2016). Resource stoichiometry and the biogeochemical consequences of nitrogen deposition in a mixed deciduous forest. *Ecology* 97, 3369–3377. doi: 10.1002/ecy.1595

Miranda, K. M., Espey, M. G., and Wink, D. A. (2001). A rapid, simple spectrophotometric method for simultaneous detection of nitrate and nitrite. *Nitric Oxide Biol. Chem.* 5, 62–71. doi: 10.1006/niox.2000.0319

Miyajima, T., Tanaka, Y., and Koike, I. (2005). Determining ^{15}N enrichment of dissolved organic nitrogen in environmental waters by gas chromatography/negative-ion chemical ionization mass spectrometry. *Limnol. Oceanogr. Methods* 3, 164–173. doi: 10.4319/lom.2005.3.164

Näsholm, T., Ekblad, A., Nordin, A., Giesler, R., Högberg, M., and Högberg, P. (1998). Boreal forest plants take up organic nitrogen. *Nature* 392, 914–916. doi: 10.1038/31921

Nordin, A., Högberg, P., and Näsholm, T. (2001). Soil nitrogen form and plant nitrogen uptake along a boreal forest productivity gradient. *Oecologia* 129, 125–132. doi: 10.1007/s004420100698

Oksanen, A. J., Blanchet, F. G., Friendly, M., Legendre, P., Minchin, P. R., O'Hara, R. B., et al. (2016). *Package 'vegan'(Version 2.4-0).*

Öpik, M., Vanatoa, A., Vanatoa, E., Moora, M., Davison, J., Kalwij, J. M., et al. (2010). The online database Maarj*AM* reveals global and ecosystemic distribution patterns in arbuscular mycorrhizal fungi (*Glomeromycota*). *N. Phytol.* 188, 223–241. doi: 10.1111/j.1469-8137.2010.03334.x

Pellitier, P. T., and Zak, D. R. (2018). Ectomycorrhizal fungi and the enzymatic liberation of nitrogen from soil organic matter: why evolutionary history matters. *N. Phytol.* 217, 68–73. doi: 10.1111/nph.14598

Phillips, R. P., Brzostek, E., and Midgley, M. G. (2013). The mycorrhizal-associated nutrient economy: A new framework for predicting carbon – nutrient couplings in temperate forests. *N. Phytol.* 199, 41–51. doi: 10.1111/nph.12221

Porras-Alfaro, A., Herrera, J., Natvig, D. O., and Sinsabaugh, R. L. (2007). Effect of long-term nitrogen fertilization on mycorrhizal fungi associated with a dominant grass in a semiarid grassland. *Plant Soil* 296, 65–75. doi: 10.1007/s11104-007-9290-9

R Core Team (2014). *R: A Language and Environment for Statistical Computing. Version 3.1. 2 [Computer Program]*. Vienna: R Foundation for Statistical Computing.

Read, D. J., and Perez-Moreno, J. (2003). Mycorrhizas and nutrient cycling in ecosystems – a journey towards relevance? *N. Phytol.* 157, 475–492. doi: 10.1046/j.1469-8137.2003.00704.x

Ren, H., Xu, Z., Isbell, F., Huang, J., Han, X., Wan, S., et al. (2017). Exacerbated nitrogen limitation ends transient stimulation of grassland productivity by increased precipitation. *Ecol. Monogr.* 87, 457–469. doi: 10.1002/ecm.1262

Rice, S. K., Westerman, B., and Federici, R. (2004). Impacts of the exotic, nitrogen-fixing black locust (*Robinia pseudoacacia*) on nitrogen-cycling in a pine-oak ecosystem. *Plant Ecol.* 174, 97–107. doi: 10.1023/B:VEGE.0000046049.21900.5a

Sato, H., and Murakami, N. (2008). Reproductive isolation among cryptic species in the ectomycorrhizal genus Strobilomyces: Population-level CAPS marker-based genetic analysis. *Mol. Phylogenet. Evol.* 48, 326–334. doi: 10.1016/j.ympev.2008.01.033

Sato, K., Suyama, Y., Saito, M., and Sugawara, K. (2005). A new primer for discrimination of arbuscular mycorrhizal fungi with polymerase chain reaction-denature gradient gel electrophoresis. *Jap. Soc. Grassl. Sci.* 51, 179–181. doi: 10.1111/j.1744-697X.2005.00023.x

Schweiger, P. F. (2016). Nitrogen isotope fractionation during N uptake via arbuscular mycorrhizal and ectomycorrhizal fungi into grey alder. *J. Plant Physiol.* 205, 84–92. doi: 10.1016/j.jplph.2016.08.004

Sigman, D. M., Casciotti, K. L., Andreani, M., Barford, C., Galanter, M., and Böhlke, J. K. (2001). A bacterial method for the nitrogen isotopic analysis of nitrate in seawater and freshwater. *Anal. Chem.* 73, 4145–4153. doi: 10.1021/ac010088e

Smith, S. E., and Read, D. J. (2008). *Mycorrhizal symbiosis*, 3rd Edn. Cambridge: Academic press.

Smith, S. E., and Smith, F. A. (2011). Roles of arbuscular mycorrhizas in plant nutrition and growth: new paradigms from cellular to ecosystem scales. *Annu. Rev. Plant Biol.* 62, 227–250. doi: 10.1146/annurev-arplant-042110-103846

Soudzilovskaia, N. A., Vaessen, S., Barcelo, M., He, J., Rahimlou, S., and Abarenkov, K. (2020). FungalRoot: global online database of plant mycorrhizal associations. *N. Phytol.* 227, 955–966. doi: 10.1111/nph.16569

Sun, T., Hobbie, S. E., Berg, B., Zhang, H., Wang, Q., Wang, Z., et al. (2018). Contrasting dynamics and trait controls in first-order root compared with leaf litter decomposition. *Proc. Natl. Acad. Sci.* 115, 10392–10397. doi: 10.1073/pnas.1716595115

Takebayashi, Y., Koba, K., Sasaki, Y., Fang, Y., and Yoh, M. (2010). The natural abundance of ^{15}N in plant and soil-available N indicates a shift of main plant N resources to NO_3^- from NH_4^+ along the N leaching gradient. *Rapid Commun. Mass Spectrom.* 24, 3567–3577. doi: 10.1002/rcm

Tanner, E. V. J., Vitousek, P. M., and Cuevas, E. (1998). Experimental investigation of nutrient limitation of forest growth on wet tropical mountains. *Ecology* 79, 10–22. doi: 10.1890/0012-96581998079[0010:EIONLO]2.0.CO;2

Tateno, R., Tokuchi, N., Yamanaka, N., Du, S., Otsuki, K., Shimamura, T., et al. (2007). Comparison of litterfall production and leaf litter decomposition between an exotic black locust plantation and an indigenous oak forest near Yan'an on the Loess Plateau, China. *For. Ecol. Manage.* 241, 84–90. doi: 10.1016/j.foreco.2006.12.026

Tatsumi, C., Taniguchi, T., Du, S., Yamanaka, N., and Tateno, R. (2019). The steps in the soil nitrogen transformation process vary along an aridity gradient via changes in the microbial community. *Biogeochemistry* 144, 15–29. doi: 10.1007/s10533-019-00569-2

Tatsumi, C., Taniguchi, T., Du, S., Yamanaka, N., and Tateno, R. (2020). Soil nitrogen cycling is determined by the competition between mycorrhiza and ammonia−oxidizing prokaryotes. *Ecology* 101:e02963. doi: 10.1002/ecy.2963

Templer, P. H., Arthur, M. A., Lovett, G. M., and Weathers, K. C. (2007). Plant and soil natural abundance 15N: indicators of relative rates of nitrogen cycling in temperate forest ecosystems. *Oecologia* 153, 399–406. doi: 10.1007/s00442-007-0746-7

Thuan, N. C., Koba, K., Yano, M., Makabe, A., Kính, C. T., Terada, A., et al. (2018). N_2O production by denitrification in an urban river: evidence from isotopes, functional genes, and dissolved organic matter. *Limnology* 19, 115–126. doi: 10.1007/s10201-017-0524-0

Treseder, K., and Allen, M. (2002). Direct nitrogen and phosphorus limitation of arbuscular mycorrhizal fungi: a model and field test. *N. Phytol.* 155, 507–515. doi: 10.1046/j.1469-8137.2002.00470.x

Uscola, M., Villar-Salvador, P., Oliet, J., and Warren, C. R. (2017). Root uptake of inorganic and organic N chemical forms in two coexisting Mediterranean forest trees. *Plant Soil* 415, 387–392. doi: 10.1007/s11104-017-3172-6

Veresoglou, S. D., Shaw, L. J., and Sen, R. (2011). *Glomus intraradices* and *Gigaspora margarita* arbuscular mycorrhizal associations differentially affect nitrogen and potassium nutrition of *Plantago lanceolata* in a low fertility dune soil. *Plant Soil* 340, 481–490. doi: 10.1007/s11104-010-0619-4

Von Holle, B., Neill, C., Largay, E. F., Budreski, K. A., Ozimec, B., Clark, S. A., et al. (2013). Ecosystem legacy of the introduced N_2-fixing tree *Robinia pseudoacacia* in a coastal forest. *Oecologia* 172, 915–924. doi: 10.1007/s00442-012-2543-1

Wang, F., Li, Z., Xia, H., Zou, B., Li, N., Liu, J., et al. (2010). Effects of nitrogen-fixing and non-nitrogen-fixing tree species on soil properties and nitrogen transformation during forest restoration in southern China. *Soil Sci. Plant Nutr.* 56, 297–306. doi: 10.1111/j.1747-0765.2010.00454.x

Wang, L., and Macko, S. A. (2011). Constrained preferences in nitrogen uptake across plant species and environments. *Plant Cell Environ.* 34, 525–534. doi: 10.1111/j.1365-3040.2010.02260.x

Wei, L., Chen, C., and Yu, S. (2015). Uptake of organic nitrogen and preference for inorganic nitrogen by two Australian native Araucariaceae species. *Plant Ecol. Divers.* 8, 259–264. doi: 10.1080/17550874.2013.871656

Wheeler, C. T., Tilak, M., Scrimgeour, C. M., Hooker, J. E., and Handley, L. L. (2000). Effects of symbiosis with Frankia and arbuscular mycorrhizal fungus on the natural abundance of ^{15}N in four species of Casuarina. *J. Exp. Bot.* 51, 287–297. doi: 10.1093/jexbot/51.343.287

Wright, S. J., Yavitt, J. B., Wurzburger, N., Turner, B. L., Tanner, E. V., Sayer, E. J., et al. (2011). Potassium, phosphorus, or nitrogen limit root allocation, tree growth, or litter production in a lowland. *Ecology* 92, 1616–1625. doi: 10.1890/10-1558.1

Yamanaka, N., Hou, Q., and Du, S. (2014). "Vegetation of the Loess Plateau," in *Restoration and Development of the Degraded Loess Plateau, China*, eds A. Tsunekawa, G. Liu, N. Yamanaka, and S. Du (Berlin: Springer), 49–60.

Yang, Y., Tang, M., Sulpice, R., Chen, H., Tian, S., and Ban, Y. (2014). Arbuscular mycorrhizal fungi alter fractal dimension characteristics of *Robinia pseudoacacia* L. seedlings through regulating plant growth, leaf water status, photosynthesis, and nutrient concentration under drought stress. *J. Plant Growth Regul.* 33, 612–625. doi: 10.1007/s00344-013-9410-0

Yoneyama, T., and Kaneko, A. (1989). Variations in the natural abundance of ^{15}N in nitrogenous fractions of komatsuna plants supplied with nitrate. *Plant Cell Physiol.* 30, 957–962.

Zhang, J., Taniguchi, T., Tateno, R., Xu, M., Du, S., Liu, G., et al. (2013). Ectomycorrhizal fungal communities of *Quercus liaotungensis* along local slopes in the temperate oak forests on the Loess Plateau, China. *Ecol. Res.* 28, 297–305. doi: 10.1007/s11284-012-1017-6

Conflict of Interest: The authors declare that the research was conducted in the absence of any commercial or financial relationships that could be construed as a potential conflict of interest.

frontiers
in Forests and Global Change

ORIGINAL RESEARCH
published: 04 March 2021
doi: 10.3389/ffgc.2021.622370

The Impact of Root-Derived Resources on Forest Soil Invertebrates Depends on Body Size and Trophic Position

Sarah L. Bluhm[1]*, Bernhard Eitzinger[1†], Christian Bluhm[1†], Olga Ferlian[1†], Kerstin Heidemann[1], Marcel Ciobanu[2], Mark Maraun[1] and Stefan Scheu[1,3]

[1] Animal Ecology, J.F. Blumenbach Institute of Zoology and Anthropology, University of Göttingen, Göttingen, Germany, [2] Department of Taxonomy and Ecology, Branch of the National Institute of Research and Development for Biological Sciences (NIRDBS) Bucharest, Institute of Biological Research, Cluj-Napoca, Romania, [3] Centre of Biodiversity and Sustainable Land Use, University of Göttingen, Göttingen, Germany

Edited by:
Alberto Canarini,
Kyoto University, Japan

Reviewed by:
Andrey S. Zaitsev,
University of Giessen, Germany
Maria Minor,
Massey University, New Zealand

***Correspondence:**
Sarah L. Bluhm
szieger@gwdg.de

†Present address:
Bernhard Eitzinger,
Chair of Nature Conservation & Landscape Ecology, University of Freiburg, Freiburg, Germany
Christian Bluhm,
Forstliche Versuchs- und Forschungsanstalt Baden-Württemberg, Freiburg, Germany
Olga Ferlian,
Institute of Biology, Leipzig University, Leipzig, Germany;
German Centre for Integrative Biodiversity Research (iDiv) Halle-Jena-Leipzig, Leipzig, Germany

Specialty section:
This article was submitted to Forest Soils, a section of the journal Frontiers in Forests and Global Change

Received: *28 October 2020*
Accepted: *03 February 2021*
Published: *04 March 2021*

Citation:
Bluhm SL, Eitzinger B, Bluhm C, Ferlian O, Heidemann K, Ciobanu M, Maraun M and Scheu S (2021) The Impact of Root-Derived Resources on Forest Soil Invertebrates Depends on Body Size and Trophic Position. Front. For. Glob. Change 4:622370. doi: 10.3389/ffgc.2021.622370

Forest soil food webs have been assumed to be fueled substantially by root-derived resources. However, until today the flux of root-derived resources into soil animals has been investigated virtually exclusively using isotope labeling experiments, whereas studies on the consequences of disrupting the flux of root-derived resources into the soil animal food web are scarce. We here investigated the importance of root-derived resources for a wide range of soil animals by interrupting the resource flux into the soil of different forest types in Central Europe using a trenching experiment. We recorded the abundance of soil animal taxa varying in body size (micro-, meso-, and macrofauna) 1 and 3 years after root trenching, and quantified changes in biomass, species composition, and trophic shift using stable isotopes and NLFA analysis. Among the microfauna groups studied (trophic groups of Nematoda) only the abundance of plant feeding nematodes showed a trend in being decreased by -58% due to root trenching. Major soil mesofauna groups, including Collembola and Oribatida, suffered to a similar extent from root trenching with their abundance and biomass being reduced by about 30–40%. The soil macrofauna groups studied (Diplopoda, Isopoda, Chilopoda, Araneae, Coleoptera) generally were only little affected by root trenching suggesting that they rely less on root-derived resources than micro- and in particular mesofauna. Notably, the community structure of micro-, meso-, and macrofauna was not affected by root trenching. Further, we observed trophic shifts only in 2 out of 10 investigated species with the shifts generally being only minor. The results indicate that soil animal communities are markedly resilient to deprivation of root-derived resources suggesting that links to root-derived resources are non-specific. However, this resilience appears to vary with body size, with mesofauna including both decomposers as well as predators being more sensitive to the deprivation of root-derived resources than microfauna (except for root feeders) and macrofauna. Overall, this suggests that body size constrains the channeling of energy through soil food webs, with root-derived resources in temperate forests being channeled predominantly via soil taxa of intermediate size, i.e., mesofauna.

Keywords: root-derived resources, mesofauna, macrofauna, trenching, forest, soil food web, stable isotopes, NLFA

INTRODUCTION

Interactions between the above- and the belowground components of terrestrial ecosystems are receiving increased attention as they strongly affect carbon (C) cycling (Bardgett and Wardle, 2010). Soil animal communities are linked to the aboveground system via two trophic pathways, i.e., via leaf litter input and root-derived resources (Wardle, 2002; Pollierer et al., 2007). Most litter C is bound in structural compounds and locked up in polymers rich in aliphatic and aromatic compounds (Tan, 2014) not readily available for soil animals without previous digestion by microbial enzymes. In addition, nitrogen (N) concentrations in litter are low (typically only 1–2%) compared to those in animal tissue (ca. 10%) (White, 1993; Vitousek et al., 2002). Nevertheless, leaf litter has been assumed to function as main food resource of soil animals as up to 90% of net primary plant production is entering the soil as detritus (Cebrian, 1999), providing ample resources for the decomposer system. However, recent studies indicate that root-derived resources may surpass those derived from leaf litter in fueling soil animal food webs (Ruf et al., 2006; Pollierer et al., 2007; Eissfeller et al., 2013; Gilbert et al., 2014). Roots release substances actively or passively into the soil (Curl and Truelove, 1986; Jones et al., 2009), which serve as an easily digestible C resource for microorganisms and are preferred compared to recalcitrant leaf litter (Farrar et al., 2003; van Hees et al., 2005). These rhizodeposits consist of sugars, organic acids, amino acids, phenols, and other secondary metabolites, as well as polysaccharides and proteins (Bais et al., 2006). Spatial and temporal patterns of the release of rhizodeposits lead to “hot spots” and “hot moments” in the rhizosphere, triggering the activity of soil microbial-driven processes (Beare et al., 1995; Kuzyakov and Blagodatskaya, 2015). The rhizosphere, thereby, is preferentially colonized by soil organisms such as bacteria, mycorrhizal and saprotrophic fungi and protists, which acquire resources from root deposits. Depending on plant species and season, 10–60% of the photosynthetically fixed C is allocated to roots (Kuzyakov and Domanski, 2000; Litton et al., 2007), and part of this C enters the soil food web via root-feeding species or animals feeding on mycorrhizal fungi and microorganisms that incorporated root-derived C (Ruf et al., 2006; Bonkowski et al., 2009; Högberg et al., 2010).

In forest soils a large fraction of the microbial biomass comprises ectomycorrhizal (ECM) fungi (Högberg and Högberg, 2002; Wallander et al., 2004; Ekblad et al., 2013). They contribute to element cycling, provide N to plants and channel large amounts of plant-derived C into the soil (Treseder et al., 2006; Clemmensen et al., 2013; Ekblad et al., 2013). The production rate of the extra-matrical mycelia of ECM fungi in the upper 10 cm of forest soil has been estimated to be about 160 kg dry matter ha^{-1} y^{-1} (Ekblad et al., 2013) and due to large biomass of ECM fungi it has been suggested as an important food resource for soil invertebrates (Fitter and Garbaye, 1994; Pollierer et al., 2012). However, recent evidence indicates that consumption of ECM fungi by soil invertebrates is limited (Potapov and Tiunov, 2016; Bluhm et al., 2019b).

The flux of root-derived resources through soil food webs and their assimilation by soil animals has been demonstrated by variations in the natural abundance of stable isotopes (Albers et al., 2006; Scheunemann et al., 2015) and isotope labeling experiments (Pollierer et al., 2007, 2009; Eissfeller et al., 2013; Scheunemann et al., 2016; Zieger et al., 2017a) conducted in grasslands (Ostle et al., 2007; Lemanski and Scheu, 2014), arable fields (Albers et al., 2006; Scheunemann et al., 2016), and forests (Pollierer et al., 2007; Zieger et al., 2017b). In long-term (Pollierer et al., 2007, 2009; Eissfeller et al., 2013) and short-term isotope labeling experiments (Scheunemann et al., 2016; Zieger et al., 2017a) it has been shown that root-derived resources are incorporated into the whole soil animal community and channeled across trophic levels. The addition of easily accessible resources, imitating root exudates, has been shown to increase the abundance of some species of soil invertebrates including Lumbricidae, Diplopoda, and Isopoda (Scheu and Schaefer, 1998; Tiunov and Scheu, 2004). However, the effect of deprivation of root-derived resources has only been investigated in Nematoda (Parmelee et al., 1993), as well as in Oribatida and Collembola by girdling of trees (Remén et al., 2008; Malmström and Persson, 2011) and trenching of roots (Siira-Pietikäinen et al., 2001, 2003).

Shortage of resources likely is among the main factors driving the abundance and biomass of soil animals (Scheu and Schaefer, 1998). Resource deprivation, however, also is likely to induce dietary shifts counteracting changes in abundance and biomass. Such dietary shifts may be traced by analyzing variations in stable isotope ratios as well as lipid patterns (Traugott et al., 2013). Variations in stable isotope ratios allow ascribing species to trophic levels as ^{15}N concentrations increase with trophic level due to fractionation processes (Post, 2002; Potapov et al., 2019b). Further, variations in ^{13}C concentrations in soil animal consumers allow to trace changes in the use of C resources (Albers et al., 2006; Pollierer et al., 2009; Potapov et al., 2019b). Neutral lipid fatty acid patterns in consumers allow to trace the incorporation of basal resources, such as bacteria, fungi and plants, into consumers as lipids in the diet are incorporated into consumers without major change (“dietary routing”; Pollierer et al., 2010; Ruess and Chamberlain, 2010).

In the present study, we investigated the effect of deprivation of resource input via tree roots on the abundance, biomass and community structure of micro-, meso-, and macrofauna in forests differing in management intensity, tree species composition and soil type in two regions of Germany using root trenching. To investigate potential shifts on basal resource use, we additionally analyzed stable isotope and neutral lipid fatty acids of abundant soil animal species.

We hypothesized that (1) the importance of root-derived resources varies with soil animal body size, with more pronounced effects on the abundance, biomass and community structure of fungal feeding micro- and mesofauna (relying heavily on root-derived resources) than macrofauna (relying more heavily on litter resources), (2) deprivation of fresh root-derived resources detrimentally affects abundance and biomass of soil animal communities with the detrimental effects increasing over time, (3) the response of microbivore soil micro- and mesofauna mirrors that of microbial biomass (and therefore varies more between regions than forest types; Bluhm et al., 2019a), and (4) soil invertebrates switch diet in response to shortage of root-derived resources, which is reflected in changes in ^{13}C and ^{15}N stable isotope values and neutral lipid fatty acid patterns.

MATERIALS AND METHODS

Study Sites and Experimental Set-Up

The experiment was established in two regions of Germany at sites of the "Biodiversity Exploratories," a large-scale and long-term biodiversity project (Fischer et al., 2010)[1]. Schorfheide-Chorin (hereafter *Schorfheide*) is located in the lowlands of Northeastern Germany (3–140 m a.s.l.) and characterized by postglacial geomorphological structures, and the Hainich-Dün (hereafter *Hainich*), located in the uplands of Central Germany (285–550 m a.s.l.). Mean annual temperatures at Schorfheide and Hainich are 8.0–8.5 and 6.5–8.0°C, and mean annual precipitation 500–600 and 500–800 mm, respectively. The forests stock on glacial till in the Schorfheide with the main soil type being Cambisol and in the Hainich on Triassic limestone with the main soil type being Luvisols with soil pH averaging 3.00 ± 0.19 and 4.59 ± 0.67, respectively. For more details on the study sites see Fischer et al. (2010) and Klarner et al. (2014). In each of the two regions four different forest types were selected: (1) managed coniferous forests with Norway spruce (*Picea abies*) in the Hainich ("spruce") and Scots pine (*Pinus sylvestris*) in the Schorfheide ("pine"), (2) 30 years old managed beech (*Fagus sylvatica*) forests ("young beech"), (3) 70 years old managed beech forests ("old beech"), and (4) unmanaged natural beech forests left out of management for at least 60 years with some trees being 120–150 years old ("unmanaged beech"). Beech forests were dominated by *F. sylvatica*, interspersed with ash (*Fraxinus excelsior*), and sycamore (*Acer pseudoplatanus*). Each forest type was replicated four times per region, resulting in 32 plots. The minimum distance between plots was 500 m.

Establishment and Maintenance of Root-Trenching Plots

In each of the 32 plots, one "trenched" and one "control" subplot 1–2 m apart from each other of 120 × 120 cm was established between September and October 2011. In the trenched subplots trenches were cut into soil to a depth of 40–50 cm using a chainsaw, thereby cutting all tree roots. To prevent re-colonization of the plots by tree roots, polyethylene barriers (120 × 60 × 0.5 cm) were inserted into the trenches on each of the four sides of the plot. In addition, aluminium linings were inserted at the edges to close the gap between adjacent barriers. Polyethylene barriers extended ca. 10 cm above the ground to restrict animal migrations between the trenched plots and the surrounding. To control for potential side effects of aboveground parts of the barriers, control plots, which were established in close vicinity of the treatment plots, were also equipped with respective barriers aboveground.

At regular intervals during the growth period above-ground parts of herbaceous plants and grasses in trenched and control plots were removed to minimize input of root-derived resources from understory plants. Soil moisture was measured gravimetrically from soil cores and water was added to control plots equalizing the amount of water in the upper 10 cm of the soil in control and trenched plots, for details see Bluhm et al. (2019a).

Sampling

Soil samples for meso- and macrofauna were taken from each control and trenched plot after one (October 2012) and three (October 2014) years. Soil mesofauna was extracted from soil cores of a diameter of 5 cm (one core per subplot). For soil macrofauna soil cores of a diameter of 20 cm were taken (one core per subplot). The litter layer and upper 5 cm of the soil from each soil core were extracted separately by a heat gradient for macrofauna (Kempson et al., 1963) and mesofauna (Macfadyen, 1961). Extracted animals were stored in 70% ethanol, sorted and identified to order level. Soil mesofauna samples included springtails (Collembola), mites (Oribatida, Mesostigmata), proturans (Protura), diplurans (Diplura), and symphylans (Symphyla). Diplura and Symphyla were taken from the 20 cm soil cores for macrofauna as their abundance in the 5 cm cores was too low for statistical analysis. The macrofauna included millipedes (Diplopoda), woodlice (Isopoda), spiders (Araneae), centipedes (Chilopoda), and beetles (Coleoptera; adults and larvae).

Soil samples for nematode extraction (one core per subplot) were taken after 3 years of the experiment (October 2014) using a steel corer (2.5 cm diameter, 10 cm deep). Nematodes were extracted by modified Baermann method, see Ruess (1995), and transferred into 3%-formaldehyde solution. Nematodes in vials were concentrated by removing part of the formaldehyde solution. At least 100 well-preserved specimens (if available in the sample) were randomly selected and identified to genus (adults and most of the juveniles) or family level (juveniles) at 400 × magnification using a Leica DMI 4000B light microscope. Nematode taxa were classified according to Bongers (1994) and then ascribed to trophic groups (Yeates et al., 1993; Bongers and Bongers, 1998; Okada et al., 2005), ordered according to the colonization–persistence gradient (c–p values) (Bongers, 1990; Bongers and Bongers, 1998) and assigned to trophic groups (Bongers and Bongers, 1998; Ferris et al., 2001).

In addition to the soil core sampling, in October 2015 Lumbricidae were collected from an area of 0.25 m^2 from each subplot by using mustard solution (Eisenhauer et al., 2008). The solution consisted of 100 g mustard powder (Semen Sinapis plv.; CAELO, Cesar & Loretz GmbH, 40721 Hilden, Germany) dissolved in 10 l water. Before applying the solution to the plots, the litter layer was removed and checked for earthworm specimens. Five liters of the solution were spilled evenly on the area, which was repeated after 15 min. Emerging Lumbricidae were hand-collected and placed into ethanol containing 5% formalin for preservation. For the analysis of trophic changes of soil animals, additional soil and litter samples were taken in

---

[1] www.biodiversity-exploratories.de

autumn 2015 and the animals were extracted by heat (Kempson et al., 1963). To obtain enough animal tissue for NLFA analysis, we sampled litter and soil from a large area of each of the plots at the end of the experiment and extracted the animals by heat (see above). These samples were stored in glycerin at −10°C for later NLFA analysis (Zieger and Scheu, 2018).

For the sampling in 2014 abundant taxa were identified to species level and species richness and biomass was calculated. Collembola and Oribatida were identified to species level using Weigmann (2006) and Hopkin (2007), respectively. Collembola were ascribed to ecological groups using Gisin (1943), Isopoda were determined using Schaefer et al. (2018), Diplopoda using Blower (1985) and Chilopoda using Latzel (1880), Koren (1992), and Barber (2008). Lumbricidae species were identified to species level using Sims and Gerard (1985).

Biomass Calculation

The biomass of Oribatida (dry weight) was calculated using regression model 4 from Caruso and Migliorini (2009) based on species-specific mean lengths and widths as given in Weigmann (2006). For Collembola, biomass (fresh weight) was calculated using the mean length of species in millimeter as given in Hopkin (2007) and the formula $\log(M_{fw}) = 1.339 + 1.992 \log(\text{length})$, with M_{fw} being the fresh weight in microgram (Mercer et al., 2001). Fresh weight was converted to dry weight by using the formula $\log(M_{dw}) = -0.5499 + 0.9402 \log(M_{fw})$ as given in Mercer et al. (2001). For Myriapoda and Isopoda the length and maximum width of all individuals were measured. For the calculation of the biomass of Geophilomorpha and Scolopendromorpha the formula given in Klarner et al. (2017) was used. For Polydesmida, Isopoda, Lithobiomorpha model 1 given in Sohlström et al. (2018) was used. For other Diplopoda the formula given in Sprengel (1986) was used. Lumbricidae were weighed using a scale (Sartorius Secura 125-1S, Göttingen, Germany). To convert fresh weight to dry weight of Polydesmida, Isopoda, *Trichoniscus* and Lithobiomorpha the following factors were used: 0.42, 0.34, 0.42, and 0.29, respectively (S. Bluhm, unpubl. data).

Stable Isotope Analysis

To investigate diet shifts we selected abundant macrofauna species (one Isopoda species and four Lumbricidae taxa). For Isopoda *Trichoniscus pusillus* from the Hainich was selected including specimens from each of the two beech forest types (beech old and beech natural); the beech young and spruce forest could not be included as *T. pusillus* was rare in these forest types. For Lumbricidae *Aporrectodea* sp. and *Octolasion lacteum* in the Hainich, and *Dendrobaena octaedra* and *Lumbricus rubellus* in the Schorfheide were used including specimens from each of the four forest types; only these species were present in sufficient numbers to allow stable isotope analysis. For the analysis appropriate amounts of animal tissue (600–1,000 μg dry weight) were transferred into tin capsules using a Sartorius Cubis scale. For Isopoda whole animals were analyzed; for Lumbricidae the first sixteen segments of each worm were detached, freeze-dried and weighed into tin capsules.

Samples of *T. pusillus* were analyzed using a system consisting of an elemental analyzer (Euro EA 3000, EuroVector S.p.A, Milano, Italy) and a mass spectrometer (Delta V Plus, Thermo Electron, Bremen, Germany) coupled by a Conflo IV interface (Thermo Electron Corporation, Bremen, Germany). Lumbricidae were measured by a coupled system consisting of an elemental analyzer (NA1110, CE-Instruments, Rodano, Milano, Italy) and a mass spectrometer (Delta Plus, Thermo Electron, Bremen, Germany) coupled by a Conflo III interface (Thermo Electron Corporation, Bremen, Germany). The computer controlled systems allow on-line measurement of stable isotopes (^{13}C, ^{15}N) (Reineking et al., 1993; Werner et al., 1999; Langel and Dyckmans, 2014). Their abundance was expressed using the δ notation with $\delta^{13}C$ and $\delta^{15}N$ (‰) = $(R_{sample} - R_{standard})/R_{standard} \times 1{,}000$. R_{sample} and $R_{standard}$ represent the $^{13}C/^{12}C$ and $^{15}N/^{14}N$ ratios of samples and standard, respectively. For ^{13}C Vienna PD belemnite (V-PDB) served as the primary standard. For ^{15}N air served as the primary standard and acetanilide (C_8H_9NO; Merck, Darmstadt, Germany) for internal calibration.

Neutral Lipid Fatty Acid Analysis

For the NFLA analysis we used species of different trophic levels (decomposers and predators) and body size (meso- and macrofauna) from samples after 4 years of root trenching (2015). Only abundant species were included as ca. 600 μg dry weight was needed for NLFA analysis. The species/taxa included one mesofauna decomposer (Collembola: Onychiuridae), one macrofauna decomposer (*T. pusillus)*, one mesofauna predator (Uropodina: *Uropoda cassidea)*, and three macrofauna predators (Chilopoda: *Strigamia acuminate* and *Schendyla nemorensis*, and Pseudoscorpionida: *Neobisium carcinoides)*. Animals were crushed and fatty acids were extracted by shaking in 5 ml single phase extraction solvent (chloroform - methanol - 0.05 M phosphate buffer, 1:2:0.8, pH 7.4) overnight, for details see Haubert et al. (2004). Neutral lipid fatty acids were dried in a rotation vacuum concentrator, saponified, methylated, and washed following the procedures given for the Sherlock Microbial Identification System (MIDI Inc., Newark, NJ, United States; see Ruess et al., 2002). Then, the lipid fraction was transferred into test tubes and stored at −20°C until analysis via gas chromatography. The gas chromatograph (CLARUS 500, Perkin Elmer, Waltham, United States) was equipped with a flame ionization detector and an Elite-5 capillary column (30 m × 0.25 mm i.d., 0.25 μm film thickness; Perkin Elmer, Waltham, United States). Fatty acid methyl esters (FAMEs) were identified by comparing retention times of samples with standard mixtures composed of 37 different FAMEs ranging from C11 to C24 and bacterial FAMEs, for details see Ferlian and Scheu (2013). NLFAs are given in percentages of total fatty acids extracted from the respective sample. The following FAs served as biomarkers for bacteria: i15:0, a15:0, i16:0, i17:0, cy17:0 and cy19:0, and 16:1ω7 and 18:1ω7 (Ruess and Chamberlain, 2010). The 18:1ω9-to-18:2ω6,9 FA ratio was used as indicator for the relative contribution of plants as compared to fungi to the diet of the animals (Ruess et al., 2007).

Statistical Analyses

Statistical analyses were performed using R v 4.0.2 (R Core Team, 2020). To inspect for the effect of trenching (control, trenching), forest type (beech old, beech young and beech natural, conifer), region (Schorfheide, Hainich) and sampling date (2012, 2014) on the abundance of the investigated order-level animal taxa, linear mixed effects models (LME) in the "nlme" package (Pinheiro et al., 2013) were conducted with the random term sampling date nested in plot identity (Plot ID/Sampling date) to account for control and trenched subplots being nested in Sampling subplots and Plot ID. To inspect for the effect of trenching, forest type and region on biomass and abundance of the investigated taxa and abundant species after 3 years of trenching (2014 data only) linear mixed effects models (LME) in the "nlme" package were conducted with the random term plot identity (Plot ID) to account for control and trenched subplots being nested in Plot ID. If necessary data were log(x + 1) transformed to improve homogeneity of variances. The effect of trenching, forest type and region on the community composition of each Collembola, Oribatida, macrofauna decomposers, and macrofauna predators from the 2014 sampling were analyzed using pManova (permutation multivariate analysis of variance) of species scores from non-metric multidimensional scaling (NMDS). NMDS was carried out using the metaMDS function in the "vegan" package (Oksanen et al., 2018). pManova was performed with Euclidean distance matrices and type II sum of square tests using the adonis.II function in the "RVAideMemoire" package (Hervé, 2020) with restricted permutation within Plot ID using strata with 9,999 permutations. To correct for multiple testing of the abundance, biomass species richness, and functional groups of Nematoda we used the Benjamini-Hochberg (BH) correction (Benjamini and Hochberg, 1995) with a false discovery rate of 5% for each of the four response variables. Corrected *p*-values were calculated using method "BH" in the "p.adjust" function in R.

To analyze if root trenching affected the trophic niche of soil animal species, the proportion of fungal marker, plant marker and sum of bacterial marker fatty acids in Onychiuridae, *T. pusillus*, *U. cassidea*, *S. acuminata* and *N. carcinoides* as well as ^{13}C and ^{15}N signatures of Lumbricidae and *T. pusillus* were analyzed using linear mixed effects models (LME) in the "nlme" package with the random term plot identity (Plot ID).

To analyze if root trenching and forest type affected the NLFA composition of each Onychiuridae, *T. pusillus*, *U. cassidea*, *S. acuminata*, and *N. carcinoides* of the 2015 sampling DFA after NMDS was carried out in Statistica version 12 (Dell Inc., Tulsa, OK, United States). Data provided in the text represent means and standard deviations.

RESULTS

Abundance and Biomass

Macrofauna. Root trenching did not affect the sum of soil macrofauna abundance (**Supplementary Table S1**). Only the abundance of Chilopoda and Coleoptera larvae was significantly lower in trenched plots, each by −23% (**Figure 1C**).

After 3 years, the biomass of the three macrofauna taxa (Isopoda, Chilopoda, Diplopoda) and that of Lumbricidae was not significantly affected by root trenching (**Figure 2** and **Supplementary Table S2**). However, the abundance of the decomposer species *Allajulus nitidus* (Diplopoda) [$F_{(1,25)} = 5.67$, $p = 0.025$] and the predator species *Monotarsobius crassipes* (Chilopoda) [$F_{(1,25)} = 4.68$, $p = 0.040$] was significantly lower in trenched plots by more than −50% (8.7 ± 4.8 and 7.7 ± 3.6 ind. m^{-2}, respectively) compared to the control (18.6 ± 6.5 and 17.7 ± 6.2 ind. m^{-2}, respectively). By contrast, the abundance of the decomposer species *T. pusillus* (Isopoda) was higher in trenched plots by +30% (259 ± 98.5 ind. m^{-2}) compared to the control (196 ± 93.4 ind. m^{-2}), but this was only marginally significant [$F_{(1,29)} = 3.36$, $p = 0.0643$].

Mesofauna. Irrespective of sampling date, total mesofauna abundance was significantly lower in trenched plots by −31%, with the abundance of Oribatida and Collembola being lowered to a similar extent (−29 and −22%, respectively) (**Figure 1A** and **Supplementary Table S1**). The abundance of Diplura was lower in trenched plots (−40%), but also their overall density was much lower than that of Oribatida and Collembola (**Figure 1B**). The abundance of Protura also was lower in trenched plots (**Figure 1B**). For Pauropoda the effect of root trenching depended on region, in the Hainich the abundance was lower in trenched plots by −85% while in the Schorfheide the abundance was similar in trenched and control plots, but this was only marginally significant after BH correction (**Supplementary Table S1**). Generally, the effect of root trenching did not vary significantly with forest type.

In addition to the significantly lower abundance of Collembola in trenched plots (−34%; **Figure 1A** and **Supplementary Table S1**) after 3 years Collembola biomass also was lower in trenched compared to control plots by −20% (**Figure 2** and **Supplementary Table S2**). The lower biomass of Collembola in trenched plots was mainly due to hemiedaphic Collembola with their biomass in trenched plots (70.8 ± 66.1 mg m^{-2}) being lower by −42% compared to control plots [40.7 ± 61.1 mg m^{-2}; $F_{(1,27)} = 11.95$, $p = 0.002$]. Similarly, the lower abundance of Oribatida in trenched plots (−36%; **Figure 1A** and **Supplementary Table S1**) was associated by −30% lower biomass of Oribatida in trenched compared to control plots, but this was only marginally significant (**Figure 2**).

In addition to abundance and biomass, in Oribatida also species richness was lower in trenched (13.4 ± 4.6 species per soil core) compared to control plots (15.6 ± 4.5 species per soil core; **Supplementary Table S2**), but this was only marginally significant after BH correction. By contrast, although the abundance of Collembola and Oribatida was reduced in trenched plots to a similar extent, in Collembola species richness did not change significantly with root trenching.

Microfauna. After 3 years, the abundance of plant feeding nematodes in trenched plots (44,029 ± 21,519 ind. m^{-2}) was lower by −58% than in control plots (103,769 ± 34,519 ind. m^{-2}; **Supplementary Table S2**), but this was only marginally significant after BH correction. Nematodes feeding on fungi generally did not significantly respond to root trenching.

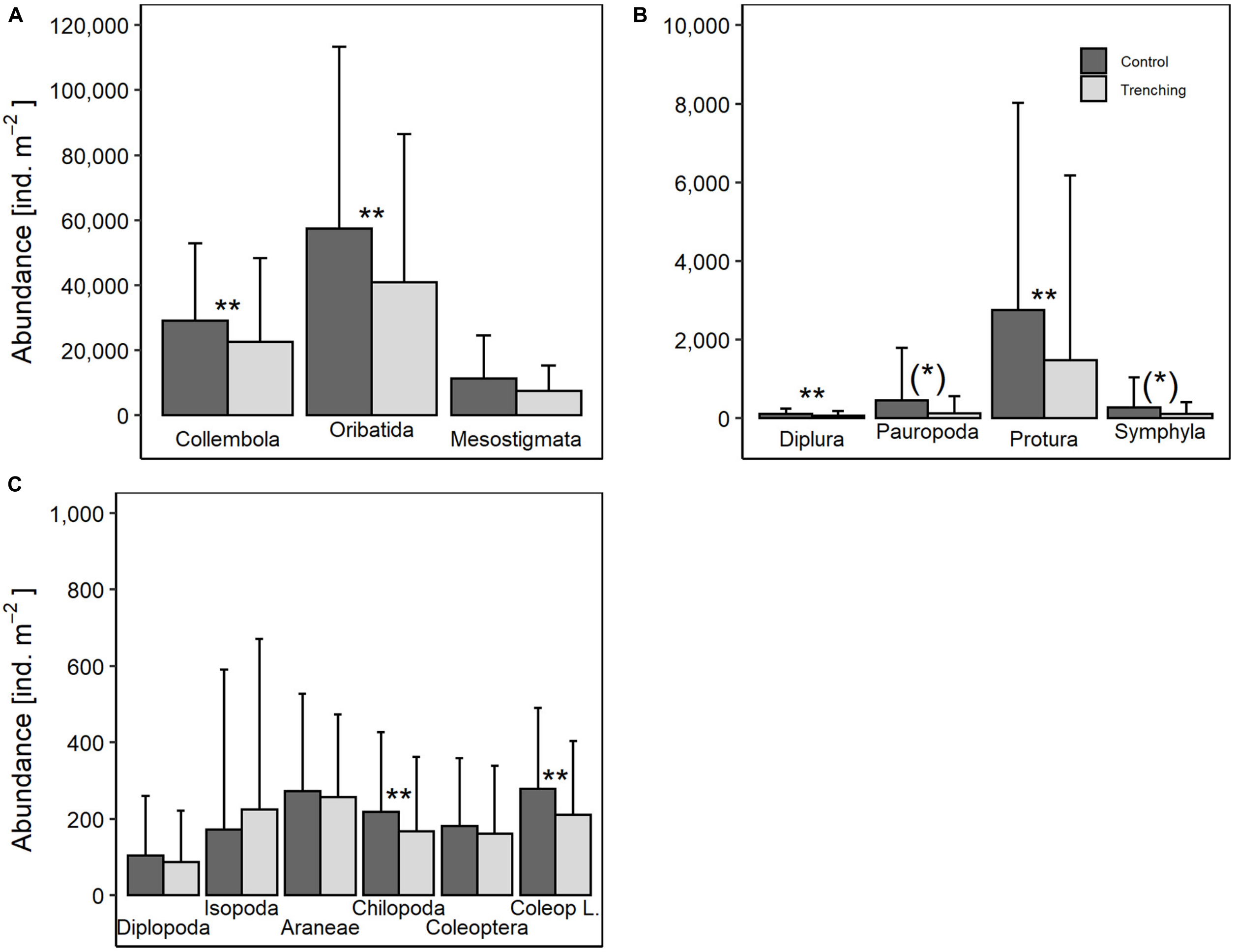

FIGURE 1 | Effect of root trenching on the abundance of mesofauna **(A,B)** and macrofauna taxa **(C)**; note different scale of y-axis in **(A,B)**; means and standard deviation pooled for forest type, region and sampling date. (*)$p < 0.1$; *$p < 0.05$; **$p < 0.01$; for statistical analyses see **Supplementary Table S1**.

Community Structure

Macrofauna community composition did not change significantly with root trenching [pManova; $F_{(1,59)} = 0.99$, $p = 0.12$; **Figure 3A**], and this was true for both macrofauna decomposers as well as macrofauna predators. Similarly, neither the community structure of Oribatida [pManova; $F_{(1,63)} = 0.50$, $p = 0.49$; **Figure 3B**] nor that of Collembola [pManova; $F_{(1,63)} = 1.17$, $p = 0.25$; **Figure 3C**] nor that of Nematoda [pManova; $F_{(1,31)} = 0.36$, $p = 0.91$; **Figure 3D**] was significantly affected by root trenching.

Trophic Shifts

The Δ^{13}C signature of Lumbricidae was not significantly affected by root trenching (**Figure 4A**). By contrast, the Δ^{15}N signature of two endogeic Lumbricidae taxa (*O. lacteum* and *Aporrectodea* sp.) were higher in trenched plots [$F_{(1,4)} = 4.63$, $p = 0.098$ and $F_{(1,4)} = 4.63$, $p = 0.098$, respectively; **Figure 4B**]. Further, Δ^{13}C values of *T. pusillus* in natural beech forests were higher in trenched compared to control plots, while the Δ^{13}C values in old beech forests were lower in trenched compared to control plots [significant Trenching × Forest type interaction; $F_{(1,6)} = 10.3$, $p = 0.018$; **Figure 4C**]. By contrast, Δ^{15}N values of *T. pusillus* were not significantly affected by root trenching (**Figure 4D**).

In addition to stable isotopes, root trenching also affected the fatty acid patterns of consumers. In *T. pusillus* the proportion of the fungal biomarker fatty acid 18:2ω6,9 was significantly lower in trenched (18.59 ± 4.71%) compared to control plots (23.87 ± 7.25%) [$F_{(1,8)} = 7.25$, $p = 0.027$]. Fatty acid patterns in the other analyzed macro- and mesofauna taxa were not significantly affected by root trenching.

DISCUSSION

Body Size-Compartments

Macrofauna. Supporting our hypothesis (1), root trenching detrimentally affected abundance and biomass of soil invertebrates with the effects varying with body size. The response of macrofauna groups varied, but with an average

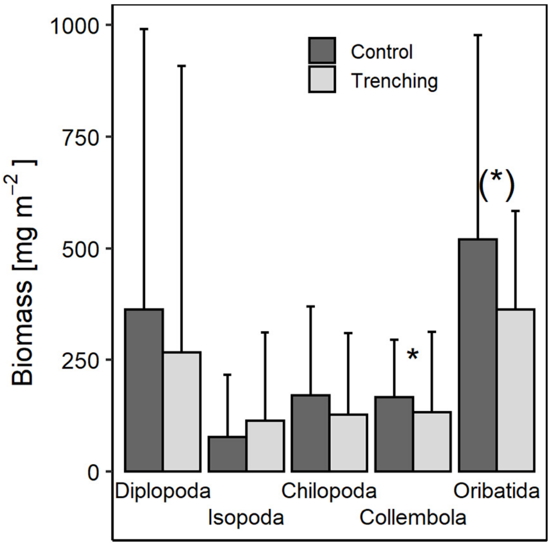

FIGURE 2 | Effect of root trenching on the biomass of soil macrofauna (Diplopoda, Isopoda, and Chilopoda) and mesofauna (Collembola and Oribatida) 3 years after root trenching; means and standard deviation pooled for forest type and region. (*)$p < 0.1$; *$p < 0.05$; for statistical analyses see **Supplementary Table S2**.

reduction in abundance of −4% in trenched plots the response was less pronounced than in mesofauna. This indicates that macrofauna more intensively integrates different energy channels than mesofauna (Wolkovich, 2016), and supports the suggestion that soil food webs are size-compartmentalized with the use of basal resources, such as bacteria, fungi and plant litter, varying with body size (Potapov et al., 2019a). Notably, the abundance and biomass of macrofauna decomposer groups (Diplopoda, Isopoda) were not significantly reduced by root trenching, indicating that they predominantly feed on litter resources as proposed earlier (Scheu and Falca, 2000; Semenyuk and Tiunov, 2011). Presumably, this is due to the ability of large detritivores to chew up leaf litter material and to use structural organic matter compounds.

Interestingly, in Isopoda the abundance of *T. pusillus* increased by 30% by root trenching, suggesting that they benefited from the deprivation of root-derived resources. This either reflects that they benefited from decomposing roots cut by trenching the plots or from the decrease in the abundance of Collembola and Oribatida, implying that certain macrofauna detritivore species are competing for food resources with mesofauna detritivores. However, as the biomass of *T. pusillus* was not affected by root trenching, the overall resources exploited presumably changed little, but trenched plots contained more small *T. pusillus* (mean dry weight of 0.26 mg in trenched plots compared to 0.28 mg in the control), suggesting that recruitment of juveniles was increased. In Diplopoda, only the density of *A. nitidus* was reduced after 3 years of root trenching. *A. nitidus* has been classified as secondary decomposer (Scheu and Falca, 2000) feeding on microorganisms and their remains after death, being an exception compared to other Diplopoda species, which have a narrow trophic niche and predominantly feed on litter and function as primary decomposers (Semenyuk and Tiunov, 2011).

Root trenching also negatively affected the abundance of two macrofauna predators, Chilopoda and Coleoptera larvae (comprising mainly of Staphylinidae), indicating that shortage of belowground resources propagates to higher trophic levels (Ruf et al., 2006; Pollierer et al., 2007). Overall, this argues for the predominance of bottom-up forces and suggests that macrofauna predators rely on mesofauna prey suffering most from deprivation of root-derived resources (see below). Although Chilopoda suffered little from root trenching, the abundance of *M. crassipes* strongly declined in root trenched plots after 3 years. Again, this supports size-compartmentalization of soil food webs. *M. crassipes* is a small Chilopoda species exploiting prey from deeper litter layers than other Chilopoda species (Günther et al., 2014; Potapov et al., 2019a), and these prey species are likely to heavily rely on root-derived resources channeled into the soil food web via bacteria as proposed earlier (Ferlian and Scheu, 2013). The abundance and biomass of Lumbricidae was also not significantly affected by root trenching even though soil microbial biomass in trenched plots was reduced by 25% (Bluhm et al., 2019a). This supports earlier findings suggesting that soil microbial biomass is a poor predictor for resource availability for (predominantly endogeic) Lumbricidae (Tiunov and Scheu, 2004), and that endogeic Lumbricidae feed little on root-derived resources (Albers et al., 2006).

Mesofauna. The abundance of soil mesofauna strongly and uniformly declined by root trenching (on average by −31%). This is in line with results of the study of Siira-Pietikäinen et al. (2001) and underlines the importance of root-derived resources for this size-compartment of the soil animal food web. All mesofauna detritivore taxa except Thysanoptera declined due to root trenching. Two pathways might have contributed to this reduction: reduced feeding on living roots and root hairs in particular by Diplura and some Collembola species (Gunn and Cherrett, 1993; Endlweber et al., 2009), or reduced feeding on fungi and bacteria associated with living roots in particular by Collembola, Oribatida and Protura (Fujii et al., 2016; Bluhm et al., 2019b). Indeed, root trenching in our study reduced vital fine roots by 50%, and also bacterial and fungal PLFA markers declined due to root trenching (Bluhm et al., 2019a). For Collembola, Oribatida and Protura it has been shown before that they rely on root-derived resources (Siira-Pietikäinen et al., 2001; Remén et al., 2008; Bluhm et al., 2019b). The fact that the abundance of both Oribatida and Collembola were reduced to a similar level indicates that both taxa are using root-derived resources to a similar extent. Notably, only hemiedaphic Collembola species were significantly affected by root trenching indicating that the importance of root-derived resources varies among ecological groups of Collembola. Supporting this conclusion, recent labeling studies also found ecological groups of Collembola to vary in their use of root-derived resources (Li et al., 2020).

Similar to mesofauna detritivores also mesofauna predators declined due to root trenching. The abundance of Diplura shown to live as predators by stable isotope studies

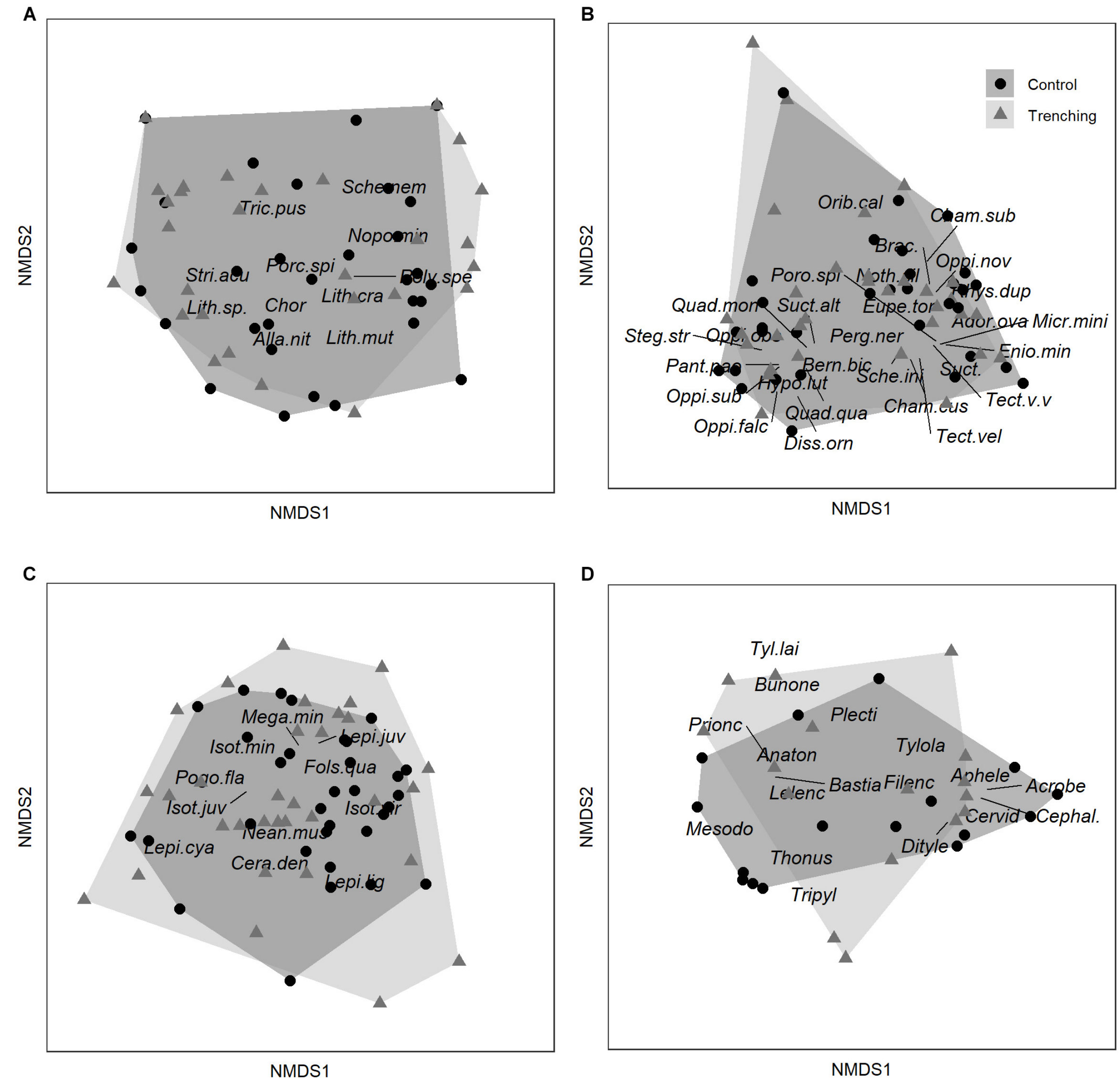

FIGURE 3 | NMDS (non-metric multidimensional scaling) of macrofauna (Diplopoda, Isopoda, Chilopoda) **(A)**, Oribatida **(B)**, Collembola **(C)**, and Nematoda communities **(D)** in control (Control) and root trenched plots (Trenching), only species significantly correlating with one of the first two NMDS axes shown. **(A)**: Macrofauna (Alla.nit, *Allajulus nitidus*; Chor, Chordeumatidae; Lith.sp., *Lithobius* sp.; Lith.cra, *Lithobius crassipes*; Lith.mut, *Lithobius mutabilis*; Nopo.min, *Nopoiulus minutus*; Poly.spe, *Polydesmus* sp.; Porc.spi, *Porcellio spinicornis*; Sche.nem, *Schendyla nemorensis*; Stri.acu, *Strigamia acuminata*; Tric.pus, *Trichoniscus pusillus*); **(B)**: Oribatida (Ador.ova, *Adoristes ovatus*; Bern.bic, *Berniniella bicarinata*; Brac., Brachychthoniidae; Cham.cus, *Chamobates cuspidatus*; Cham.sub, *Chamobates subglobulus*; Diss.orn, *Dissorhina ornata*; Enio.min, *Eniochthonius minutissimus*; Eupe.tor, *Eupelops torulosus*; Hypo.lut, *Hypochthonius luteus*; Micr.mini, *Microtritia minima*; Noth.sil, *Nothrus silvestris*; Oppi.falc, *Oppiella falcata*; Oppi.nov, *Oppiella nova*; Oppi.obs, *Oppiella obsoleta*; Oppi.sub, *Oppiella subpectinata*; Orib.cal, *Oribatella calcarata*; Pant.pao, *Pantelozetes paolii*; Perg.ner, *Pergalumna nervosa*; Poro.spi, *Porobelba spinosa*; Quad.mon, *Quadroppia monstruosa*; Quad.qua, *Quadroppia quadricarinata*; Rhys.dup, *Rhysotritia duplicata*; Sche.ini, *Scheloribates initialis*; Steg.str, *Steganacarus striculus*; Suct.alt, *Suctobelba altvateri*; Suct., *Suctobelbella* spp.; Tect.vel, *Tectocepheus velatus* sp.; Tect.v.v, *Tectocepheus velatus velatus*); **(C)**: Collembola (Cera.den, *Ceratophysella denticulata*; Fols.qua, *Folsomia quadroculata*; Isot.vir, *Isotoma viridis*; Isot.juv, Isotomidae juvenil; Isot.min, *Isotomiella minor*; Lepi.cya, *Lepidocyrtus cyaneus*; Lepi.juv, *Lepidocyrtus* juvenil; Lepi.lig, *Lepidocyrtus lignorum*; Mega.min, *Megalothorax minimus*; Nean.mus, *Neanura muscorum*; Pogo.fla, *Pogonognathellus flavescens*); **(D)**: Nematoda (Acrobe, *Acrobeloides*; Anaton, *Anatonchus*; Aphele, Aphelenchoides; Bastia, *Bastiania*; Bunone, *Bunonema*; Cephal., Cephalobidae; Cervid, *Cervidellus*; Dityle, *Ditylenchus*; Filenc, *Filenchus*; Lelenc, *Lelenchus*; Mesodo, *Mesodorylaimus*; Plecti, Plectidae; Prionc, *Prionchulus*; Thonus, *Thonus*; Tripyl, *Tripyla*; Tyl.lai, *Tylencholaimus*; Tylola, *Tylolaimophorus*).

(Scheu and Falca, 2000; Albers et al., 2006) declined by −40% and the density of Mesostigmata showed a decreasing trend (−33%; **Figure 1A**) indicating that they suffered from the decline in mesofauna prey.

Microfauna. In contrast to our hypothesis (1), root trenching did not significantly reduce the abundance of fungal feeding Nematoda. This suggests that either fungal feeding Nematoda do not feed on ECM fungi or they were

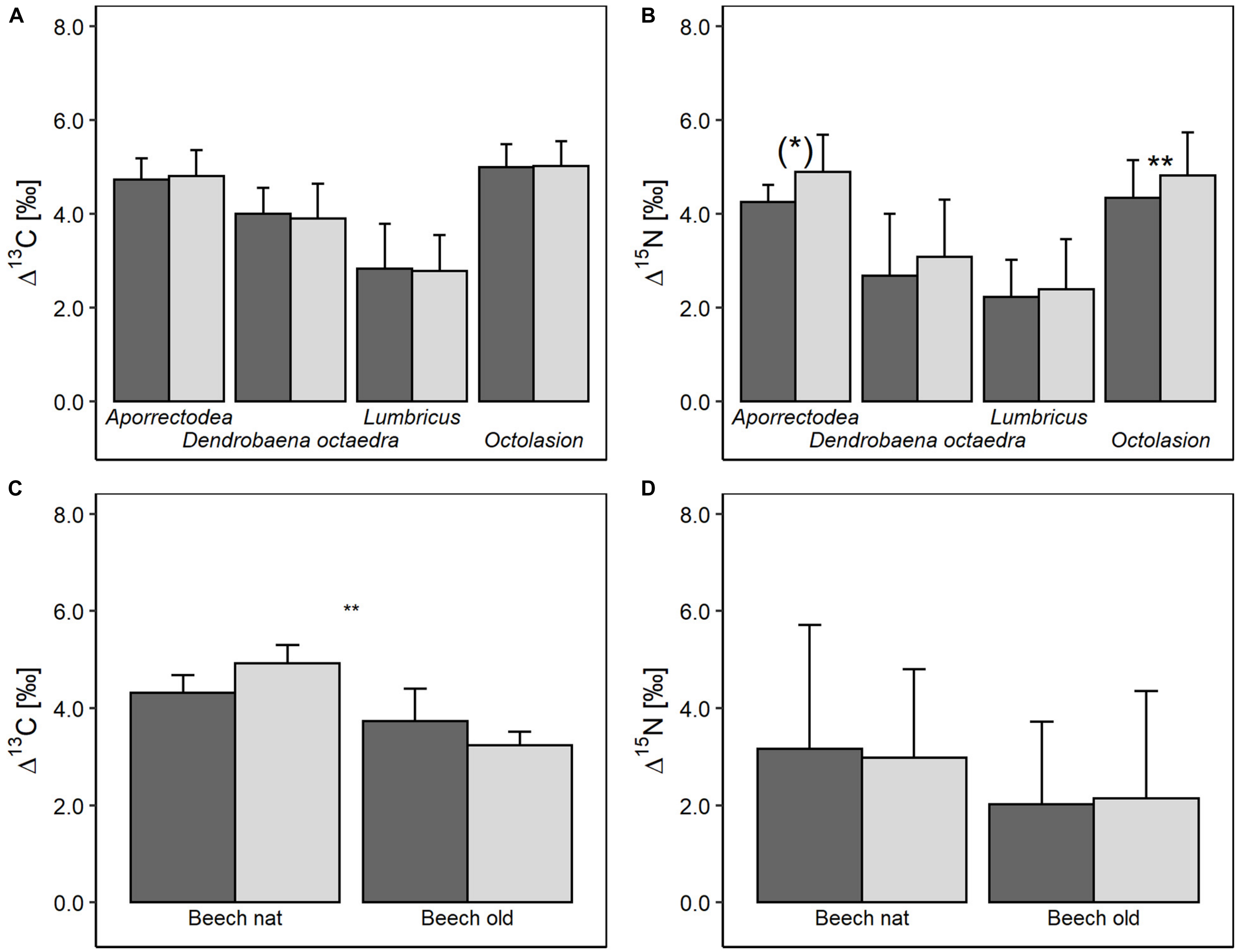

FIGURE 4 | Effect of root trenching on stable isotope values of ^{13}C **(A)** and ^{15}N **(B)** of Lumbricidae taxa, and on stable isotope values of ^{13}C **(C)** and ^{15}N **(D)** of the isopod *Trichoniscus pusillus* in natural (Beech nat) and 70 years old beech stands (Beech old). Stable isotope values are calibated against stable isotope values of litter in the respective plot; means and standard deviation. (*)$p < 0.1$; **$p < 0.01$.

able to compensate for the reduction in ECM fungi by switching to feeding on saprotrophic fungi. The findings are in contrast to results of the study of Li et al. (2009), who found the abundance of fungivorous Nematoda to be reduced after tree girdling. However, plant feeding Nematoda showed a trend of being reduced by root trenching, on average by −58%, presumably due to reduced vital root biomass and the inability of root feeding nematodes to switch to other food resources.

Community Structure

In contrast to our hypothesis (1), the community composition (only analyzed after 3 years of root trenching, see "Materials and Methods") was not affected in macrofauna (Isopoda, Diplopoda, Chilopoda), mesofauna (Oribatida and Collembola), and microfauna (Nematoda). Similarly, Siira-Pietikäinen et al. (2001) documented that, despite the abundance of Oribatida decreased, the community structure remained unaffected due to exclusion of roots in a coniferous forest in Finland. The lack of changes in community structure due to root trenching indicates that virtually all analyzed species suffered to a similar extent from the deprivation of root-derived resources or were independent of it.

Temporal Changes

Contrasting our hypothesis (2), detrimental effects did not increase with time after root trenching. This is consistent with the response of microorganisms to root trenching where the effect even decreased with time suggesting that they compensated for the deprivation of root-derived resources (Bluhm et al., 2019a). Presumably, decomposing roots (and associated mycorrhizal fungi) cut by trenching increased the availability of resources to microorganisms and this may also have alleviated the detrimental effect of root trenching for soil animals later in the experiment (Hagerman et al., 1999).

Variations With Forest Type and Region

Supporting our hypothesis (3), the effect of root trenching generally did not vary with forest type and only little with region. The stronger reduction in microbial biomass due to root trenching in the Hainich compared to the Schorfheide (Bluhm et al., 2019a) was only paralleled in one of the studied taxa of soil animals, i.e., Pauropda. Soils in the Hainich are rich in nutrients and characterized by shallow organic layers, while those in the Schorfheide are poor in nutrients and characterized by thick organic layers. Unfortunately, however, information on food resources of Pauropoda is lacking almost entirely (Starling, 1944; Voigtländer et al., 2016) and the parallel response to microorganisms may not necessarily have been due to trophic interactions.

Trophic Shifts

In contrast to our hypothesis (4), root trenching little affected the composition of food resources of soil animals as indicated by stable isotope and NLFA analysis. The decomposer species *T. pusillus* (Isopoda) was among the most responsive macrofauna species to root trenching, with its abundance being increased by trenching, but this was only marginally significant after BH correction (see above). Stable isotope analysis showed that the increase in abundance was associated by a shift in the carbon resources used, but the changes varied with forest types and were restricted to the Hainich. Also, in Lumbricidae root trenching resulted in changes in stable isotope values. However, in contrast to *T. pusillus*, the changes were due to changes in $\delta^{15}N$ values of the two endogeic Lumbricidae species analyzed (Hainich only). Presumably, root trenching resulted in a dietary shift towards older, more decomposed carbon resources more enriched in ^{15}N (Kramer et al., 2003; Potapov et al., 2019b).

Unexpectedly, root trenching did not affect the NLFA composition of any of the analyzed detritivore or predator species except in trend for *T. pusillus*. This likely reflects that, although microbial biomass was reduced strongly by root trenching, it did not alter microbial community composition as measured by PLFA analysis (Bluhm et al., 2019a). In *T. pusillus* the fungal marker fatty acid showed a trend of being reduced by root trenching indicating that this species switched its diet towards bacteria based diets. This shift paralleled the decreased fungal and increased bacterial PLFAs in trenched plots in the Hainich after 3 years of root trenching (Bluhm et al., 2019a). As the trophic shift in *T. pusillus* was associated by an increase in abundance but not biomass in trenched plots, the shift only beneficially affected recruitment of juveniles of this species (see above).

Experimental Limitations

Investigating the role of root-derived resources for the belowground system by using root trenching also has limitations. Due to cutting of roots soil moisture might be increased during the growing period due to the lack of water uptake by plants. To control for the reduced water uptake by trees in trenched plots we irrigated the control plots, but this may not have fully equalized soil moisture conditions in control and trenched plots. Further, dead roots in the trenched plots may serve as additional resource for decomposers. However, the general reduction in soil microorganisms as well as soil arthropod taxa in trenched plots argues that additional dead roots were of minor importance as resource for the decomposer food web, at least in the studied upper litter and soil horizons.

CONCLUSION

Root trenching affected the abundance and biomass of soil animal taxa but the effect depended on the size of the taxa. Macrofauna and microfauna were only slightly decreased due to trenching of roots, while mesofauna declined much stronger. The consistent detrimental effect across mesofauna taxa suggests that energy in soil food webs is channeled via size-based pathways with mesofauna detritivores as well as mesofauna predators relying heavily on root-derived resources. The effect of root trenching generally did not vary with forest type and only little with region. Only one taxon responded parallel to that of microorganisms, suggesting that microbial biomass inadequately reflects basal resources of the soil animal food web. Notably, despite the in part marked reduction in abundance and biomass of soil animal taxa by root trenching, community composition of each micro-, meso-, and macrofauna remained unaffected. This suggests that the species of the detrimentally affected taxa suffered in a similar way from deprivation of root-derived resources, pointing to the dominance of generalist/omnivore species in soil food webs. The lack of or only slight change in the diet of soil animals to root trenching either points to the inability of soil animals to switch diet or reflects that root-derived resources only little affect the composition of microbial communities. Overall, the findings indicate that root-derived resources are predominantly incorporated into soil animal food webs via mesofauna taxa affecting both their abundance and biomass, whereas community composition and trophic niches of soil animals generally are not or only little affected by root-derived resources. The fact that mesofauna detritivores and predators suffered to a similar extent from root trenching points to the dominance of bottom-up forces in regulating this size-compartment of soil animal food webs.

DATA AVAILABILITY STATEMENT

The datasets generated for this study can be found in the online repositories. The names of the repository/repositories and accession number(s) can be found below: the datasets will be public available after acceptance of the manuscript for publication: the datasets IDs 27526, 27487, 27486, 27468, 27467, 27308, 27307, and 27306 for this study can be found in the BExIS (Biodiversity Exploratories Information System), https://www.bexis.uni-jena.de/PublicData/PublicData.aspx.

AUTHOR CONTRIBUTIONS

BE, OF, CB, MM, and SS: conceptualization. SB: formal analysis. MM and SS: funding acquisition. SB, BE, CB, OF, KH, MC, MM,

and SS: investigation and writing—review and editing: SB and SS: visualization and writing—original draft. All authors contributed to the article and approved the submitted version.

FUNDING

The work has been funded by the German Research Foundation (DFG Priority Program 1374 "Infrastructure-Biodiversity-Exploratories," DFG- SCHE 376/22-3).

ACKNOWLEDGMENTS

We are indebted to Andreas Küttner, Bernhard Klarner, Christoph Digel, Dana Augustin, Emily Solly, David Ott, Christel Fischer, Guido Humpert, and Dieter Nünchert for help during field and laboratory work. We thank Anton Potapov for valuable comments on the manuscript. We thank the managers of the two Exploratories Hainich-Dün and Schorfheide-Chorin, Kerstin Wiesner, Katrin Lorenzen, Martin Gorke, and all former managers for their work in maintaining the plot and project infrastructure; Simone Pfeiffer, Christiane Fischer, and Victoria Grießmeier for giving support through the central office, Britta König-Ries, Michael Owonibi, and Andreas Ostrowski for managing the central data base, and Markus Fischer, Eduard Linsenmair, Dominik Hessenmöller, Daniel Prati, Ingo Schöning, François Buscot, Ernst-Detlef Schulze, Wolfgang W. Weisser, and the late Elisabeth Kalko for their role in setting up the Biodiversity Exploratories project. Field work permits were issued by the responsible state environmental offices of Thüringen and Brandenburg.

SUPPLEMENTARY MATERIAL

The Supplementary Material for this article can be found online at: https://www.frontiersin.org/articles/10.3389/ffgc.2021.622370/full#supplementary-material

REFERENCES

Albers, D., Schaefer, M., and Scheu, S. (2006). Incorporation of plant carbon into the soil animal food web of an arable system. *Ecology* 87, 235–245. doi: 10.1890/04-1728

Bais, H. P., Weir, T. L., Perry, L. G., Gilroy, S., and Vivanco, J. M. (2006). The role of root exudates in rhizosphere interactions with plants and other organisms. *Annu. Rev. Plant Biol.* 57, 233–266. doi: 10.1146/annurev.arplant.57.032905.105159

Barber, A. D. (2008). *Key to the Identification of British Centipedes*. Shrewsbury: Field Studies Council.

Bardgett, R. D., and Wardle, D. A. (2010). *Aboveground- Belowground Linkages. Biotic Interactions, Ecosystem Processes, and Global Change*. Oxford: Oxford University Press.

Beare, M. H., Coleman, D. C., Crossley, D. A., Hendrix, P. F., and Odum, E. P. (1995). A hierarchical approach to evaluating the significance of soil biodiversity to biogeochemical cycling. *Plant Soil* 170, 5–22. doi: 10.1007/BF02183051

Benjamini, Y., and Hochberg, Y. (1995). Controlling the false discovery rate: a practical and powerful approach to multiple testing. *J. R. Stat. Soc. Ser. B* 57, 289–300. doi: 10.1111/j.2517-6161.1995.tb02031.x

Blower, J. G. (1985). *Millipedes: Keys and Notes for the Identification of the Species*. Leiden: Backhuys Publishers.

Bluhm, S. L., Eitzinger, B., Ferlian, O., Bluhm, C., Schröter, K., Pena, R., et al. (2019a). Deprivation of root-derived resources affects microbial biomass but not community structure in litter and soil. *PLoS One* 14:e0214233. doi: 10.1371/journal.pone.0214233

Bluhm, S. L., Potapov, A. M., Shrubovych, J., Ammerschubert, S., Polle, A., and Scheu, S. (2019b). Protura are unique: first evidence of specialized feeding on ectomycorrhizal fungi in soil invertebrates. *BMC Ecol.* 19:10. doi: 10.1186/s12898-019-0227-y

Bongers, T. (1990). The maturity index: an ecological measure of environmental disturbance based on nematode species composition. *Oecologia* 83, 14–19. doi: 10.1007/BF00324627

Bongers, T. (1994). *De Nematoden van Nederland. 2*. Utrecht: K.N.NV.

Bongers, T., and Bongers, M. (1998). Functional diversity of nematodes. *Appl. Soil Ecol.* 10, 239–251. doi: 10.1016/S0929-1393(98)00123-1

Bonkowski, M., Villenave, C., and Griffiths, B. S. (2009). Rhizosphere fauna: the functional and structural diversity of intimate interactions of soil fauna with plant roots. *Plant Soil* 321, 213–233. doi: 10.1007/s11104-009-0013-2

Caruso, T., and Migliorini, M. (2009). Euclidean geometry explains why lengths allow precise body mass estimates in terrestrial invertebrates: the case of oribatid mites. *J. Theor. Biol.* 256, 436–440. doi: 10.1016/j.jtbi.2008.09.033

Cebrian, J. (1999). Patterns in the fate of production in plant communities. *Am. Nat.* 154, 449–468. doi: 10.1086/303244

Clemmensen, K. E., Bahr, A., Ovaskainen, O., Dahlberg, A., Ekblad, A., Wallander, H., et al. (2013). Roots and associated fungi drive long-term carbon sequestration in boreal forest. *Science* 339, 1615–1618. doi: 10.1126/science.1231923

Curl, E. A., and Truelove, B. (1986). *The Rhizosphere*. Berlin: Springer-Verlag.

Eisenhauer, N., Straube, D., and Scheu, S. (2008). Efficiency of two widespread non-destructive extraction methods under dry soil conditions for different ecological earthworm groups. *Eur. J. Soil Biol.* 44, 141–145. doi: 10.1016/j.ejsobi.2007.10.002

Eissfeller, V., Beyer, F., Valtanen, K., Hertel, D., Maraun, M., Polle, A., et al. (2013). Incorporation of plant carbon and microbial nitrogen into the rhizosphere food web of beech and ash. *Soil Biol. Biochem.* 62, 76–81. doi: 10.1016/j.soilbio.2013.03.002

Ekblad, A., Wallander, H., Godbold, D. L., Cruz, C., Johnson, D., Baldrian, P., et al. (2013). The production and turnover of extramatrical mycelium of ectomycorrhizal fungi in forest soils: role in carbon cycling. *Plant Soil* 366, 1–27. doi: 10.1007/s11104-013-1630-3

Endlweber, K., Ruess, L. R., and Scheu, S. (2009). Collembola switch diet in presence of plant roots thereby functioning as herbivores. *Soil Biol. Biochem.* 41, 1151–1154. doi: 10.1016/j.soilbio.2009.02.022

Farrar, J., Hawes, M., Jones, D., and Lindow, S. (2003). How roots control the flux of carbon to the rhizosphere. *Ecology* 84, 827–837.

Ferlian, O., and Scheu, S. (2013). Shifts in trophic interactions with forest type in soil generalist predators as indicated by complementary analyses of fatty acids and stable isotopes. *Oikos* 123, 1182–1191. doi: 10.1111/j.1600-0706.2013.00848.x

Ferris, H., Bongers, T., and de Goede, R. G. M. (2001). A framework for soil food web diagnostics: extension of the nematode faunal analysis concept. *Appl. Soil Ecol.* 18, 13–29. doi: 10.1016/S0929-1393(01)00152-4

Fischer, M., Bossdorf, O., Gockel, S., Hänsel, F., Hemp, A., Hessenmöller, D., et al. (2010). Implementing large-scale and long-term functional biodiversity research: the biodiversity Exploratories. *Basic Appl. Ecol.* 11, 473–485. doi: 10.1016/j.baae.2010.07.009

Fitter, A. H., and Garbaye, J. (1994). Interactions between mycorrhizal fungi and other soil organisms. *Plant Soil* 159, 123–132. doi: 10.1007/BF00000101

Fujii, S., Mori, A. S., Kominami, Y., Tawa, Y., Inagaki, Y., Takanashi, S., et al. (2016). Differential utilization of root-derived carbon among collembolan species. *Pedobiologia* 59, 225–227. doi: 10.1016/j.pedobi.2016.05.001

Gilbert, K. J., Fahey, T. J., Maerz, J. C., Sherman, R. E., Bohlen, P., Dombroskie, J. J., et al. (2014). Exploring carbon flow through the root channel in a temperate forest soil food web. *Soil Biol. Biochem.* 76, 45–52. doi: 10.1016/j.soilbio.2014.05.005

Gisin, H. (1943). ökologie und Lebensgemeinschaften der Collembolen im schweizerischen Exkursionsgebiet Basels. *Rev. Suisse Zool.* 50, 131–224.

Gunn, A., and Cherrett, J. M. (1993). The exploitation of food resources by soil meso-invertebrates and macro-invertebrates. *Pedobiologia* 37, 303–320.

Günther, B., Rall, B. C., Ferlian, O., Scheu, S., and Eitzinger, B. (2014). Variations in prey consumption of centipede predators in forest soils as indicated by molecular gut content analysis. *Oikos* 123, 1192–1198. doi: 10.1111/j.1600-0706.2013.00868.x

Hagerman, S. M., Jones, M. D., Bradfield, G. E., Gillespie, M., and Durall, D. M. (1999). Effects of clear-cut logging on the diversity and persistence of ectomycorrhizae at a subalpine forest. *Can. J. For. Res.* 29, 124–134. doi: 10.1139/x98-186

Haubert, D., Häggblom, M. M., Scheu, S., and Ruess, L. R. (2004). Effects of fungal food quality and starvation on the fatty acid composition of *Protaphorura fimata* (Collembola). *Comp. Biochem. Physiol. Biochem. Mol. Biol.* 138, 41–52. doi: 10.1016/j.cbpc.2004.02.009

Hervé, M. (2020). *RVAideMemoire: Testing and Plotting Procedures for Biostatistics. R package version 0.9-77*. Available online at: https://CRAN.R-project.org/package=RVAideMemoire

Högberg, M. N., Briones, M. J. I., Keel, S. G., Metcalfe, D. B., Campbell, C., Midwood, A. J., et al. (2010). Quantification of effects of season and nitrogen supply on tree below-ground carbon transfer to ectomycorrhizal fungi and other soil organisms in a boreal pine forest. *New Phytol.* 187, 485–493. doi: 10.1111/j.1469-8137.2010.03274.x

Högberg, M. N., and Högberg, P. (2002). Extramatrical ectomycorrhizal mycelium contributes one-third of microbial biomass and produces, together with associated roots, half the dissolved organic carbon in a forest soil. *New Phytol.* 154, 791–795. doi: 10.1046/j.1469-8137.2002.00417.x

Hopkin, S. P. (2007). *A Key to the Collembola (Springtails) of Britain and Ireland*. Shrewsbury: Field Studies Council.

Jones, D. L., Nguyen, C., and Finlay, R. D. (2009). Carbon flow in the rhizosphere: carbon trading at the soil-root interface. *Plant Soil* 321, 5–33. doi: 10.1007/s11104-009-9925-0

Kempson, D., Lloyd, M., and Ghelardi, R. (1963). A new extractor for woodland litter. *Pedobiologia* 3, 1–21.

Klarner, B., Ehnes, R. B., Erdmann, G., Eitzinger, B., Pollierer, M. M., Maraun, M., et al. (2014). Trophic shift of soil animal species with forest type as indicated by stable isotope analysis. *Oikos* 123, 1173–1181. doi: 10.1111/j.1600-0706.2013.00939.x

Klarner, B., Winkelmann, H., Krashevska, V., Maraun, M., Widyastuti, R., and Scheu, S. (2017). Trophic niches, diversity and community composition of invertebrate top predators (Chilopoda) as affected by conversion of tropical lowland rainforest in Sumatra (Indonesia). *PLoS One* 12:e0180915. doi: 10.1371/journal.pone.0180915

Koren, A. (1992). Die Chilopodenfauna von Kärnten und Osttirol, Teil 2: Lithobiomorpha. *Carinthia II* 52, 1–138.

Kramer, M. G., Sollins, P., Sletten, R. S., and Swart, P. K. (2003). N isotope fractionation and measures of organic matter alteration during decomposition. *Ecology* 84, 2021–2025. doi: 10.1890/02-3097

Kuzyakov, Y., and Blagodatskaya, E. (2015). Microbial hotspots and hot moments in soil: concept & review. *Soil Biol. Biochem.* 83, 184–199. doi: 10.1016/j.soilbio.2015.01.025

Kuzyakov, Y., and Domanski, G. (2000). Carbon input by plants into the soil. Review. *J. Plant Nutr. Soil Sci.* 163, 421–431.

Langel, R., and Dyckmans, J. (2014). Combined (13) C and (15) N isotope analysis on small samples using a near-conventional elemental analyzer/isotope ratio mass spectrometer setup. *Rapid Commun. Mass Spectrom.* 28, 1019–1022. doi: 10.1002/rcm.6878

Latzel, R. (1880). *Die Myriopoden der Österreichisch-ungarischen Monarchie. Erste Hälfte: Die Chilopoda*. Wien: Hölder.

Lemanski, K., and Scheu, S. (2014). Fertilizer addition lessens the flux of microbial carbon to higher trophic levels in soil food webs of grassland. *Oecologia* 176, 487–496. doi: 10.1007/s00442-014-3037-0

Li, Y., Yang, X., and Wu, J. (2009). Response of soil nematode communities to tree girdling in a subtropical evergreen broad-leaved forest of southwest China. *Soil Biol. Biochem.* 41, 877–882. doi: 10.1016/J.SOILBIO.2008.07.031

Li, Z., Scheunemann, N., Potapov, A. M., Shi, L., Pausch, J., Scheu, S., et al. (2020). Incorporation of root-derived carbon into soil microarthropods varies between cropping systems. *Biol. Fertil. Soils* 56, 839–851. doi: 10.1007/s00374-020-01467-8

Litton, C. M., Raich, J. W., and Ryan, M. G. (2007). Carbon allocation in forest ecosystems. *Glob. Chang. Biol.* 13, 2089–2109. doi: 10.1111/j.1365-2486.2007.01420.x

Macfadyen, A. (1961). Improved funnel-type extractors for soil arthropods. *J. Anim. Ecol.* 30, 171–184. doi: 10.2307/2120

Malmström, A., and Persson, T. (2011). Responses of Collembola and Protura to tree girdling – some support for ectomycorrhizal feeding. *Soil Org.* 83, 279–285.

Mercer, R. D., Gabriel, A. G. A., Barendse, J., Marshall, D. J., and Chown, S. L. (2001). Invertebrate body sizes from Marion Island. *Antarct. Sci.* 13, 135–143. doi: 10.1017/S0954102001000219

Okada, H., Harada, H., and Kadota, I. (2005). Fungal-feeding habits of six nematode isolates in the genus Filenchus. *Soil Biol. Biochem.* 37, 1113–1120. doi: 10.1016/J.SOILBIO.2004.11.010

Oksanen, J., Blanchet, F. G., Friendly, M., Kindt, R., Legendre, P., McGlinn, D., et al. (2018). *vegan: Community Ecology Package. R Packag. version 2.4–6*. Available online at: https//CRAN.R-project.org/package=vegan

Ostle, N. J., Briones, M. J. I., Ineson, P., Cole, L., Staddon, P., and Sleep, D. (2007). Isotopic detection of recent photosynthate carbon flow into grassland rhizosphere fauna. *Soil Biol. Biochem.* 39, 768–777. doi: 10.1016/j.soilbio.2006.09.025

Parmelee, R. W., Ehrenfeld, J. G., and Tate, R. L. (1993). Effects of pine roots on microorganisms, fauna, and nitrogen availability in two soil horizons of a coniferous forest spodosol. *Biol. Fertil. Soils* 15, 113–119. doi: 10.1007/BF00336428

Pinheiro, J., Bates, D., DebRoy, S., and Sarkar, D. (2013). *nlme: Linear and Nonlinear Mixed Effects Models. R Package Version 3.1-109*. Vienna: R Foundation for Statistical Computing.

Pollierer, M. M., Dyckmans, J., Scheu, S., and Haubert, D. (2012). Carbon flux through fungi and bacteria into the forest soil animal food web as indicated by compound-specific 13C fatty acid analysis. *Funct. Ecol.* 26, 978–990. doi: 10.1111/j.1365-2435.2012.02005.x

Pollierer, M. M., Langel, R., Körner, C., Maraun, M., and Scheu, S. (2007). The underestimated importance of belowground carbon input for forest soil animal food webs. *Ecol. Lett.* 10, 729–736. doi: 10.1111/j.1461-0248.2007.01064.x

Pollierer, M. M., Langel, R., Scheu, S., and Maraun, M. (2009). Compartmentalization of the soil animal food web as indicated by dual analysis of stable isotope ratios (15N/14N and 13C/12C). *Soil Biol. Biochem.* 41, 1221–1226. doi: 10.1016/j.soilbio.2009.03.002

Pollierer, M. M., Scheu, S., and Haubert, D. (2010). Taking it to the next level: trophic transfer of marker fatty acids from basal resource to predators. *Soil Biol. Biochem.* 42, 919–925. doi: 10.1016/j.soilbio.2010.02.008

Post, D. M. (2002). Using stable isotopes to estimate trophic position: models, methods, and assumptions. *Ecology* 83, 703–718. doi: 10.2307/3071875

Potapov, A. M., Brose, U., Scheu, S., and Tiunov, A. V. (2019a). Trophic position of consumers and size structure of food webs across aquatic and terrestrial ecosystems. *Am. Nat.* 194, 823–839. doi: 10.1086/705811

Potapov, A. M., Tiunov, A. V., and Scheu, S. (2019b). Uncovering trophic positions and food resources of soil animals using bulk natural stable isotope composition. *Biol. Rev.* 94, 37–59. doi: 10.1111/brv.12434

Potapov, A. M., and Tiunov, A. V. (2016). Stable isotope composition of mycophagous collembolans versus mycotrophic plants: Do soil invertebrates feed on mycorrhizal fungi? *Soil Biol. Biochem.* 93, 115–118. doi: 10.1016/j.soilbio.2015.11.001

R Core Team (2020). "R: A language and environment for statistical computing", in *R Foundation for Statistical Computing*, Vienna. Available online at: https://www.R-project.org/

Reineking, A., Langel, R., and Schikowski, J. (1993). C-On-line Measurements with an Elemental Analyser (Carlo Erba, Isotopenpraxis. *Isot. Environ. Health Sci.* 29, 169–174. doi: 10.1080/10256019308046151

Remén, C., Persson, T., Finlay, R. D., and Ahlström, K. (2008). Responses of oribatid mites to tree girdling and nutrient addition in boreal coniferous forests. *Soil Biol. Biochem.* 40, 2881–2890. doi: 10.1016/j.soilbio.2008.08.006

Ruess, L. (1995). Studies on the nematode fauna of an acid forest soil: spatial distribution and extraction. *Nematologica* 41, 229–239. doi: 10.1163/003925995X00198

Ruess, L. R., and Chamberlain, P. M. (2010). The fat that matters: soil food web analysis using fatty acids and their carbon stable isotope signature. *Soil Biol. Biochem.* 42, 1898–1910. doi: 10.1016/j.soilbio.2010.07.020

Ruess, L. R., Häggblom, M. M., Zapata, E. J. G., and Dighton, J. (2002). Fatty acids of fungi and nematodes—possible biomarkers in the soil food chain? *Soil Biol. Biochem.* 34, 745–756.

Ruess, L. R., Schütz, K., Migge-Kleian, S., Häggblom, M. M., Kandeler, E., and Scheu, S. (2007). Lipid composition of Collembola and their food resources in deciduous forest stands—Implications for feeding strategies. *Soil Biol. Biochem.* 39, 1990–2000. doi: 10.1016/j.soilbio.2007.03.002

Ruf, A., Kuzyakov, Y., and Lopatovskaya, O. (2006). Carbon fluxes in soil food webs of increasing complexity revealed by 14C labelling and 13C natural abundance. *Soil Biol. Biochem.* 38, 2390–2400. doi: 10.1016/j.soilbio.2006.03.008

Schaefer, M., Ansorge, H., Brehm, G., Fiedler, K., Sattler, K., Scheu, S., et al. (2018). *Brohmer - Fauna von Deutschland*, 25th Edn, ed. M. Schaefer (Wiebelsheim: Quelle & Meyer).

Scheu, S., and Falca, M. (2000). The soil food web of two beech forests (Fagus sylvatica) of contrasting humus type: stable isotope analysis of a macro- and a mesofauna-dominated community. *Oecologia* 123, 285–296. doi: 10.1007/s004420051015

Scheu, S., and Schaefer, M. (1998). Bottom-up control of the soil macrofauna community in a beechwood on limestone: manipulation of food resources. *Ecology* 79, 1573–1585. doi: 10.2307/176777

Scheunemann, N., Maraun, M., Scheu, S., and Butenschoen, O. (2015). The role of shoot residues vs. crop species for soil arthropod diversity and abundance of arable systems. *Soil Biol. Biochem.* 81, 81–88. doi: 10.1016/j.soilbio.2014.11.006

Scheunemann, N., Pausch, J., Digel, C., Kramer, S., Scharroba, A., Kuzyakov, Y., et al. (2016). Incorporation of root C and fertilizer N into the food web of an arable field: variations with functional group and energy channel. *Food Webs* 9, 39–45. doi: 10.1016/j.fooweb.2016.02.006

Semenyuk, I. I., and Tiunov, A. V. (2011). Isotopic signature (15N/14N and 13C/12C) confirms similarity of trophic niches of millipedes (Myriapoda, Diplopoda) in a temperate deciduous forest. *Biol. Bull.* 38, 283–291. doi: 10.1134/S1062359011030137

Siira-Pietikäinen, A., Haimi, J., and Fritze, H. (2003). Organisms, decomposition and growth of pine seedlings in boreal forest soil affected by sod cutting and trenching. *Biol. Fertil. Soils* 37, 163–174. doi: 10.1007/s00374-002-0571-4

Siira-Pietikäinen, A., Haimi, J., Kanninen, A., Pietikäinen, J., and Fritze, H. (2001). Responses of decomposer community to root-isolation and addition of slash. *Soil Biol. Biochem.* 33, 1993–2004. doi: 10.1016/S0038-0717(01)00135-3

Sims, R. W., and Gerard, B. M. (1985). *Earthworms: Keys and Notes for the Identification and Study of the Species*. Leiden: Brackish-Water Sciences.

Sohlström, E. H., Marian, L., Barnes, A. D., Haneda, N. F., Scheu, S., Rall, B. C., et al. (2018). Applying generalized allometric regressions to predict live body mass of tropical and temperate arthropods. *Ecol. Evol.* 8, 12737–12749. doi: 10.1002/ece3.4702

Sprengel, T. (1986). *Die Doppelfüßer (Diplopoda) eines Kalkbuchenwaldes und ihre Funktion beim Abbau der Laubstreu*. Ph.D. dissertation, Universität Göttingen, Göttingen.

Starling, J. H. (1944). Ecological studies of the Pauropoda of the Duke Forest. *Ecol. Monogr.* 14, 291–310. doi: 10.2307/1948445

Tan, K. H. (2014). *Humic Matter in Soil and the Environment: Principles and Controversies*, 2nd Edn. Oakville: CRC Press.

Tiunov, A. V., and Scheu, S. (2004). Carbon availability controls the growth of detritivores (Lumbricidae) and their effect on nitrogen mineralization. *Oecologia* 138, 83–90. doi: 10.1007/s00442-003-1391-4

Traugott, M., Kamenova, S., Ruess, L., Seeber, J., and Plantegenest, M. (2013). Empirically Characterising Trophic Networks: What Emerging DNA- Based Methods, Stable Isotope and Fatty Acid Analyses Can Offer. *Adv. Ecol. Res.* 49, 177–224. doi: 10.1016/B978-0-12-420002-9.00003-2

Treseder, K. K., Torn, M. S., and Masiello, C. A. (2006). An ecosystem-scale radiocarbon tracer to test use of litter carbon by ectomycorrhizal fungi. *Soil Biol. Biochem.* 38, 1077–1082. doi: 10.1016/j.soilbio.2005.09.006

van Hees, P. A. W., Jones, D. L., Finlay, R., Godbold, D. L., and Lundström, U. S. (2005). The carbon we do not see—the impact of low molecular weight compounds on carbon dynamics and respiration in forest soils: a review. *Soil Biol. Biochem.* 37, 1–13. doi: 10.1016/j.soilbio.2004.06.010

Vitousek, P. M., Hättenschwiler, S., Olander, L., and Allison, S. (2002). Nitrogen and nature. *Ambio* 31, 97–101. doi: 10.1579/0044-7447-31.2.97

Voigtländer, K., Decker, P., Burkhardt, U., and Spelda, J. (2016). The present knowledge of the Symphyla and Pauropoda (Myriapoda) in Germany – An annotated checklist. *Acta Soc. Zool. Bohem.* 80, 51–85.

Wallander, H., Göransson, H., and Rosengren, U. (2004). Production, standing biomass and natural abundance of 15N and 13C in ectomycorrhizal mycelia collected at different soil depths in two forest types. *Oecologia* 139, 89–97. doi: 10.1007/s00442-003-1477-z

Wardle, D. A. (2002). *Communities and Ecosystems: Linking the Aboveground and Belowground Components*. Princeton, NJ: Princeton University Press.

Weigmann, G. (2006). *Hornmilben (Oribatida) (Die Tierwelt Deutschlands)*. Keltern: Goecke & Evers.

Werner, R. A., Bruch, B. A., and Brand, W. A. (1999). ConFlo III - an interface for high precision δ13C and δ15N analysis with an extended dynamic range. *Rapid Commun. Mass Spectrom.* 13, 1237–1241.

White, T. C. R. (1993). *The Inadequate Environment: Nitrogen and the Abundance of Animals*. Berlin: Springer. doi: 10.1007/978-3-642-78299-2

Wolkovich, E. M. M. (2016). Reticulated channels in soil food webs. *Soil Biol. Biochem.* 102, 18–21. doi: 10.1016/j.soilbio.2016.06.021

Yeates, G. W., Bongers, T., De Goede, R. G., Freckman, D. W., and Georgieva, S. S. (1993). Feeding habits in soil nematode families and genera-an outline for soil ecologists. *J. Nematol.* 25, 315–331.

Zieger, S. L., Ammerschubert, S., Polle, A., and Scheu, S. (2017a). Root-derived carbon and nitrogen from beech and ash trees differentially fuel soil animal food webs of deciduous forests. *PLoS One* 12:e0189502. doi: 10.1371/journal.pone.0189502

Zieger, S. L., Holczinger, A., Sommer, J., Rath, M., Kuzyakov, Y., Polle, A., et al. (2017b). Beech trees fuel soil animal food webs via root-derived nitrogen. *Basic Appl. Ecol.* 22, 28–35. doi: 10.1016/j.baae.2017.06.006

Zieger, S. L., and Scheu, S. (2018). Effects of storage and handling on neutral lipid fatty acid profiles of two woodlice (Isopoda, Crustacea) species differing in size. *Appl. Soil Ecol.* 130, 178–184. doi: 10.1016/j.apsoil.2018.04.009

Conflict of Interest: The authors declare that the research was conducted in the absence of any commercial or financial relationships that could be construed as a potential conflict of interest.

frontiers
in Plant Science

ORIGINAL RESEARCH
published: 30 June 2021
doi: 10.3389/fpls.2021.683658

Responses of Low-Cost Input Combinations on the Microbial Structure of the Maize Rhizosphere for Greenhouse Gas Mitigation and Plant Biomass Production

Caio Augusto Yoshiura[1], Andressa Monteiro Venturini[1†], Lucas Palma Perez Braga[1†], Aline Giovana da França[1], Maria do Carmo Catanho Pereira de Lyra[2], Siu Mui Tsai[1‡] and Jorge Luiz Mazza Rodrigues[3‡]*

[1] *Cell and Molecular Biology Laboratory, Center for Nuclear Energy in Agriculture, University of São Paulo, Piracicaba, Brazil,* [2] *Genome Laboratory, Agronomic Institute of Pernambuco, Recife, Brazil,* [3] *Soil EcoGenomics Laboratory, University of California, Davis, Davis, CA, United States*

Edited by:
Catherine Preece,
University of Antwerp, Belgium

Reviewed by:
Mónica Montoya,
Polytechnic University of Madrid, Spain
Antoine Berger,
University of Florida, United States

***Correspondence:**
Caio Augusto Yoshiura
caio.yoshiura@alumni.usp.br

†These authors share second authorship

‡These authors share last authorship

Specialty section:
This article was submitted to Plant Symbiotic Interactions, a section of the journal Frontiers in Plant Science

Received: *21 March 2021*
Accepted: *18 May 2021*
Published: *30 June 2021*

Citation:
Yoshiura CA, Venturini AM, Braga LPP, França AG, Lyra MCCP, Tsai SM and Rodrigues JLM (2021) Responses of Low-Cost Input Combinations on the Microbial Structure of the Maize Rhizosphere for Greenhouse Gas Mitigation and Plant Biomass Production. Front. Plant Sci. 12:683658. doi: 10.3389/fpls.2021.683658

The microbial composition of the rhizosphere and greenhouse gas (GHG) emissions under the most common input combinations in maize (*Zea mays* L.) cultivated in Brazil have not been characterized yet. In this study, we evaluated the influence of maize stover coverage (S), urea-topdressing fertilization (F), and the microbial inoculant *Azospirillum brasilense* (I) on soil GHG emissions and rhizosphere microbial communities during maize development. We conducted a greenhouse experiment and measured methane (CH_4), carbon dioxide (CO_2), and nitrous oxide (N_2O) fluxes from soil cultivated with maize plants under factorial combinations of the inputs and a control treatment (F, I, S, FI, FS, IS, FIS, and control). Plant biomass was evaluated, and rhizosphere soil samples were collected at V5 and V15 stages and DNA was extracted. The abundance of functional genes (*mcrA*, *pmoA*, *nifH*, and *nosZ*) was determined by quantitative PCR (qPCR) and the structure of the microbial community was assessed through 16S rRNA amplicon sequencing. Our results corroborate with previous studies which used fewer input combinations and revealed different responses for the following three inputs: F increased N_2O emissions around 1 week after application; I tended to reduce CH_4 and CO_2 emissions, acting as a plant growth stimulator through phytohormones; S showed an increment for CO_2 emissions by increasing carbon-use efficiency. IS and FIS treatments presented significant gains in biomass that could be related to Actinobacteria (19.0%) and Bacilli (10.0%) in IS, and Bacilli (9.7%) in FIS, which are the microbial taxa commonly associated with lignocellulose degradation. Comparing all factors, the IS (inoculant + maize stover) treatment was considered the best option for plant biomass production and GHG mitigation since FIS provides small gains toward the management effort of F application.

Keywords: microbial ecology, denitrification, mesocosm, plant growth-promoting rhizobacteria, methanotrophy, methanogenesis

INTRODUCTION

Several inputs have been studied and documented to improve crop development and production, increasing soil health and plant resistance to pathogens and seasonal variations (Thangarajan et al., 2013; Wang et al., 2016; Abbott et al., 2018; Sharma and Bali, 2018). However, the excessive and indiscriminate use of synthetic nitrogen fertilizers can cause an imbalance in the nitrogen cycle at huge economic costs. These are associated with human health problems due to drinking water contamination by high nitrate concentrations and environmental problems, such as freshwater eutrophication and climate change by the increase of nitrous oxide (N_2O) and carbon dioxide (CO_2) emissions (Galloway et al., 2008; Ward, 2009; Zamanian et al., 2018), enforcing the continuous search for alternatives to improve food production. Currently, three inputs – synthetic nitrogen fertilizers, commercial microbial inoculants, and plant residues coverage from the adoption of no-tillage practices – have been commonly used in agricultural practices to increase crop yield and production. Microbial inoculants, such as plant-growth-promoting rhizobacteria (PGPR) are alternatives to nitrogen fertilization and are commonly employed as biofertilizers, phytostimulators, and biocontrollers (Okon and Labandera-Gonzalez, 1994; Bloemberg and Lugtenberg, 2001). On the other hand, no-tillage practices have been increasing among crop management systems around the globe since they provide plant residues for soil coverage and nutrient supply (Busari et al., 2015; Pittelkow et al., 2015) and improve the physicochemical characteristics and carbon storage of the soil by increasing the CO_2 sequestration (Rigon and Calonego, 2020). For instance, no-tillage areas in Brazil, the United States, and China are implemented in more than 50% of their total crop areas (He et al., 2010; USDA, 2010; Freitas and Landers, 2014).

Brazil is the third worldwide producer of maize (*Z. mays* L.), the second most important crop for the country, whose production increased more than 6% through the last 10 years (CONAB, 2019). Recently, studies on the evaluation of maize managements are focused on crop yield, soil greenhouse gas (GHG) emissions (Calvo et al., 2016; Cambouris et al., 2016; Müller et al., 2016), or the characterization of bulk and rhizosphere soil microbial communities using molecular approaches (Peiffer et al., 2013; Li et al., 2014). These studies about crop management are driven mostly by the increasing demand for food to feed human populations (FAO, 2009) and global climate changes due to the increase of GHG emissions, which are responsible for extreme weather events and rising sea levels, among other environmental impacts, in addition to threatening wildlife, as reported by the IPCC (2014).[1] However, few studies have characterized the microbial composition of the maize rhizosphere, aiming to prospect for potential mitigators of GHG emissions, and test the combined effects of agricultural inputs commonly used in Brazil (Teixeira et al., 2019), thus evaluating combinations for balanced and sustainable managements with less GHG emissions and higher maize production. In Brazil, around 35.7 Gg of N_2O [i.e., 10.6 Tg in carbon dioxide equivalent (CO_2 equivalent)] was emitted in 2010 from nitrogen fertilization (Brasil, 2016). Aiming at N_2O mitigation, recent technologies have been developed to reduce losses from fertilizers by volatilization and leaching, such as fertilizer coating or the addition of urease inhibitors (Barbarena et al., 2019; Bortoletto-Santos et al., 2019). The losses from fertilizers are closely related to the conventional urea that represents about 50% of the total N applied in Brazilian agriculture in the last two decades due to its low cost (Santos et al., 2020). Although the stabilized and slow-release urea is an alternative to reduced nitrogen losses by volatilization, it did not increase the nitrogen content in plants compared to conventional urea (Cancellier et al., 2016). Nevertheless, information about nitrogen fertilization remains incomplete and more than ever, results are needed to help establish sustainable management to reduce N_2O without compromising crop yields (Abalos et al., 2016).

Microbial processes in the rhizosphere affect plant growth (Bonkowski et al., 2000), provide protection against pathogens and environmental stress (Liu et al., 2020; Tkacz and Poole, 2021), and are responsible for relevant activities related to biogeochemical cycles (Li et al., 2014). Roots modify soil properties by releasing several low-molecular-mass compounds, polymerized sugars, root border cells, and dead root cap cells that alter the structure, functions, and interactions of the microbial populations (Philippot et al., 2013). Besides these, the incorporation of inputs also modifies the soil quality and nutrient content, feeding plants and microbial populations (Wieland et al., 2001; Geisseler and Scow, 2014). Therefore, bioaugmentation using PGPR, such as *Azospirillum brasilense*, could act as diazotrophic bacteria for biological nitrogen (N_2) fixation (Hartmann and Burris, 1987; Somers et al., 2005; Bashan et al., 2014; Backer et al., 2018) and promote other activities, such as phosphate solubilization, degradation of siderophores, and biological control of soil-borne pathogens (Bashan et al., 2004).

Toward the problem of the excessive use of urea as a nitrogen fertilizer in Brazilian fields, our hypothesis was to evaluate the necessity of urea-topdressing fertilization to increase plant biomass for high crop yield since the use of microbial inoculants and no-tillage practices are beneficial alternatives. In this study, we evaluated the influence of maize stover coverage, urea-topdressing fertilizer, and the microbial inoculant, *A. brasilense* on soil GHG emissions and the microbial composition of the maize rhizosphere during plant development through a mesocosm experiment. Hereby, we established direct comparisons among all factorial treatments, covering knowledge gaps related to the effects of these input combinations on soil GHG fluxes and microbial communities.

MATERIALS AND METHODS

Experimental Design and Setup

A factorial mesocosm experiment (**Figure 1**) was assembled to test the influence of maize stover, urea-topdressing

---

[1] https://www.ipcc.ch/

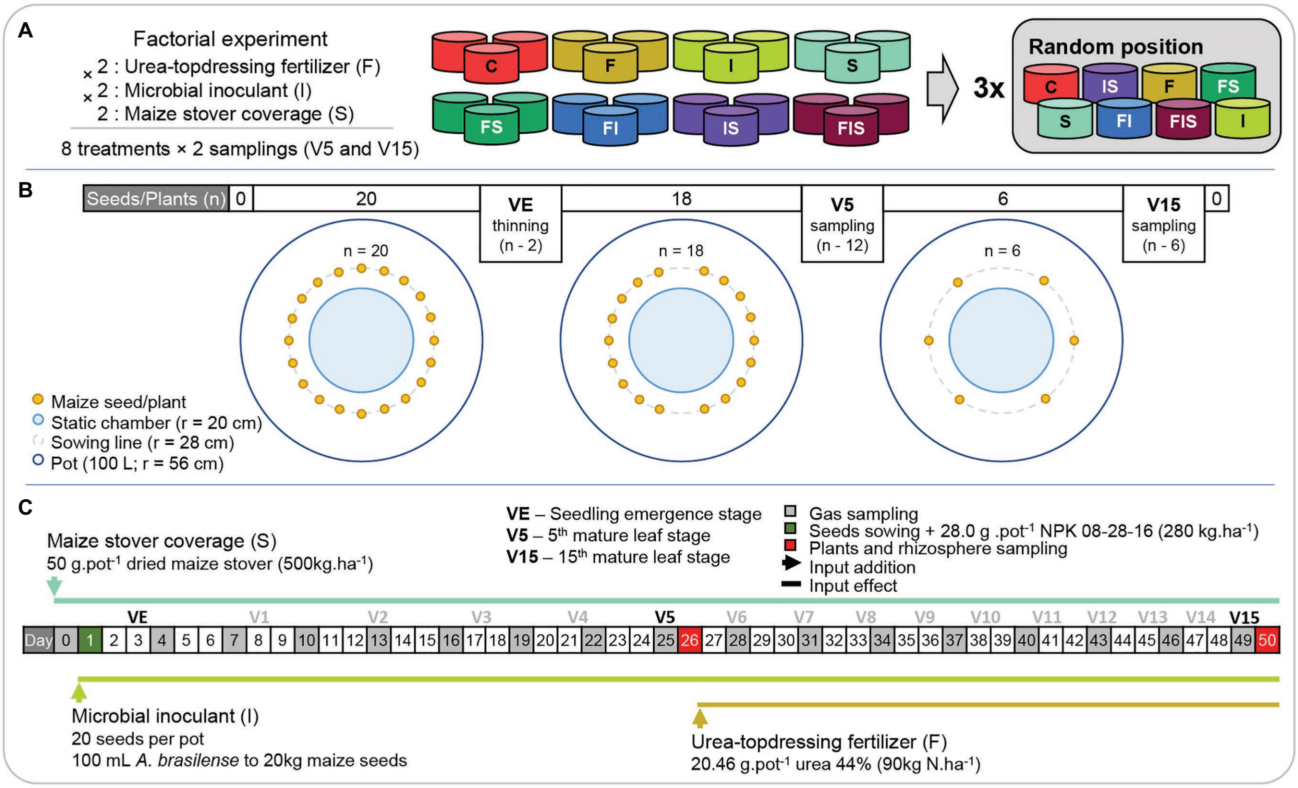

FIGURE 1 | Schemes of the **(A)** experimental design and **(B)** mesocosm pots through the **(C)** timeline. Treatments: C, Control; F, Urea-topdressing fertilization at V5; I, *A. brasilense* inoculant on seeds sowing; FI, F + I; S, Maize stover coverage; FS, F + S; IS, I + S; FIS, F + I + S.

fertilization, and microbial inoculant (*A. brasilense*) – 2 (with and without urea-topdressing fertilization) × 2 (with and without microbial inoculant) × 2 (with and without maize stover) × 2 (V5 and V15 sampling times; **Figure 1A**) – on the microbial composition of the maize rhizosphere, maize biomass gains, and GHG emissions. The factorial design resulted in eight treatments [urea-topdressing fertilization (F), microbial inoculant (I), maize stover coverage (S), and the combinations F + I (FI), F + S (FS), I + S (IS), F + I + S (FIS), and a control treatment (C)] with the following two sampling times: the next morning after the observation of the 5th mature leaf (V5) and maize stage of the 15th mature leaf (V15). All treatments were established in three replicates, in which each replicate was placed randomly in one block, that is, the experiment totalized three blocks containing eight pots each.

The mesocosm experiment was assembled in a greenhouse at the University of São Paulo – Center for Nuclear Energy in Agriculture (USP-CENA) in the maize second-crop season (Summer–Fall) of 2016. The topsoil (from 0 to 25 cm) from about 30 m^2 was obtained from an agricultural field at the Anhumas Experimental Station (22°50′28.22″S, 48°1′1.7″W). Twenty-four pots of 100 L (with 8 cm of gravel in the bottom layer for water drainage) were filled with the homogenized topsoil. The soil was classified as a dystrophic red-yellow latosol (IBGE, 2018) – oxisol, according to the US Soil Taxonomy (Soil Survey Staff, 1999), or Ferralsols, in the International Soil Classification System (IUSS Working Group WRB, 2015); and it was selected on the basis that dystrophic latosols represent a major part of soils used for maize production in Brazil (CONAB, 2018; IBGE, 2018). After sampling, aliquots (approximately 300 g) were sent to the Department of Soils of the University of São Paulo – Luiz de Queiroz College of Agriculture (USP-ESALQ) for physicochemical analysis, established for tropical soils according to the Agronomic Institute of Campinas (IAC; van Raij et al., 2001), to calculate the correction of soil fertility. Therefore, 28 g per pot (280 kg ha^{-1}) of a 08-28-16 NPK formulation was added to the seed furrows during sowing, according to the fertility recommendation (productivity more than 6 t ha^{-1}; EMBRAPA, 2015) for plant health maintenance until the V15 sampling.

Maize plants were grown using seeds with VT Pro Yieldgard technology (AG 8088; Sementes Agroceres – Monsanto, Brazil), suitable for grain and silage production on the first and second crops with high-temperature tolerance. In each pot, 20 seeds were sowed at 9.5 cm of distance in a circular line (r = 28 cm; **Figure 1B**). After seedling emergence (VE), 18 seedlings were kept until the V5 sampling time. At V5, 12 plants were collected, the remaining six for the V15 sampling time. Therefore, the experiment design was planned to simulate the planting population rates of 60,000 plants per hectare at V15.

The inputs were added to the experiment as described in the timeline (**Figure 1C**). Dried maize stover was collected from the Anhumas Experimental Station and applied in a proportion of 50 g per pot, simulating in-field conditions of maize residue coverage (500 kg ha^{-1}; S treatments). The strains, AbV5 and AbV6 of *A. brasilense* commercialized with a minimum concentration of 2×10^8 UFC ml^{-1} by Stoller do Brasil LTDA (Brazil) as the liquid inoculant Masterfix L Gramíneas was sprayed at 1 ml per 200 g of seeds (100 ml per hectare is equivalent to 100 ml per 20 kg of seeds) following the instructions of the manufacturer (I treatments). In non-inoculated treatments, 1 ml of sterilized water was sprayed instead. Urea-topdressing fertilization was applied after the V5 sampling time according to the field management conditions for a high yield of maize (90 kg N ha^{-1}), representing 20.46 g of urea (44% N) per pot (F treatments; EMBRAPA, 2015).

The different times of the application of the inputs implied different activation times of their effects. The maize stover coverage and *A. brasilense* inoculant inputs started their influence at the beginning of the experiment, and the urea-topdressing fertilization started its influence after V5. This means that F treatments (F, FI, FS, and FIS) have the same characteristics as C, I, S, and IS, respectively before V5 treatments.

The experiment was conducted for 50 days until the V15 stage of the development of the maize plants. During the experiment, soil moisture was kept similar among treatments with daily irrigation – 1 L at initial stages (VE stage and after) and up to 8 L before reproductive stages (before V15) per pot – based on maize water consumption, considering each phenological phase, treatment, and weather (EMBRAPA, 2015). Soil temperature oscillated from 21 to 30°C, and the air temperature inside the greenhouse varied from 21 to 45°C, at daylight hours, during the experimental period.

Gas Sampling and Analyses

Static round-chambers (20-cm inner diameter) were installed in the center of each pot to monitor the differences in gas fluxes during the growth of maize plants until V15. The anchors of the chambers were placed at 5 cm depth from the surface so as not to affect the soil water movement and to ensure the retention of gases in the chambers (Cerri et al., 2013).

Gas samplings were carried out in the morning between 10 a.m. and 12 p.m. (BRT; UTC-3:00) before the beginning of the experiment (Day 0) and at every 72 h after seed sowing until V15 (Days 4, 7, 10, 13, 16, 19, 22, 25, 28, 31, 34, 37, 40, 43, 46, and 49; **Figure 1B**). After attaching the chamber lids on their anchors, gas samples of 20 ml were collected for 45 min (1, 15, 30, and 45 min; i.e., T1, T15, T30, and T45, respectively) from each chamber in plastic syringes to be read (after the gas sampling) in the SRI 8610C gas chromatography instrument (SRI Instruments, United States) that was set to detect methane (CH_4) and CO_2 by a flame ionization detector (FID), and N_2O gas by an electron capture detector (ECD), according to the operating manual of the manufacturer. In addition, a sample of the ambient air at the initial time (T0) of each sampling day was collected as quality control for gas measurement normalization, and air temperature data were collected for gas law correction (Cerri et al., 2013).

Greenhouse gas emissions were evaluated from 1 day before sowing seeds until V15 (50 days) of the development of the maize plants. The emissions of CH_4, CO_2, and N_2O were determined by the mean of total cumulative fluxes from the same treatment, obtained through the linear projection of emission times (T1–T45) from each sampling day and the sum of the results obtained throughout the experimental period (Day 0–49). The values of CH_4 and N_2O were transformed into carbon dioxide equivalent (CO_2 equivalent in g pot^{-1}) by multiplying with 34 and 298, respectively, based on the 100-year global warming potential (GWP_{100}) with climate-carbon feedbacks (IPCC, 2013).

Rhizosphere Soil Sampling and Biomass of Maize Plants

The entire maize plants – V5 (12 plants) and V15 (6 plants) – from each pot were harvested, totalizing 48 samples during the experiment. After sampling, the excess of soil on the plant roots (40 cm length) was removed by shaking, and the soil firmly attached (moistened) by exudates was considered as the rhizosphere. Rhizosphere soil samples from each plant were collected, homogenized, conditioned in 15 ml tubes, fast-frozen using liquid nitrogen (N_2), and stored at −80°C for further analysis. Soil samples were also collected to check physicochemical characteristics at V15 (**Supplementary Table 1**; **Supplementary Figure 1**). Shoots of plants harvested were dried in the oven at 60°C for 5 days and weighted to evaluate the development of plants and biomass gains during the experiment.

Genomic Analysis

For molecular analysis, DNA extraction from 0.5 g of each rhizosphere soil sample was carried out using DNeasyPowerSoil Kit (Qiagen, CA, United States), following the protocol of the manufacturer. The concentration and quality of the DNA samples were evaluated on 1% GelRed-stained agarose gels (electrophoresis conditions of 80 V by 40 min) in sodium boric acid buffer (Brody and Kern, 2004) and on a Nanodrop 2000 c spectrophotometer (Thermo Fisher Scientific, MA, United States). The DNA samples were stored at −20°C for molecular analysis.

Quantitative PCR

Generalist primer sets for functional microbial groups were used in qPCR assays. Primers related to CH_4 and N_2O production and consumption and nitrogen fixation were retrieved from the literature. However, primers associated with the N_2O production – nitric oxide reductase genes (*norB* and *P450nor*) – remained unsatisfactory for a wide range of taxonomic groups (Ma et al., 2019) and were not used in this study. Thus, primers targeting particulate methane monooxygenase (*pmoA*) and methyl-coenzyme M reductase (*mcrA*) genes were selected to evaluate the consumption and production of CH_4, respectively.

Primers targeting nitrous oxide reductase (*nosZ*) and nitrogenase iron protein (*nifH*) genes were selected to evaluate the denitrification of N_2O to dinitrogen (N_2) and the atmospheric N_2 fixation, respectively.

Standard curves for absolute quantification were prepared from serial dilutions containing between 10^5 and 10^0 copies of the target genes, obtained from strains of the German Collection of Microorganisms and Cell Cultures (DSMZ, Germany): *nifH* from *Bradyrhizobium japonicum* (DSMZ 30131), *nosZ* from *Paraburkholderia phymatum* (DSMZ 17167), *mcrA* from *Methanolinea mesofila* (DSMZ 23604), and *pmoA* from *Methylosinus sporium* (DSMZ 17706).

Quantitative PCR assays from the samples of V5 and V15 were carried out, under modified thermal cycling conditions (**Supplementary Table 2**), in triplicates containing 1X Maxima SYBR Green/ROX qPCR Master Mix (2X; Thermo Fisher Scientific, Vilnius, Lithuania), 1.0 μm of each universal primer (**Supplementary Table 2**), 10 ng of DNA, and ultrapure deionized water to complete 10 μl. All qPCR assays were carried out in a StepOnePlus Real-Time PCR System instrument (Applied Biosystems, MA, United States) and analyzed using the StepOne Software v2.3, reaching efficiency between 90 and 100% and 0.99 of pipetting error. Gene abundance comparisons were performed relative to each other using the initial amount of sample DNA as a normalization parameter among treatments and considered in the calculations.

16S rRNA Amplicon Sequencing

The taxonomic composition of microbial communities influenced by the treatments at V15 (24 samples) was investigated by 16S rRNA amplicon sequencing. For this, PCRs were carried out containing 1X Phusion Hot Start II High-Fidelity PCR Master Mix (2X; Thermo Fisher Scientific, MA, United States), 0.5 μm of each primer set (forward + reverse for each sample, as described in **Supplementary Table 3**) for the V4 region from the Earth Microbiome Project (EMP),[2] 1 μl of DNA, and ultrapure deionized water to complete 20 μl. The thermal cycling conditions were 30 s of denaturation at 98°C, followed by 27 rounds of temperature cycling (98°C for 30 s, 50°C for 30 s, and 72°C for 20 s) and a final extension at 72°C for 7 min. All reactions were carried out in a C1000 Touch™ Thermal Cycler with Dual 48/48 Fast Reaction Module (Bio-Rad, CA, United States). Aliquots (5 μl) of the PCR products were checked on 1% GelRed-stained agarose gels running at 80 V for 40 min and quantified using Qubit 2.0 Fluorometer (Invitrogen, MA, United States) following the instructions of the manufacturer. All PCR products were purified using QIAquick PCR Purification Kit (Qiagen, Hilden, Germany) following the instructions of the manufacturer. The purified PCR products were sent to the Genome Center Facility of the University of California Davis (Davis, CA, United States) for paired-end amplicon sequencing (2 × 250 bp) in a HiSeq 2500 platform (Illumina Inc., CA, United States).

Computational and Statistical Analysis

The gas fluxes were analyzed by Shapiro–Wilk and Kolmogorov–Smirnov normality tests and Levene's homogeneity test in order to define the most appropriate statistical test to be used to evaluate differences among treatments. Two-way analysis of variance (ANOVA) followed by the Tukey Honest Significant Difference (HSD) *post-hoc* test for multiple comparisons at $p < 0.05$ were performed using the agricolae package v1.2-8 (Mendiburu, 2017). For non-parametric data, Kruskal–Wallis with the *post-hoc* Dunn's test from the dunn.test package v1.3.5 (Dinno, 2017) was implemented, all in R-statistical environment (version 3.4.3.; R Core Team, 2017).

Comparisons of plant biomass, soil physicochemical properties, and gene abundance were also performed by two-way ANOVA, as previously described.

Raw nucleotide sequences of 16S rRNA amplicons were analyzed using Qiime2 microbiome bioinformatics platform version 2018.8 (Bolyen et al., 2019). Sequences were treated using dada2 version 2017.6.0 (sequences were maintained if $Q > 30$, truncated to 175 bp, and chimeric filtered; Callahan et al., 2016), then rarefied to 50,000 sequences and aligned to Silva 132 release database (Quast et al., 2013) based on 99% sequence identity as the taxonomic reference. Raw sequences were deposited in the SRA database (accession number PRJNA495686).

Diversity indices were calculated from the aligned sequences at the order level using Qiime2. Non-metric multidimensional scaling (NMDS) analysis (Bray-Curtis) and phylogenetic (weighted UniFrac) were generated using vegan v2.4-6 (Oksanen et al., 2017) and ape v5.0 (Paradis et al., 2004) packages and plotted using ggplot2 v2.2.1 (Wickham, 2009) in R-statistical environment (R Core Team, 2017).

STAMP v2.1.3 (Parks et al., 2014), a graphical software for statistical analysis of taxonomical and functional profiles, was used to determine statistical differences among rhizosphere-soil treatments. The values of p were calculated using Welch's t-test two-sided with Welch's inverted method to calculate confidence intervals at 95%. The Storey False Discovery Rate (FDR) multiple test correction was applied ($p < 0.05$) with an effect size filter of difference between proportions ($DP < 1.00$).

RESULTS

Gas Emissions

As a reference, total GHG emissions in the control group were equivalent to 435.79 ± 11.73 g pot^{-1} in CO_2 equivalent (**Figure 2A**). Carbon dioxide fluxes from soils were higher than N_2O and CH_4 fluxes in all treatments.

Considering the total sum of GHG emissions (**Figure 2A**), treatments containing *A. brasilense* (I/FI/IS/FIS) presented, respectively, with a reduction of 11.9, 8.4, 16.2, and 1.6% in emissions compared to its "control treatment" without the inoculant (C, F, S, and FS, respectively), with the IS treatment demonstrating the most pronounced effect of GHG mitigation ($p < 0.05$). The GHG emissions obtained from the urea-topdressing fertilization treatments compared to the other groups

---

[2] https://earthmicrobiome.org/

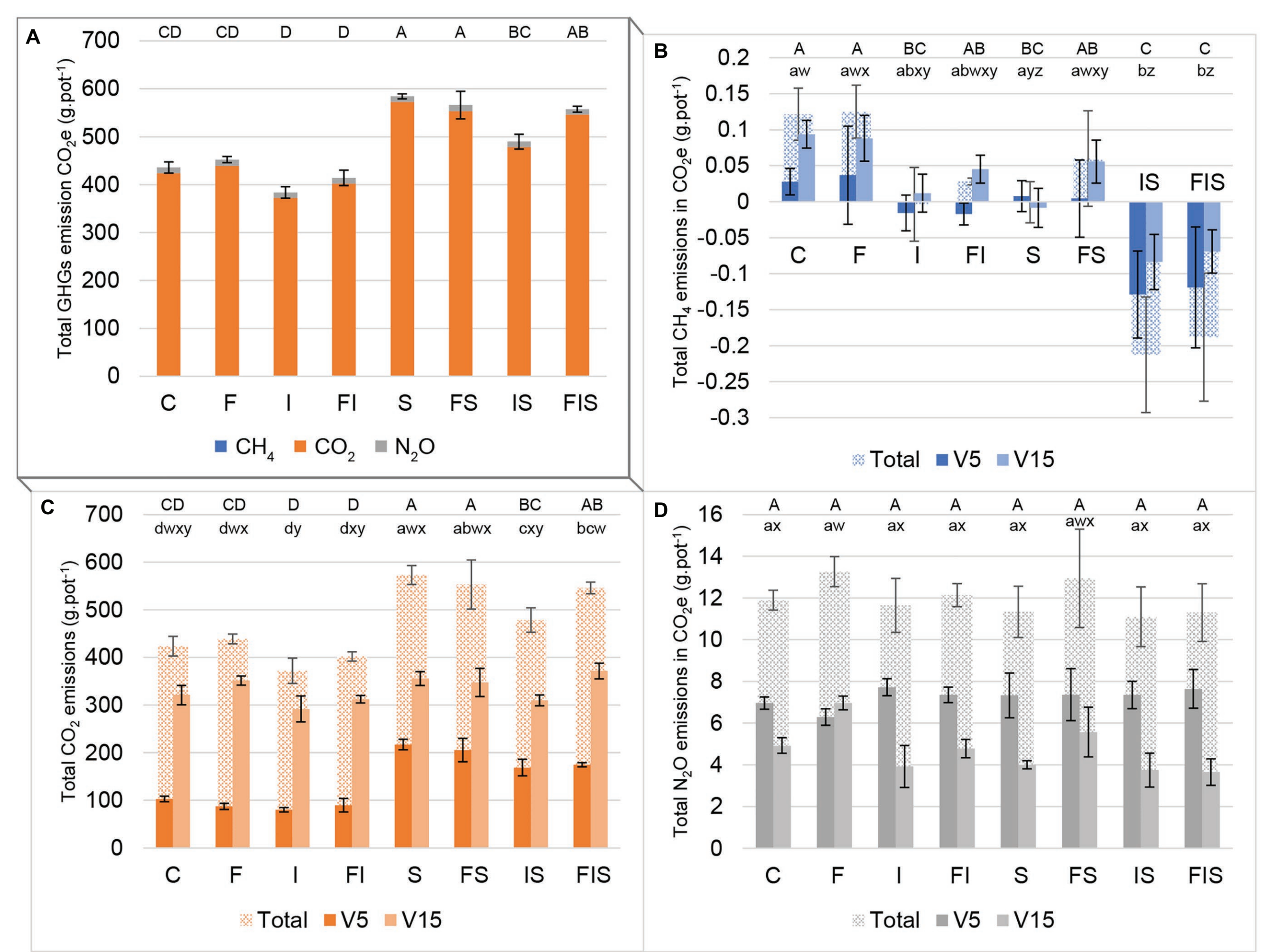

FIGURE 2 | Emissions in carbon dioxide equivalent (CO_2 equivalent) from the maize soil-rhizosphere experiment: **(A)** sum of all three main GHGs, **(B)** methane (CH_4), **(C)** carbon dioxide (CO_2), and **(D)** nitrous oxide (N_2O). Bars with the same letter are not significantly different ($p < 0.05$). Three groups of series of letters compare treatments: uppercase letters (ABCD) on the top of bars compare differences among total emissions of the entire experiment; lowercase letters close to bars compare each stage period (*abcd* for V5 and *wxyz* for V15). V5 includes accumulated gas measurements before the rhizosphere sampling at V5, while V15 includes accumulated gas measurements between both rhizosphere sampling times (V5 and V15). Total bars are the sum of both periods (V5 and V15). Treatments: C, Control; F, Urea-topdressing fertilization at V5; I, *A. brasilense* inoculant on seeds sowing; FI, F + I; S, Maize stover coverage; FS, F + S; IS, I + S; FIS, F + I + S.

(i.e., F:C, FI:I, FS:S, and FIS:IS) varied 3.8, 7.9, −3.1%, and 13.8%, respectively. Finally, the treatments influenced by stover (i.e., S, FS, IS, and FIS), strongly increased the GHG emissions by 34.1, 25.2, 27.5, and 34.5% in comparison to the other treatments (i.e., C, F, I, and FI).

Analyzing individually (**Figures 2B–D**), treatments, I and FI presented a tendency to reduce CH_4 emissions before V5, while the S treatment presented the same tendency after V5. This tendency of reduction of CH_4 from I, FI, and S treatments was potentialized and become significant when combined in IS and FIS treatments, before and after V5 (**Figure 2B**).

The CO_2 measurements (**Figure 2C**) showed that S treatments (i.e., S, FS, IS, and FIS) are related to increments in gas emissions until V5. However, I treatments except for FIS (i.e., I, FI, and IS) presented reduced emissions after V5 in comparison to the other treatments.

Comparisons between F treatments and their "control treatment" (i.e., F:C, FI:I, FS:S, and FIS:IS) after V5, urea-topdressing fertilizer significantly increased by 41.4% N_2O emissions (**Figure 2D**) in F:C comparison ($p < 0.01$) and showed a slight increment of 39.2% in FS:S comparison. However, increment differences in FI:I and FIS:IS comparisons were not significant, with 21.9 and 2.5%, respectively.

Maize Plant Biomass

At V5, maize plants from IS and FIS treatments (identical treatments before the urea-topdressing fertilization) showed a tendency for the highest gains in plant biomass – i.e., highest individual plant biomass gain. However, the average increases were not different from others ($n = 12$), probably due to the influence of the initial fertility correction. This tendency of plant biomass gains raised at V15, and both IS and FIS

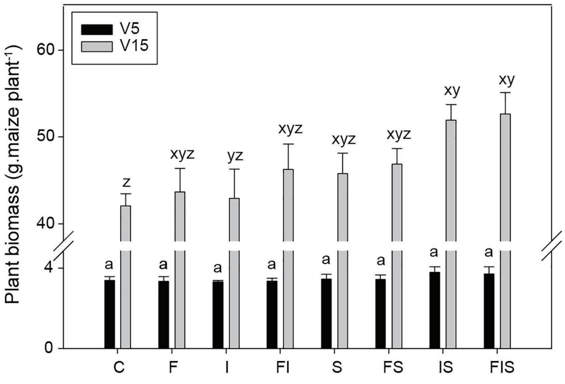

FIGURE 3 | Biomass average of maize plants collected at V5 (n = 12) and V15 (n = 6). Bars with the same letter are not significantly different ($p < 0.05$). Two groups of series of letters compare treatments from distinctly stage periods (*a* for V5 and *xyz* for V15). Treatments: C, Control; F, Urea-topdressing fertilization at V5; I, *A. brasilense* inoculant on seeds sowing; FI, F + I; S, Maize stover coverage; FS, F + S; IS, I + S; FIS, F + I + S.

treatments presented a significant increase in biomass ($n = 6$; $p < 0.05$), with 23.4 and 25.2% more than C condition, respectively (**Figure 3**). However, they were considered similar to the other treatments.

Quantitative PCR

At V5, the average number of copies per gram of soil (copies.g soil^{-1-1}) ranged from 6.64×10^3 to 5.52×10^4 for the *mcrA* gene; from 3.28×10^3 to 6.38×10^3 for *pmoA*; from 9.07×10^4 to 2.60×10^5 for *nifH*; and from 3.26×10^4 to 2.48×10^5 for *nosZ*. In comparison, the quantification of V15 samples ranged from 5.67×10^2 to 2.04×10^3 for the *mcrA* gene; from 3.35×10^3 to 9.50×10^3 for *pmoA*; from 1.67×10^3 to 1.32×10^5 for *nifH*; and from 4.81×10^4 to 1.75×10^5 for *nosZ* (**Supplementary Figure 2**).

In general, the S treatments (S, FS, IS, and FIS) contained more copies of the *mcrA* gene (above 4.00×10^4copies.g soil^{-1}) than the other treatments at V5, and *pmoA* (above 7.00×10^3copies.g soil^{-1}) at V15. However, all treatments

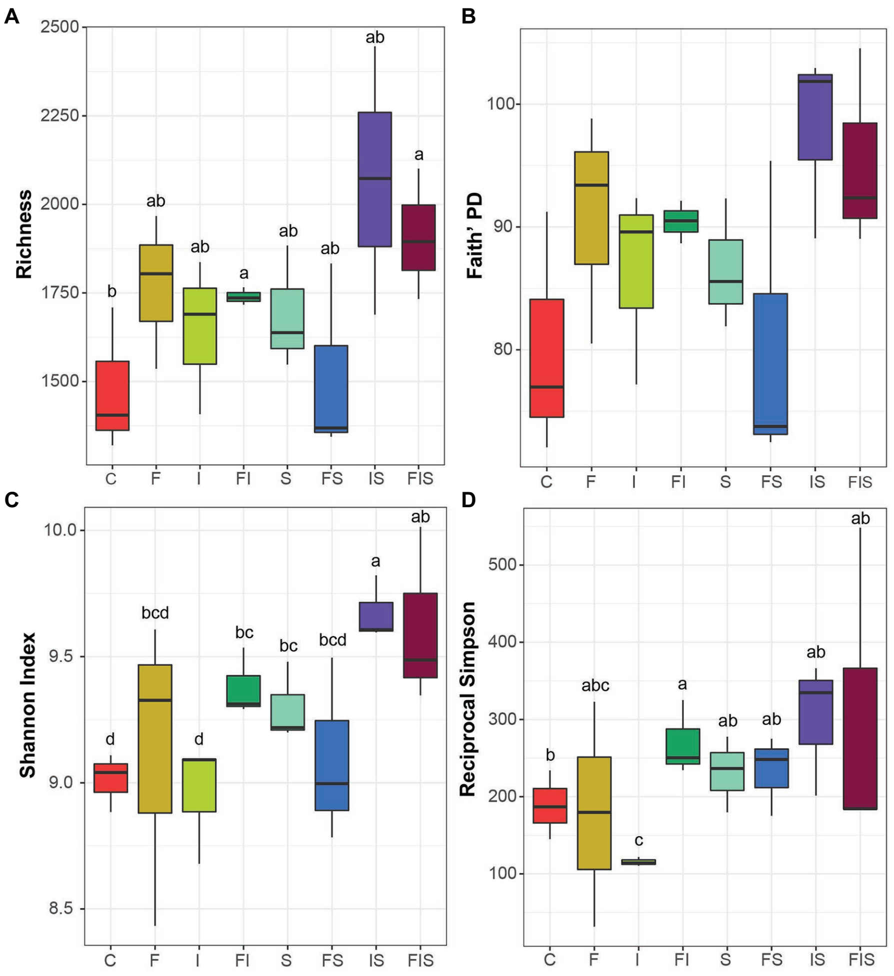

FIGURE 4 | Alpha diversity boxplots from the rhizosphere microbial communities (order level) at the V15 stage: **(A)** total species richness, **(B)** Faith's phylogenetic diversity, **(C)** Shannon index, and **(D)** Reciprocal Simpson index (1/D). Boxplots with the same letter or in absence are not significantly different ($p < 0.05$). Treatments: C, Control; F, Urea-topdressing fertilization at V5; I, *A. brasilense* inoculant on seeds sowing; FI, F + I; S, Maize stover coverage; FS, F + S; IS, I + S; FIS, F + I + S.

presented a small number of copies (up to 2.04×10^3copies.g soil^{-1}) of *mcrA* at V15.

Nevertheless, differences with undistinguishable patterns between the sampling times (V5 and V15) among treatments were observed for all genes (**Supplementary Table 2**).

Alpha and Beta Diversity Analyses

Rarefaction curves demonstrated sufficient sequencing coverage for each sample (**Supplementary Figure 3**). The number of amplicon sequence variants (ASVs) reached an asymptote for all treatments. Alpha diversity indices presented a considerable variability among treatment replicates with few significant differences (**Figure 4**), except for the comparisons (in general) against IS and FIS treatments. The abundance of ASVs was greater in IS and FIS than in C condition, and other treatments had intermediate diversity. This result shows that IS and FIS treatments tended to differ from the others.

Taxonomic (Bray-Curtis-R = 0.4157, $p < 0.002$) and phylogenetic (weighted UniFrac-R = 0.461, $p < 0.001$) approaches used to estimate community dissimilarities and beta diversity among rhizosphere-soil samples (**Figure 5**) demonstrated that IS and FIS were distinctly grouped from all other treatments.

Structure of Microbial Communities

A total of 10,497 ASVs were classified and distributed in 38 phyla, using Silva 132 99% database (Quast et al., 2013; **Figure 6**). The most abundant classes (>5% at least in one treatment), include Acidobacteriia, Actinobacteria, Alphaproteobacteria, Bacilli, Gammaproteobacteria, Gemmatimonadetes, and Thermoleophilia (**Table 1**), with significant increments of Actinobacteria (19.0%) and Bacilli (17.3%) in IS treatment, and Bacilli (9.7%) in FIS treatment.

At the class level, microbial taxa that significantly changed in abundance in IS compared to all other treatments, including Actinobacteria (19%), Alphaproteobacteria (12.8%), Bacilli (10%), Acidobacteriia (5.1%), Gemmatimonadetes (4.2%), Verrucomicrobiae (2%), and Bacteroidia (1.1%), with special attention to the increments of Actinobacteria and Bacilli in IS (**Figure 7A**). The FIS treatment had a significant reduction in Alphaproteobacteria (10.9%), Acidobacteriia (5%), Bacilli (11.5%), Gemmatimonadetes (3.7%), and Verrucomicrobia (1.5%) compared to all other treatments (**Figure 7B**).

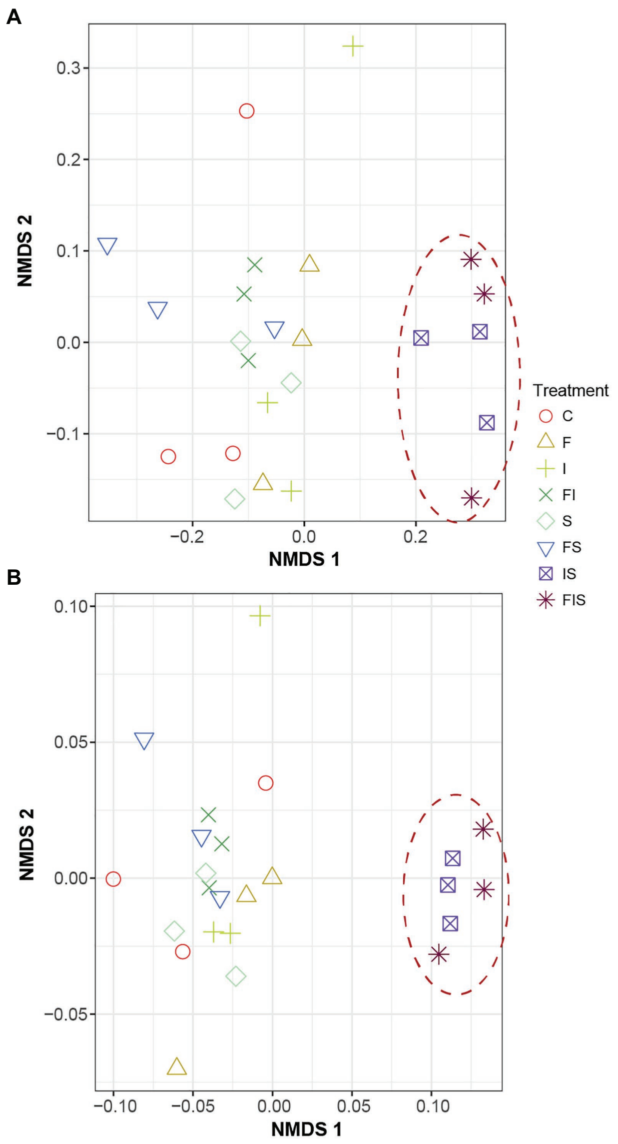

FIGURE 5 | Non-metric multidimensional distance scaling (NMDS) analysis of the composition of the rhizosphere microbial communities among treatments at V15. **(A)** Taxonomic similarity (Bray-Curtis) and **(B)** phylogenetic similarity (weighted UniFrac). Treatments: C, Control; F, Urea-topdressing fertilization at V5; I, *A. brasilense* inoculant on seeds sowing; FI, F + I; S, Maize stover coverage; FS, F + S; IS, I + S; FIS, F + I + S.

DISCUSSION

Our results showed a high baseline effect promoted by the initial NPK fertilization in the furrow before seed sowing, which restricted our findings to each input effect. Even with this baseline, the effect of the inputs on treatments containing *A. brasilense* inoculant showed a reduction of soil CH_4 emissions after V15 and before V5 to CO_2 emissions. In addition, a tendency for plant biomass increases at V15 was also observed (maize plants are not fully grown at this stage, presenting early kernel development, which means only a prediction of plant biomass potential for the mature kernel stage). Such an effect is consistent with the expected benefit promoted by this PGPR, which can reduce nitrate and produce phytohormones like auxins – for example, indole-3-acetic acid (IAA; Bothe et al., 1992; Costacurta et al., 1994; Bashan et al., 2004), thus stimulating plants for a better root system development at initial stages and preparing them to an open-wide nutrient intake system for the subsequent reproductive stages (Vacheron et al., 2013; EMBRAPA, 2015).

Apparently, *A. brasilense* interactions with other microbes in rhizosphere communities respond to the maize stover addition and can reduce carbon-based GHG (CH_4 and CO_2) emissions.

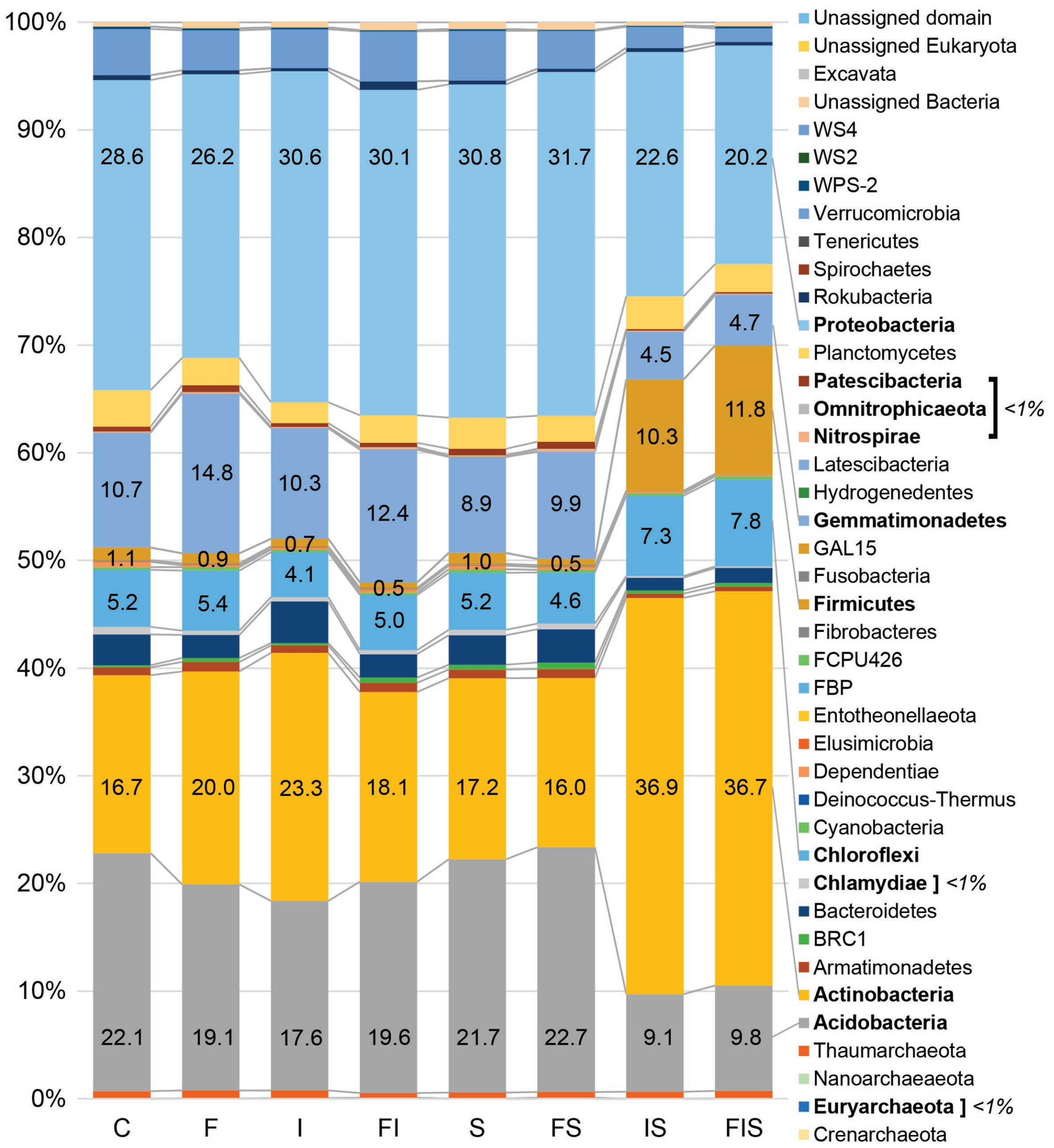

FIGURE 6 | Relative abundances of the microbial communities at the phylum level from the 16S rRNA sequencing from the rhizosphere at V15 (n = 3). Sequences ($Q > 30$) were aligned against Silva 132 99% database using Qiime2 software platform version 2018.8 (https://qiime2.org/). Bars with percentages and names in bold are the most representative and significant phyla ($p < 0.05$). Treatments: C, Control; F, Urea-topdressing fertilization at V5; I, *A. brasilense* inoculant on seeds sowing; FI, F + I; S, Maize stover coverage; FS, F + S; IS, I + S; FIS, F + I + S.

This was possibly the same phenomenon observed by Steinweg et al. (2008) as a consequence of carbon-use efficiency that has been increasing the soil carbon assimilation throughout the years (Allison et al., 2010). Despite the similar results of N_2O among treatments, the growth promotion of the root system stimulated by *A. brasilense* (Costa et al., 2015) can contribute to nitrogen-use efficiency by plants from nitrogen inputs, removing nitrogen availability to denitrification pathways and allowing plant biomass gains as verified in-fields condition (Araújo et al., 2015). These carbon and nitrogen use efficiencies are correlated to a variation in the C:N ratio, serving as indicators of ecological stoichiometry, which can be used to monitor crop field conditions (Agren, 2004).

Although the presence of *A. brasilense* was not observed (data not shown) in our 16S rRNA amplicon sequencing data at the V15 sampling time, its benefits combined with the maize stover addition were determinant for biomass gains. In this case, the activation of the inoculation effects in our experiment occurred before V15, and *A. brasilense* may have been replaced by other microorganisms. In addition, Bonkowski et al. (2021)

TABLE 1 | The most abundant classes in treatments (more than 5% in at least one treatment).

Class	Control (C)	Fertilizer (F)	Inoculant (I)	F + I (FI)	Stover (S)	F + S (FS)	I + S (IS)	F + I + S (FIS)
Acidimicrobiia	1.2%	1.7%	1.5%	1.7%	1.6%	1.8%	1.6%	1.6%
Acidobacteriia*	16.1%	12.8%	11.7%	11.7%	15.7%	17.0%	5.1%	5.0%
Actinobacteria*	5.2%	5.6%	10.9%	5.8%	6.0%	5.3%	19.0%	17.3%
Alphaproteobacteria*	15.4%	13.8%	17.1%	15.7%	17.7%	17.8%	12.8%	10.9%
Bacilli*	1.1%	0.9%	0.7%	0.5%	1.0%	0.5%	10.0%	9.7%
Bacteroidia*	2.5%	1.9%	3.7%	2.0%	2.5%	2.8%	1.1%	1.0%
Blastocatellia (Subgroup 4)*	1.6%	2.1%	1.9%	2.2%	1.5%	1.6%	0.9%	1.0%
Deltaproteobacteria*	2.9%	3.5%	3.4%	3.7%	3.0%	2.8%	2.5%	2.6%
Gammaproteobacteria	10.5%	9.0%	10.3%	10.7%	10.2%	11.3%	7.4%	7.8%
Gemmatimonadetes*	10.2%	14.5%	10.0%	12.1%	8.5%	9.4%	4.2%	3.7%
KD4-98*	1.3%	1.0%	1.0%	1.6%	1.3%	1.1%	1.9%	2.1%
Ktedonobacteria	1.7%	2.0%	1.4%	1.3%	1.7%	1.2%	2.7%	2.4%
Planctomycetacia*	2.7%	1.8%	1.5%	1.7%	2.2%	1.6%	2.6%	2.5%
Subgroup 6	3.7%	3.5%	3.2%	4.3%	3.3%	3.0%	2.6%	3.6%
Thermoleophilia	9.7%	12.1%	10.2%	9.4%	8.8%	8.2%	15.7%	18.0%
Verrucomicrobiae*	4.3%	3.7%	3.6%	4.6%	4.6%	3.5%	2.0%	1.5%
Others	9.8%	10.1%	8.1%	10.8%	10.3%	10.9%	8.0%	9.3%

*Significant difference at $p < 0.05$.

reported that the influence of plant growth stages is more significant than the fertilization level on the microbial community shift. Besides, the mature time of different roots and their rhizo deposits play an important role in microbiome assembly, which can cause the fluctuation in gene quantifications, as observed in our study.

On average, amendments of maize stover coverage since the beginning of the experiment (S treatments) stimulate a better development of maize plants (**Figure 3**) and can incite groups of microorganisms (Actinobacteria, Firmicutes, and Proteobacteria), allowing them to rise as a dominant later, as observed at V15 in the 16S rRNA amplicon sequencing profile. So, maize stover provides nutrients in favor of the bioaugmentation of these microbial groups as a prebiotic compound. On the other hand, maize stover decomposition seems to be primarily responsible for the increase in CO_2 emissions during the entire experiment. However, these CO_2 emissions from soils were reduced in the interaction of maize stover coverage with *A. brasilense* (IS treatment) among all combinations with stover coverage, mainly after V5. The increase of soil CO_2 emissions could be an advantage for plant photosynthesis with the rapid availability of this gas for plant growth (Bond-Lamberty and Thomsom, 2010). Also, CO_2 emissions might act as an offset to other GHG emissions due to the equilibrium of microbial activities (Liu and Greaver, 2009), as observed in our experiments with low levels of CH_4 and N_2O in comparison to CO_2. Even though no significant differences were found in IS at V15 compared to the other treatments, the biomass of the plant could reach around 3.12 tons in-field conditions for IS, which means an increment of 0.6 tons and 0.34 tons compared to C and FI (the second in biomass gains at lower GHG emissions), respectively. It is worth mentioning that FIS was discarded from this in-field calculation for using more input with a small increment of 0.04 tons in comparison to IS. Small increments of each plant can improve biomass gains on a larger scale (60,000 plants ha^{-1}), especially if the production has reached through low-cost management, such as the use of microbial inoculants (Santini et al., 2018).

Yang et al. (2017) also found a reduction in CO_2 emissions (~4.5%) in treatments with biochar in comparison to maize stover, as amendments in maize crop. Biochar has a structural reordination of lignocellulose chains (after pyrolysis) that allows being colonized by beneficial groups of microorganisms (e.g., Proteobacteria, Actinobacteria, and Firmicutes) as found by Cannavan et al. (2016). However, Actinobacteria and Firmicutes were likely favored by the inoculation of *A. brasilense* and plant residues, increasing their abundance in IS and FIS treatments (**Figure 6**). Functionally, the maize rhizosphere actively selects groups from bulk soil that acts on carbon fixation and degradation, among other pathways, including exopolysaccharides and antibiotic production, to control soil-borne pathogens (Li et al., 2014). These functional groups are expected to be promoted since maize roots exudate, considering their production and composition, can largely support the microbiota demands (Carvalhais et al., 2011; Li et al., 2014). The favored bacterial groups that distinguished IS and FIS

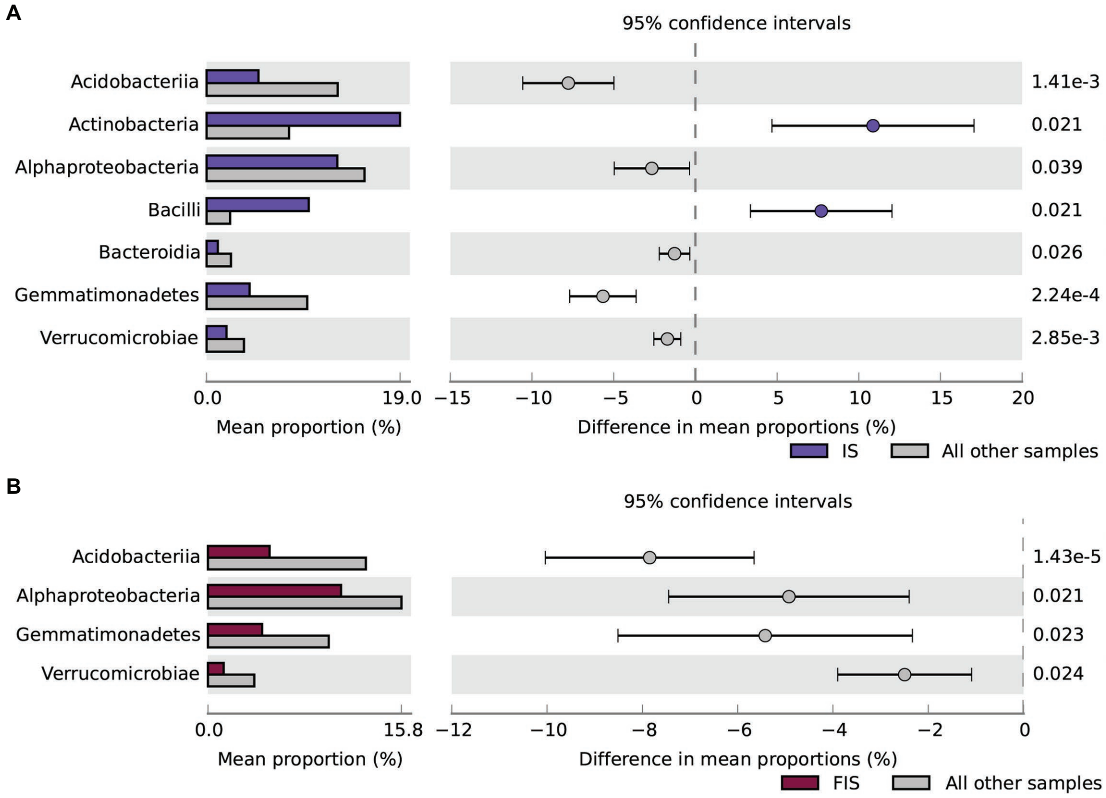

FIGURE 7 | Statistical differences of representative microbial communities at the class level from the rhizosphere at V15. **(A)** *A. brasilense* inoculant at seed sowing + Maize stover coverage (IS) against all other treatments; **(B)** Urea-topdressing fertilization at V5 + *A. brasilense* inoculant at seed sowing + Maize stover coverage (FIS) against all other treatments. Classes overrepresented in IS and FIS (colored/dark) correspond to positive differences among proportions, and other samples (gray/light) correspond to negative differences among proportions. Error bars are the standard deviations. The *q*-values were calculated using the Storey FDR approach ($p < 0.05$) with effect size filter in difference among proportions ($DP < 1.00$).

treatments from others (**Figure 6**) can act, indirectly, on the rhizosphere structure due to their influence as tenacious substrate competitors and antimicrobial producers. Besides, these groups have the ability of sporulation to survive in adverse conditions, such as drought. All these characteristics could make classes like Actinobacteria and Bacilli persistent in the environment (**Figure 7A**) – Actinobacteria are known as antibiotic producers, saprophytes, and PGPR (Doumbou et al., 2001), while Bacilli are PGPR, cellulose, and hemicellulose degraders, biosurfactants, and carotenoids producers, and act as biopesticides (Lee et al., 2008; Di Pasqua et al., 2014). However, the abundance of Acidobacteria dropped down in IS, an unexpected behavior of a ubiquitous and versatile class of microorganisms, which participate in carbohydrate and nitrogen metabolism (Kielak et al., 2016; Eichorst et al., 2018). All these functions need to be accessed using more detailed molecular approaches to evaluate these treatment interactions and identify the microorganisms at a more specific taxonomic level. Overall, the three factors evaluated separately (i.e., single-variable treatments) showed that: (a) urea-topdressing fertilization increased N_2O emissions around 1-week after the application, as also reported by Calvo et al. (2016); (b) the inoculant, *A. brasilense* induced the reduction of CH_4 and CO_2 emissions; and (c) maize stover coverage showed an increment for CO_2 emissions.

Following these patterns, when the inputs were combined, their effects were potentialized or merged: (a) the FI treatment showed intermediate values (between F and I treatments) of total CO_2 and N_2O emissions; (b) FS showed similar N_2O and CO_2 emissions in comparison to F and S treatments, respectively; (c) FIS merged patterns of GHG emissions from F, I, and S treatments; however, for CH_4, FIS potentialized the responses of I and S for emission reduction, with the advantage of higher levels of biomass gains; and (d) the IS treatment showed similar positive responses to FIS, with the inoculant influence on the reduction of CO_2 emissions, therefore rising as the best production treatment with low-cost input for higher biomass production and less GHG emissions. In conclusion, this study revealed the effects of input combinations on the maize soil-rhizosphere microbiota and GHG fluxes. The combination of microbial inoculant and maize stover coverage was found to be the best input option, aiming for high biomass production of maize plants with the beneficial reduction of CO_2 equivalent emissions of the main GHGs. In addition, the microbial structure presented increments in the abundance of taxa related to carbon fixation, lignocelluloses degradation, and antibiotic production that might be responsible for GHG mitigation. Through our results related to the structure of the microbial communities, the stover coverage was pointed out as one of the responsible factors modulating microbial GHG fluxes, which should be evaluated using other more specific omics tools, such as metatranscriptomics and metaproteomics. Finally, it is worth mentioning that Glass and Orphan (2012) have tracked the composition of each enzyme related to CH_4 and N_2O pathways, indicating iron (Fe) and copper (Cu) as essential metal cofactors that might be explored in future research.

DATA AVAILABILITY STATEMENT

The original contributions presented in the study are publicly available. This data can be found at: The sequences are deposited in Sequence Read Archive (SRA) repository, the accession number is PRJNA495686, and the link is https://www.ncbi.nlm.nih.gov/bioproject/PRJNA495686/.

AUTHOR CONTRIBUTIONS

CY, LB, and ST conceived the project and designed the experiment. CY performed the greenhouse experiment. CY, AV, AF, and ML performed the molecular analyses. CY, LB, AV, and AF analyzed and contributed to interpreting the data. CY, LB, and AV wrote the manuscript. ST and JR critically reviewed the manuscript. All authors contributed to the article and approved the submitted version.

FUNDING

This work was financially supported by Fundação de Amparo à Pesquisa do Estado de São Paulo (FAPESP – NSF-BIOTA Thematic Project grant 2014/50320-4 and the grant no. Fellowships 2013/22845-2, 2015/08564-6, 2015/13546-7, 2015/19979-2, 2016/11268-2, and 2019/25931-3), the National Science Foundation – Dimensions of Biodiversity DEB 14422214, Conselho Nacional de Desenvolvimento Científico e Tecnológico (CNPq – grant no. Fellowships 149662/2014-9, 140032/2015-0, and 311008/2016-0), and the Coordenação de Aperfeiçoamento de Pessoal de Nível Superior – Brasil (CAPES) – Finance code 001.

ACKNOWLEDGMENTS

The authors would like to thank Karine Calderan Yoshiura for the indispensable help during the greenhouse experiment and organization of samples, the laboratory technician Wagner Picinini for the greenhouse experiment assembling, and Stoller do Brasil LTDA that provided the free sample of microbial inoculant for the experiment at our request.

SUPPLEMENTARY MATERIAL

The Supplementary Material for this article can be found online at: https://www.frontiersin.org/articles/10.3389/fpls.2021.683658/full#supplementary-material

REFERENCES

Abalos, D., Smith, W. N., Grant, B. B., Drury, C. F., MacKell, S., and Wagner-Riddle, C. (2016). Scenario analysis of fertilizer managements practices for N_2O mitigation from corn systems in Canada. *Sci. Total Environ.* 573, 356–365. doi: 10.1016/j.scitotenv.2016.08.153

Abbott, L. K., Macdonald, L. M., Wong, M. T. F., Webb, M. J., Jenkins, S. N., and Farrell, M. (2018). Potential roles of biological amendments for profitable grain production – a review. *Agric. Ecosyst. Environ.* 256, 34–50. doi: 10.1016/j.agee.2017.12.021

Agren, G. I. (2004). The C:N:P stoichiometry of autotrophs – theory and observations. *Ecol. Lett.* 7, 185–191. doi: 10.1111/j.1461-0248.2004.00567.x

Allison, S. D., Wallenstein, M. D., and Bradford, M. A. (2010). Soil-carbon response to warming dependent on microbial physiology. *Nat. Geosci.* 3, 336–340. doi: 10.1038/ngeo846

Angel, R., Claus, P., and Conrad, R. (2012). Methanogenic archaea are globally ubiquitous in aerated soils and become active under wet anoxic conditions. *ISME J.* 6, 847–862. doi: 10.1038/ismej.2011.141

Araújo, E. D. O., Martins, M. R., Vitorino, A. C. T., Mercante, F. M., and Urquiaga, S. G. (2015). Effect of nitrogen fertilization associated with diazotrophic bacteria inoculation on nitrogen use efficiency and its biological fixation by corn determined using 15N. *Afr. J. Microbiol. Res.* 9, 643–650. doi: 10.5897/AJMR2014.7072

Backer, R., Stefan Rokem, J., Ilangumaran, G., Lamont, J., Praslickova, D., Ricci, E., et al. (2018). Plant growth-promoting rhizobacteria: context, mechanisms of action, and roadmap to commercialization of biostimulants for sustainable agriculture. *Front. Plant Sci.* 9:1473. doi: 10.3389/fpls.2018.01473

Barbarena, I. M., Espindula, M. C., Araújo, L. F. B., and Marcolan, A. L. (2019). Use of urease inhibitors to reduce ammonia volatilization in Amazonian soils. *Pesq. Agropec. Bras.* 54:e00253. doi: 10.1590/s1678-3921.pab2019.v54.00253

Bashan, Y., De-Bashan, L. E., Prabhu, S., and Hernandez, J.-P. (2014). Advances in plant growth-promoting bacterial inoculant technology: formulations and practical perspectives (1998–2013). *Plant Soil* 378, 1–33. doi: 10.1007/s11104-013-1956-x

Bashan, Y., Holguin, G., and de-Bashan, L. E. (2004). Azospirillum-plant relationships: physiological, molecular, agricultural, and environmental advances (1997–2003). *Can. J. Microbiol.* 50, 521–577. doi: 10.1139/w04-035

Bloemberg, G. V., and Lugtenberg, B. J. J. (2001). Molecular basis of plant growth promotion and biocontrol by rhizobacteria. *Curr. Opin. Plant Biol.* 4, 343–350. doi: 10.1016/S1369-5266(00)00183-7

Bolyen, E., Rideout, J. R., Dillon, M. R., Bokulich, N. A., Abnet, C. C., Al-Ghalith, G. A., et al. (2019). Reproducible, interactive, scalable and extensible microbiome data science using QIIME 2. *Nat. Biotechnol.* 37, 852–857. doi: 10.1038/s41587-019-0209-9

Bond-Lamberty, B., and Thomsom, A. (2010). Temperature-associated increases in the global soil respiration record. *Nature* 464, 579–582. doi: 10.1038/nature08930

Bonkowski, M., Cheng, W., Griffiths, B. S., Alphei, J., and Scheu, S. (2000). Microbial-faunal interactions in the rhizosphere and effects on plant growth. *Eur. J. Soil Biol.* 36, 135–147. doi: 10.1016/S1164-5563(00)01059-1

Bonkowski, M., Tarkka, M., Razavi, B. S., Schmidt, H., Blagodatskaya, E., Koller, R., et al. (2021). Spatiotemporal dynamics of maize (*Zea mays* L.) root growth and its potential consequences for the assembly of the rhizosphere microbiota. *Front. Microbiol.* 12:619499. doi: 10.3389/fmicb.2021.619499

Bortoletto-Santos, R., Guimarães, G. G. F., Roncato Junior, V., Cruz, D. F., Polito, W. L., and Ribeiro, C. (2019). Biodegradable oil-based polymeric coatings on urea fertilizer: N release kinetic transformations of urea in soil. *Sci. Agric.* 77:e20180033. doi: 10.1590/1678-992x-2018-0033

Bothe, H., Korsgen, H., Lehmacher, T., and Hundeshagen, B. (1992). Differential effects of *Azospirillum*, auxin and combined nitrogen on the growth of the roots of wheat. *Symbiosis* 13, 167–179.

Brasil (2016). Ministério da Ciência, Tecnologia e Inovação. Secretaria de Políticas e Programas de Pesquisa e Desenvolvimento. Coordenação-Geral de Mudanças Globais de Clima. Terceira Comunicação Nacional do Brasil à Convenção-Quadro das Nações Unidas sobre Mudança do Clima – Volume III/ Ministério da Ciência, Tecnologia e Inovação. Brasília: Ministério da Ciência, Tecnologia e Inovação. ISBN: 978-85-88063-19-8.

Brody, J. R., and Kern, S. E. (2004). Sodium boric acid: a Tris-free, cooler conductive medium for DNA electrophoresis. *Biotechniques* 36, 214–216. doi: 10.2144/04362BM02

Busari, M. A., Kukal, S. S., Kaur, A., Bhatt, R., and Dulazi, A. A. (2015). Conservation tillage impacts on soil, crop and the environment. *Int. Soil Water Conserv. Res.* 3, 119–129. doi: 10.1016/j.iswcr.2015.05.002

Callahan, B. J., McMurdie, P. J., Rosen, M. J., Han, A. W., Johnson, A. J. A., and Holmes, S. P. (2016). DADA2: high-resolution sample inference from Illumina amplicon data. *Nat. Methods* 13, 581–583. doi: 10.1038/nmeth.3869

Calvo, P., Watts, D. B., Kloepper, J. W., and Torbert, H. A. (2016). The influence of microbial-based inoculants on N_2O emissions from soil planted with corn (*Zea mays* L.) under greenhouse conditions with different nitrogen fertilizer regimens. *Can. J. Microbiol.* 62, 1041–1056. doi: 10.1139/cjm-2016-0122

Cambouris, A. N., Ziad, N., Perron, I., Alotaibi, K. D., Luce, M. S., and Tremblay, N. (2016). Corn yield components response to nitrogen fertilizer as a function of soil texture. *Can. J. Soil Sci.* 96, 386–399. doi: 10.1139/cjss-2015-0134

Cancellier, E. L., Silva, D. R. G., Faquin, V., Gonçalves, B. A., Cancellier, L. L., and Spehar, C. R. (2016). Ammonia volatilization from enhanced-efficiency urea on no-till maize in braziliancerrado with improved soil fertility. *Ciênc. Agrotrec.* 40, 133–144. doi: 10.1590/1413-70542016402031115

Cannavan, F. S., Nakamura, F. M., Germano, M. G., de Souza, L. F., and Tsai, S. M. (2016). "Next-generation sequencing to elucidate biochar-effected microbial community dynamics," in *Biochar Application: Essential Soil Microbial Ecology*. eds. J. K. Ralebitso-Senior and C. H. Orr (Amsterdam, the Netherlands and Boston, MA, USA: Elsevier), 109–132.

Carvalhais, L. C., Dennis, P. G., Fedoeyenko, D., Hajirezaei, M.-R., Borriss, R., and von Wirén, N. (2011). Root exudation of sugars, amino acids, and organic acids by maize as affected by nitrogen, phosphorus, potassium, and iron deficiency. *J. Plant Nutr. Soil Sci.* 174, 3–11. doi: 10.1002/jpln.201000085

Cerri, C. E. P., Galdos, M. V., Carvalho, J. L. N., Feigl, B. J., and Cerri, C. C. (2013). Quantifying soil carbon stocks and greenhouse gas fluxes in the sugarcane agrosystem: point of view. *Sci. Agric.* 70, 361–368. doi: 10.1590/S0103-90162013000500011

CONAB (2018). Companhia Nacional de Abastecimento. Mapas de Produção Agrícola. Milho 1ª e 2ª Safra 2014/2015. Available at: http://www.conab.gov.br/conteudos.php?a=1101&t=2 (Accessed January 10, 2018).

CONAB (2019). Companhia Nacional de Abastecimento. Boletim da Safra de Grãos. Available at: https://www.conab.gov.br/info-agro/safras/graos/boletim-da-safra-de-graos (Accessed April 01, 2019).

Costa, R. R., Quirino, G. D., Naves, D. C., Santos, C. B., and Rocha, A. F. (2015). Efficiency of inoculant with *Azospirillum brasilense* on the growth and yield of second-harvest maize. *Pesquisa Agropecuária Tropical* 45, 304–311. doi: 10.1590/1983-40632015v4534593

Costacurta, A., Keijers, V., and Vanderleyden, J. (1994). Molecular cloning and sequence analysis of an *Azospirillum brasiliense* indole-3-pyruvate decarboxylase gene. *Mol. Gen. Genet.* 243, 463–472. doi: 10.1007/BF00280477

Costello, A. M., and Lidstrom, M. E. (1999). Molecular characterization of functional and phylogenetic genes from natural populations of methanotrophs in Lake sediments. *Appl. Environ. Microbiol.* 65, 5066–5074. doi: 10.1128/AEM.65.11.5066-5074.1999

Dinno, A. (2017). dunn.test: Dunn's Test of Multiple Comparisons Using Rank Sums. R package version 1.3.5. Available at: https://CRAN.R-project.org/package=dunn.test (Accessed January 10, 2018).

Di Pasqua, R., Valeria, V., Aliberti, A., Robertiello, A., Faraco, V., Viscardi, S., et al. (2014). Influence of different lignocellulose sources on Endo-1,4-ß-Glucanase gene expression and enzymatic activity of *Bacillus amyloliquefaciens* B31C. *Bioresources* 9, 1303–1310. doi: 10.15376/biores.9.1.1303-1310

Doumbou, C. L., Hamby Salove, M. K., Crawford, D. L., and Beaulieu, C. (2001). Actinomycetes, promising tools to control plant diseases and to promote plant growth. *Phytoprotection* 82, 85–102. doi: 10.7202/706219ar

Eichorst, S. A., Trojan, D., Roux, S., Herbold, C., Rattei, C., and Woebken, D. (2018). Genomic insights into the Acidobacteria reveal strategies for their success in terrestrial environments. *Environ. Microbiol.* 20, 1041–1063. doi: 10.1111/1462-2920.14043

EMBRAPA (2015). Empresa Brasileira de Pesquisa Agropecuária, Embrapa Milho e Sorgo. Sistema de Produção – Cultivo do Milho. ISSN 1679-012X. Available at: https://www.spo.cnptia.embrapa.br/temas-publicados (Accessed 10 jan 2018).

FAO (2009). Global agriculture towards 2050. High-level expert forum. Available at: <http://www.fao.org/fileadmin/templates/wsfs/docs/Issues_papers/HLEF2050_Global_Agriculture.pdf> (Accessed January 10, 2018).

Freitas, P. L., and Landers, J. N. (2014). The transformation of agriculture in Brazil through development and adoption of zero tillage conservation agriculture. *Int. Soil Water Conserv. Res.* 2, 35–46. doi: 10.1016/S2095-6339(15)30012-5

Galloway, J. N., Townsend, A. R., Willem Erisman, J., Bekunda, M., Cai, Z., Freney, J. R., et al. (2008). Transformation of the nitrogen cycle: recent trends, questions, and potential solutions. *Science* 320, 889–892. doi: 10.1126/science.1136674

Geisseler, D., and Scow, K. M. (2014). Long-term effects of mineral fertilizers on soil microorganisms – a review. *Soil Biol. Biochem.* 75, 54–63. doi: 10.1016/j.soilbio.2014.03.023

Glass, J., and Orphan, V. (2012). Trace metal requirements for microbial enzymes involved in the production and consumption of methane and nitrous oxide. *Front. Microbiol.* 3:61. doi: 10.3389/fmicb.2012.00061

Hartmann, A., and Burris, R. H. (1987). Regulation of nitrogenase activity by oxygen in *Azospirillum brasilense* and *Azospirillum lipoferum*. *J. Bacteriol.* 169, 944–948. doi: 10.1128/JB.169.3.944-948.1987

He, J., Li, H.-W., Wang, Q.-J., Gao, H.-W., Li, W.-Y., Zhang, X.-M., et al. (2010). The adoption of conservation tillage in China. *Ann. N. Y. Acad. Sci.* 1195, E96–E106. doi: 10.1111/j.1749-6632.2009.05402.x

Henry, S., Bru, D., Stres, B., Hallet, S., and Philippot, L. (2006). Quantitative detection of the *nosZ* gene, encoding nitrous oxide reductase, and comparison of the abundances of 16S rRNA, narG, nirK, and *nosZ* genes in soils. *Appl. Environ. Microbiol.* 72, 5181–5189. doi: 10.1128/AEM.00231-06

Holmes, A. J., Costello, A., Lidstrom, M. E., and Murrell, J. C. (1995). Evidence that particulate methane monooxygenase and ammonia monooxygenase may be evolutionarily related. *FEMS Microbiol. Lett.* 132, 203–208. doi: 10.1111/j.1574-6968.1995.tb07834.x

IBGE (2018). Instituto de Brasileiro de Geografia e Estatística. Mapas de Solos do Brasil. Available at: https://mapas.ibge.gov.br/tematicos/solos (Accessed January 10, 2018).

IPCC (2013). Climate Change 2013: The Physical Science Basis. Contribution of Working Group I to the Fifth Assessment Report of the Intergovernmental Panel on Climate Change. eds. T. F. Stocker, D. Qin, G.-K. Plattner, M. Tignor, S. K. Allen, J. Boschung et al (United Kingdom and New York, NY, USA: Cambridge University Press, Cambridge) 1535.

IPCC (2014). Climate Change 2014: Synthesis Report. Contribution of Working Groups I, II and III to the Fifth Assessment Report of the Intergovernmental Panel on Climate Change. eds. Core Writing Team, R.K. Pachauri and L.A. Meyer (Geneva, Switzerland: IPCC) 151

IUSS Working Group WRB (2015). World reference base for soil resources 2014, update 2015: International soil classification system for naming soils and creating legends for soil maps. World Soil Resources Reports No. 106. FAO, Rome. Available at: http://www.fao.org/soils-portal/data-hub/soil-classification/world-reference-base/en/ (Accessed April 1, 2019).

Kielak, A. M., Barreto, C. C., Kowalchuk, G. A., van Veen, J. A., and Kuramae, E. E. (2016). The ecology of Acidobacteria: moving beyond genes and genomes. *Front. Microbiol.* 7:744. doi: 10.3389/fmicb.2016.00744

Lee, Y. J., Kim, B. K., Lee, B. H., Jo, K. I., Lee, N. K., Chung, C. H., et al. (2008). Purification and characterization of cellulase produced by *Bacillus amyoliquefaciens* DL-3 utilizing rice hull. *Bioresour. Technol.* 99, 378–386. doi: 10.1016/j.biortech.2006.12.013

Li, X., Rui, J., Xiong, J., Li, J., He, Z., Zhou, J., et al. (2014). Functional potential of soil microbial communities in the maize rhizosphere. *PLoS One* 9:e112609. doi: 10.1371/journal.pone.0112609

Liu, H., Brettell, L. E., Qiu, Z., and Singh, B. K. (2020). Microbiome-mediated stress resistance in plants. *Trends Plant Sci.* 25, 733–743. doi: 10.1016/j.tplants.2020.03.014

Liu, L., and Greaver, T. L. (2009). A review of nitrogen enrichment effects on three biogenic GHGs: the CO_2 sink may be largely offset by stimulated N_2O and CH_4 emission. *Ecol. Lett.* 12, 1103–1117. doi: 10.1111/j.1461-0248.2009.01351.x

Ma, Y., Zilles, J. L., and Kent, A. D. (2019). An evaluation of primers for detecting denitrifiers via their functional genes. *Environ. Microbiol.* 21, 1196–1210. doi: 10.1111/1462-2920.14555

Mendiburu, F. (2017). agricolae: Statistical Procedures for Agricultural Research. R package version 1.2-6. Available at: https://CRAN.R-project.org/package=agricolae (Accessed January 10, 2018).

Müller, T. M., Sandini, I. E., Rodrigues, J. D., Novakowiski, J. H., Basi, S., and Kaminski, T. H. (2016). Combination of inoculation methods of *Azopirillum brasilense* with broadcasting of nitrogen fertilizer increases corn yield. *Ciência Rural* 46, 210–215. doi: 10.1590/0103-8478cr20131283

Okon, Y., and Labandera-Gonzalez, C. A. (1994). Agronomic applications of *Azospirillum*: an evaluation of 20 years worldwide field inoculation. *Soil Biol. Biochem.* 26, 1591–1601. doi: 10.1016/0038-0717(94)90311-5

Oksanen, J., Blanchet, F. G., Friendly, M., Kindt, R., Legendre, P., McGlinn, D., et al. (2017). vegan: Community Ecology Package. R package version 2.4-3. Vienna, 2017. Available at: https://CRAN.R-project.org/package=vegan (Accessed January 10, 2018).

Paradis, E., Claude, J., and Strimmer, K. (2004). APE: analyses of phylogenetics and evolution in R language. *Bioinformatics* 20, 289–290. doi: 10.1093/bioinformatics/btg412

Parks, D. H., Tyson, G. W., Hugenholtz, P., and Beiko, R. G. (2014). STAMP: statistical analysis of taxonomic and functional profiles. *Bioinformatics* 30, 3123–3124. doi: 10.1093/bioinformatics/btu494

Peiffer, J. A., Spor, A., Koren, O., Jin, Z., Tringe, S. G., Dangl, J. L., et al. (2013). Diversity and heritability of the maize rhizosphere microbiome under field conditions. *Proc. Natl. Acad. Sci. U. S. A.* 110, 6548–6553. doi: 10.1073/pnas.1302837110

Philippot, L., Raaijmakers, J. M., Lemanceau, P., and van der Putten, W. H. (2013). Going back to the roots: the microbial ecology of the rhizosphere. *Nat. Rev. Microbiol.* 11, 789–799. doi: 10.1038/nrmicro3109

Pittelkow, C. M., Linquist, B. A., Lundy, M. E., Liang, X., Jan van Groenigen, K., Lee, J., et al. (2015). When does no-till yield more? A global meta-analysis. *Field Crop Res.* 183, 156–168. doi: 10.1016/j.fcr.2015.07.020

Quast, C., Pruesse, E., Yilmaz, P., Gerken, J., Schweer, T., Yarza, P., et al. (2013). The SILVA ribosomal RNA gene database project: improved data processing and web-based tools. *Nucleic Acids Res.* 41, D590–D596. doi: 10.1093/nar/gks1219

R Core Team (2017). R: A language and environment for statistical computing. R Foundation for Statistical Computing, Vienna, Austria. Available at: https://www.R-project.org/ (Accessed January 10, 2018).

Rigon, J. P. G., and Calonego, J. C. (2020). Soil carbon fluxes and balances of crop rotations under long-term no-till. *Carbon Balance Manag.* 15, 1–11. doi: 10.1186/s13021-020-00154-3

Rösch, C., Mergel, A., and Bothe, H. (2002). Biodiversity of denitrifying and dinitrogen-fixing bacteria in an acid forest soil. *Appl. Environ. Microbiol.* 68, 3818–3829. doi: 10.1128/AEM.68.8.3818-3829.2002

Santini, J. M. K., Buzetti, S., Teixeira Filho, M. C. M., Galindo, F. S., Coaguila, D. N., and Boleta, E. H. M. (2018). Doses and forms of *Azospirillum brasilense* inoculation on maize crop. *Revista Brasileira de Engenharia Agrícola e Ambiental* 22, 373–377. doi: 10.1590/1807-1929/agriambi.v22n6p373-377

Santos, W. M., Alves, B. J. R., Urquiaga, S., Pacheco, E. P., Barros, I., Fernandes, M. F., et al. (2020). Ammonia volatilization and yield of corn fertilized with different nitrogen sources in the Brazilian semiarid. *Pesq. Agrop. Brasileira* 55:e01036. doi: 10.1590/s1678-3921.pab2020.v55.01036

Sharma, L. K., and Bali, S. K. (2018). A review of methods to improve nitrogen use efficiency in agriculture. *Sustainability* 10:51. doi: 10.3390/su10010051

Soil Survey Staff (1999). *Soil Taxonomy: A Basic System of Soil Classification for Making and Interpreting Soil Surveys. 2nd Edn.* Natural Resources Conservation Service, U.S. Department of Agriculture Handbook, 436.

Somers, E., Ptacek, D., Gysegom, P., Srinivasan, M., and Vanderleyden, J. (2005). *Azospirillum brasiliense* produces the auxin-like phenylacetic acid by using the key enzyme for indole-3-acetic acid biosynthesis. *Appl. Environ. Microbiol.* 71, 1803–1810. doi: 10.1128/AEM.71.4.1803-1810.2005

Steinberg, L. M., and Regan, J. M. (2009). *mcrA*-targeted real-time quantitative PCR method to examine methanogen communities. *Appl. Environ. Microbiol.* 75, 4435–4442. doi: 10.1128/AEM.02858-08

Steinweg, J. M., Plante, A. F., Conant, R. T., Paul, E. A., and Tanaka, D. L. (2008). Patterns of substrate utilization during long-term incubations at different temperatures. *Soil Biol. Biochem.* 40, 2722–2728. doi: 10.1016/j.soilbio.2008.07.002

Teixeira, R. S., Santos, R. S., de Sousa, R. N., de Sousa, I. V., Reis, T. G., Milagres, J. J. M., et al. (2019). Short-term effects of maize rhizosphere and N-fertilization on stable organic matter in a tropical soil. *J. Agric. Sci.* 11:418. doi: 10.5539/jas.v11n1p418

Thangarajan, R., Bolan, N. S., Tian, G., Naidu, R., and Kunhikrishnan, A. (2013). Role of organic amendment application on greenhouse gas emission from soil. *Sci. Total Environ.* 465, 72–96. doi: 10.1016/j.scitotenv.2013.01.031

Tkacz, A., and Poole, P. (2021). The plant microbiome: The dark and dirty secrets of plant growth. *Plants People Planet* 3, 124–129. doi: 10.1002/ppp3.10167

USDA (2010). U.S. Department of Agriculture, Economic Research Service. Economic Information Bulletin Number 70. "No-Till" Farming Is a Growing Practice. Available at: https://www.ers.usda.gov/webdocs/publications/44512/8086_eib70.pdf?v=41055 (Accessed January 10, 2018).

Vacheron, J., Desbrosses, G., Bouffaud, M.-L., Touraine, B., Moënne-Loccoz, Y., Muller, D., et al. (2013). Plant growth-promoting rhizobacteria and root system functioning. *Front. Plant Sci.* 4:356. doi: 10.3389/fpls.2013.00356

van Raij, B., Andrade, J. C. d. e., Cantarella, H., and Quaggio, J. A. (2001). *Análise Química Para Avaliação da Fertilidade de Solos Tropicais*. Campinas: IAC, 285

Wang, Z., Qi, Z., Xue, L., and Bukovsky, M. (2016). RZWQM2 simulated management practices to mitigate climate change impacts on nitrogen losses and corn production. *Environ. Model Softw.* 84, 99–111. doi: 10.1016/j.envsoft.2016.06.016

Ward, M. H. (2009). Too much of a good thing? Nitrate from nitrogen fertilizers and cancer. *Rev. Environ. Health* 24, 357–363. doi: 10.1515/reveh.2009.24.4.357

Wickham, H. (2009). *ggplot2: Elegant Graphics for Data Analysis*. New York: Springer-Verlag.

Wieland, G., Neumann, R., and Backhaus, H. (2001). Variation of microbial communities in soil, rhizosphere, and rhizoplane in response to crop species, soil type, and crop development. *Appl. Environ. Microbiol.* 67, 5849–5854. doi: 10.1128/AEM.67.12.5849-5854.2001

Yang, X., Lan, Y., Meng, J., Chen, W., Huang, Y., Cheng, X., et al. (2017). Effects of maize stover and its derived biochar on greenhouse gases emissions and C-budget of brown earth in Northeast China. *Environ. Sci. Pollut. Res.* 24, 8200–8209. doi: 10.1007/s11356-017-8500-0

Zamanian, K., Zarebanadkouki, M., and Kuzyakov, Y. (2018). Nitrogen fertilization raises CO_2 efflux from inorganic carbon: a global assessment. *Glob. Chang. Biol.* 24, 2810–2817. doi: 10.1111/gcb.14148

Conflict of Interest: The authors declare that the research was conducted in the absence of any commercial or financial relationships that could be construed as a potential conflict of interest.

frontiers
in Forests and Global Change

ORIGINAL RESEARCH
published: 13 July 2021
doi: 10.3389/ffgc.2021.698191

Trade-Offs in Phosphorus Acquisition Strategies of Five Common Tree Species in a Tropical Forest of Puerto Rico

Daniela Yaffar[1,2], Camille E. Defrenne[1], Kristine G. Cabugao[1,2], Stephanie N. Kivlin[2], Joanne Childs[1], Niko Carvajal[3] and Richard J. Norby[1,2]*

[1] Oak Ridge National Laboratory, Environmental Sciences Division and Climate Change Science Institute, Oak Ridge, TN, United States, [2] Ecology and Evolutionary Biology, University of Tennessee, Knoxville, Knoxville, TN, United States, [3] Viticulture and Enology, University of California, Davis, Davis, CA, United States

OPEN ACCESS

Edited by:
Erik Verbruggen,
University of Antwerp, Belgium

Reviewed by:
Kerstin Pierick,
University of Göttingen, Germany
Thomas Kuyper,
Wageningen University and Research,
Netherlands

***Correspondence:**
Daniela Yaffar
danielayaffar@gmail.com;
dyaffar@vols.utk.edu

Specialty section:
This article was submitted to
Forest Soils,
a section of the journal
Frontiers in Forests and Global
Change

Received: 20 April 2021
Accepted: 11 June 2021
Published: 13 July 2021

Citation:
Yaffar D, Defrenne CE,
Cabugao KG, Kivlin SN, Childs J,
Carvajal N and Norby RJ (2021)
Trade-Offs in Phosphorus Acquisition
Strategies of Five Common Tree
Species in a Tropical Forest of Puerto
Rico.
Front. For. Glob. Change 4:698191.
doi: 10.3389/ffgc.2021.698191

Tree species that are successful in tropical lowlands have different acquisition strategies to overcome soil phosphorus (P) limitations. Some of these strategies belowground include adjustments in fine-root traits, such as morphology, architecture, association with arbuscular mycorrhizal fungi, and phosphatase activity. Trade-offs among P-acquisition strategies are expected because of their respective carbon cost. However, empirical evidence remains scarce which hinders our understanding of soil P-acquisition processes in tropical forests. Here, we measured seven fine-root functional traits related to P acquisition of five common tree species in three sites of the Luquillo Experimental Forest in Puerto Rico. We then described species-specific P-acquisition strategies and explored the changes in fine-root trait expression from 6 months before to 6 months after two consecutive hurricanes, Irma and María, passed over the island. We found that variations in root trait expression were driven mainly by the large interspecific differences across the three selected sites. In addition, we revealed a trade-off between highly colonized fine roots with high phosphatase activity and fine roots that have a high degree of branching. Furthermore, the former strategy was adopted by pioneer species (*Spathodea campanulata* and *Cecropia schreberiana*), whereas the latter was adopted by non-pioneer species (mostly *Dacryodes excelsa* and *Prestoea montana*). Additionally, we found that root trait expression did not change comparing 6 months before and after the hurricanes, with the exception of root phosphatase activity. Altogether, our results suggest a combination of structural and physiological root traits for soil P acquisition in P-poor tropical soils by common tropical tree species, and show stability on most of the root trait expression after hurricane disturbances.

Keywords: root architecture, specific root length, root diameter, phosphorus concentration, Luquillo Experimental Forest, phosphatase activity, root traits

INTRODUCTION

The availability of soil inorganic phosphorus (orthophosphate; hereafter, available P) strongly limits plant growth in lowland tropical forests where climate conditions lead to high soil weathering rates (Walker and Syers, 1976; Vitousek and Sanford, 1986; Reed et al., 2011; Lugli et al., 2021). Tree species that are successful in tropical lowlands have multiple acquisition strategies to overcome P limitation (Zalamea et al., 2016; Lugli et al., 2021). Aboveground, plants may increase P-use efficiency, which in turn leads to higher retention time of P in the canopy and higher resorption efficiency of P as tissues senesce (Paoli et al., 2005; Dalling et al., 2016). Belowground, plants optimize P acquisition by displaying multiple strategies commonly described by the expression of the traits of the narrowest, most absorptive roots (i.e., fine roots) and their mycorrhizal symbionts (Bardgett et al., 2014; Kramer-Walter et al., 2016; Weemstra et al., 2016; McCormack and Iversen, 2019; Bergmann et al., 2020; Lugli et al., 2021). Fine-root and mycorrhizal fungal trait expression is closely related to root function, such as resource foraging and uptake. For example, specific root length (SRL) and root branching are linked to soil space occupancy while root phosphatase activity and mycorrhizal colonization are critical determinants of P uptake (Lee, 1988; McCormack et al., 2017; Freschet et al., 2021).

Belowground, adjustments in morphology, architecture, association with arbuscular mycorrhizal fungi, and phosphatase activity expression may be all viable P-acquisition strategies. First, plants may alter the morphology of their fine roots in such a way as to increase their total absorptive length per unit of biomass (i.e., high SRL) and to decrease their thickness (Treseder and Vitousek, 2001; Santiago, 2015). These morphological adjustments enable plants to maximize resource acquisition while minimizing the cost of root tissue construction and maintenance (Valverde-Barrantes et al., 2015; Weemstra et al., 2016; McCormack and Iversen, 2019). Within the conceptual framework of the root economic space, this strategy is named the "do-it-yourself" strategy (Bergmann et al., 2020), which associates a competitive advantage with exploration of a larger soil volume and faster P assimilation over species that build shorter, thicker-diameter roots (Hodge, 2004; Kong et al., 2014; Liu et al., 2015). Second, plants that construct short, thick, fine roots may still acquire P effectively by outsourcing to mycorrhizal fungi—also called the "outsourcing" strategy (Comas et al., 2014; Kong et al., 2014; Eissenstat et al., 2015; Liu et al., 2015; Kramer-Walter et al., 2016; Ma et al., 2018; Bergmann et al., 2020). Arbuscular mycorrhizal (AM) fungi associate with most neotropical trees and efficiently forage for P in spaces away from P-depleted rhizospheres *via* extraradical hyphae. In turn, P is translocated to the plant host within arbuscules and intracellular hyphal coils in exchange for photosynthetically fixed carbon (Smith and Smith, 2011). Third, plants may adjust fine-root physiological traits to overcome soil P-limitation by regulating the exudation of phosphatase (Hinsinger, 2001; Treseder and Vitousek, 2001; Vance et al., 2003; Olander and Vitousek, 2004; Lambers et al., 2006). The mineralization of organic P by both root and microbial phosphatase, such as phosphomonoesterase (PME) is especially important in soils of tropical forests where organic P can comprise 30–60% of soil P (Smith and Read, 2008; Kong et al., 2014; Liu et al., 2015; Cabugao et al., 2017; Lugli et al., 2019).

Research on belowground P-acquisition strategies suggests that plants simultaneously adjust the expression of multiple fine-root traits related to P-acquisition to overcome soil P limitation (Lugli et al., 2019, 2021). Therefore, root morpho-architectural adjustments, association with AM fungi, and phosphatase activity may be complementary strategies as opposed to alternatives (Smith and Read, 2008; Turner, 2008; Nasto et al., 2019), but empirical evidence remains scarce in tropical ecosystems. For example, Lugli et al. (2019) found no relationship between mycorrhizal colonization and fine-root morphological traits at the ecosystem level, but SRL and phosphatase activity were shown to be related (Lugli et al., 2019; Cabugao et al., 2021). However, at the species level, thicker roots exhibited higher AM fungal colonization and more P-mobilizing exudates (Zangaro et al., 2005; Wen et al., 2019). Furthermore, the relationship between fine-root architectural traits (i.e., root branching) and mycorrhizal colonization has received little attention at the species level in the tropics (Kong et al., 2014; Liu et al., 2015). Altogether, the relationships among fine-root morphology, architecture, root phosphatase activity, and microbial associations remain understudied in tropical plant species, and the place of these relationships within the root economic space remains indeterminate (Treseder and Vitousek, 2001; Lugli et al., 2019; Nasto et al., 2019). This partly stems from the paucity of studies that measure "hard" traits, such as root enzymatic activity and mycorrhizal colonization. However, "hard" traits generally strongly relate to root function compared to the commonly measured "soft" traits, such as SRL and root nitrogen concentration (Freschet et al., 2015, 2021). To date, knowledge on the relationships among plant fine-root traits related to P acquisition in lowland tropical forests mostly comes from community or ecosystem level studies (Lugli et al., 2019, 2021; Addo-Danso et al., 2020; Cabugao et al., 2021). Consequently, individual relationships between fine-root morphology, phosphatase activity, and mycorrhizal colonization at the species level are underexplored. Yet, plant species can have a strong influence on root and microbial phosphatase activity (Cabugao et al., 2017; Guilbeault-Mayers et al., 2020) and they are likely to differ widely in their nutrient requirement (Townsend et al., 2007). Furthermore, plant species of different successional status are likely to differ in their fine-root trait expression, which may inform their resource acquisition strategies (Coll et al., 2008; Xiang et al., 2013; Caplan et al., 2019).

Here, we describe belowground P-acquisition strategies of five common tree species that have different successional status (two pioneers and three non-pioneers) growing in the lowland tropical wet forests of Puerto Rico, where residence time of soil labile P is short (Liptzin et al., 2015). For each species, we explored relationships among fine-root traits related to P acquisition (Freschet et al., 2021), such as (i) morphological, architectural, and chemical traits (SRL, diameter, P concentration, branching intensity, and branching ratio) and (ii) physiological and microbial traits (root phosphatase activity and mycorrhizal colonization intensity). Based on results from tropical lowland studies (Lugli et al., 2019) and the conceptual root economic space framework (Bergmann et al., 2020), we hypothesized that: (H1) root phosphatase activity and architectural traits would covary with morphological traits, such that high root phosphatase activity would relate to high root branching ratio or intensity and high SRL, representing complementary P-acquisition strategies (combined strategy); and (H2) mycorrhizal colonization would negatively covary with phosphatase activity, branching ratio or intensity, and SRL, representing a trade-off in P-acquisition strategies. Furthermore, (H3) both strategies would covary with root P concentration assuming that root P is an indicator of plant P status and likely reflects P acquisition (based on our analysis of data in Holdaway et al., 2011; Schreeg et al., 2014; **Supplementary Figure 1**). Altogether, we expected that the existence of a trade-off between these two strategies would lead tree species to adopt one or the other. Most of the analyses we made in this study focused on fine roots collected 6 months after two consecutive hurricanes passed through Puerto Rico in 2017. We used this unique opportunity to also explore differences in some of the aforementioned root traits before and after the hurricanes for each tree species.

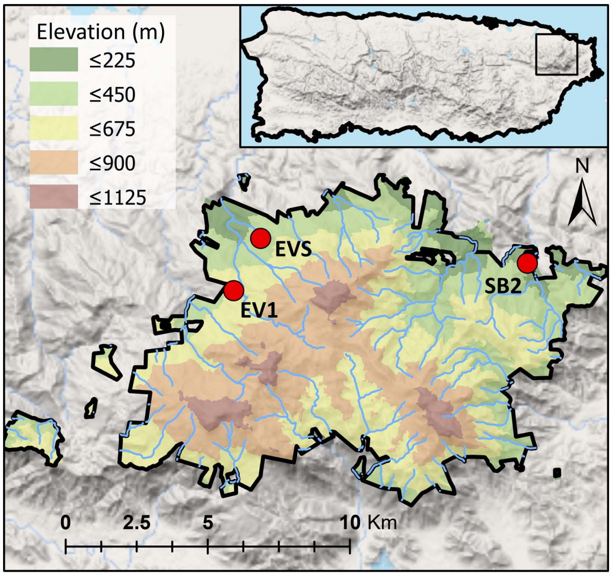

FIGURE 1 | Map of the Luquillo Experimental Forest (LEF)—Puerto Rico, with the location of the studied sited (red circles). Two sites (EV1 and EVS) were located near El Verde Field Station, and one site (SB2) was located near the USDA Forest Service Sabana Field Research Station.

MATERIALS AND METHODS

Study Site and Sampling

In March 2017, we selected three sites in the Luquillo Experimental Forest (LEF; **Figure 1** and **Table 1**) in Puerto Rico. Two sites were close to El Verde Field Station (EVS and EV1; ca. 550 m a.s.l.), and one site was near the USDA Forest Service Sabana Field Research Station (SB2; 150 m a.s.l.). The EVS site is a mature forest with the greatest concentration of soil organic P of the three sites, EV1 is a secondary forest, and SB2 is a young secondary forest with the greatest concentration of soil available P (Brown et al., 1983; Scatena, 1989; Uriarte and Zimmerman, 2017; **Table 1**). We sampled fine roots of the most common tree species at these sites including (1) *Cecropia schreberiana* Miq. (Urticaceae) (native pioneer), (2) *Dacryodes excelsa* Vahl (Burceraceae), *Prestoea montana* (Graham) G. Nicholson (Arecaceae) and *Calophyllum calaba* L. (Calophyllaceae) (native non-pioneers) and (3) *Spathodea campanulata* P. Beauv. (Bignoniaceae) (non-native pioneer). Only *Prestoea* occurred at the three sites, *Cecropia*, and *Calophyllum* occurred at both EV1 and SB2, while *Spathodea* only occurred at SB2, and *Dacryodes* was collected only from EVS. All tree species form symbioses with AM fungi.

We selected three mature individuals (>10 cm of DBH) from each species that were at least 10 m away from each other and collected at least two root samples from each tree (composed of multiple fine-root branches) by tracing out two coarse roots of each tree from the tree bole until reaching the fine-root system (∼ 2 m away from the tree boles). We combined the two samples per tree, and then we used three subsamples for subsequent root analyses: (i) we assessed mycorrhizal colonization at the Center of Applied Tropical Ecology and Conservation of the University of Puerto Rico (samples were kept in 75% ethanol), (ii) we measured phosphatase activity at Oak Ridge National Laboratory (ORNL; Cabugao et al., 2021), and (iii) we conducted morphological and architectural analyses at the USDA Sabana Field Station Puerto Rico; once dried, we used those samples to measure root P concentration at ORNL. Due to sampling restrictions, we did not measure root phosphatase activity for *Spathodea*, and we did not assess mycorrhizal colonization before the hurricanes; we made all other measurements both before and after the hurricanes (March 2017 and 2018, respectively).

Fine-Root Trait Measurements

We measured seven fine-root traits from which five were directly related to P acquisition according to Freschet et al. (2021): root phosphatase activity, mycorrhizal colonization, SRL, root branching ratio, root branching intensity. We included root diameter as often this trait is related to mycorrhizal colonization (Bergmann et al., 2020), and root P concentration assuming this trait is an indicator of plant P status and reflects P acquisition (based on our analysis of data in Holdaway et al., 2011 and Schreeg et al., 2014; **Supplementary Figure 1**).

We used the subsample for morphological and architectural trait measurements (ca. five branches in total) from each tree species and separated them by root order following the morphometric classification approach (Pregitzer et al., 2002). We scanned the first two root orders separately using WinRHIZO (version 12, 1,400 dpi, Regent Instruments Inc., Quebec City, Canada) to obtain total root length (cm) and average diameter (mm). We calculated root branching intensity as the number of first-order roots per length of second-order roots and root branching ratio as the number of first-order roots per number of second-order roots. We dried each group of root orders separately at 65°C until samples reached a stable weight,

TABLE 1 | Environmental conditions of the studied sites at the Luquillo Experimental Forest (LEF).

Region	Site name	Latitude Longitude	Elevation (m a.s.l.)	MAT (°C)	MAP (mm yr^{-1})	Forest age (years)	Soils order	Soil available P (µg g^{-1})		Soil organic P (mg g^{-1})	
								2017	2018	2017	2018
El Verde	EVS	18.321, −65.818	200–600	24	3500	>100	Oxisol	NA	0.25	NA	0.19
El Verde	EV1	18.311, −65.826	200–600	24	3500	62–76	Oxisol	0.14	0.09	0.12	0.12
Sabana	SB2	18.322, −65.732	150	24	3500	35–62	Ultisol	0.87	0.36	0.19	0.14

Soil available P and organic P are from before the hurricanes (February, 2017), and after the hurricanes (February, 2018). MAT, mean annual temperature; MAP, mean annual precipitation; NA, not available.
NB: Methods for soil measurements are available in ***Supplementary Methods*** *and soil orders were determined according to Brown et al. (1983), Scatena (1989), and Stone et al. (2014).*

and we calculated SRL by dividing total root length by root dry weight (cm mg^{-1}). We then shipped the dried root samples to ORNL for P concentration measurements (first- and second-order roots were combined). At ORNL, we ground the samples in 50 ml falcon tubes using a Geno/Grinder 2010 (Spex Sampler Prep, Metuchen, NJ, United States) and measured root P concentration (%) using a Lachat BD40 block digestor for the high temperature digestion and a Lachat QuikChem 8000 series for the flow injection analysis (Hach Company, Loveland CO, United States) following methods described by Cabugao et al. (2021).

Mycorrhizal Colonization and Phosphatase Activity

We cleared, stained and de-stained first- and second-order roots previously preserved in ethanol following Kormanik and Mcgraw (1982) to measure AM fungal colonization. Specifically, we cleared fine roots in potassium hydroxide in a water bath (40°C), stained them with acid fuchsin and de-stained them in glycerol. We then recorded the presence of mycorrhizal structures (100 intersections per sample) disregarding the nature of the structures (e.g., hyphae, arbuscules, coils, vesicles) under a compound microscope (200× magnification) following McGonigle et al. (1990).

We measured root phosphatase activity as the phosphomonoesterase (PME) activity from the first and second-order roots using a modified version of the colorimetric para-nitrophenyl (pNP) phosphate assay (Tabatabai and Bremner, 1969; Cabugao et al., 2017; Png et al., 2017). This assay consists of measuring the activity of PME bound to the root surface in the presence of an organic P substrate (para-nitrophenyl phosphate). We washed the root samples (∼1 g) with milliQ water multiple times, mixed them with 9 ml of 50 mM sodium acetate-acetic acid (for 1 L: 2.88 g sodium acetate; pH = 5.0 using acetic acid) and 1 ml of 50 mM pNP (1.856 g pNP in 100 ml sodium acetate buffer), and incubated in a shaker at 27°C for 1 h. We then took 0.5 ml of this solution, added 4.5 ml of 0.11 M NaOH to terminate the reaction and measured the concentration of the product (para-nitrophenol) by spectrophotometry (405 nm, spectrophotometer 110, Cole Parmer, East Banker Court Vernon Hills, Illinois). Standard curves were made using 0, 100, 200, 400, 1,000 µM of pNP. PME activity is expressed as µmol pNP $g_{root}{}^{-1}$ hr^{-1}.

Hurricane Events

Most of the analyses we made in this study focused on fine roots collected 6 months after two consecutive hurricanes passed through Puerto Rico. However, we had also collected roots samples 6 months before the hurricanes Irma on September 6th, 2017 (category 5) and María 2 weeks after, on September 20th 2017 (category 4). Sustained winds reached 250 km hr^{-1} (among the strongest on record for the island; Lugo, 2020) and precipitation over 500 mm in just 24 h from María (Pasch et al., 2019). The hurricanes had a strong effect on the forest structure, which was still evident when we performed sample collection 6 months following the hurricanes. Tree mortality as a consequence of the disturbance was high (∼15%; Uriarte et al., 2019), and it included two trees we previously measured, which we replaced by a nearby individual of the same species and similar DBH. There was a large reduction in canopy cover (from ∼90 to 30%), and soil available P concentration decreased at EV1 and SB2, while organic P concentration decreased only at SB2 (**Table 1**).

Data Analysis

We conducted all statistical analyses in R version 3.3.4 (R Core Team, 2019) and considered statistically significant results at $P \leq 0.05$. To test for outliers in the data, we used the *check_outliers* function from the "*performance*" package in R (Lüdecke et al., 2020), and dropped two datapoints from all the analysis that were statistical outliers and ecologically improbable based on the literature (FRED 3.0; Iversen et al., 2018). To test for changes in root trait expression among species and sites separately we performed ANOVAs followed by *post-hoc* HSD Tukey's tests (Chambers et al., 2017). For multiple testing, we corrected *P*-values with the Bonferroni correction (McDonald, 2014). All mycorrhizal colonization data were transformed to percentages. To normalize the distribution of the mycorrhizal colonization percentage, we used a logit transformation (*gtools* package, Fox and Weisberg, 2019). To visualize dimensions in root trait variation among species and sites, we used Non-metric Multi-Dimensional Scaling (Kruskal, 1964). To explore bivariate relationships among root traits (for example, the effect of mycorrhizal colonization on root phosphatase activity) we used linear mixed effects models with the *lmer* function (*lme4* package, Bates et al., 2015) considering site, and species within sites as nested random intercepts as two separate models (see

Supplementary Table 2), and reported the one with only site in the results. To test for models' assumptions, we used the *check_model* function from the "*performance*" package in R, based on these results we log transformed the data from root phosphatase activity. Confidence intervals for the model parameters were estimated using the *confint* function (*stats* package; Ponciano et al., 2009; R Core Team, 2019). To test for differences in root trait expression and soil P concentration before and after the hurricanes we also fitted a linear mixed effect model where tree within species within sites was the nested random intercept. We did not consider mycorrhizal colonization in this last analysis due to sample restrictions before the hurricanes. We used the estimated marginal means using the *emmeans* function from the *emmeans* package to compare traits expression before and after the hurricane (Lenth et al., 2020).

RESULTS

Inter- and Intraspecific Root Trait Variation

Most fine-root traits we measured had greater variation among species within sites (interspecific mean variation, *CV* = 62.4%) than within species among sites (intraspecific mean variation, *CV* = 40.5%; **Supplementary Table 1**). However, root phosphatase activity and branching ratio varied in only one species among sites, while root P concentration did not differ among species (**Supplementary Table 1**). Overall, root trait expression did not vary among sites (**Figure 2A**), whereas root branching ratio, phosphatase activity and mycorrhizal colonization explained most of the variation ($>$50%) among species (**Figure 2B**).

Calophyllum displayed the thickest first-order root diameter (0.46 mm) that had the lowest values of SRL (0.79 cm mg^{-1}; **Figures 3A,B**) while the pioneers *Cecropia* and *Spathodea* had the greatest SRL values (10.3 and 10.6 cm mg^{-1}, respectively) and the highest percentage mycorrhizal colonization (70 and 75%, respectively; **Figure 3E**). In addition, fine roots of *Cecropia* had the highest phosphatase activity (272.9 μmol pNP $\text{g}_{\text{root}}{}^{-1}\,\text{hr}^{-1}$; **Figure 3F**), while those of *Spathodea* had the highest P concentration values (0.1%; **Figure 3G**), although differences among species for root P concentration were not statistically significant. Lastly, *Prestoea* built highly branched fine roots (branching ratio of 5.9; **Figure 3C**) that had the smallest diameter (first-order root measured 0.2 mm), the lowest activity of phosphatase (16.4 μmol pNP $\text{g}_{\text{root}}{}^{-1}\,\text{hr}^{-1}$) and lowest mycorrhizal colonization (12%). *Dacryodes* had the highest root branching intensity (**Figure 3D**).

Bivariate Relationships Among Fine-Root Traits

Bivariate relationships between fine-root traits were driven by interspecific variations (**Supplementary Table 2** and **Figure 4**). Mycorrhizal colonization covaried with root phosphatase activity such that root phosphatase activity increased linearly by 3.06 μmol pNP $\text{g}_{\text{root}}{}^{-1}\,\text{hr}^{-1}$ for every percent increase in mycorrhizal colonization ($p < 0.01$; R^2m = 0.43; **Supplementary Table 2** and **Figure 4A**). Conversely, root phosphatase activity decreased by 21.2 μmol pNP $\text{g}_{\text{root}}{}^{-1}\,\text{hr}^{-1}$ for every number of first-order root per number of second-order root increase in branching ratio (p = 0.02; R^2m = 0.17; **Supplementary Table 2** and **Figure 4B**). Mycorrhizal colonization was also negatively related to root branching ratio, decreasing by 6.5% for every number of first-order root per number of second-order root increase in branching ratio (p = 0.04; R^2m = 0.25; **Supplementary Table 2** and **Figure 4C**), and positively related to SRL, increasing by 3.4% for every 1 cm mg^{-1} increase (p = 0.02; R^2m = 0.19; **Supplementary Table 2** and **Figure 4D**). Furthermore, root diameter, SRL, root P concentration, and root branching intensity were not related to root phosphatase activity (**Supplementary Figures 2A–D** and **Supplementary Table 2**), nor were root branching intensity and root diameter related to mycorrhizal colonization (**Supplementary Figures 2E,F** and **Supplementary Table 2**). Root P concentration was positively related to mycorrhizal colonization (p = 0.05; R^2m = 0.14; **Supplementary Table 2** and **Figure 4E**), root branching intensity (p = 0.02; R^2m = 0.12; **Supplementary Table 2** and **Figure 4F**), and soil available P (**Supplementary Table 2**). No other root measurement was related to soil available P (not shown).

Fine-Root Measurement Before vs. After the Hurricanes

After two consecutive hurricanes in September 2017, most of the tree species did not display changes in morphological, architectural, or chemical root trait expression (**Figures 5A–D,F**). For instance, the estimated marginal mean of SRL was 4.72 cm mg^{-1} pre-hurricanes and 4.78 cm mg^{-1} post-hurricanes. We found a strong decrease in the activity of root phosphatase overall (**Figure 5E**) (when we fitted a model with trees nested within species within sites; **Supplementary Table 3**). Estimated marginal means for root phosphatase activity were 220.0 μmol $\text{pNPg}_{\text{root}}{}^{-1}\,\text{hr}^{-1}$ pre-hurricanes and 76.9 μmol $\text{pNPg}_{\text{root}}{}^{-1}\,\text{hr}^{-1}$ post-hurricanes.

DISCUSSION

Tropical forests are highly productive, comprising one fourth of the planet's terrestrial carbon stored in aboveground vegetation biomass (Bonan, 2008). This high productivity might be modulated by feedbacks between plant functional traits and the P cycle (Quesada et al., 2010; Cernusak et al., 2013). However, the role of belowground plant functional traits in soil P acquisition remains unclear, in part because knowledge on the relationships among fine-root traits and potential trait trade-offs is limited (Freschet et al., 2021). Here, we explored relationships among a suite of fine-root traits related to P acquisition in the P-poor soils of a lowland tropical forest of Puerto Rico. Variations in root trait expression of the five tree species we studied were mainly driven by the large interspecific differences across the three selected sites. Our results contradict

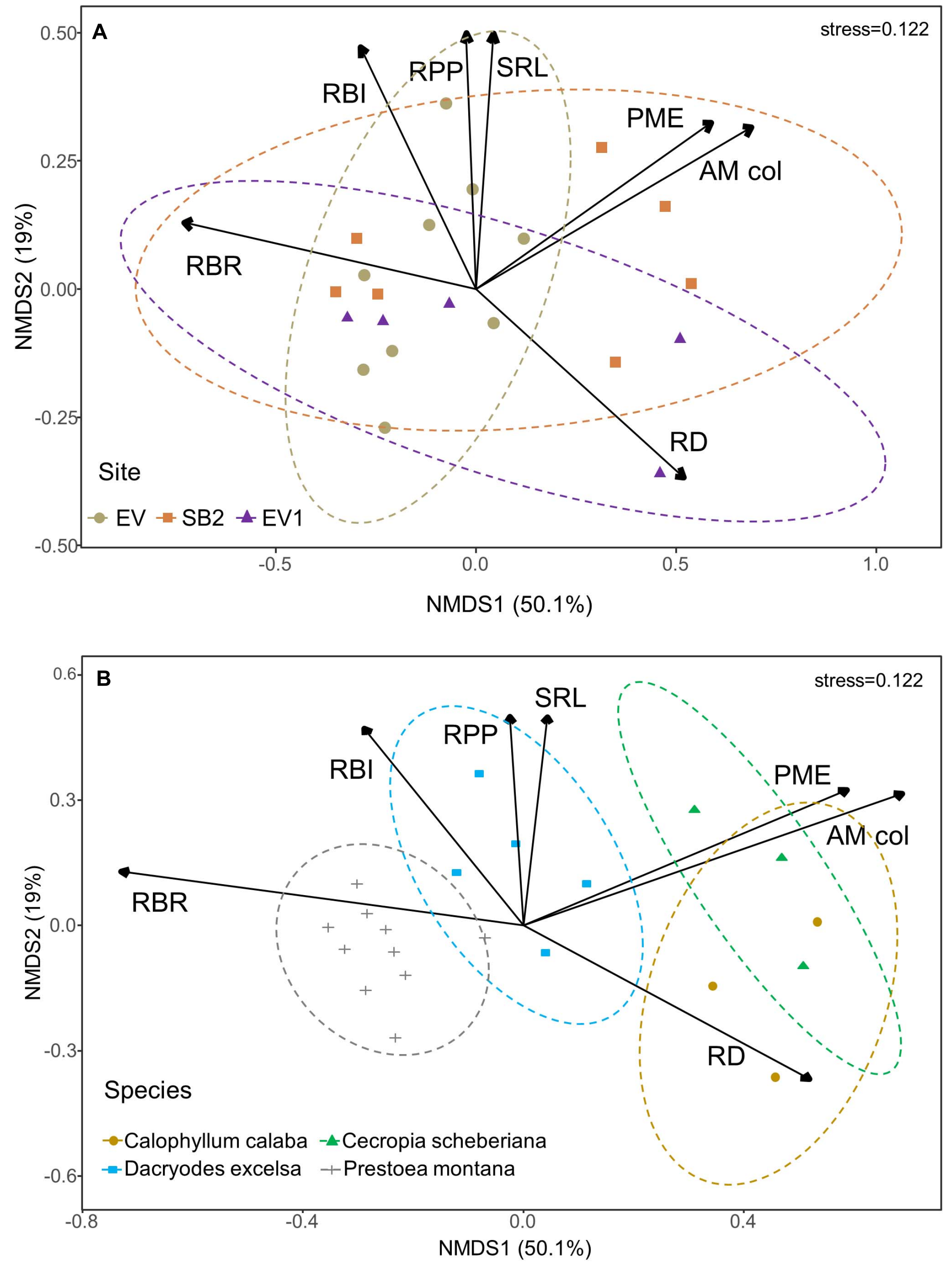

FIGURE 2 | Functional root traits of the first two fine-root orders of five common tree species at the Luquillo Experimental Forest in Puerto Rico. Non-Metric Multi-Dimensional Scaling (NMDS) of the fine-root traits: root branching ratio (RBR), root branching intensity (RBI), specific root length (SRL), root phosphatase activity (phosphomonoesterase; PME), root diameter (RD), root phosphorus concentration (RPP), and arbuscular mycorrhizal colonization (AM col). The NMDS plots are grouped by **(A)** Sites and **(B)** Species. Data are shown after the hurricanes that passed over the island in 2017. Due to sampling constraints, root PME activity was not measured for *Spathodea campanulata.*

our hypotheses of a trade-off in phosphorus acquisition strategies between (H1) fine roots with high phosphatase activity, high SRL, and high root branching, and (H2) fine roots with greater mycorrhizal colonization. In contrast, we reveal a trade-off between highly colonized fine roots with high phosphatase activity and fine roots that have a high degree of branching. Furthermore, the former strategy was adopted by the pioneer trees (*Spathodea* and *Cecropia*) whereas the latter was adopted by the non-pioneer trees (mostly *Dacryodes* and *Prestoea*). Our results confirmed that both high root branching and high mycorrhizal colonization are two contrasting strategies that covaried with root P concentration (H3). Additionally, we found that none of the root traits except phosphatase activity changed when comparing 6 months before and after the hurricanes. Our study, although encompassing only five tree species, highlights the need to combine measurements of

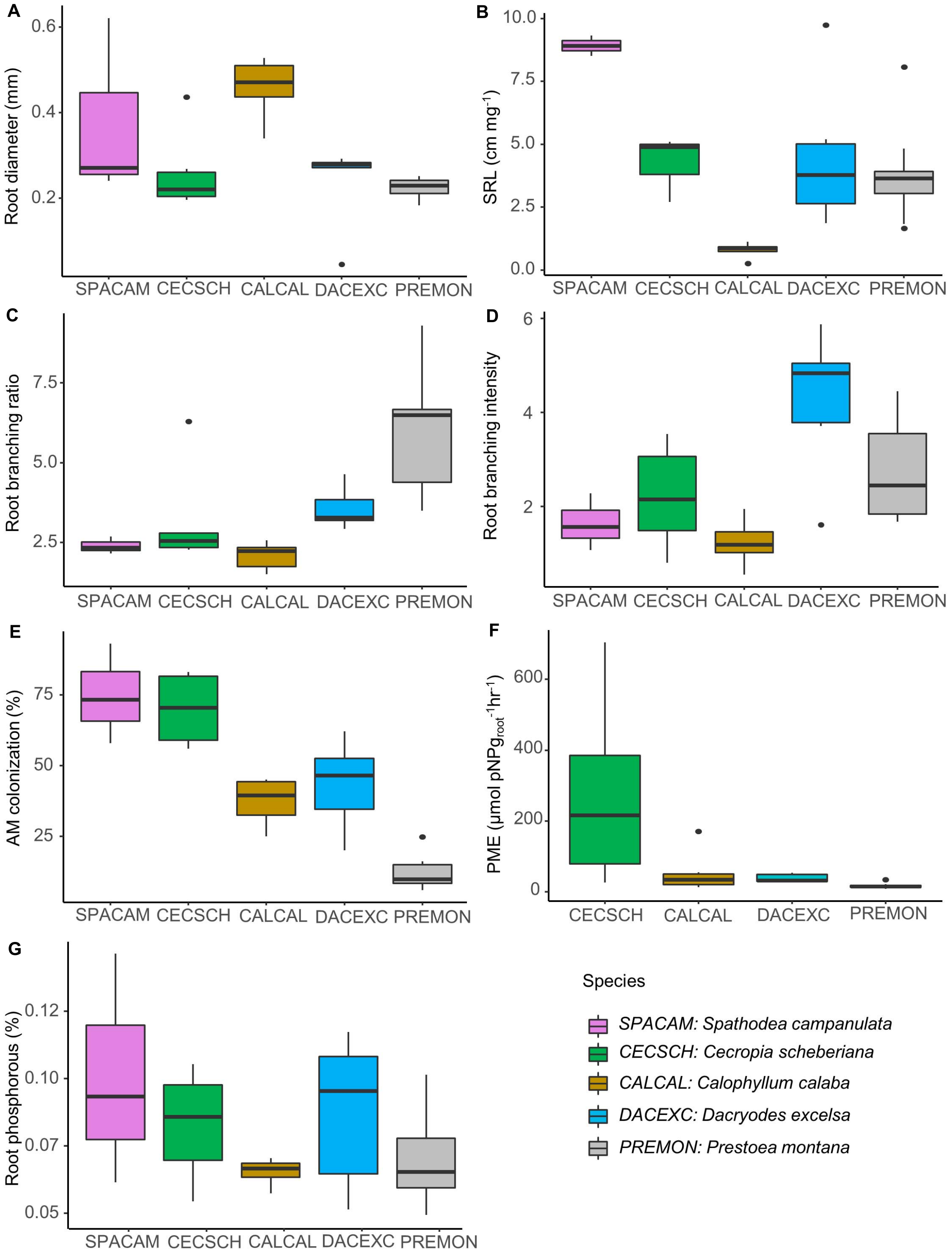

FIGURE 3 | Fine-root trait values for five common trees species at the Luquillo Experimental Forest in Puerto Rico. **(A)** Root diameter and **(B)** specific root length (SRL) were measured from 1st root order. **(C)** Root branching ratio, **(D)** root branching intensity, **(E)** arbuscular mycorrhizal (AM) colonization, **(F)** root phosphatase activity (phosphomonoesterase; PME), and **(G)** root phosphorus concentration were measured from 1st and 2nd orders combined. Data are shown after the hurricanes that passed over the island in 2017. Due to sampling constraints, root PME activity was not measured for *Spathodea campanulata*.

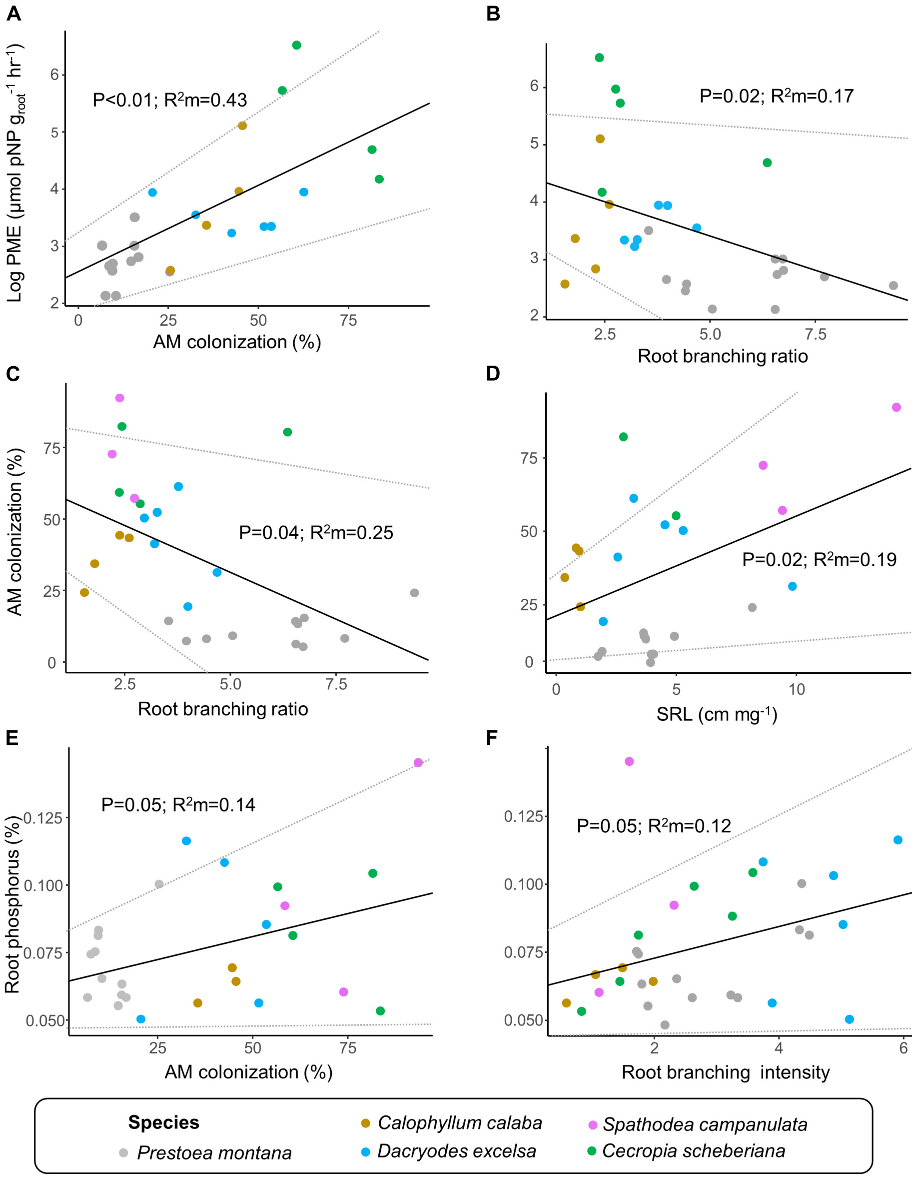

FIGURE 4 | Bivariate significant relationships among the seven fine-root traits measured in this study. Linear mixed-effects models were fitted for each root trait combination to account for the hierarchical nature of our dataset (see **Supplementary Table 2**). We report the marginal R^2 of each model which represents the variance explained by the fixed effect. The dotted gray lines represent the confidence interval for a given model parameter. The relationships include root phosphatase activity (phosphomonoesterase; PME) with **(A)** arbuscular mycorrhizal (AM) colonization and with **(B)** root branching ratio; AM colonization with **(C)** root branching ratio and with **(D)** specific root length (SRL); and root phosphorus concentration with **(E)** AM colonization and with **(F)** root branching intensity. Data are shown after the hurricanes that passed over the island in 2017. Due to sampling constraints, root PME activity was not measured for *Spathodea campanulata*.

fine-root morphology, architecture, physiology, and mycorrhizal colonization to better define belowground plant P-acquisition strategies in the tropics.

Large Interspecific Fine-Root Trait Variation

Interspecific root trait variation was high among the five tree species selected and for most of the traits. Interspecific fine-root trait variation has been widely explored at the global and biome scales, and some traits are phylogenetically constrained, such as SRL and root diameter (Ryser and Eek, 2000; Kong et al., 2014; Ma et al., 2018; Wang R. et al., 2018; Liu et al., 2019; Valverde-Barrantes et al., 2020). Nonetheless, the expression of other functional traits, such as mycorrhizal colonization and root branching ratio could vary greatly with environmental conditions (Kong et al., 2014; Weemstra et al., 2016). Accordingly, we found that root branching ratio and phosphatase activity varied between sites and within species (**Supplementary Table 1**), which confirms our previous findings in Cabugao et al. (2017). However,

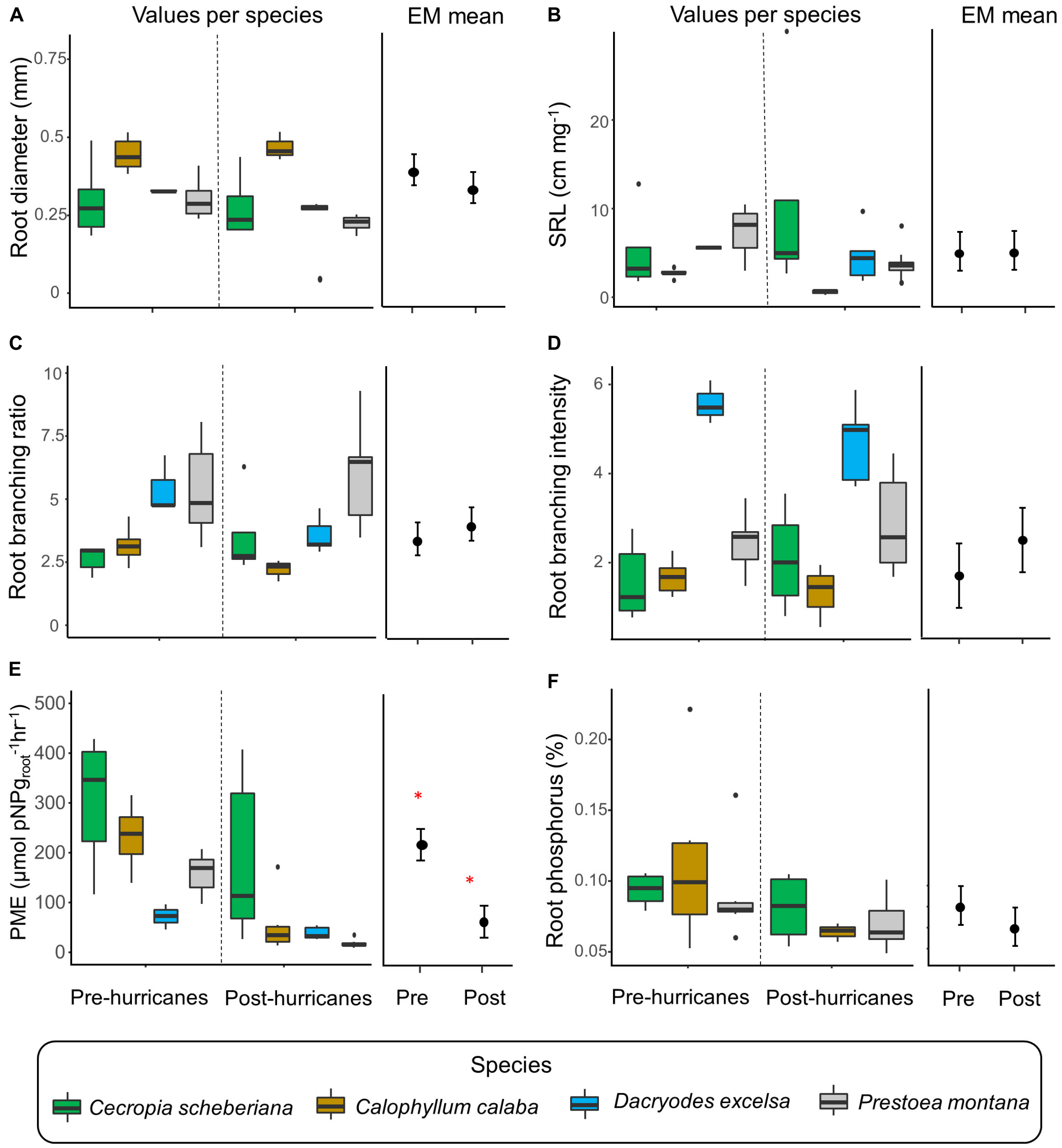

FIGURE 5 | Fine-root trait values for four common trees species at the Luquillo Experimental Forest in Puerto Rico before and after two consecutive hurricanes (boxplots on the left of each panel). We fitted linear mixed-effects models with tree within species within sites as a nested random effect and report the estimated marginal means (EM means; right plot of each panel) and standard error of the means for each root trait. **(A)** Root diameter and **(B)** specific root length (SRL) were measured from 1st root order. **(C)** Root branching ratio, **(D)** root branching intensity, **(E)** root phosphatase activity (phosphomonoesterase; PME), and **(F)** root phosphorus concentration were measured from 1st and 2nd orders combined. Significant differences in (mean) root trait values before and after the hurricanes are marked with a red asterisk. Due to sampling restriction, root phosphatase activity (phosphomonoesterase; PME) was not measured for *Spathodea campanulata* and root phosphorus concentration was not estimated for *Dacryodes excelsa*.

the percent of mycorrhizal colonization was similar within species present in at least two of our three sites (**Supplementary Table 1**). Similarly, site differences in environmental conditions did not appear to drive variation in AM hyphal length in tropical forests of Costa Rica, Panama, Peru, and Brazil (Powers et al., 2005). In addition, some studies suggest that AM fungi may colonize root cortical tissue independently of soil P availability, due to a lack of efficient plant mechanisms to control mycorrhizal colonization (Johnson, 2010; Valverde-Barrantes et al., 2016).

We found that the pioneers *Cecropia* and *Spathodea* had greater mycorrhizal colonization than non-pioneers. This has also been shown in some studies from Brazil where AM colonization decreased as species composition changed during forest succession (Zangaro et al., 2008, 2012). However, other studies from Puerto Rico showed that pioneer plant species were more independent of their fungal mycorrhizal partners than non-pioneers (Myster et al., 2013; Bachelot and Lee, 2018). These apparent contradictions represent a genuine challenge in the rhizosphere ecology. Although broader studies are needed in tropical ecosystems, we can attribute some of the differences between our study and others to the selection of tree species, sample size, and tree age, as most other studies estimated mycorrhizal colonization on seedlings, whereas we sampled mature trees.

No Trade-Off Between Fine-Root Physiology and Mycorrhizal Colonization

We hypothesized that high root phosphatase activity and adjustments in architectural and morphological traits would represent a combined strategy for P acquisition (H1), which would be in contrast with a strategy of high mycorrhizal colonization (H2). In theory, both strategies represent a significant cost to the plants, which can either invest in P-mineralizing enzymes, high length per unit biomass, and high number of first-order roots or in mycorrhizal symbionts (Treseder and Vitousek, 2001; Liu et al., 2015; Nasto et al., 2017, 2019; Cabugao et al., 2021). In addition, root phosphatase activity has been shown to relate positively to SRL at the community level within the LEF (Cabugao et al., 2021), which implies that root phosphatase activity would be part of the "do-it-yourself" end of the collaboration gradient, opposite from mycorrhizal colonization (Bergmann et al., 2020). However, we partially rejected both hypotheses as no relationships were detected between root phosphatase activity and branching intensity or SRL (**Supplementary Figure 2**) except for the negative relationship between phosphatase activity and branching ratio, and as mycorrhizal colonization and root phosphatase activity were positively related (when considering site variation only). This suggests that enzyme exudation and mycorrhizal colonization are not contrasting strategies for the five species considered at the LEF. This could partly be attributed to the large interspecific variations in root trait expression because the relationship between mycorrhizal colonization and phosphatase activity was not statistically significant when considering species within sites as a random effect in the models (**Supplementary Table 2**). In addition, our results suggest that in our five tree species, both fine roots and AM fungi may have contributed to phosphatase activity given that 43% of the root phosphatase activity variation was explained by the mycorrhizal colonization in our model (**Figure 4A**). Mycorrhizal fungi, such as AM fungi are capable of exuding phosphatase, yet their ability to hydrolyze organic P is still controversial (Koide and Kabir, 2000; Smith and Read, 2008). This points out the additional work needed to understand the contribution of AM fungi to root phosphatase activity.

The percent of root colonization by AM fungi was weakly positively related to SRL of first-order roots (19% of variation explained; **Figure 4D**), contradicting the root economic space framework in which mycorrhizal colonization is expected to co-vary positively with root diameter and thus, negatively with SRL (Brundrett, 2002; Kong et al., 2014; Bergmann et al., 2020). However, another study in a tropical forest of Brazil found a positive relationship between mycorrhizal colonization and SRL (Zangaro et al., 2008). Furthermore, SRL observations across a world-wide range of species have also shown that plants can construct roots with many combinations of morphological traits (Kramer-Walter et al., 2016; Weemstra et al., 2016; Bergmann et al., 2020) and that mycorrhizal colonization is highly dependent on tree developmental stage and the anatomy of the fine root (i.e., cortex cell properties; Brundrett, 2002; Bachelot et al., 2017). Thus, the relationship among these traits is complex and depends on different species-specific factors. When fitting models with species within sites as a random effect, SRL and mycorrhizal colonization were no longer positively correlated; in contrast mycorrhizal colonization appeared to be positively related to root diameter, as predicted by the root economic space framework (**Supplementary Table 2**). This highlights that root trait trade-offs at the species level inform species-specific resource acquisition strategies that may differ from patterns at the global scale (Freschet et al., 2021).

Trade-Offs Between Mycorrhizae, Root Branching, and Phosphatase Activity

Fine-root branching ratio and colonization by AM fungi were negatively related, such that species exhibiting high levels of colonization had a lower number of first-order roots per number of second-order roots (less branching). This partially supports our hypotheses (H1 and H2) as root branching and mycorrhizal colonization represent different strategies for soil P acquisition. Both AM fungi and root branching greatly contribute to soil P foraging (Treseder, 2013; Liu et al., 2018; Wang Y. et al., 2018), yet plants must balance their investment in these P strategies due to their significant costs (Eissenstat et al., 2015). Moreover, as hypothesized (H3), both traits representing contrasting strategies were weakly positively related to root P concentration, which is a good indicator of plant P status (and this correlation holds even when including site and species within sites as random effects in the models). Although we have no direct measure of P acquisition (e.g., instantaneous P uptake rate by roots or annual whole-plant P increment), root P concentration potentially reflects P acquisition due to its strong correlation to both leaf P concentration (Holdaway et al., 2011) and soil inorganic and total P (Holdaway et al., 2011; Schreeg et al., 2014; Freschet et al., 2021; **Supplementary Figure 1A**) which we also found in this study (**Supplementary Figure 1B**). Finally root branching was weakly negatively related to phosphatase activity (17% of variation explained; **Figure 4B**), probably due to the possible combined phosphatase activity from roots and their fungal partners.

P-Acquisition Strategies Vary Across Species

We considered two pioneer species *Spathodea campanulata* and *Cecropia schreberiana* that generally display acquisitive leaf traits (e.g., high leaf nitrogen concentration; Lugo and Abelleira Martínez, 2018), and three non-pioneer species *Calophyllum calaba*, *Dacryodes excelsa*, and *Prestoea montana* that display conservative leaf traits (e.g., high specific leaf area; Harris and Medina, 2013; **Figure 6**). These differences

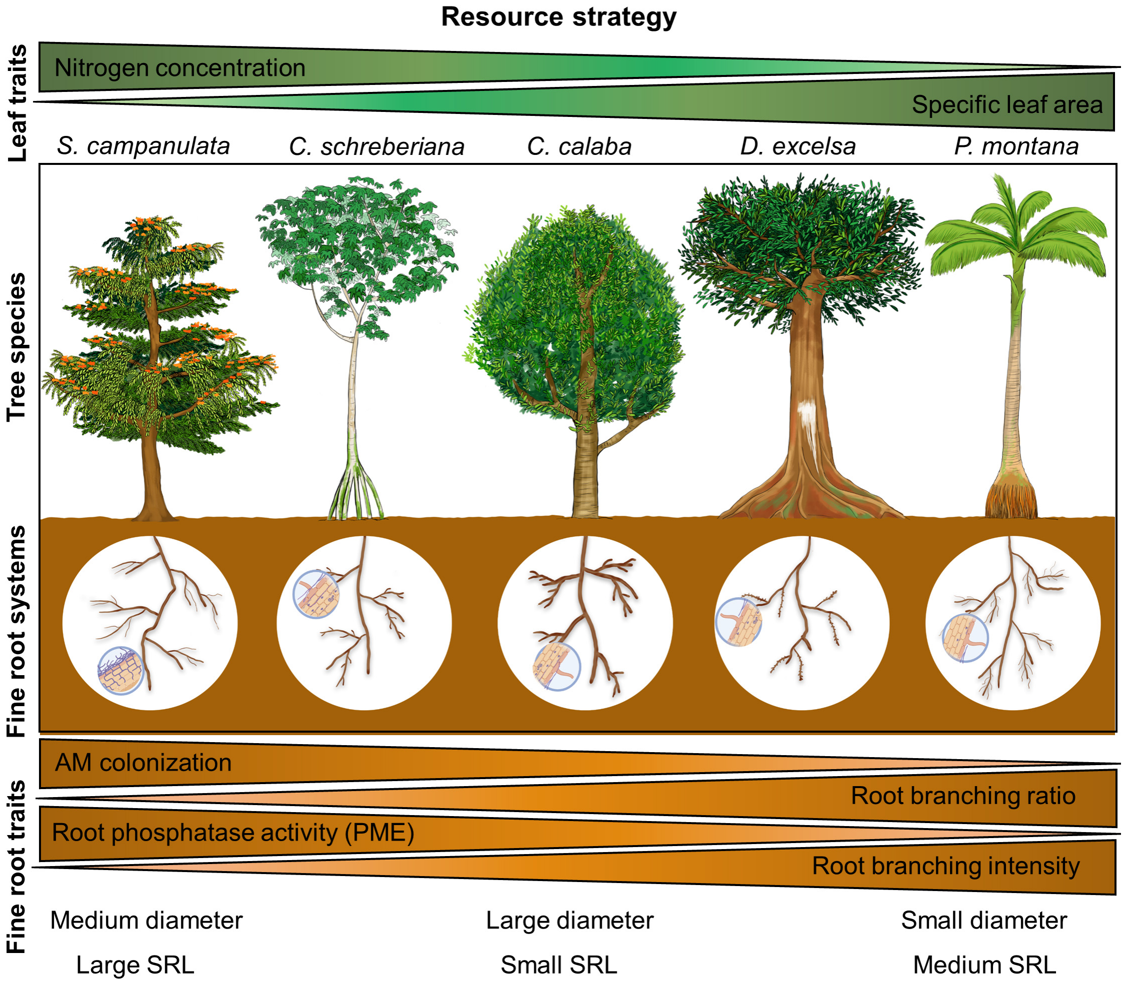

FIGURE 6 | Conceptual diagram of belowground phosphorus-acquisition strategies of five tropical tree species from Puerto Rico. Our results highlight a trade-off between highly colonized fine roots with high phosphatase activity and fine roots that have a high degree of branching. Furthermore, the former strategy is adopted by pioneer species (*Spathodea campanulata* and *Cecropia schreberiana*), whereas the latter is adopted by non-pioneer species (mostly *Dacryodes excelsa* and *Prestoea montana*). Root phosphorus concentration was not included here because no clear pattern was found across species.

in plant leaf traits for resource acquisition and resource conservation typically divide fast-growing pioneer species from slow-growing non-pioneer species (Grime, 1977; Wright et al., 2004; Weemstra et al., 2016). Similarly, some studies also found important root trait differences across different plant successional status (Coll et al., 2008; Zangaro et al., 2012; Xiang et al., 2013; Caplan et al., 2019). Accordingly, we found that fine-root architectural traits, phosphatase activity, and mycorrhizal colonization are all important in separating pioneers from non-pioneer tree species, but there was no equivalent pattern for morphological traits (**Figure 6**).

Both fast-growing pioneers, *Spathodea* and *Cecropia*, had greater mycorrhizal colonization, and *Cecropia* had the highest phosphatase activity compared to the other species studied. Investing carbon in fungal partners to outsource nutrient acquisition could benefit plants with higher P nutrient demand, and therefore enable faster growth (Wright et al., 2004; Freschet et al., 2021), which appears to support both the collaboration and the conservation gradient framework (Bergmann et al., 2020). The combined above- and belowground P-acquisition strategies from these pioneer species might partially explain their large dominant presence in Puerto Rico (Brandeis et al., 2003), and may help them thrive in gaps formed from natural and anthropogenic disturbances (i.e., hurricanes; for *Cecropia*) and in degraded soils (for *Spathodea*; Aide et al., 2000; Francis, 2000; Lugo et al., 2011). In contrast, the slow-growing non-pioneers, *Dacryodes* and *Prestoea*, showed greater root branching ratio and intensity compared to the other species, which represents a greater carbon investment in root construction for nutrient exploration (Hodge, 2004; Liese et al., 2017; **Figure 6**). Because root branching is considered a leading root trait due to its plasticity and relationship with mycorrhizal association type and resource exploitation (Kong et al., 2014; Liese et al., 2017; Freschet et al., 2021), the high values of branching ratio and intensity might play an important role in the large dominant presence of *Dacryodes* and *Prestoea* in the mature wet forests of the LEF (Aide et al., 2000; Francis, 2000). Further, although *Calophyllum* is a non-pioneer species, it had low values of root branching, compared to the other non-pioneer species, and low values of phosphatase activity, and mycorrhizal colonization compared to the pioneer species (**Figure 6**). This species' distribution is mostly attributed to its use for reforestation on degraded soils (Francis, 2000), and its soil P-acquisition strategy might be related to other root trait syndromes that we have not considered in this study.

Stability of Root Trait Expression Before vs. After the Hurricanes

We showed no apparent changes in most root trait expression 6 months after hurricanes Irma and María impacted the forest compared to their pre-hurricane values. Root phosphatase activity, however, was significantly different after the hurricanes. This difference may have reflected normal seasonal environmental changes (Sardans et al., 2007), but it is likely that there also were effects of the numerous changes in forest structure, soil biogeochemistry, and environmental conditions created by the hurricanes. These influences could have included changes in soil available P (Dakora and Phillips, 2002; Burns et al., 2013; Dalling et al., 2016; Margalef et al., 2017). However, although we expected that the decrease in root phosphatase activity could have been triggered by an increase in soil available P, we in fact measured a decrease in soil available P in our sites (**Table 1**). Reed et al. (2020) also reported an initial decrease in soil available P (first 3 months after Hurricane María), but soon after, they measured a sharp increase. Differences in methods assessing soil available P can account for important differences in *P*-values (Neyroud and Lischer, 2003), which represents a challenge and limitation in tropical forest ecology. Nevertheless, other potential factors influencing changes in root phosphatase activity could have been related to changes in soil moisture (SB2 was flooded for several months), a decrease of plant demand for P because of extensive defoliation, or changes in competition from understory vegetation abundance (Kennard et al., 2020; Reed et al., 2020). We cannot separate these different possible influences but note that the responsiveness of root phosphatase to environmental change may be an important consideration in evaluating phosphorus nutrition of tropical forests.

CONCLUSION

To overcome soil P limitation in lowland tropical forests, plants employ multiple strategies belowground, such as increasing SRL, root branching, root phosphatase activity and their reliance on AM fungi. However, relationships and potential trade-offs among these strategies are poorly understood. This limits our ability to predict potential feedbacks between plant traits and the P cycle in these ecosystems. Here, we reveal a trade-off between highly colonized fine roots with high root phosphatase activity and fine roots that have a high degree of branching, using five tree species growing in Puerto Rico. Tree successional status was a good predictor of belowground P-acquisition strategies as pioneers invested resources in mycorrhizal fungi and root phosphatase activity, whereas non-pioneers increased fine-root branching. In addition, most root traits before and after two consecutive hurricanes did not show significant changes in the species we studied. Root phosphatase activity, however, did vary when comparing pre- and post-hurricanes, and the causation of this variation might be relevant to future studies. Finally, expanding studies on belowground traits in the tropics to include "hard" functional traits, such as phosphatase activity should help to predict plant responses to natural disturbances and aid in the simulation of trait diversity and coexistence under resource limitation in tropical forests.

DATA AVAILABILITY STATEMENT

The data used in this study are publicly available at the NGEE Tropics repository under the DOI: 10.15486/ngt/1778242.

AUTHOR CONTRIBUTIONS

DY developed the concept for the project, took the field and laboratory measurements, analyzed the data, and wrote the manuscript. CD provided essential insight to the concept of the project and to writing the manuscript. KGC helped to developed the concept for the project, took field and laboratory measurements, and reviewed the manuscript. SNK assisted in data analysis, reviewed, and edited the manuscript. JC and NC participated in the field and laboratory measurements and reviewed the manuscript. RJN developed the concept for the project, helped with the field and laboratory measurements, helped in data analysis, and reviewed and edited the manuscript. All authors contributed to the article and approved the submitted version.

FUNDING

This research was supported by the Next Generation Ecosystem Experiments-Tropics, funded by the United States Department of Energy, Office of Science, Office of Biological and Environmental Research. Oak Ridge National Laboratory is managed by UT-Battelle, LLC, for the United States Department of Energy under contract DE-AC05–00OR22725.

ACKNOWLEDGMENTS

We acknowledge Joshua Price, Benjamin Branoff, and Lalasia Bialic-Murphy for the statistical and graphical guidance in the analysis; Ariel Lugo, Colleen Iversen, Elvira Cuevas, Jean Lodge, and Tana Wood for their essential insights and equipment; Deanne Brice, Nathan Stenson, and Holly Vander Stel for the help in the field and in the laboratory; and Gabriela Moncada for the tree designs.

SUPPLEMENTARY MATERIAL

The Supplementary Material for this article can be found online at: https://www.frontiersin.org/articles/10.3389/ffgc.2021.698191/full#supplementary-material

REFERENCES

Addo-Danso, S. D., Defrenne, C. E., McCormack, M. L., Ostonen, I., Addo-Danso, A., Foli, E. G., et al. (2020). Fine-root morphological trait variation in tropical forest ecosystems: an evidence synthesis. *Plant Ecol.* 221, 1–13. doi: 10.1007/s11258-019-00986-1

Aide, M. T., Zimmerman, J. K., Pascarella, J. B., Rivera, L., and Marcano-Vega, H. (2000). Forest regeneration in a chronosequence of tropical abandoned pastures: implications for restoration ecology. *Restor. Ecol.* 8, 328–338. doi: 10.1046/j.1526-100X.2000.80048.x

Bachelot, B., and Lee, C. T. (2018). Dynamic preferential allocation to arbuscular mycorrhizal fungi explains fungal succession and coexistence. *Ecology* 99, 372–384. doi: 10.1002/ecy.2080

Bachelot, B., Uriarte, M., McGuire, K. L., Thompson, J., and Zimmerman, J. (2017). Arbuscular mycorrhizal fungal diversity and natural enemies promote coexistence of tropical tree species. *Ecology* 98, 712–720. doi: 10.1002/ecy.1683

Bardgett, R. D., Mommer, L., and De Vries, F. T. (2014). Going underground: Root traits as drivers of ecosystem processes. *Trends Ecol. Evol.* 29, 692–699. doi: 10.1016/j.tree.2014.10.006

Bates, D., Mächler, M., Bolker, B. M., and Walker, S. C. (2015). Fitting linear mixed-effects models using lme4. *J. Stat. Softw.* 67, 1–48. doi: 10.18637/jss.v067.i01

Bergmann, J., Weigelt, A., Van Der Plas, F., Laughlin, D. C., Kuyper, T. W., Guerrero-Ramirez, N., et al. (2020). The fungal collaboration gradient dominates the root economics space in plants. *Sci. Adv.* 6:27. doi: 10.1126/sciadv.aba3756

Bonan, G. B. (2008). Forests and climate change: forcings, feedbacks, and the climate benefits of forests. *Science* 320, 1444–1449. doi: 10.1126/science.1155121

Brandeis, T. J., Helmer, E. H., and Oswalt, S. N. (2003). *The Status of Puerto Rico's Forests, 2003.* Resource Bulletin SRS-119. Asheville, NC: U.S. Department of Agriculture Forest Service.

Brown, S., Lugo, A. E., Silander, S., and Liegel, L. (1983). *Research History and Opportunities in the Luquillo Experimental Forest.* General Technical Report SO-44. New Orleans, LA: U.S. Dept of Agriculture, Forest Service, doi: 10.2737/SO-GTR-44

Brundrett, M. C. (2002). Coevolution of roots and mycorrhizas of land plants. *New Phytol.* 154, 275–304. doi: 10.1046/j.1469-8137.2002.00397.x

Burns, R. G., DeForest, J. L., Marxsen, J., Sinsabaugh, R. L., Stromberger, M. E., Wallenstein, M. D., et al. (2013). Soil enzymes in a changing environment: current knowledge and future directions. *Soil Biol. Biochem.* 58, 216–234. doi: 10.1016/j.soilbio.2012.11.009

Cabugao, K. G., Timm, C. M., Carrell, A. A., Childs, J., Lu, T. Y. S., Pelletier, D. A., et al. (2017). Root and rhizosphere bacterial phosphatase activity varies with tree species and soil phosphorus availability in puerto rico tropical forest. *Front. Plant Sci.* 8:1834. doi: 10.3389/fpls.2017.01834

Cabugao, K. G., Yaffar, D., Stenson, N., Childs, J., Phillips, J., Mayes, M. A., et al. (2021). Bringing function to structure: root–soil interactions shaping phosphatase activity throughout a soil profile in Puerto Rico. *Ecol. Evol.* 11, 1150–1164. doi: 10.1002/ece3.7036

Caplan, J. S., Meiners, S. J., Flores-Moreno, H., and McCormack, M. L. (2019). Fine-root traits are linked to species dynamics in a successional plant community. *Ecology* 100:e02588. doi: 10.1002/ecy.2588

Cernusak, L. A., Winter, K., Dalling, J. W., Holtum, J. A. M., Jaramillo, C., Körner, C., et al. (2013). Tropical forest responses to increasing atmospheric CO2: current knowledge and opportunities for future research. *Funct. Plant Biol.* 40, 531–551. doi: 10.1071/FP12309

Chambers, J. M., Freeny, A. E., and Heiberger, R. M. (2017). "Analysis of variance; designed experiments," in *Statistical Models in S*, eds J. M. Chambers and T. J. Hastie (Boca Raton, FL: Routledge), doi: 10.1201/9780203738535

Coll, L., Potvin, C., Messier, C., and Delagrange, S. (2008). Root architecture and allocation patterns of eight native tropical species with different successional status used in open-grown mixed plantations in Panama. *Trees Struct. Funct.* 22:585. doi: 10.1007/s00468-008-0219-6

Comas, L. H., Callahan, H. S., and Midford, P. E. (2014). Patterns in root traits of woody species hosting arbuscular and ectomycorrhizas: implications for the evolution of belowground strategies. *Ecol. Evol.* 4, 2979–2990. doi: 10.1002/ece3.1147

Dakora, F. D., and Phillips, D. A. (2002). "Root exudates as mediators of mineral acquisition in low-nutrient environments," in *Food Security in Nutrient-Stressed Environments: Exploiting Plants' Genetic Capabilities*, ed. J. J. Adu-Gyamfi (Dordrecht: Springer), 201–213. doi: 10.1023/A:1020809400075

Dalling, J. W., Heineman, K., Lopez, O. R., Wright, S. J., and Turner, B. L. (2016). "Nutrient availability in tropical rain forests: the paradigm of phosphorus limitation," in *Tropical tree physiology*, eds G. Guillermo and L. S. Santiago (Cham: Springer International Publishing), 261–273. doi: 10.1007/978-3-319-27422-5_12

Eissenstat, D. M., Kucharski, J. M., Zadworny, M., Adams, T. S., and Koide, R. T. (2015). Linking root traits to nutrient foraging in arbuscular mycorrhizal trees in a temperate forest. *New Phytol.* 208, 114–124. doi: 10.1111/nph.13451

Fox, J., and Weisberg, S. (2019). *CAR – An R Companion to Applied Regression.* Thousand Oaks, CA: Sage.

Francis, J. K. (2000). *Bioecología de Arboles Nativos y Exóticos de Puerto Rico y las Indias Occidentales.* General Technical Report IITF-15. Río Piedras, PR: USDA.

Freschet, G. T., Kichenin, E., and Wardle, D. A. (2015). Explaining within-community variation in plant biomass allocation: A balance between organ biomass and morphology above vs below ground? *J. Veg. Sci.* 26, 431–440. doi: 10.1111/jvs.12259

Freschet, G. T., Roumet, C., Comas, L. H., Weemstra, M., Bengough, A. G., Rewald, B., et al. (2021). Root traits as drivers of plant and ecosystem functioning: current understanding, pitfalls and future research needs. *New Phytol.* doi: 10.1111/nph.17072

Grime, J. P. (1977). Evidence for the existence of three primary strategies in plants and its relevance to ecological and evolutionary theory. *Am. Nat.* 111, 1169–1194. doi: 10.1086/283244

Guilbeault-Mayers, X., Turner, B. L., and Laliberté, E. (2020). Greater root phosphatase activity of tropical trees at low phosphorus despite strong variation among species. *Ecology* 101:e03090. doi: 10.1002/ecy.3090

Harris, N. L., and Medina, E. (2013). Changes in leaf properties across an elevation gradient in the luquillo mountains. *Puerto Rico. Ecol. Bull.* 54, 169–180.

Hinsinger, P. (2001). Bioavailability of soil inorganic P in the rhizosphere as affected by root-induced chemical changes: a review. *Plant Soil* 237, 173–195. doi: 10.1023/A:1013351617532

Hodge, A. (2004). The plastic plant: root responses to heterogeneous supplies of nutrients. *New Phytol.* 162, 9–24. doi: 10.1111/j.1469-8137.2004.01015.x

Holdaway, R. J., Richardson, S. J., Dickie, I. A., Peltzer, D. A., and Coomes, D. A. (2011). Species- and community-level patterns in fine root traits along a 120000-year soil chronosequence in temperate rain forest. *J. Ecol.* 99, 954–963. doi: 10.1111/j.1365-2745.2011.01821.x

Iversen, C. M., Powell, A. S., McCormack, M. L., Blackwood, C. B., Freschet, G. T., Kattge, J., et al. (2018). *Fine-Root Ecology Database (FRED): A Global Collection of Root Trait Data with Coincident Site, Vegetation, Edaphic, and Climatic Data, Version 2.* Oak Ridge National Lab. TES SFA. Oak Ridge, TN: U.S. Department Energy.

Johnson, N. C. (2010). Resource stoichiometry elucidates the structure and function of arbuscular mycorrhizas across scales. *New Phytol.* 185, 631–647. doi: 10.1111/j.1469-8137.2009.03110.x

Kennard, D. K., Matlaga, D., Sharpe, J., Wood, T. E., Alonso-Rodríguez, A. M., Reed, S. C., et al. (2020). Tropical understory herbaceous community responds more strongly to hurricane disturbance than to experimental warming. *Ecol. Evol.* 10, 8906–8915. doi: 10.1002/ece3.6589

Koide, R. T., and Kabir, Z. (2000). Extraradical hyphae of the mycorrhizal fungus Glomus intraradices can hydrolyse organic phosphate. *New Phytol.* 148, 511–517. doi: 10.1046/j.1469-8137.2000.00776.x

Kong, D., Ma, C., Zhang, Q., Li, L., Chen, X., Zeng, H., et al. (2014). Leading dimensions in absorptive root trait variation across 96 subtropical forest species. *New Phytol.* 203, 863–872. doi: 10.1111/nph.12842

Kormanik, P. P., and Mcgraw, A. C. (1982). "Quantification of vesicular-arbuscular mycorrhizas in plant roots," in *Methods and Principles of Mycorrhizal Research,* ed. N. C. Schenck (St Paul, MI: The American Phytopathological Society), 37–45.

Kramer-Walter, K. R., Bellingham, P. J., Millar, T. R., Smissen, R. D., Richardson, S. J., and Laughlin, D. C. (2016). Root traits are multidimensional: specific root length is independent from root tissue density and the plant economic spectrum. *J. Ecol.* 104, 1299–1310. doi: 10.1111/1365-2745.12562

Kruskal, J. B. (1964). Multidimensional scaling by optimizing goodness of fit to a nonmetric hypothesis. *Psychometrika* 29, 1–27. doi: 10.1007/BF02289565

Lambers, H., Shane, M. W., Cramer, M. D., Pearse, S. J., and Veneklaas, E. J. (2006). Root structure and functioning for efficient acquisition of phosphorus: matching morphological and physiological traits. *Ann. Bot.* 98, 693–713. doi: 10.1093/aob/mcl114

Lee, R. B. (1988). Phosphate influx and extracellular phosphatase activity in barley roots and rose cells. *New Phytol.* 109, 141–148. doi: 10.1111/j.1469-8137.1988.tb03701.x

Lenth, R., Singmann, H., Love, J., Buerkner, P., and Herve, M. (2020). *Estimated Marginal Means, Aka Least-Squares Means.* R Package version 1.5.0. Available online at: https://CRAN.R-project.orgpackage=emmeans (accessed April 23, 2021).

Liese, R., Alings, K., and Meier, I. C. (2017). Root branching is a leading root trait of the plant economics spectrum in temperate trees. *Front. Plant Sci.* 8:315. doi: 10.3389/fpls.2017.00315

Liptzin, D., Silver, W. L., and Pan, Y. (2015). Spatial patterns in oxygen and redox sensitive biogeochemistry in tropical forest soils. *Ecosphere* 6, 1–14. doi: 10.1890/ES14-00309.1

Liu, B., Li, H., Zhu, B., Koide, R. T., Eissenstat, D. M., and Guo, D. (2015). Complementarity in nutrient foraging strategies of absorptive fine roots and arbuscular mycorrhizal fungi across 14 coexisting subtropical tree species. *New Phytol.* 208, 125–136. doi: 10.1111/nph.13434

Liu, C., Ravnskov, S., Liu, F., Rubæk, G. H., and Andersen, M. N. (2018). Arbuscular mycorrhizal fungi alleviate abiotic stresses in potato plants caused by low phosphorus and deficit irrigation/partial root-zone drying. *J. Agric. Sci.* 156, 46–58. doi: 10.1017/S0021859618000023

Liu, C., Xiang, W., Zou, L., Lei, P., Zeng, Y., Ouyang, S., et al. (2019). Variation in the functional traits of fine roots is linked to phylogenetics in the common tree species of Chinese subtropical forests. *Plant Soil* 436, 347–364. doi: 10.1007/s11104-019-03934-0

Lüdecke, D., Makowski, D., Waggoner, P., and Patil, I. (2020). *Performance: Assessment of Regression Models Performance*. Available online at: https://cran.r-project.org/package=performance (accessed April 23, 2021).

Lugli, L. F., Andersen, K. M., Aragão, L. E. O. C., Cordeiro, A. L., Cunha, H. F. V., Fuchslueger, L., et al. (2019). Multiple phosphorus acquisition strategies adopted by fine roots in low-fertility soils in Central Amazonia. *Plant Soil* 450, 49–63. doi: 10.1007/s11104-019-03963-9

Lugli, L. F., Rosa, J. S., Andersen, K. M., Di Ponzio, R., Almeida, R. V., Pires, M., et al. (2021). Rapid responses of root traits and productivity to phosphorus and cation additions in a tropical lowland forest in Amazonia. *New Phytol.* 230, 116–128. doi: 10.1111/nph.17154

Lugo, A. E. (2020). Effects of extreme disturbance events: from ecesis to social–ecological–technological systems. *Ecosystems* 23, 1726–1747. doi: 10.1007/s10021-020-00491-x

Lugo, A. E., Abelleira, O. J., Collado, A., Viera, C. A., Santiago, C., Vélez, D. O., et al. (2011). Allometry, biomass, and chemical content of Novel African Tulip Tree (*Spathodea campanulata*) forests in puerto rico. *New For.* 42, 267–283. doi: 10.1007/s11056-011-9258-8

Lugo, A. E., and Abelleira Martínez, O. L. (2018). Stoichiometry of decomposing Spathodea campanulata leaves in novel puertorrican forests. *For. Ecol. Manage.* 430, 176–187. doi: 10.1016/j.foreco.2018.07.059

Ma, Z., Guo, D., Xu, X., Lu, M., Bardgett, R. D., Eissenstat, D. M., et al. (2018). Evolutionary history resolves global organization of root functional traits. *Nature* 555, 94–97. doi: 10.1038/nature25783

Margalef, O., Sardans, J., Fernández-Martínez, M., Molowny-Horas, R., Janssens, I. A., Ciais, P., et al. (2017). Global patterns of phosphatase activity in natural soils. *Sci. Rep.* 7: 1337. doi: 10.1038/s41598-017-01418-8

McCormack, M. L., Guo, D., Iversen, C. M., Chen, W., Eissenstat, D. M., Fernandez, C. W., et al. (2017). Building a better foundation: improving root-trait measurements to understand and model plant and ecosystem processes. *New Phytol.* 215, 27–37. doi: 10.1111/nph.14459

McCormack, M. L., and Iversen, C. M. (2019). Physical and functional constraints on viable belowground acquisition strategies. *Front. Plant Sci.* 10:1215. doi: 10.3389/fpls.2019.01215

McDonald, J. H. (2014). *Multiple comparisons – Handbook of Biological Statistics*. Baltimore, MD: Sparky House Publishing.

McGonigle, T. P., Miller, M. H., Evans, D. G., Fairchild, G. L., and Swan, J. A. (1990). A new method which gives an objective measure of colonization of roots by vesicular—arbuscular mycorrhizal fungi. *New Phytol.* 115, 495–501. doi: 10.1111/j.1469-8137.1990.tb00476.x

Myster, R. W., Lebron, L., Loayza, A. B. P., and Zimmerman, J. K. (2013). Mycotrophic strategy of 13 common neotropical trees and shrubs. *J. Trop. For. Sci.* 25, 34–41.

Nasto, M. K., Osborne, B. B., Lekberg, Y., Asner, G. P., Balzotti, C. S., Porder, S., et al. (2017). Nutrient acquisition, soil phosphorus partitioning and competition among trees in a lowland tropical rain forest. *New Phytol.* 214, 1506–1517. doi: 10.1111/nph.14494

Nasto, M. K., Winter, K., Turner, B. L., and Cleveland, C. C. (2019). Nutrient acquisition strategies augment growth in tropical N2-fixing trees in nutrient-poor soil and under elevated CO2. *Ecology* 100:e02646. doi: 10.1002/ecy.2646

Neyroud, J. A., and Lischer, P. (2003). Do different methods used to estimate soil phosphorus availability across Europe give comparable results? *J. Plant Nutr. Soil Sci.* 166, 422–431. doi: 10.1002/jpln.200321152

Olander, L. P., and Vitousek, P. M. (2004). Biological and geochemical sinks for phosphorus in soil from a wet tropical forest. *Ecosystems* 7, 404–419. doi: 10.1007/s10021-004-0264-y

Paoli, G. D., Curran, L. M., and Zak, D. R. (2005). Phosphorus efficiency of Bornean rain forest productivity: evidence against the unimodal efficiency hypothesis. *Ecology* 86, 1548–1561. doi: 10.1890/04-1126

Pasch, R. J., Penny, A. B., and Berg, R. (2019). *National Hurricane Center Tropical Cyclone Report: Hurricane Maria (AL152017)*. Silver Spring, MD: National Weather Service.

Png, G. K., Turner, B. L., Albornoz, F. E., Hayes, P. E., Lambers, H., and Laliberté, E. (2017). Greater root phosphatase activity in nitrogen-fixing rhizobial but not actinorhizal plants with declining phosphorus availability. *J. Ecol.* 105, 1246–1255. doi: 10.1111/1365-2745.12758

Ponciano, J. M., Taper, M. L., Dennis, B., and Lele, S. R. (2009). Hierarchical models in ecology: confidence intervals, hypothesis testing, and model selection using data cloning. *Ecology* 90, 356–362. doi: 10.1890/08-0967.1

Powers, J. S., Treseder, K. K., and Lerdau, M. T. (2005). Fine roots, arbuscular mycorrhizal hyphae and soil nutrients in four neotropical rain forests: patterns across large geographic distances. *New Phytol.* 165, 913–921. doi: 10.1111/j.1469-8137.2004.01279.x

Pregitzer, K. S., DeForest, J. L., Burton, A. J., Allen, M. F., Ruess, R. W., and Hendrick, R. L. (2002). Fine root architecture of nine north american trees. *Ecol. Monogr.* 72, 293–309. doi: 10.2307/3100029

Quesada, C. A., Lloyd, J., Schwarz, M., Patiño, S., Baker, T. R., Czimczik, C., et al. (2010). Variations in chemical and physical properties of Amazon forest soils in relation to their genesis. *Biogeosciences* 7, 1515–1541. doi: 10.5194/bg-7-1515-2010

R Core Team (2019). *R: A Language and Environment for Statistical Computing*. Vienna: R Foundation Statistics Computing.

Reed, S. C., Reibold, R., Cavaleri, M. A., Alonso-Rodríguez, A. M., Berberich, M. E., and Wood, T. E. (2020). Soil biogeochemical responses of a tropical forest to warming and hurricane disturbance. *Adv. Ecol. Res.* 62, 226–248. doi: 10.1016/bs.aecr.2020.01.007

Reed, S. C., Townsend, A. R., Taylor, P. G., and Cleveland, C. C. (2011). "Phosphorus cycling in tropical forests growing on highly weathered soils," in *Phosphorus in Action. Soil Biology*, Vol. 26, eds E. Bünemann, A. Oberson, and E. Frossard (Berlin: Springer), doi: 10.1007/978-3-642-15271-9_14

Ryser, P., and Eek, L. (2000). Consequences of phenotypic plasticity vs. interspecific differences in leaf and root traits for acquisition of aboveground and belowground resources. *Am. J. Bot.* 87, 402–411. doi: 10.2307/2656636

Santiago, L. S. (2015). Nutrient limitation of eco-physiological processes in tropical trees. *Trees Struct. Funct.* 29, 1291–1300. doi: 10.1007/s00468-015-1260-x

Sardans, J., Peñuelas, J., and Estiarte, M. (2007). Seasonal patterns of root-surface phosphatase activities in a Mediterranean shrubland. Responses to experimental warming and drought. *Biol. Fertil. Soils* 43, 779–786. doi: 10.1007/s00374-007-0166-1

Scatena, F. N. (1989). *An Introduction to the Physiography and History of the Bisley Experimental Watersheds in the Luquillo Mountains of Puerto Rico.* General Technical Report SO-72. New Orleans, LA: Forest Service Southern Forest Experiment Station, 22.

Schreeg, L. A., Santiago, L. S., Wright, S. J., and Turner, B. L. (2014). Stem, root, and older leaf N: P ratios are more responsive indicators of soil nutrient availability than new foliage. *Ecology* 95, 2062–2068. doi: 10.1890/13-1671.1

Smith, S., and Read, D. (2008). *Mycorrhizal Symbiosis*, 3rd Edn. London: Academic Press, doi: 10.1016/B978-0-12-370526-6.X5001-6

Smith, S. E., and Smith, F. A. (2011). Roles of arbuscular mycorrhizas in plant nutrition and growth: new paradigms from cellular to ecosystem scales. *Annu. Rev. Plant Biol.* 62, 227–250. doi: 10.1146/annurev-arplant-042110-103846

Stone, M. M., DeForest, J. L., and Plante, A. F. (2014). Changes in extracellular enzyme activity and microbial community structure with soil depth at the Luquillo Critical Zone Observatory. *Soil Biol. Biochem.* 75, 237–247. doi: 10.1016/j.soilbio.2014.04.017

Tabatabai, M. A., and Bremner, J. M. (1969). Use of p-nitrophenyl phosphate for assay of soil phosphatase activity. *Soil Biol. Biochem.* 1, 301–307. doi: 10.1016/0038-0717(69)90012-1

Townsend, A. R., Cleveland, C. C., Asner, G. P., and Bustamante, M. M. C. (2007). Controls over foliar N: P ratios in tropical rain forests. *Ecology* 88, 107–118. doi: 10.1890/0012-9658(2007)88[107:cofnri]2.0.co;2

Treseder, K. K. (2013). The extent of mycorrhizal colonization of roots and its influence on plant growth and phosphorus content. *Plant Soil.* 371, 1–13. doi: 10.1007/s11104-013-1681-5

Treseder, K. K., and Vitousek, P. M. (2001). Effects of soil nutrient availability on investment in acquisition of N and P in Hawaiian rain forests. *Ecology* 82, 946–954. doi: 10.1890/0012-9658(2001)082[0946:eosnao]2.0.co;2

Turner, B. L. (2008). Resource partitioning for soil phosphorus: a hypothesis. *J. Ecol.* 96, 698–702. doi: 10.1111/j.1365-2745.2008.01384.x

Uriarte, M., and Zimmerman, J. (2017). *El Yunque Chronosequence Tree Census Data ver 17. Environmental Data Initiative.* Available online at: https://doi.org/10.6073/pasta/7a8315e46e841e20413968144c9e3076 (accessed June 27, 2021).

Uriarte, M., Thompson, J., and Zimmerman, J. K. (2019). Hurricane María tripled stem breaks and doubled tree mortality relative to other major storms. *Nat. Commun.* 10, 1–7. doi: 10.1038/s41467-019-09319-2

Valverde-Barrantes, O. J., Horning, A. L., Smemo, K. A., and Blackwood, C. B. (2016). Phylogenetically structured traits in root systems influence arbuscular mycorrhizal colonization in woody angiosperms. *Plant Soil* 404, 1–12. doi: 10.1007/s11104-016-2820-6

Valverde-Barrantes, O. J., Maherali, H., Baraloto, C., and Blackwood, C. B. (2020). Independent evolutionary changes in fine-root traits among main clades during the diversification of seed plants. *New Phytol.* 228, 541–553. doi: 10.1111/nph.16729

Valverde-Barrantes, O. J., Smemo, K. A., and Blackwood, C. B. (2015). Fine root morphology is phylogenetically structured, but nitrogen is related to the plant economics spectrum in temperate trees. *Funct. Ecol.* 29, 796–807. doi: 10.1111/1365-2435.12384

Vance, C. P., Uhde-Stone, C., and Allan, D. L. (2003). Phosphorus acquisition and use: Critical adaptations by plants for securing a nonrenewable resource. *New Phytol.* 157, 423–447. doi: 10.1046/j.1469-8137.2003.00695.x

Vitousek, P. M., and Sanford, R. L. (1986). Nutrient cycling in moist tropical forest. *Annu. Rev. Ecol. Syst.* 17, 137–167. doi: 10.1146/annurev.es.17.110186.001033

Walker, T. W., and Syers, J. K. (1976). The fate of phosphorus during pedogenesis. *Geoderma* 15, 1–19. doi: 10.1016/0016-7061(76)90066-5

Wang, R., Wang, Q., Zhao, N., Xu, Z., Zhu, X., Jiao, C., et al. (2018). Different phylogenetic and environmental controls of first-order root morphological and nutrient traits: evidence of multidimensional root traits. *Funct. Ecol.* 32, 29–39. doi: 10.1111/1365-2435.12983

Wang, Y., Wang, M., Li, Y., Wu, A., and Huang, J. (2018). Effects of arbuscular mycorrhizal fungi on growth and nitrogen uptake of *Chrysanthemum morifolium* under salt stress. *PLoS One* 13:e0196408. doi: 10.1371/journal.pone.0196408

Weemstra, M., Mommer, L., Visser, E. J. W., van Ruijven, J., Kuyper, T. W., Mohren, G. M. J., et al. (2016). Towards a multidimensional root trait framework: a tree root review. *New Phytol.* 211, 1159–1169. doi: 10.1111/nph.14003

Wen, Z., Li, H., Shen, Q., Tang, X., Xiong, C., Li, H., et al. (2019). Tradeoffs among root morphology, exudation and mycorrhizal symbioses for phosphorus-acquisition strategies of 16 crop species. *New Phytol.* 223, 882–895. doi: 10.1111/nph.15833

Wright, I. J., Reich, P. B., Westoby, M., Ackerly, D. D., Baruch, Z., Bongers, F., et al. (2004). The worldwide leaf economics spectrum. *Nature* 428, 821–827. doi: 10.1038/nature02403

Xiang, W., Wu, W., Tong, J., Deng, X., Tian, D., Zhang, L., et al. (2013). Differences in fine root traits between early and late-successional tree species in a Chinese subtropical forest. *Forestry* 86, 343–351. doi: 10.1093/forestry/cpt003

Zalamea, P. C., Turner, B. L., Winter, K., Jones, F. A., Sarmiento, C., and Dalling, J. W. (2016). Seedling growth responses to phosphorus reflect adult distribution patterns of tropical trees. *New Phytol.* 212, 400–408. doi: 10.1111/nph.14045

Zangaro, W., Alves, R. A., Lescano, L. E., Ansanelo, A. P., and Nogueira, M. A. (2012). Investment in fine roots and arbuscular mycorrhizal fungi decrease during succession in three brazilian ecosystems. *Biotropica* 44, 141–150. doi: 10.1111/j.1744-7429.2011.00781.x

Zangaro, W., De Assis, R. L., Rostirola, L. V., De Souza, P. B., Gonçalves, M. C., Andrade, G., et al. (2008). Changes in arbuscular mycorrhizal associations and fine root traits in sites under different plant successional phases in southern Brazil. *Mycorrhiza* 19, 37–45. doi: 10.1007/s00572-008-0202-5

Zangaro, W., Nishidate, F. R., Spago Camargo, F. R., Romagnoli, G. G., and Vandressen, J. (2005). Relationships among arbuscular mycorrhizas, root morphology and seedling growth of tropical native woody species in southern Brazil. *J. Trop. Ecol.* 21, 529–540. doi: 10.1017/S0266467405002555

Conflict of Interest: The authors declare that the research was conducted in the absence of any commercial or financial relationships that could be construed as a potential conflict of interest.

frontiers in Plant Science

ORIGINAL RESEARCH
published: 21 July 2021
doi: 10.3389/fpls.2021.682142

Shifts in the Abundances of Saprotrophic and Ectomycorrhizal Fungi With Altered Leaf Litter Inputs

Sara Marañón-Jiménez[1,2]*, Dajana Radujković[3], Erik Verbruggen[3], Oriol Grau[1,2,4], Matthias Cuntz[5], Josep Peñuelas[1,2], Andreas Richter[6], Marion Schrumpf[7] and Corinna Rebmann[8]

[1] Center for Ecological Research and Forestry Applications (CREAF), Bellaterra, Spain, [2] Spanish National Research Council (CSIC), Global Ecology Unit CREAF-CSIC-UAB, Bellaterra, Spain, [3] Centre of Excellence Plant and Ecosystems (PLECO), Department of Biology, University of Antwerp, Antwerp, Belgium, [4] French Agricultural Research Centre for International Development (CIRAD), Joint Research Unit Ecology of Guianan Forests-UMR EcoFoG (AgroParisTech, CNRS, INRA, University of Antilles, University of Guyane), Kourou, French Guiana, [5] Université de Lorraine, French National Institute of Agricultural Research, AgroParisTech, UMR 1434 Silva, Nancy, France, [6] Department of Microbiology and Ecosystem Science, University of Vienna, Wien, Austria, [7] Department for Biogeochemical Processes, Max Planck Institute for Biogeochemistry, Jena, Germany, [8] UFZ-Helmholtz Centre for Environmental Research, Department of Computational Hydrosystems, Leipzig, Germany

Edited by:
Camille Eichelberger Granada,
Universidade Do Vale Do
Taquari–Univates, Brazil

Reviewed by:
Valeria Prigione,
University of Turin, Italy
Erica Lumini,
Institute for Sustainable Plant
Protection, National Research Council
(CNR), Italy
Evelise Bach,
Federal University of Rio Grande Do
Sul, Brazil

***Correspondence:**
Sara Marañón-Jiménez
s.maranon@creaf.uab.es

Specialty section:
This article was submitted to
Plant Symbiotic Interactions,
a section of the journal
Frontiers in Plant Science

Received: 17 March 2021
Accepted: 22 June 2021
Published: 21 July 2021

Citation:
Marañón-Jiménez S, Radujković D,
Verbruggen E, Grau O, Cuntz M,
Peñuelas J, Richter A, Schrumpf M
and Rebmann C (2021) Shifts in the
Abundances of Saprotrophic and
Ectomycorrhizal Fungi With Altered
Leaf Litter Inputs.
Front. Plant Sci. 12:682142.
doi: 10.3389/fpls.2021.682142

Ectomycorrhizal (EcM) and saprotrophic fungi interact in the breakdown of organic matter, but the mechanisms underlying the EcM role on organic matter decomposition are not totally clear. We hypothesized that the ecological relations between EcM and saprotroph fungi are modulated by resources availability and accessibility, determining decomposition rates. We manipulated the amount of leaf litter inputs (No-Litter, Control Litter, Doubled Litter) on Trenched (root exclusion) and Non-Trenched plots (with roots) in a temperate deciduous forest of EcM-associated trees. Resultant shifts in soil fungal communities were determined by phospholipid fatty acids and DNA sequencing after 3 years, and CO_2 fluxes were measured throughout this period. Different levels of leaf litter inputs generated a gradient of organic substrate availability and accessibility, altering the composition and ecological relations between EcM and saprotroph fungal communities. EcM fungi dominated at low levels of fresh organic substrates and lower organic matter quality, where short-distances exploration types seem to be better competitors, whereas saprotrophs and longer exploration types of EcM fungi tended to dominate at high levels of leaf litter inputs, where labile organic substrates were easily accessible. We were, however, not able to detect unequivocal signs of competition between these fungal groups for common resources. These results point to the relevance of substrate quality and availability as key factors determining the role of EcM and saprotroph fungi on litter and soil organic matter decay and represent a path forward on the capacity of organic matter decomposition of different exploration types of EcM fungi.

Keywords: CO_2 fluxes, Gadgil effect, ectomycorrhiza fungal exploration types, litter decomposition, soil fungal communities, plant detritus

INTRODUCTION

Plants adjust the amount of carbon (C) invested in above- vs. belowground parts in response to soil nutrient availability to optimize biomass returns of invested carbon (Shipley and Meziane, 2002; Dybzinski et al., 2011). Accordingly, plants have been shown to allocate more C to mycorrhizal fungi in exchange for nutrients at elevated CO_2 and lower nutrient availability (Treseder, 2004; Alberton et al., 2005; Högberg et al., 2010; Phillips et al., 2011). Shifts in the amount of above- and belowground organic matter inputs to the soil may also shape the composition and activity of fungal communities (Yarwood et al., 2009; de Graaff et al., 2010; Kaiser et al., 2010), with potential implications for decomposition rates of organic matter and soil C storage.

EcM and saprotrophic fungi interact in the breakdown of litter-derived organic substrates, determining the decomposition rates, the fate and the stabilization of soil organic matter (SOM) (Lindahl and Tunlid, 2015). Many EcM fungi have the ability to produce oxidative enzymes for the breakdown of organic compounds (Bödeker et al., 2009; Nicolás et al., 2019), which can alter the degradability of residual SOM by the saprotroph community (Rineau et al., 2012). However, EcM fungi may also compete with the saprotrophic community for limiting water, nutrients or space (Lindahl et al., 2001; Koide and Wu, 2003; Bödeker et al., 2016). This competition has been long hypothesized to slow down decomposition rates (i.e., "Gadgil effect," Gadgil and Gadgil, 1971, 1975), leading to the prediction of larger C storage in forest soils (Orwin et al., 2011; Averill et al., 2014). Nonetheless, EcM fungi have shown both no effect (Mayor and Henkel, 2006; but see McGuire et al., 2010) and a stimulation of decomposition rates (Entry et al., 1991; Zhu and Ehrenfeld, 1996; Brzostek et al., 2015) and the mechanisms underlying the EcM role on organic matter decomposition are not totally clear (Fernandez and Kennedy, 2015).

Despite sharing common ancestors (Tedersoo et al., 2010), saprotrophs and ectomycorrhiza fungi have evolved into two fungal groups with well-differentiated resource needs and acquisition strategies. Some EcM guilds have retained the capacity to breakdown organic nitrogen (N) substrates (Shah et al., 2016; Nicolás et al., 2019) and can exploit litter selectively for N (Rineau et al., 2012; Bödeker et al., 2014). The direct supply of C from the plant host may confer an advantage to EcM fungi when organic substrates are not easily available, allowing them to allocate more resources to exploit and acquire N (Rineau et al., 2013; Lindahl and Tunlid, 2015). In line with this, fungal communities have shown segregated niche distribution with depth, where saprotrophs dominate in organic and cellulose-rich litter layers and EcM fungi are more abundant at greater depths, where the acquisition of N from more recalcitrant organic substrates also requires higher energy investment (Lindahl et al., 2007; Baldrian et al., 2012). Saprotrophic decomposition may be progressively restricted as the organic substrates become less accessible and the energy return of their decomposition declines (Baldrian, 2009; Sterkenburg et al., 2018). This niche segregation may be then the consequence of the specialization of each fungal group on divergent target resources and the development of different evolutionary strategies for their acquisition. Changes in substrates quality and availability can, therefore, drive shifts in the composition and abundance of EcM and saprotrophic fungi thereby modulating their ecological interactions and the decomposition rates of organic matter as a result.

In order to elucidate how resource availability govern the ecological feedbacks between saprotrophs and EcM fungal communities, we manipulated the amount of leaf litter inputs (No-Litter "NL," Control Litter "CL," Doubled Litter "DL") on Trenched ("T," root exclusion) and Non-Trenched plots ("NT," with roots) of a temperate deciduous forest composed of ectomycorrhiza-associated species (oak and beech). Resultant shifts in the diversity and composition of soil fungal communities as detected by ITS1 metabarconding and phospholipid fatty acids (PLFAs) and in the microbial biomass, dissolved organic C, and C and N stocks were determined after 3 years, and CO_2 fluxes were measured throughout this period. We hypothesized that: (1) Changes in the availability and accessibility of organic substrates in soil in response to altered leaf litter inputs modulate the dominance and ecological interactions between EcM and saprotroph fungi; (2) Conditions of limited access to organic substrates will benefit EcM over saprotroph fungi, leading to exacerbated competition between both groups for N sources, while plentiful and easily accessible organic matter inputs will benefit the proliferation of saprotrophs and relax the competition; (3) The exclusion of EcM fungi in Trenched plots will, therefore, increase saprotrophic abundance and decomposition rates in a larger extent at low litter inputs, resulting in a higher increase in the litter-derived CO_2 flux at "Control Litter" inputs compared to "Doubled Litter" inputs.

MATERIALS AND METHODS

Study Site

The study was conducted in a mixed deciduous forest ("Hohes Holz") in the area of the Magdeburger Boerde in central Germany (52°05′N, 11°13′E, 210 m above sea level). Climate in the study area is subatlantic-submontane. Mean annual temperature is 9.1°C (climatic period 1981–2010, station Ummendorf of German Weather Service), with mean minimum temperature in the coldest month (January) of 0.7°C, and mean maximum of the warmest month (July) of 18.3°C. Annual mean precipitation was 563 mm during the climatic period 1981–2010, while annual precipitation during the experiment measured locally at the site was 550 mm in 2015 and 390 mm in 2016. The forest stand is located in a mainly municipal forest area, managed by regional forestry. The experiment was conducted inside a 1 ha fenced area with ungulate enclosure since 2011, composed of sessile oak [*Quercus petraea* (Matt.) Liebl.] and European beech (*Fagus sylvatica* L.) as the dominant species (45 and 38% of total basal area, respectively) with accompanying hornbeam (*Carpinus betulus* L., 13%) and birch (*Betula pendula* Roth, 4%). Tree height and diameter at breast height were 27.0 ± 11.9 (SD) m, and 0.38 ± 0.2 m on average for beech and oak. The bedrock is Pleistocene sandy loess above till and Mesozoic muschelkalk, with Haplic Cambisol as predominant soil type. Soil texture at 0–20 cm depth was 3.0 ± 1.8% sand, 87.1 ± 2.1% silt, and 10.0 ± 2.2% clay,

TABLE 1 | Initial soil parameters measured prior to the establishment of the trenching and leaf litter input treatments.

Soil depth (cm)	SOC (%)	TN (%)	C:N$_{soil}$	Soil depth (cm)	ρ_{soil} (g cm^{-3})
0–5	5.67 ± 0.39	0.335 ± 0.020	16.71 ± 0.26	0–5	1.15 ± 0.07
5–15	2.14 ± 0.17	0.121 ± 0.008	17.48 ± 0.33		
15–30	0.79 ± 0.05	0.051 ± 0.002	15.02 ± 0.38	20–25	1.35 ± 0.03
30–60	0.31 ± 0.02	0.035 ± 0.001	9.025 ± 0.41	40–45	1.49 ± 0.02
60–100	0.22 ± 0.01	0.032 ± 0.001	6.78 ± 0.27	60–65	1.55 ± 0.02

SOC, soil organic carbon; TN, total soil nitrogen; C:N$_{soil}$, soil C:N ratios; ρ_{soil}, soil bulk density.

with a pH of 8.0. The main soil variables determined before the experiment establishment are described in **Table 1**.

Experimental Design

Three levels of leaf litter inputs (No-Litter "NL," Control Litter "CL," Doubled Litter "DL") were established in pairs of Trenched ("T," root exclusion) and Non-Trenched plots ("NT," with roots) following a factorial randomized block design. For this, five blocks were randomly distributed over 1 ha area, each one consisting of one trenched plot and a similar non-trenched plot of 2×3 m each, within a distance <10 m between them (**Figure 1**). The root exclusion in the Trenched plots was achieved by excavating a trench 20 cm wide and 70 cm depth around each plot in November 2013, 6 months before the start of the measurements. Trench walls were subsequently covered by a polyethylene foil and the trench was refilled back with soil in order to avoid the re-colonization of new roots. Soil remained unperturbed within the 2×3 m area of each plot. Understory vegetation was also removed in Trenched plots at the time of the experimental setting and every ca. 2 weeks during the growing season since the establishment of the experiment to exclude plant root contribution. Two 1×1 m replicate subplots per litter input level (NL, CL, DL) were randomly distributed in a 2×3 m grid within each plot in April 2014 (n = 5 blocks × 2 trenching levels (paired plots) × 3l inputs levels × 2 replicate subplots = 60). Leaf litter was removed from No-Litter subplots (NL) and immediately added and distributed as evenly as possible to Doubled Litter subplots (DL) once a month and every 2 weeks during autumn. Litter was left undisturbed in the Control Litter subplots (CL), representing the litter amount that naturally falls over the forest floor (325 ± 49 g m^{-2} y^{-1}). The distance from the center of each subplot to the nearest oak and beech tree were also measured.

Soil CO$_2$ Fluxes and Soil Environmental Variables

Prior to the establishment of litter input treatments in April 2014, a PVC collar (diameter 20 cm × height 11.5 cm) was inserted in the soil to ca. 5 cm depth in the center of each subplot. CO$_2$ fluxes were measured on the inserted collars every 2 weeks from June 2014 to December 2016 using a portable dark, closed chamber connected to an automated CO$_2$ analyzer system (Li-Cor 8100, Lincoln, NE, USA). Snow prevented the location of the PVC collars and CO$_2$ measurements during winter. At each measuring campaign, CO$_2$ fluxes were taken simultaneously with soil temperature at 10 cm depth using a probe thermometer (DET3R, Voltcraft, Wernberg-Köblitz, Germany), and with volumetric water content using a soil moisture probe (8100-204 Delta-T ThetaProbe, Cambridge, UK). Measurements were generally performed between 8 am to 4 pm. The order of measurement was rotated among the blocks and treatments over the campaigns. Vegetation cover was estimated visually from 0 to 100% for each campaign (Sutherland, 1996). Vegetation inside the collars was not removed in the case of Non-Trenched plots. Thus, CO$_2$ fluxes reported in this study could include some above-ground autotrophic respiration. However, for practical proposes and because the latter are likely negligible, we use "soil CO$_2$ fluxes" as shorthand for the CO$_2$ flux measured at the soil surface, which are compounded of soil respiration and litter decomposition in case of DL and CL litter input levels.

Soil Sampling

Three years after the experiment establishment (May 2017), samples of mineral soil were collected from a randomly chosen subplot per block, litter input and trenching level at two depths (0–5 cm and 5–10 cm) (n = 5 blocks × 2 trenching level × 3l input × 2 depths = 60 soil samples). Soil samples were immediately sieved to 2 mm and homogenized. The bulk density was calculated with the dry weight and volume of the soil fraction <2 mm. The fraction of soil >2 mm (stones, hereafter) was also weighted. The root biomass in each soil sample was carefully washed and oven dried at 60°C until constant weight. The fresh sieved soil samples were split into three soil subsamples: A 50 g subsample of fresh soil was weighted, transferred to a paper bag and oven dried at 105°C for 48 h for gravimetric determination of water content by the difference between fresh and dry weight, and stored for elemental analyses of inorganic and organic soil C and total soil N. A second 50 g subsample from the upper 5 cm of soil was frozen at −20°C within 24 h after sampling for further analyses of fungal community composition by DNA sequencing and PLFAs analyses. The remaining fresh soil was immediately stored at 4°C for further analyses (see below).

Litter Sampling

Litter samples were also collected from the same randomly chosen subplot per block, litter (only CL and DL) and trenching levels (n = 5 blocks × 2 trenching levels × 2l input levels = 20l samples) at the same time as the soil sampling (3 years after the experiment establishment, May 2017). For that, a 15 × 15 cm quadrant was placed randomly in each subplot and

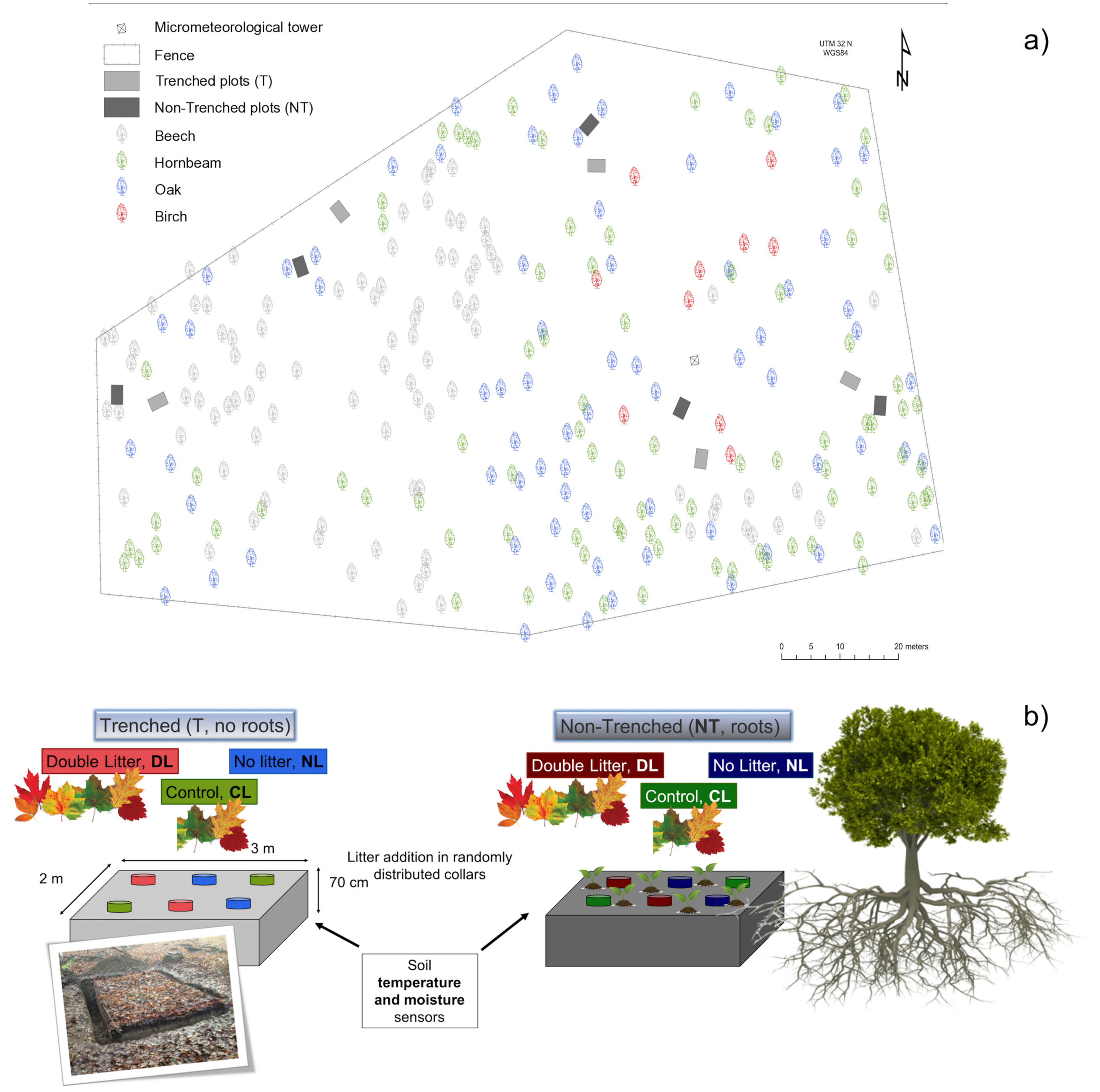

FIGURE 1 | (a) Location of the paired Trenched and Non-Trenched plots in the study area. **(b)** Scheme of the experimental design showing the distribution of the trenching and leaf litter input treatments within each block.

the total amount of litter and organic layer falling within the quadrant perimeter was collected. No roots were found growing in the litter layer. Litter samples were then oven dried at 60°C, weighted, ground and thereby homogenized prior to the C and N elemental analysis.

Soil Extractions and Chemical Analyses

A 6 g subsample of fresh mineral soil was extracted with 30 ml of 0.05M K_2SO_4 within 24 h of soil sampling. Another 6 g subsample was fumigated with $CHCl_3$ for 24 h in vacuum to release the nutrients from the microbial biomass (fumigation-extraction method; Jenkinson and Powlson, 1976), after which the soil was also extracted with 0.05 M K_2SO_4 as above. Dissolved organic C (DOC) in fumigated and non-fumigated K_2SO_4 extracts was determined with a vario TOC cube (Elementar Analysensysteme GmbH, Hanau) and microbial C (C_{micro}) was determined from the difference of DOC between fumigated and non-fumigated subsamples. We were only interested in relative differences among treatments, so the concentrations in the microbial fraction presented here were not corrected for extraction efficiency.

Total soil inorganic C, organic C (SOC), total soil N (TN), total litter C, and total litter N were determined from dry and homogenized soil and litter samples by dry combustion with an Elemental Analyzer (VarioMax CN, Elementar Analysensysteme GmbH, Hanau, Germany for soil samples and Vario EL II, Elementar Analysensysteme GmbH, Hanau, Germany for litter samples). C:N ratios of soil ($C:N_{soil}$) and leaf litter ($C:N_{soil}$) were calculated on a mass basis. The relative accessibility of the DOC pool was calculated as its ratio to the SOC pool. All fractions are presented relative to dry mass.

Phospholipids Fatty Acid Analyses

Soil samples from the upper 5 cm of soil were freeze-dried and total lipids were extracted with a mixture of chloroform, methanol and citrate buffer (1:2:0.8, v/v/v) and fractionated by solid-phase extraction on silica columns according to Gorka et al. (2019). Phospholipids were derivatized to methyl esters via alkaline methanolysis and dried under a constant stream of N_2. Resulting fatty acid methyl esters were re-dissolved in iso-octane and identified and quantified on a gas chromatograph (Agilent 7890B GC; Santa Clara, CA, USA) coupled to a time-of-flight mass spectrometer (Pegasus HT; LECO corporation, Saint-Joseph, MI, USA) on a DB5 column (60 m × 0.25 mm × 0.25 μm). Bacterial fatty acid methyl esters (BAME CP mix, Supelco; 37 Component FAME mix, Supelco) were used as qualitative standards. Prior to methylation nonadecanoic acid (19:0) was added to samples and used as an internal standard for quantification.

PLFA 18:2ω6,9 was used as an indicator of fungal abundance (Olsson, 1999). Since the proportions of individual PLFA differ between different types of bacteria (Ratledge and Wilkinson, 1988) and we were not interested on the shifts of bacterial communities, we grouped the bacterial PLFA to produce less variable results and ease the interpretation (Frostegård and Bååth, 1996; Zelles, 1999). Nonetheless, shifts in bacterial communities were also explored in order to check potential effects on the abundances of saprotrophic and ectomycorrhizal fungi. Beta-hydroxil, cyclopropane, and branched chain PLFAs were considered bacterial PLFAs (Zelles, 1999; Ruess and Chamberlain, 2010). The ratio between fungal and bacterial PLFAs was calculated and considered an indicator of fungal to bacterial biomass ratio. Total PLFAs were considered as a further estimation of total microbial biomass.

DNA Extraction and Sequencing

DNA was extracted from 0.25 to 0.35 g of the mineral soil samples using the DNeasy PowerSoil Kit (Qiagen, Venlo, the Netherlands) following the manufacturer's protocol. The first PCR was performed using ITS1f and ITS2 primers (Smith and Peay, 2014) with Illumina Nextera labels (Illumina Inc; San Diego, CA, USA) targeting fungal ITS1 region. The 25 μl reaction mixtures contained 2 μl of DNA template, 480 nM forward and reverse primers and 1X PCR buffer, 200 μM of each dNTPsand 1 U of Phusion High-Fidelity DNA polymerase (New England Biolabs, Ispwich, MA, USA). PCR conditions were as follows: initial denaturation step at 98°C for 60 s, followed by 35 cycles of: denaturation step at 98°C for 30 s, annealing at 55°C for 30 s, extension at 72°C for 30 s; and final extension step of 72°C for 10 min. The mixture for the second PCR contained 2.5 μl of 50 × diluted PCR product and 0.1 μM of dual barcoded primers with Illumina adapters. The conditions were: initial step at 98°C for 60 s, 12 cycles: at 98°C for 10 s, 63°C for 30 s, 72°C for 30 s; and 72°C for 5 min. Following the gel electrophoresis (1.5% agarose gel) successful amplicons were normalized and purified from PCR artifacts using the SequalPrep Normalization Plate Kit (ThermoFisher Scientific; Waltham, MA, USA). Samples were then pooled into a single library and purified using QIAquick Gel Extraction Kit (Qiagen; Venlo, the Netherlands). Subsequently, the library was quantified with qPCR (KAPA Library Quantification Kits, Kapa Biosystems, Wilmington, MA, USA) and sequenced on the Illumina MiSeq platform (Illumina Inc; San Diego, CA, USA) with 300 cycles for paired-end reads.

Bioinformatic Analyses

The bioinformatics analyses were performed using the USEARCH software following the UPARSE pipeline (Edgar, 2013). The sequences were first trimmed to 250 bp, forward and reverse reads were merged and primers were removed. Quality filtering was performed using a maximum expected error threshold of 0.5. After dereplication and singleton removal the sequences were clustered into operational taxonomic units (OTUs) based on 97% similarity using the UPARSE-OTU algorithm (Edgar, 2013) yielding 810 OTUs in total. The original reads were then mapped to the OTUs with the identity threshold of 0.97. The sequence counts of all samples (abundances matrixes) were normalized by random subsampling to the minimal number of reads per sample (2,986 sequences, rarefaction) to avoid potential artifacts due to library size and lower the false discovery rates (Weiss et al., 2017). We calculated rarefied OTU accumulation curves ("vegan" R package; Oksanen et al., 2020) to explore the completeness of our sampling. While rarefaction curves indicated that additional sequencing depth would yield additional taxa in most samples, depth was relatively balanced among the treatments (**Supplementary Figure 1A**), so unlikely to bias the abundance patterns after subsampling to a common read number.

The OTUs were taxonomically assigned by comparing representative sequences to the UNITE database (Kõljalg et al., 2015) (release date 01.08.2015), using the BLAST algorithm with default settings. The OTUs were assigned to particular taxa by selecting the hits with the lowest E-value and with a minimum alignment length of 75 bp. OTUs were subsequently assigned to functional groups if their genus was successfully matched with one of the genera whose trophic type have been described in Tedersoo et al. (2014). If the trophic type at the genus level was unknown, trophic type was assigned at family level if more than 80% of genera within that family, containing at least four genera, belonged to the same trophic type. EcM fungi were further assigned to different exploration types (contact, short, short-medium, medium and long) based on the description of functional traits of EcM genera in Lilleskov et al. (2011). As a result, 46.3% of total OTUs were assigned to a trophic type and 98.2% of OTUs assigned to EcM fungi could be grouped into an exploration type, which are similar to the percentages found in global studies on fungal functional ecology (e.g., Tedersoo et al., 2014).

Statistical Analyses

The effect of root and litter inputs on monthly soil CO_2 fluxes, soil temperature and soil moisture and its variation along the time was tested by repeated measures ANOVAs split-plot design, with trenching and litter input as main fixed factors between subjects, and date as factor within subjects. The analysis was thus run using mean monthly values per each treatment combination and block, which allowed us to produce integrated data of soil respiration per month. The excess of CO_2 flux caused by the addition the litter inputs (hereafter "litter-derived CO_2 flux") was calculated as the difference of CO_2 fluxes between levels with litter inputs (DL and CL) and the correspondent litter exclusion level (NL) in Trenched (root exclusion) and Non-Trenched plots (root presence). Litter-derived CO_2 fluxes, as calculated here, have previously been shown to be reliable indicators for long-term litter decomposability and litter carbon dynamics (Bowden et al., 1993; Aerts and Caluwe, 1997; Xiao et al., 2014). Nonetheless, these fluxes should be interpreted as metric of the effect (direct and indirect) of the litter addition on CO_2 fluxes, and not as a strict measure of C released exclusively from the litter. The effect of trenching, leaf litter inputs and their interactions on the mean and CO_2 excess flux was tested using two-ways ANOVAs, with trenching and leaf litter inputs as fixed factors. Differences among leaf litter inputs levels within each trenching level were further tested by *post-hoc* tests with Tukey correction for multiple testing.

The effect of trenching, leaf litter inputs, soil depth and their interactions on soil DOC, C_{micro}, SOC, TN, $C:N_{soil}$, ρ_{soil}, and on root biomass was tested using three-ways ANOVAs, with trenching, leaf litter inputs and soil depth as fixed factors. The effect of trenching and leaf litter inputs was also tested on the same variables averaged across soil depths using two-ways ANOVAs, since the effect of soil depth was consistent across treatments (no interactions with the rest of factors). Differences among leaf litter inputs levels within each trenching level were further tested by *post-hoc* tests with Tukey correction for multiple testing.

We investigated the similarity of the soil fungal communities amongst root and leaf litter inputs treatments by non-metric multidimensional scaling (NMDS) ordinations with the read-abundance data using the Bray–Curtis index ("BiodiversityR" package; Kindt and Coe, 2005). For exploratory purposes and to check the robustness of the data, we also performed ordinations using non-rarefied data, giving similar results (**Supplementary Figure 2**). We calculated the relative abundance of the different functional groups (number of reads of a given functional group/total number of reads per sample) and the relative abundance of the different EcM exploration types (number of reads of a given EcM exploration type/total number of reads of identified EcM fungi per sample) to assess the effect of root and leaf litter inputs on the relative abundances of each group and to account for the variation in the relative abundance of different functional groups and EcM exploration types amongst the samples. We then used the "envfit" function ("vegan" R package; Oksanen et al., 2020) to fit the relative abundances of different functional groups and the environmental variables onto the NMDS ordination. Environmental variables were previously standardized.

The dissimilarity between pairs of samples of each root and leaf litter input treatment levels (i.e., beta-diversity) was calculated using the Bray-Curtis distances to the centroid ("vegdist" and "betadisper" functions from "vegan" R package), and the homogeneity of multivariate group of dispersions was then tested using multi-factor analyses of variance for dissimilarity matrices ("dissmfacw" function from "TraMineR" R package, Studer and Ritschard, 2016). Since the dispersion around centroids of soil fungal communities differed significantly among trenching levels (see Fungal community shifts in Results section), the effect of root and leaf litter treatments on the fungal community composition was tested using analyses of deviance for multivariate generalized linear models ("manyglm" R function from "mvabund" R package, Wang et al., 2012), with trenching and leaf litter inputs as fixed factors, block as a random factor and a negative binomial as a link function.

The effect of root and leaf litter inputs on leaf litter variables, PLFAs groups and on the relative abundances of saprotrophic and EcM fungi was tested by two-ways ANOVAs, with trenching and leaf litter inputs as fixed factors. The effect of each factor was further explored by one-way ANOVAs for each trenching and leaf litter input level. Similarly, the effect of leaf litter inputs on EcM exploration types in NT plots (root trenching suppressed virtually all EcM fungi) was tested by one-ways ANOVAs with leaf litter inputs as fixed factor. Correlations between the relative abundances of different fungal trophic types and EcM exploration types and the soil and environmental variables were also explored by Pearson correlations.

Variables were transformed when required to improve normality and homoscedasticity (Quinn and Keough, 2009). Statistical analyses and model construction were performed using JMP 13.0 (SAS Institute) and R v.3.4.3 (R Core Team, 2016). All results are presented as means ± standard errors.

RESULTS

Soil Variables and Microbial Biomass

Trenching reduced the amount of roots present in the soil, which was consistent across leaf litter input levels and depths (**Table 2**; **Figure 2a**). Leaf litter manipulation treatments also successfully altered the amount of leaf litter decomposing over the soil surface. As such, the dry weight of litter per unit of surface at the DL litter input treatment was approximately twice the amount of litter in the C litter input treatment both in T and NT plots (**Table 2**; **Figure 2b**), and the amount of leaf litter decomposing over the soil surface did not differ between T and NT plots. Litter C and N percentages were also similar across leaf litter and root litter inputs (**Table 2**), without changes in C:N ratios across treatments (**Figure 2c**).

TABLE 2 | Results of the ANOVAs on soil and microbial fractions and root and leaf litter variables.

Factor	Trenching	Leaf litter input	Depth	Trenching*Leaf litter input	Trenching*Depth	Leaf litter input*Depth	Trenching*Leaf litter input*Depth
DOC	0.76	**12.39*****	**25.21*****	1.31	1.21	0.3	0.08
C_{micro}	**14.27*****	1.12	**105.21*****	1.01	0.09	0.2	0.12
SOC	0.01	0.76	**77.34*****	0.1	0.24	0.05	0.31
TN	0.08	0.69	**106.18*****	0.22	0.05	0.03	0.25
$C:N_{soil}$	0.58	0.51	**12.50*****	0.34	1.28	0.82	0.02
ρ_{soil}	0.36	0.42	0.01	0.05	0.27	0.03	0.19
Dry weight roots	**7.27****	0.03	**10.11****	0.18	0.88	1.13	1.22
Dry weight litter	2.48	**30.38*****		0.77			
C_{litter}	0.00	0.56		0.92			
N_{litter}	1.81	0.15		0.04			
$C:N_{litter}$	3.53	0.44		3.32			
18:2ω6,9 PLFA	**7.25***	0.4		1.06			
Bacterial PLFAs	2.01	0.8		0.22			
Fungal:bacterial PLFAs	**8.35****	1.00		0.22			
Total PLFAs	**7.10***	0.01		1.48			
Relative EcM abundance	**59.55*****	1.21		**4.30***			
Relative Saprotrophs abundance	**12.13****	0.38		**3.43***			
Contact-distances EcM		1.27					
Short-distances EcM		1.97					
Short-medium-distances EcM		**4.23***					
Medium-distances EcM		0.55					
Long distances EcM		0.63					

Values of the F statistic are presented. The effects of trenching, leaf litter inputs, soil depth, and their interactions are shown. The effect of soil depth is not applicable for litter variables. The effect of soil depth and trenching is not applicable for ectomycorrhiza exploration types, since the root trenching suppressed virtually all ectomycorrhizal fungi. DOC, Dissolved organic carbon; C_{micro}, microbial carbon; SOC, soil organic carbon; TN, total soil nitrogen; $C:N_{soil}$, soil C:N ratios; ρ_{soil}, soil bulk density; C_{litter}, carbon concentration in litter; N_{litter}, nitrogen concentration in litter; $C:N_{litter}$, C:N ratios in litter; PLFAs, phospholipid fatty acids. Statistically significant effects are marked in bold. $^{*}0.01 < P \leq 0.05$; $^{**}0.001 < P \leq 0.01$; $^{***}P \leq 0.001$.

Microbial biomass was consistently higher in NT plots across soil depths (0–5 and 5–10 cm), but it was not affected significantly by the amount of litter addition (**Table 2**; **Figure 2d**). On the contrary, the soil DOC increased consistently with the amount of leaf litter inputs, but not with the presence of roots (**Table 2**; **Figure 2e**). Neither the amount of leaf litter nor the root exclusion by trenching provoked significant changes in SOC, soil TN, C:N ratios or soil bulk density 3 years after the experiment establishment (**Table 2**; **Figure 2f**), and therefore, treatments did not affect soil C and N stocks significantly either. DOC, microbial biomass C, SOC, and TN decreased consistently with soil depth (**Table 2**), while the soil C:N ratios showed an increase at the sub-superficial 5–15 cm depth (**Table 1**).

Fungal Community Shifts

The root exclusion by trenching altered the fungal communities present in the upper 5 cm of mineral soil and drastically reduced the proportion of EcM fungi DNA reads (**Table 3**; **Figure 3a**). By contrast, T plots showed a higher proportion of saprotrophs, particularly of filamentous fungi. The amount of leaf litter inputs also altered the composition of soil fungal communities (**Figure 3b**), with a marginal interaction between root and leaf litter inputs. Soil moisture was higher and less variable (lower standard deviation) where roots were excluded (**Table 3**; **Figure 3c**). Soil CO_2 fluxes, soil temperature, fungal and total PLFAs, soil C and N stocks and the distance to the closer oak tree showed an increasing gradient in the direction of NT plots. Fungal communities were also more heterogeneous (higher pair-wise dissimilarities) in presence of roots than when roots were excluded ($F = 2.09$, $P = 0.001$, **Figure 3b**), while dissimilarities were not altered by litter inputs. Nonetheless, dissimilarity indices showed highest values in the combined NT and NL plots.

In accordance with microbial biomass, fungal PLFA 18:2ω6,9, total PLFAs and fungal to bacterial PLFA ratios were higher at NT plots (**Table 2**; **Figures 4a,d**) as well as Actinobacteria ($P = 0.0264$), while effect of leaf litter inputs on these PLFA groups was not statistically significant. Bacterial PLFA, by contrast, was not affected by the trenching or litter addition treatments (**Figure 4c**), and the same was true for Gram positive and Gram negative bacteria separately, and for Eukariota microbial communities.

The reduction of EcM fungi by root trenching is also evidenced by a 94–73% decrease in their relative abundances (**Table 2**; **Figure 4b**). Overall, relative EcM abundances were not significantly affected by the leaf litter inputs, but they increased in NT plots with decreasing leaf litter inputs, causing a significant effect of leaf litter inputs in NT plots ($P = 0.0346$) and a significant Trenching*Leaf litter input interaction

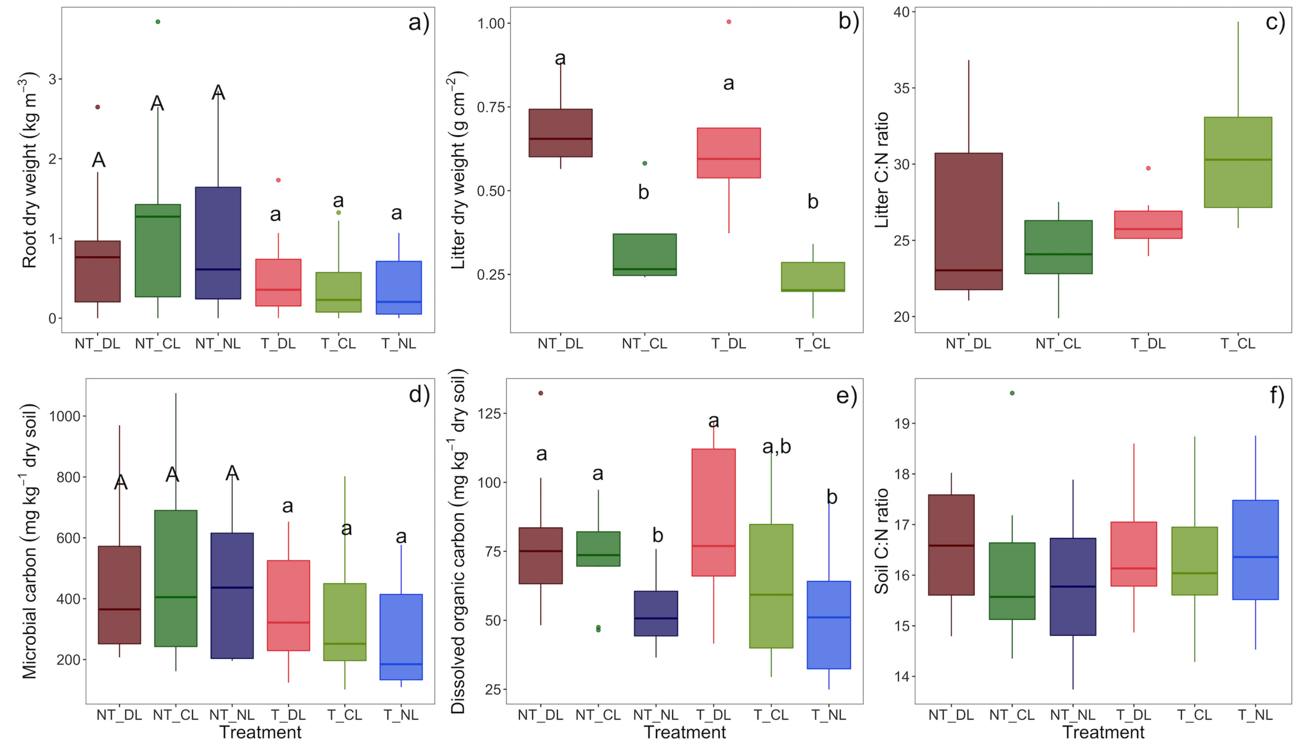

FIGURE 2 | **(a)** Root biomass, **(b)** leaf litter biomass, **(c)** leaf litter C:N ratios, **(d)** microbial biomass carbon, **(e)** dissolved organic carbon, and **(f)** soil C:N ratios in each of the root and leaf litter input treatments. Averaged values of 0–5 and 5–10 cm soil depths for the case of root and soil variables. Box-plots represent the values of $n = 5$ plots per treatment. Different letter case indicates significant effect of trenching according two-ways ANOVA. Different letters indicate significant differences among leaf litter input levels within each trenching level. Microbial biomass carbon is not corrected for extraction efficiency. NT_DL, Non-Trenched and Doubled Litter; NT_CL, Non-Trenched and Control Litter; NT_NL, Non-Trenched and No-Litter; T_DL, Trenched and Doubled Litter; T_CL, Trenched and Control Litter; T_NL, Trenched and No-Litter.

($P = 0.0248$). EcM relative abundance in NT plots was positively correlated with soil C:N ratios in absence of leaf litter inputs (NL, **Figure 5a**), whereas the slopes of this correlation decreased progressively with the amount of leaf litter inputs (CL and DL). Contrary to the relative EcM abundances, the relative abundances of saprotrophic fungi increased in T plots. Leaf litter inputs also did not have an overall effect on saprotrophs relative abundances, but they increased with leaf litter inputs in NT plots, causing a marginal leaf litter effect on NT plots ($P = 0.0814$) and a significant Trenching*Leaf litter input interaction ($P = 0.0474$, **Figure 4b**). Saprotroph relative abundance in NT plots was, moreover, positively correlated with the DOC accessibility in soil relative to total SOC (**Figure 5b**).

The amount of leaf litter inputs also determined the presence of EcM fungal communities with different exploration strategies in NT plots (**Figure 6**), although the effect of leaf litter input was not significant in all the exploration types due to the high variability among blocks (**Table 2**). Short-medium, medium and long-distances exploration types of EcM fungi tended to dominate at doubled leaf litter inputs ($P = 0.0939$ for the sum of these exploration types and $P = 0.0406$ for short-medium distances), while short-distance exploration strategies tended to be more abundant, although not significantly, in absence of leaf litter inputs.

The high variability in the relative abundance of fungal groups among blocks and within treatments was associated, besides to spatial variability of soil properties and microclimate, to the differences in the distances from roots of the different tree species (oak and beech). We detected positive correlations between the distance to the nearest oak tree and the relative abundance of ectomycorrhizal fungi ($P = 0.0034$, $R^2 = 0.7032$) and negative correlations with the relative abundances of plant pathogen ($P = 0.0076$, $R^2 = 0.6584$) and arbuscular mycorrhizal fungi ($P = 0.056$, $R^2 = 0.6767$) in NT plots. In the same plots, there were also positive correlations between the distances to the nearest beech tree and the relative abundances of arbuscular mycorrhiza ($P = 0.0016$, $R^2 = 0.7391$) and plant pathogen fungi ($P = 0.0007$, $R^2 = 0.7723$).

Soil CO_2 Fluxes

Soil CO_2 fluxes were consistently highest in NT and increased with leaf litter inputs (DL > CL > NL) (**Table 4**; **Figures 7a**, **8a**), without significant interactions between trenching and leaf litter inputs. Nonetheless, the excess of CO_2 flux associated to litter inputs did not differ significantly between T and NT (**Figure 8b**) and differences between litter input levels also disappeared when fluxes were standardized per unit of leaf litter C, although fluxes were slightly lower in NT plots (**Figure 8c**). Soil CO_2 fluxes also

TABLE 3 | Regression weights of the variables fitted in the NMDS analysis in **Figure 3c**.

Category	Variable	NMDS1	NMDS2	r^2	*P*
Trophic type	Animal parasite	−0.710	−0.704	0.089	0.313
	Plant pathogen	−0.587	−0.809	0.033	0.628
	Mycoparasite	−0.666	−0.746	0.090	0.287
	Sapro Brown rot	0.312	0.950	0.025	0.679
	Sapro Filamentous	0.287	−0.958	0.445	**0.002**
	Sapro White rot	−0.907	−0.422	0.103	0.263
	Sapro Yeast	−0.930	−0.368	0.023	0.751
	Arbuscular mycorrhiza	−0.481	−0.877	0.019	0.803
	Ectomycorrhiza	0.163	0.987	0.587	**0.001**
Soil and environmental variables	Soil bulk density	0.47735	0.87871	0.0891	0.317
	% Stones	0.85290	−0.52207	0.0360	0.610
	Inorganic C	0.78558	−0.61876	0.0077	0.901
	Distance to closer oak	0.90257	0.43055	0.3629	**0.003**
	Distance to closer beech	−0.92891	−0.37031	0.0643	0.448
	Root biomass	0.23218	0.97267	0.1468	0.138
	Soil moisture	−0.70474	−0.70947	0.6324	**0.001**
	Soil moisture S.D.	0.51806	0.85534	0.5492	**0.001**
	Soil temperature	0.85110	0.52500	0.3300	**0.011**
	Soil temperature S.D.	−0.60766	−0.79420	0.0430	0.595
	Soil CO_2 flux	0.72530	0.68843	0.2739	**0.025**
	Litter dry weight	0.64275	−0.76608	0.0341	0.644
	Litter C	0.58819	−0.80872	0.0484	0.552
	Litter N	0.61027	−0.79219	0.0435	0.586
	Litter C:N ratio	0.65895	−0.75219	0.0435	0.590
	SOC	−0.86350	−0.50435	0.1256	0.206
	TN	−0.91565	−0.40198	0.0634	0.445
	Soil C:N ratio	−0.78242	−0.62276	0.3075	0.052
	DOC	−0.61375	−0.78950	0.0730	0.372
	Microbial biomass C	0.33463	0.94235	0.1121	0.237
	Soil C stock	−0.01278	0.99992	0.3497	**0.008**
	Soil N stock	−0.04971	0.99876	0.3396	**0.009**
	C18:2ω6,9 PLFA	0.43539	0.90024	0.2387	**0.050**
	Total PLFAs	0.57168	0.82047	0.2384	**0.040**

r^2, Squared Pearson correlation; P, Critical probability of the analysis. Statistically significant effects are marked in bold.

varied with time (**Table 4**), with a lower contribution from roots during winter and a higher contribution from leaf litter from early summer to autumn (**Figures 7a,b**).

Soil temperature in the upper 10 cm of soil was not affected by the presence of roots or the amount of litter inputs to the soil (**Table 4**; **Figure 7c**). By contrast, soil moisture was lowest in NT plots, where roots were present (**Table 4**; **Figure 7d**), particularly during the growing season.

DISCUSSION

The ecological relations between EcM and saprotroph fungi can determine the fate of SOM and soil C stabilization (Lindahl and Tunlid, 2015; Wang et al., 2017). The amount of aboveground litter inputs modulates the availability and accessibility of organic substrates in soil. We present evidences suggesting that this generates ecological niches for different fungal trophic types (saprotrophs vs. EcM fungi) and EcM lineages (EcM exploration types) that are favored according to their resource demands and acquisition strategies, determining their abundances. As a result, substrate availability and accessibility may modulate the ecological relations between EcM and saprotrophic fungal communities and, ultimately, the relative role of EcM vs. saprotroph fungi on litter decay and SOM transformation.

Mechanisms Modulating the ecological Relations Between EcM and Saprotrophic Fungi

Fungal communities in soil are largely structured by the availability of limiting substrates (Waldrop et al., 2006; Cline and Zak, 2015), among other factors. We hypothesized that the amount of leaf litter inputs, which generates a range of availability

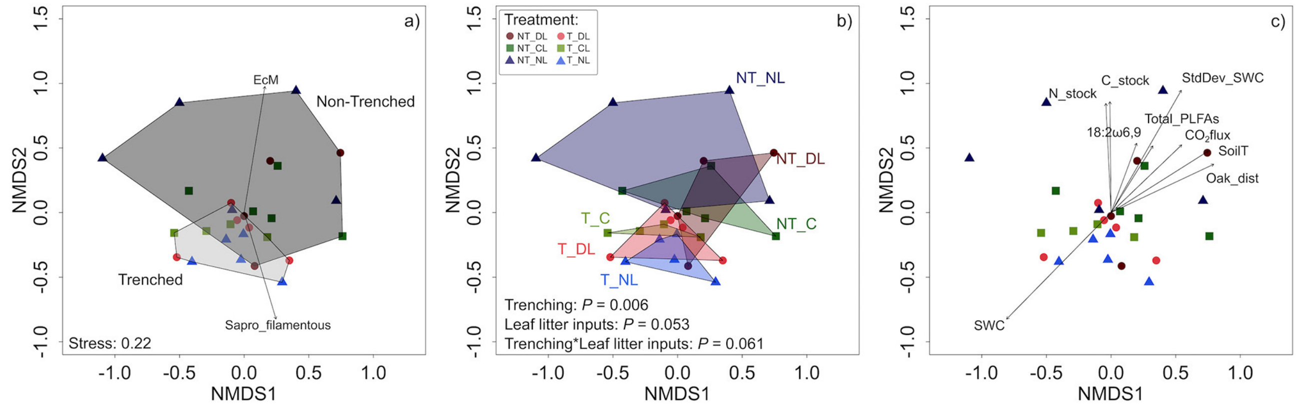

FIGURE 3 | Non-metric multidimensional matrix of soil fungal communities in the trenching and leaf litter inputs treatments. **(a)** Trenching levels are indicated by shaded polygons and relative abundances of fungal trophic types represented by vectors. **(b)** Leaf litter levels are indicated by different colored polygons. **(c)** Gradient direction and strength of environmental variables indicated by vectors. Only variables with a $P < 0.05$ are shown. EcM, ectomycorrhiza abundance; Sapro_filamentous, filamentous saprotroph abundance; SWC, soil moisture; N_stock, soil N stock; C_stock, soil C stock; 18:2ω6,9, 18:2ω6,9 PLFA; StdDev_SWC, soil moisture standard deviation; Total_PLFAs, Total PLFAs; CO_2flux, CO_2 flux; SoilT, soil temperature; Oak_dist, distance to the closest oak tree; NT_DL, Non-Trenched and Doubled Litter; NT_CL, Non-Trenched and Control Litter; NT_NL, Non-Trenched and No-Litter; T_DL, Trenched and Doubled Litter; T_CL, Trenched and Control Litter; T_NL, Trenched and No-Litter.

and accessibility of organic substrates in soil, determines the ecological interactions between EcM and saprotroph fungi and creates diverse niches in which the most adapted fungal guilds are selected according to their resource demands and acquisition strategies. Increasing amounts of litter inputs certainly created a gradient of dissolved organic C in the upper 10 cm of soil, both in Trenched and Non-Trenched plots (**Table 2**; **Figure 2e**), although soil organic C, total soil N concentrations and C:N ratios did not show significant changes after 3 years of altered root and leaf litter inputs (**Table 2**; **Figure 2f**). The root exclusion succeeded in suppressing virtually all ectomycorrhizal fungi (**Figure 4b**), contributing to the decrease in the total microbial biomass C, fungal and total PLFAs in soil (**Table 2**; **Figures 2d**, **4a**). Microbial biomass C and fungal PLFAs however did not change in response to the DOC gradient created in soil by the litter manipulation, but the relative abundances of EcM and saprotroph fungi shifted with leaf litter inputs in Non-Trenched plots (**Figures 3b**, **4b**). The amount of litter inputs therefore selected different fungal communities according to their resources demands and acquisition strategies, altering the abundances of saprotrophic and EcM fungi.

Saprotrophs increased with leaf litter inputs and with soil DOC accessibility in Non-Trenched plots (**Figure 5b**), which evidences the higher reliance of saprotrophs on fresh and accessible organic substrates compared to EcM fungi. On the other hand, EcM fungal abundance increased progressively with decreasing leaf litter inputs, and they proliferated more at higher soil C:N ratios in absence of leaf litter inputs (NL, **Figure 5a**). Conditions of limited access to organic substrates in NL resulted advantageous for EcM, where they resulted better competitors at lower organic matter quality. Declines in EcM fruiting bodies, EcM species richness and dominance have been reported in response to increases in the litter layer and N deposition in Europe and US (Arnolds, 1991; Peter et al., 2001; Averill et al., 2018; Jo et al., 2019). The removal of litter and humus layer have been actually used as practices to restore EcM fungal diversity (Baar and Kuyper, 1998; Smit et al., 2003). Trees generally reduce the belowground C allocation to EcM fungi with increasing N availability at regional or larger scales (Phillips et al., 2011). At the moderate levels of soil N availability in our study, low decomposition and N mineralization rates in the litter exclusion treatment may have acted as a local stress signal for the trees, increasing root elongation, exudation, and the C supply to EcM fungi to enhance N acquisition in exchange (Drew, 1975; Hodge, 2005).

The direct access to plant host sugars may also facilitate EcM fungi an efficient interception and immobilization of N leaching through the soil (Pena et al., 2013) and the production of extracellular peroxidases needed to acquire the N sequestered in complex recalcitrant compounds (Smith and Read, 2008; Bödeker et al., 2009; Lindahl and Tunlid, 2015). Accordingly, Steidinger et al. (2019) have shown that EcM trees dominate in climatic areas of low decomposition rates. Moreover, the amount C transferred from roots to EcM fungi have shown to decrease drastically in presence of saprotroph wood-decomposing fungi (Leake et al., 2001). It is therefore likely that litter inputs, organic matter quality and nutrient availability interact to select functionally distinct fungi, affecting in turn, plant nutrition and C allocation.

Our results point to the emergence of divergent specialization strategies to the available substrates, but we were not able to detect unequivocal signs of competition between saprotrophs and EcM fungi for common resources. Despite the relative abundance of saprotroph fungi increased when EcM fungi were excluded in Trenched plots (**Figure 4b**), trenching also decreased the total fungal abundance (**Figure 4a**), precluding

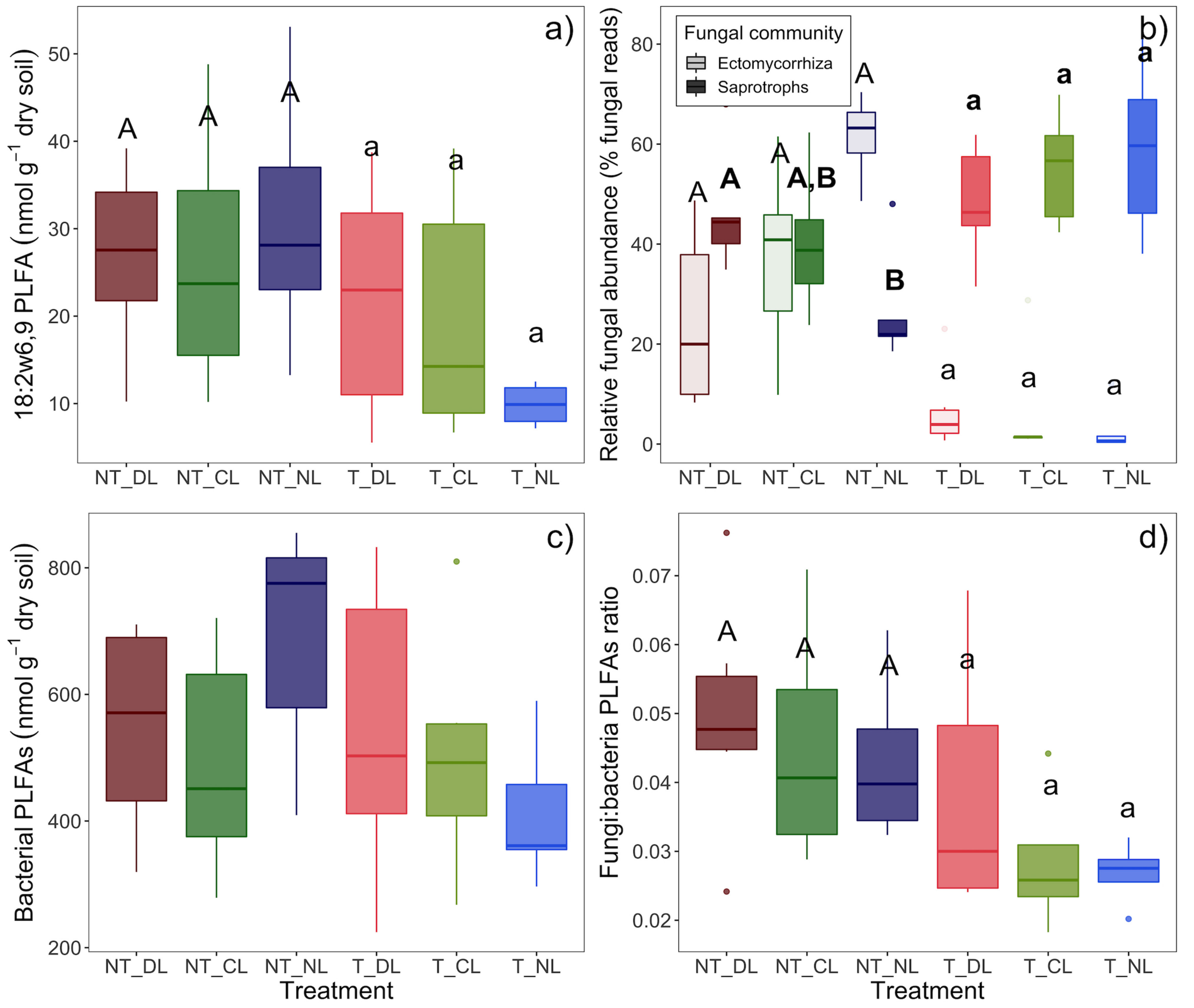

FIGURE 4 | Abundance estimations of soil microbial groups in the trenching and leaf litter inputs treatments. **(a)** 18:2ω6,9 PLFA marker (fungal abundance), **(b)** relative abundances of saprotrophic and ectomycorrhizal fungi (% of fungal DNA reads), **(c)** sum of bacterial PLFAs, **(d)** ratio of fungal to bacterial PLFAs. Box-plots represent the values of $n = 5$ plots per treatment. Different letter case indicates significant effect of trenching according two-ways ANOVA, different letters indicate significant differences among leaf litter input levels within each trenching level according one-ways ANOVA. In **(b)**, bold letters indicate treatment effects on saprotrophic fungi and normal letters indicate treatment effects on ectomycorrhizal fungi. NT_DL, Non-Trenched and Doubled Litter; NT_CL, Non-Trenched and Control Litter; NT_NL, Non-Trenched and No-Litter; T_DL, Trenched and Doubled Litter; T_CL, Trenched and Control Litter; T_NL, Trenched and No-Litter.

to detect significant changes in the absolute abundances of saprotrophs between T and NT plots. The proportion of unassigned OTUs may have had some contribution on the lack of unequivocal signs of competition between ectomycorrhizal and saprotrophic fungi. The proportion of unassigned OTUs was higher in Trenched plots (**Supplementary Figure 3**, $P = 0.003$), which most likely belong to saprotrophic fungi, since EcM fungi are fairly well-known and well-represented in the DNA databases. Nonetheless, our data do not show a clear deceleration of decomposition rates in presence of EcM fungi. The litter-derived CO_2 fluxes per unit of litter C did not differ significantly between Trenched (without EcM fungi) and Non-Trenched plots (with EcM fungi) (**Figure 8c**). If any, the inhibiting effect of EcM fungi on litter decomposition rates was very low to be detected in this case, considering that lower levels of soil moisture in presence of roots (**Table 4**; **Figure 7d**) may have also contributed to underestimate the litter-associated excess CO_2 flux in Non-Trenched plots. Smith and Wan, 2019 have recently found that ectomycorrhizal fungi slow leaf litter decomposition only in forests where litter inputs are highly recalcitrant. In agreement to that, soil C:N ratios in our study (**Table 1**) were relatively low compared to other studies where

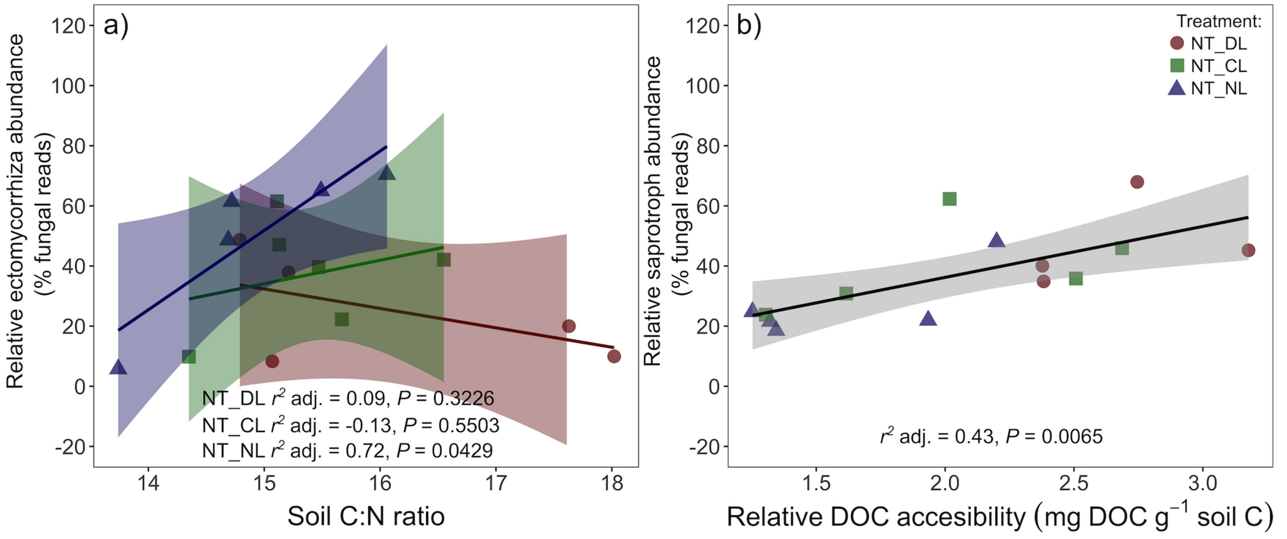

FIGURE 5 | Correlation between the **(a)** relative abundance of ectomycorrhizal fungi and the soil C:N ratios in the different leaf litter input treatments in Non-Trenched plots and **(b)** the relative abundance of saprotroph fungi and the relative accessibility of the soil DOC pool in Non-Trenched plots. The relative accessibility of the DOC pool was calculated as the ratio of DOC to the SOC pool in soil. r^2 adj. = Adjusted Pearson correlation. Shaded areas indicate the 95% confidence intervals. NT_DL, Non-Trenched and Doubled Litter; NT_CL, Non-Trenched and Control Litter; NT_NL, Non-Trenched and No-Litter; T_DL, Trenched and Doubled Litter; T_CL, Trenched and Control Litter; T_NL, Trenched and No-Litter.

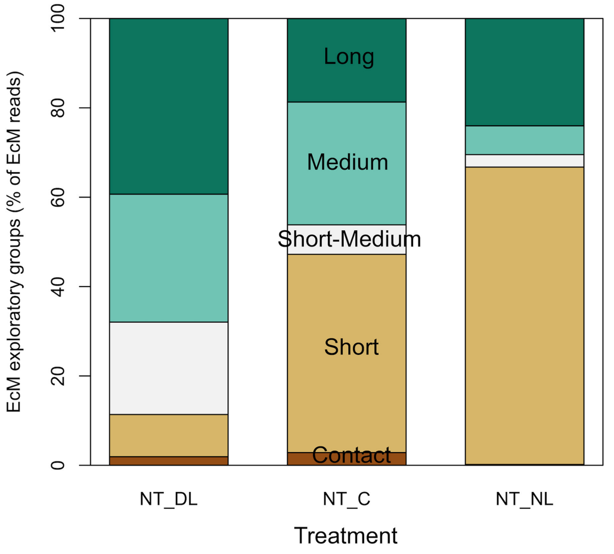

FIGURE 6 | Shifts in the relative abundances of ectomycorrhizal fungi groups of different exploratory strategies for each leaf litter input treatment. Only abundances of ectomycorrhizal fungi in Non-Trenched plots are presented, since the root trenching suppressed virtually all ectomycorrhizal fungi. NT_DL, Non-Trenched and Doubled Litter; NT_CL, Non-Trenched and Control Litter; NT_NL, Non-Trenched and No-Litter; T_DL, Trenched and Doubled Litter; T_CL, Trenched and Control Litter; T_NL, Trenched and No-Litter.

a negative effect of EcM fungi on litter decomposition rates have been reported (Gadgil and Gadgil, 1971, 1975; Koide and Wu, 2003; C:N = 26 and C:N = 43.6, respectively). Higher soil temperatures may have also contributed to faster microbial mineralization rates and N release from SOM in our case. Higher N availability in these soils and the specialization of EcM and saprotroph fungi on divergent target substrates may have allowed them to co-exist without any apparent signs of competition. In support to that, Kyaschenko et al. (2017) found a higher proliferation of saprotrophs, oxidative enzymatic activities and N cycling in fertile sites with higher productivity and N availability, whereas EcM fungi suppressed enzymatic oxidation in less fertile soils. Similarly, Sterkenburg et al. (2018) showed that the effect of EcM fungi on decomposition rates changed across stages of SOM decomposition, where EcM fungi slow down litter decomposition at the soil surface but accelerate SOM decomposition at deeper soil layers. Taken together, these results support the idea that the influence of EcM fungi on litter and SOM decay is strongly context dependent (Fernandez and Kennedy, 2015; Zak et al., 2019), where N availability, SOM quality and the accessibility of organic substrates are key factors that will determine the structure of the soil fungal community, their ecological relations and the net effect of EcM fungi on SOM transformation.

Shifts in Exploration Types of EcM Fungi

EcM fungal communities were not only more successful when organic substrates were scarce, but they can also optimize resource acquisition through different exploration strategies according to available substrates (Agerer, 2006; Tedersoo and Smith, 2013). Short-distances exploration types of EcM fungi tended to dominate in the litter exclusion treatment (**Figure 6**), although the effect was not statistically significant. These EcM guilds are argued to predominantly utilize simple N forms or byproducts from advanced stages of decomposition (ammonium, nitrate and simple aminoacids, Hobbie and Agerer, 2010). Short-distances EcM fungi also invest lower amounts of C on hyphae

TABLE 4 | Summary of Repeated Measures Analysis of Variance (rmANOVA) for the monthly means of soil CO_2 fluxes, soil temperature, and soil moisture.

Source	**Soil CO_2 flux**			**Soil temperature**			**Soil moisture**		
Between-subject	**df**	***F***	***P***	**df**	***F***	***P***	**df**	***F***	***P***
Trenching	1, 24	19.97	0.0002	1, 24	0.02	0.8813	1, 24	21.43	<0.0001
Leaf litter input	2, 24	29.35	<0.0001	2, 24	0.52	0.6001	2, 24	1.41	0.2634
Trenching*Leaf litter input	2, 24	0.22	0.8061	2, 24	0.99	0.3842	2, 24	0.06	0.9386
Within-subject	**df**	***F***	***P***	**df**	***F***	***P***	**df**	***F***	***P***
Date	29, 696	152.47	<0.0001	26, 624	1045.36	<0.0001	29, 696	42.52	<0.0001
Date*Trenching	29, 696	2.08	0.0008	26, 624	0.60	0.9416	29, 696	6.07	<0.0001
Date*Leaf litter input	58, 696	4.14	<0.0001	52, 624	1.01	0.4613	58, 696	0.65	0.9783
Date*Trenching*Leaf litter input	58, 696	0.96	0.5684	52, 624	0.12	1.0000	58, 696	0.67	0.9699

df = degrees of freedom of the numerator and denominator, respectively. F = Value of the F statistic, according to unadjusted univariate F-tests for contrasts within subjects. P = Critical probability of the analysis.

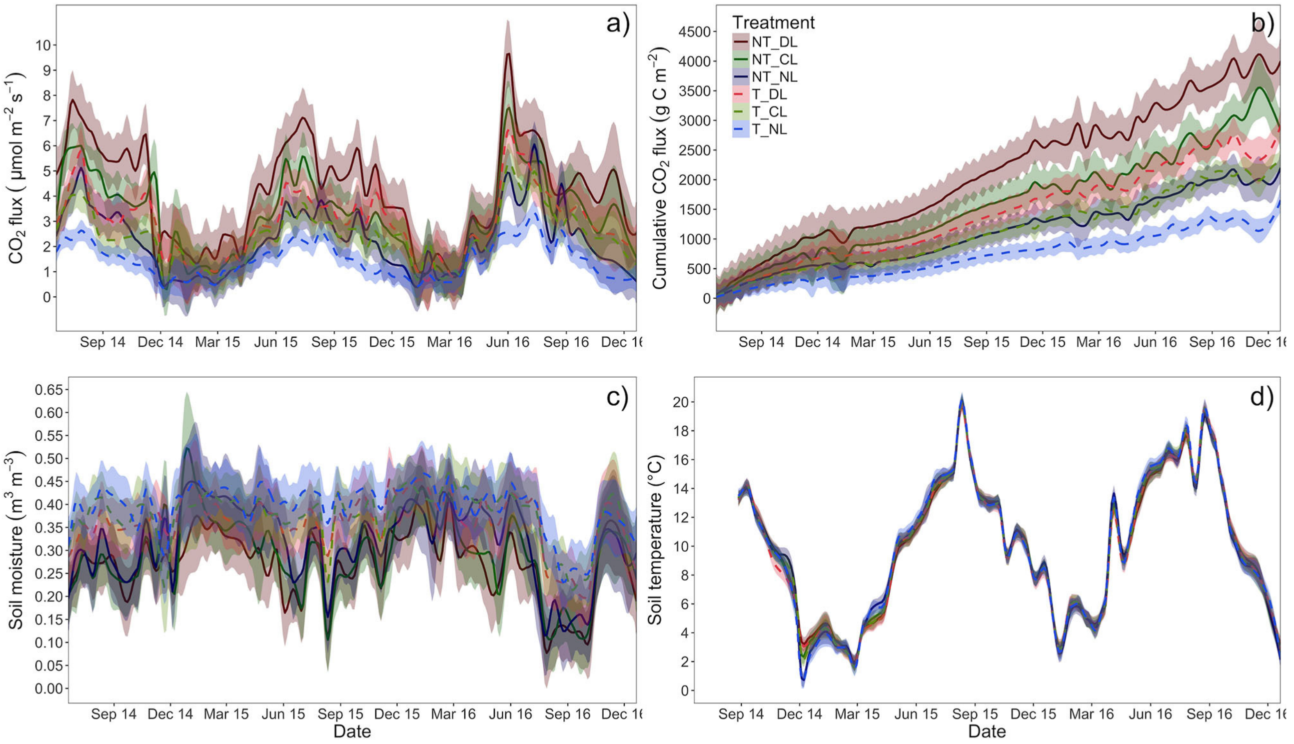

FIGURE 7 | (a) Time course of soil CO_2 fluxes, **(b)** cumulative soil CO_2 fluxes, **(c)** soil moisture, and **(d)** soil temperature in each of the trenching and leaf litter input treatments. Lines represent the loess smooth of $n = 5$ per treatment and date. Shadowed areas around lines represent the 95% confidence interval of the mean. NT_DL, Non-Trenched and Doubled Litter; NT_CL, Non-Trenched and Control Litter; NT_NL, Non-Trenched and No-Litter; T_DL, Trenched and Doubled Litter; T_CL, Trenched and Control Litter; T_NL, Trenched and No-Litter.

elongation, which represents a carbon-conservative strategy that may make them more competitive in areas with higher EcM fungal density (Peay et al., 2011). By contrast, shifts to a higher abundance of long, medium and short-medium-distance exploration types at increasing litter inputs suggests a shift in the target substrate. Long-distance EcM guilds utilize widely dispersed, spatially concentrated resources and have higher capacity of SOM oxidation and organic nitrogen uptake (Hobbie and Agerer, 2010; Lilleskov et al., 2011, Nicolás et al., 2019). Despite the high variability among replicate blocks in our study did not allowed to support this hypothesis, it may be possible that increasing levels of leaf litter inputs enhance the proliferation of EcM fungal groups with the ability to exploit organic N substrates at larger distances from the plant root, such as the decomposing

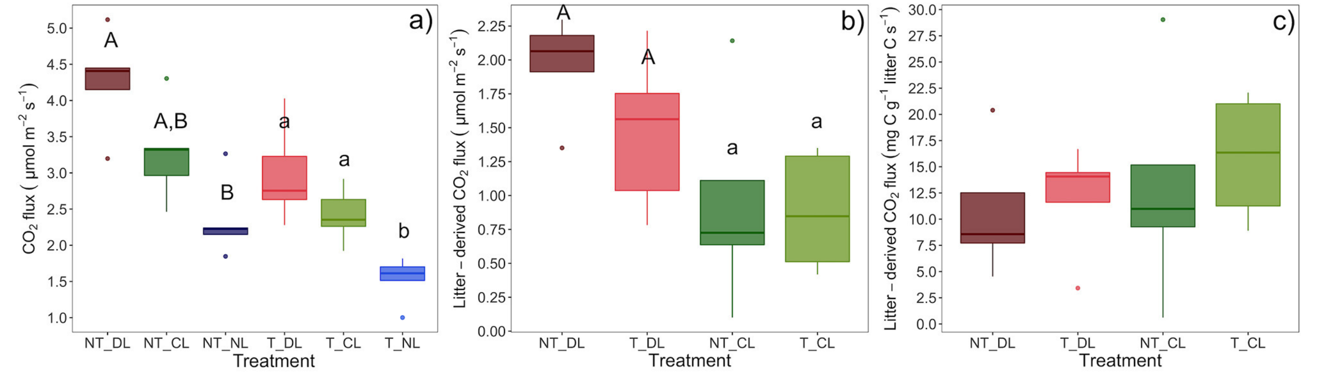

FIGURE 8 | (a) Mean CO_2 flux, **(b)** CO_2 flux excess associated to the leaf litter inputs taking the No-Litter treatment as a baseline in each of the trenching and leaf litter input treatments and **(c)** CO_2 flux excess associated to the leaf litter inputs per unit of leaf litter carbon. Box-plots represent the values of $n = 5$ plots per treatment. Different letter case indicates significant effect of trenching **(a)** or litter **(b)** according two-ways ANOVAs. Different letters indicate significant differences among leaf litter inputs **(a)** or trenching levels **(b)** within each level of the other factor. NT_DL, Non-Trenched and Doubled Litter; NT_CL, Non-Trenched and Control Litter; NT_NL, Non-Trenched and No-Litter; T_DL, Trenched and Doubled Litter; T_CL, Trenched and Control Litter; T_NL, Trenched and No-Litter.

litter (Rineau et al., 2013). These results represent an open door to future research on the role that different exploration types of EcM fungi may have on litter decomposition.

CONCLUSIONS

The ecological interaction between saprotroph and EcM fungal communities can have crucial implications for organic matter decomposition and soil C stabilization. Our results show the proliferation of saprotrophs and EcM fungi of different exploration types based on their acquisition strategies and the available target substrates. The amount of leaf litter inputs, and consequently, substrate availability and accessibility, modulated the abundances of these fungal groups and their ecological relations. EcM fungi were generally favored at low levels of leaf litter inputs and lower SOM quality, where short-distances exploration types may be more competitive, whereas saprotrophs and longer exploration types of EcM fungi tended to dominate at high levels of leaf litter inputs and accessibility of labile organic substrates. These patterns, if confirmed in further studies, may have important implications for decomposition rates in the face of global driven changes in plant allocation patterns. Accordingly, saprotroph fungi may have a key contribution on the breakdown of organic substrates at increasing levels of aboveground tree productivity and leaf litter inputs, whereas the role of EcM fungi on enhancing plant N acquisition may become increasingly relevant at low levels of plant aboveground litter inputs. These results also represent a path forward for future experiments testing the role of different EcM exploration types of fungi on litter and SOM decomposition rates.

DATA AVAILABILITY STATEMENT

The datasets presented in this study can be found in online repositories. The names of the repository/repositories and accession number(s) can be found at: Sequence Read Archive (SRA, http://www.ncbi.nlm.nih.gov/bioproject/747155, BioProject ID PRJNA74715). Data on soil variables and CO_2 fluxes are archived and publicly available at the online archives of the Helmholtz Centre for Environmental Research GmbH - UFZ (https://www.ufz.de/record/dmp/archive/7013/de/ and https://www.ufz.de/record/dmp/archive/7016/de/, respectively).

AUTHOR CONTRIBUTIONS

SM-J, CR, and MC conceived the research. SM-J, DR, EV, AR, MS, and CR contributed data. SM-J conducted analyses, generated figures, and prepared the original draft. All authors provided comments on the manuscript.

FUNDING

This research was supported by the European Union's Seventh Framework Programme and the Ministry of Economy, Innovation, Science and Employment of the Junta de Andalucía (postdoctoral fellowship of the Andalucía Talent Hub Program, Marie Skłodowska-Curie actions, COFUND—Grant agreement No. 291780, to SM-J), the European Union's Horizon 2020 Research and Innovation Programme (Marie Skłodowska-Curie grant agreement No. 750252 to SM-J), the Serra Hunter fellowship Programme from the regional government of Catalonia, the European Research Council Synergy grant 610028 (IMBALANCE-P), as well as by the German Federal Ministry of Education and Research—INFLUINS (03 IS 2001 A) and ICOS-D (01LK1224G).

ACKNOWLEDGMENTS

We thank the forestry office of Hohes Holz for lending the land and their support in the maintenance of the research sites. Special thanks goes to all members of the field-research group of the UFZ Department Computational Hydrosystems for their support during field and lab experiments, in particular to Sebastian Gimper, Hendrik Zöphel, Laura Dienstbach, and Inmaculada García Quirós.

SUPPLEMENTARY MATERIAL

The Supplementary Material for this article can be found online at: https://www.frontiersin.org/articles/10.3389/fpls.2021.682142/full#supplementary-material

REFERENCES

Aerts, R., and Caluwe, H. (1997). Initial litter respiration as indicator for long-term leaf litter decomposition of *Carex* species. *Oikos* 80, 353–361. doi: 10.2307/3546603

Agerer, R. (2006). Fungal relationships and structural identity of their ectomycorrhizae. *Mycol. Prog.* 5, 67–107. doi: 10.1007/s11557-006-0505-x

Alberton, O., Kuyper, T. W., and Gorissen, A. (2005). Taking mycocentrism seriously: mycorrhizal fungal and plant responses to elevated CO_2. *New Phytol.* 167, 859–868. doi: 10.1111/j.1469-8137.2005.01458.x

Arnolds, E. (1991). Decline of ectomycorrhizal fungi in Europe. *Agric. Ecosyst. Environ.* 35, 209–244. doi: 10.1016/0167-8809(91)90052-Y

Averill, C., Dietze, M. C., and Bhatnagar, J. M. (2018). Continental-scale nitrogen pollution is shifting forest mycorrhizal associations and soil carbon stocks. *Glob. Chang. Biol.* 24, 4544–4553. doi: 10.1111/gcb.14368

Averill, C., Turner, B. L., and Finzi, A. C. (2014). Mycorrhiza-mediated competition between plants and decomposers drives soil carbon storage. *Nature* 505, 543–545. doi: 10.1038/nature12901

Baar, J., and Kuyper, T. W. (1998). Restoration of aboveground ectomycorrhizal flora in stands of pinus sylvestris (Scots Pine) in The Netherlands by removal of litter and humus. *Restor. Ecol.* 6, 227–237. doi: 10.1046/j.1526-100X.1998.00635.x

Baldrian, P. (2009). Ectomycorrhizal fungi and their enzymes in soils: is there enough evidence for their role as facultative soil saprotrophs? *Oecologia* 161, 657–660. doi: 10.1007/s00442-009-1433-7

Baldrian, P., Kolarik, M., Stursova, M., Kopecky, J., Valaskova, V., Vetrovsky, T., et al. (2012). Active and total microbial communities in forest soil are largely different and highly stratified during decomposition. *ISME J.* 6, 248–258. doi: 10.1038/ismej.2011.95

Bödeker, I., Lindahl, B. D., Olson, A., and Clemmensen, K. E. (2016). Mycorrhizal and saprotrophic fungal guilds compete for the same organic substrates but affect decomposition differently. *Funct. Ecol.* 30, 1967–1978. doi: 10.1111/1365-2435.12677

Bödeker, I. T. M., Clemmensen, K. E., de Boer, W., Martin, F., Olson, Å., and Lindahl, B. D. (2014). Ectomycorrhizal Cortinarius species participate in enzymatic oxidation of humus in northern forest ecosystems. *New Phytol.* 203, 245–256. doi: 10.1111/nph.12791

Bödeker, I. T. M., Nygren, C. M. R., Taylor, A. F. S., Olson, Å., and Lindahl, B. D. (2009). ClassII peroxidase-encoding genes are present in a phylogenetically wide range of ectomycorrhizal fungi. *ISME J.* 3, 1387–1395. doi: 10.1038/ismej.2009.77

Bowden, R. D., Nadelhoffer, K. J., Boone, R. D., Melillo, J. M., and Garrison, J. B. (1993). Contributions of aboveground litter, belowground litter, and root respiration to total soil respiration in a temperate mixed hardwood forest. *Can. J. For. Res.* 23, 1402–1407. doi: 10.1139/x93-177

Brzostek, E. R., Dragoni, D., Brown, Z. A., and Phillips, R. P. (2015). Mycorrhizal type determines the magnitude and direction of root-induced changes in decomposition in a temperate forest. *New Phytol.* 206, 1274–1282. doi: 10.1111/nph.13303

Cline, L. C., and Zak, D. R. (2015). Soil microbial communities are shaped by plant-driven changes in resource availability during secondary succession. *Ecology* 96, 3374–3385. doi: 10.1890/15-0184.1

de Graaff, M.-A., Classen, A. T., Castro, H. F., and Schadt, C. W. (2010). Labile soil carbon inputs mediate the soil microbial community composition and plant residue decomposition rates. *New Phytol.* 188, 1055–1064. doi: 10.1111/j.1469-8137.2010.03427.x

Drew, M. C. (1975). Comparison of the effects of a localised supply of phosphate, nitrate, ammonium and potassium on the growth of the seminal root system, and the shoot, in barley. *New Phytol.* 75, 479–490. doi: 10.1111/j.1469-8137.1975.tb01409.x

Dybzinski, R., Farrior, C., Wolf, A., Reich, P. B., and Pacala, S. W. (2011). Evolutionarily stable strategy carbon allocation to foliage, wood, and fine roots in trees competing for light and nitrogen: an analytically tractable, individual-based model and quantitative comparisons to data. *Am. Nat.* 177, 153–166. doi: 10.1086/657992

Edgar, R. C. (2013). UPARSE: highly accurate OTU sequences from microbial amplicon reads. *Nat. Methods* 10, 996–998. doi: 10.1038/nmeth.2604

Entry, J. A., Rose, C. L., and Cromack, K. (1991). Litter decomposition and nutrient release in ectomycorrhizal mat soils of a Douglas fir ecosystem. *Soil Biol. Biochem.* 23, 285–290. doi: 10.1016/0038-0717(91)90065-R

Fernandez, C. W., and Kennedy, P. G. (2015). Revisiting the 'Gadgil effect': do interguild fungal interactions control carbon cycling in forest soils? *New Phytol.* 209, 1382–1394. doi: 10.1111/nph.13648

Frostegård, A., and Bååth, E. (1996). The use of phospholipid fatty acid analysis to estimate bacterial and fungal biomass in soil. *Biol. Fertil. Soils* 22, 59–65. doi: 10.1007/s003740050076

Gadgil, R. L., and Gadgil, P. D. (1971). Mycorrhiza and litter decomposition. *Nature* 233:133. doi: 10.1038/233133a0

Gadgil, R. L., and Gadgil, P. D. (1975). Suppression of litter decomposition by mycorrhizal roots of *Pinus radiata*. *N. Z. J. For. Sci.* 5, 35–41.

Gorka, S., Dietrich, M., Mayerhofer, W., Gabriel, R., Wiesenbauer, J., Martin, V., et al. (2019). Rapid transfer of plant photosynthates to soil bacteria via ectomycorrhizal hyphae and its interaction with Nitrogen availability. *Front. Microbiol.* 10:168. doi: 10.3389/fmicb.2019.00168

Hobbie, E. A., and Agerer, R. (2010). Nitrogen isotopes in ectomycorrhizal sporocarps correspond to belowground exploration types. *Plant Soil* 327, 71–83. doi: 10.1007/s11104-009-0032-z

Hodge, A. (2005). "Nitrogen in soils. Plant uptake," in *Encyclopedia of Soils in the Environment*, ed D. Hillel (Cambridge, MA: Academic Press), 39–46.

Högberg, M. N., Briones, M. J. I., Keel, S. G., Metcalfe, D. B., Campbell, C., Midwood, A. J., et al. (2010). Quantification of effects of season and nitrogen supply on tree below-ground carbon transfer to ectomycorrhizal fungi and other soil organisms in a boreal pine forest. *New Phytol.* 187, 485–493. doi: 10.1111/j.1469-8137.2010.03274.x

Jenkinson, D. S., and Powlson, D. S. (1976). Effects of biocidal treatments on metabolism in soil. 5. Method for measuring soil biomass. *Soil Biol. Biochem.* 8, 209–213. doi: 10.1016/0038-0717(76)90005-5

Jo, I., Fei, S., Oswalt, C. M., Domke, G. M., and Phillips, R. P. (2019). Shifts in dominant tree mycorrhizal associations in response to anthropogenic impacts. *Sci. Adv.* 5:6358. doi: 10.1126/sciadv.aav6358

Kaiser, C., Koranda, M., Kitzler, B., Fuchslueger, L., Schnecker, J., Schweiger, P., et al. (2010). Belowground carbon allocation by trees drives seasonal patterns of extracellular enzyme activities by altering microbial community composition in a beech forest soil. *New Phytol.* 187, 843–858. doi: 10.1111/j.1469-8137.2010.03321.x

Kindt, R., and Coe, R. (2005). *Tree Diversity Analysis. A Manual and Software for Common Statistical Methods for Ecological and Biodiversity Studies*. Nairobi: World Agroforestry Centre (ICRAF).

Koide, R. T., and Wu, T. (2003). Ectomycorrhizas and retarded decomposition in a *Pinus resinosa* plantation. *New Phytol.* 158, 401–407. doi: 10.1046/j.1469-8137.2003.00732.x

Kõljalg, U., Larsson, K. H., Abarenkov, K., et al. (2015). UNITE: a database providing web-based methods for the molecular identification of ectomycorrhizal fungi. *New Phytol.* 166, 1063–1068. doi: 10.1111/j.1469-8137.2005.01376.x

Kyaschenko, J., Clemmensen, K. E., Hagenbo, A., Karltun, E., and Lindahl, B. D. (2017). Shift in fungal communities and associated enzyme activities along an age gradient of managed Pinus sylvestris stands. *ISME J.* 11, 863–874. doi: 10.1038/ismej.2016.184

Leake, J. R., Donnelly, D. P., Saunders, E. M., Boddy, L., and Read, D. J. (2001). Rates and quantities of carbon flux to ectomycorrhizal mycelium following 14C pulse labeling of Pinus sylvestris seedlings: effects of litter patches and interaction with a wood-decomposer fungus. *Tree Physiol.* 21, 71–82. doi: 10.1093/treephys/21.2-3.71

Lilleskov, E. A., Hobbie, E. A., and Horton, T. R. (2011). Conservation of ectomycorrhizal fungi: exploring the linkages between functional and taxonomic responses to anthropogenic N deposition. *Fungal Ecol.* 4, 174–183. doi: 10.1016/j.funeco.2010.09.008

Lindahl, B., Stenlid, J., and Finlay, R. D. (2001). Effects of resource availability on mycelial interactions and 32P transfer between a saprotrophic and an ectomycorrhizal fungus in soil microcosms. *FEMS Microbiol. Ecol.* 38, 43–52. doi: 10.1111/j.1574-6941.2001.tb00880.x

Lindahl, B. D., Ihrmark, K., Boberg, J., Trumbore, S. E., Hogberg, P., Stenlid, J., et al. (2007). Spatial separation of litter decomposition and mycorrhizal nitrogen uptake in a boreal forest. *New Phytol.* 173, 611–620. doi: 10.1111/j.1469-8137.2006.01936.x

Lindahl, B. D., and Tunlid, A. (2015). Ectomycorrhizal fungi–potential organic matter decomposers, yet not saprotrophs. *New Phytol.* 205, 1443–1447. doi: 10.1111/nph.13201

Mayor, J. R., and Henkel, T. W. (2006). Do ectomycorrhizas alter leaf-litter decomposition in monodominant tropical forests of Guyana? *New Phytol.* 169, 579–588. doi: 10.1111/j.1469-8137.2005.01607.x

McGuire, K. L., Zak, D. R., Edwards, I. P., Blackwood, C. B., and Upchurch, R. (2010). Slowed decomposition is biotically mediated in an ectomycorrhizal, tropical rain forest. *Oecologia* 164, 785–795. doi: 10.1007/s00442-010-1686-1

Nicolás, C., Martin-Bertelsen, T., Floudas, D., Bentzer, J., Smits, M., Johansson, T., et al. (2019). The soil organic matter decomposition mechanisms in ectomycorrhizal fungi are tuned for liberating soil organic nitrogen. *ISME J.* 13, 77–988. doi: 10.1038/s41396-018-0331-6

Oksanen, J., Blanchet, G., Friendly, M., Kindt, R., Legendre, P., McGlinn, D., et al. (2020). *Vegan: Community Ecology Package.* R package version 2.5-7.

Olsson, P. A. (1999). Signature fatty acids provide tools for determination of the distribution and interactions of mycorrhizal fungi in soil. *FEMS Microbiol. Ecol.* 29, 303–310. doi: 10.1111/j.1574-6941.1999.tb00621.x

Orwin, K. H., Kirschbaum, M. U., St John, M. G., and Dickie, I. A. (2011). Organic nutrient uptake by mycorrhizal fungi enhances ecosystem carbon storage: a model-based assessment. *Ecol. Lett.* 14, 493–502. doi: 10.1111/j.1461-0248.2011.01611.x

Peay, K. G., Kennedy, P. G., and Bruns, T. D. (2011). Rethinking ectomycorrhizal succession: are root density and hyphal exploration types drivers of spatial and temporal zonation? *Fungal Ecol.* 4, 233–240. doi: 10.1016/j.funeco.2010.09.010

Pena, R., Tejedor, J., Zeller, B., Dannenmann, M., and Polle, A. (2013). Interspecific temporal and spatial differences in the acquisition of litter-derived nitrogen by ectomycorrhizal fungal assemblages. *New Phytol.* 199, 520–528. doi: 10.1111/nph.12272

Peter, M., Ayer, F., and Egli, S. (2001). Nitrogen addition in a Norway spruce stand altered macromycete sporocarp production and belowground ectomycorrhizal species composition. *New Phytol.* 149, 311–325. doi: 10.1046/j.1469-8137.2001.00030.x

Phillips, R. P., Finzi, A. C., and Bernhardt, E. S. (2011). Enhanced root exudation induces microbial feedbacks to N cycling in a pine forest under long-term CO2 fumigation. *Ecol. Lett.* 14, 187–194. doi: 10.1111/j.1461-0248.2010.01570.x

Quinn, G. P., and Keough, M. J. (2009). *Experimental Design and Data Analysis for Biologists*. Cambridge: Cambridge University Press.

R Core Team (2016). *A Language and Environment for Statistical Computing.* Vienna: R Core Team.

Ratledge, C., and Wilkinson, S. G. (1988). *Microbial Lipids.* London: Academic Press.

Rineau, F., Roth, D., Shah, F., Smits, M., Johansson, T., Canback, B., et al. (2012). The ectomycorrhizal fungus *Paxillus involutus* converts organic matter in plant litter using a trimmed brown-rot mechanism involving Fenton chemistry. *Environ. Microbiol.* 14, 1477–1487. doi: 10.1111/j.1462-2920.2012.02736.x

Rineau, F., Shah, F., Smits, M. M., Persson, P., Johansson, T., Carleer, R., et al. (2013). Carbon availability triggers the decomposition of plant litter and assimilation of nitrogen by an ectomycorrhizal fungus. *ISME J.* 7, 2010–2022. doi: 10.1038/ismej.2013.91

Ruess, L., and Chamberlain, P. M. (2010). The fat that matters: soil food web analysis using fatty acids and their carbon stable isotope signature. *Soil Biol. Biochem.* 42, 1898–1910. doi: 10.1016/j.soilbio.2010.07.020

Shah, F., Nicolás, C., Bentzer, J., Ellström, M., Smits, M., Rineau, F., et al. (2016). Ectomycorrhizal fungi decompose soil organic matter using oxidative mechanisms adapted from saprotrophic ancestors. *New Phytol.* 209, 1705–1719. doi: 10.1111/nph.13722

Shipley, B., and Meziane, D. (2002). The balanced-growth hypothesis and the allometry of leaf and root biomass allocation. *Funct. Ecol.* 16, 326–331. doi: 10.1046/j.1365-2435.2002.00626.x

Smit, E., Veenman, C., and Baar, J. (2003). Molecular analysis of ectomycorrhizal basidiomycete communities in a *Pinus sylvestris* L. stand reveals long-term increased diversity after removal of litter and humus layers. *Fems Microbiol. Ecol.* 45, 49–57. doi: 10.1016/S0168-6496(03)00109-0

Smith, D. P., and Peay, K. G. (2014). Sequence depth, not PCR replication, improves ecological inference from next generation DNA sequencing. *PLoS ONE* 9:90234. doi: 10.1371/journal.pone.0090234

Smith, G. R., and Wan, J. (2019). Resource-ratio theory predicts mycorrhizal control of litter decomposition. *New Phytol.* 223, 1595–1606. doi: 10.1111/nph.15884

Smith, S. E., and Read, D. J. (2008). *Mycorrhizal Symbiosis.* New York, NY: Academic Press.

Steidinger, B. S., Crowther, T. W., Liang, J., Van Nuland, M. E., Werner, G. D. A., Reich, P. B., et al. (2019). Climatic controls of decomposition drive the global biogeography of forest-tree symbioses. *Nature* 569, 404–408. doi: 10.1038/s41586-019-1128-0

Sterkenburg, E., Clemmensen, K. E., Ekblad, A., Finlay, R. D., and Lindahl, B. D. (2018). Contrasting effects of ectomycorrhizal fungi on early and late stage decomposition in a boreal forest. *ISME J.* 12, 2187–2197. doi: 10.1038/s41396-018-0181-2

Studer, M., and Ritschard, G. (2016). What matters in differences between life trajectories: a comparative review of sequence dissimilarity measures. *J. R. Stat. Soc. Ser. A* 179, 481–511. doi: 10.1111/rssa.12125

Sutherland, W. J. (1996). *Ecological Census Techniques: A Handbook*. Cambridge: Cambridge University Press.

Tedersoo, L., Bahram, M., Põlme, S., Kõljalg, U., Yorou, N. S., Wijesundera, R., et al. (2014). Global diversity and geography of soil fungi. *Science* 346:1256688. doi: 10.1126/science.1256688

Tedersoo, L., May, T. W., and Smith, M. E. (2010). Ectomycorrhizal lifestyle in fungi: global diversity, distribution, and evolution of phylogenetic lineages. *Mycorrhiza* 20, 217–263. doi: 10.1007/s00572-009-0274-x

Tedersoo, L., and Smith, M. E. (2013). Lineages of ectomycorrhizal fungi revisited: foraging strategies and novel lineages revealed by sequences from belowground. *Fungal Biol. Rev.* 27, 83–99. doi: 10.1016/j.fbr.2013.09.001

Treseder, K. K. (2004). A meta-analysis of mycorrhizal responses to nitrogen, phosphorus, and atmospheric CO_2 in field studies. *New Phytol.* 164, 347–355. doi: 10.1111/j.1469-8137.2004.01159.x

Waldrop, M. P., Zak, D. R., Blackwood, C. B., Curtis, C. D., and Tilman, D. (2006). Resource availability controls fungal diversity across a plant diversity gradient. *Ecol. Lett.* 9, 1127–1135. doi: 10.1111/j.1461-0248.2006.00965.x

Wang, T., Tian, Z., Bengtson, P., Tunlid, A., and Persson, P. (2017). Mineral surface-reactive metabolites secreted during fungal decomposition contribute to the formation of soil organic matter. *Environ. Microbiol.* 19, 5117–5129. doi: 10.1111/1462-2920.13990

Wang, Y., Naumann, U., Wright, S. T., and Warton, D. I. (2012). mvabund–an R package for model-based analysis of multivariate abundance data. *Methods Ecol. Evol.* 3, 471–474. doi: 10.1111/j.2041-210X.2012.00190.x

Weiss, S., Xu, Z. Z., Peddada, S., Amir, A., Bittinger, K., Gonzalez, A., et al. (2017). Normalization and microbial differential abundance strategies depend upon data characteristics. *Microbiome* 5:27. doi: 10.1186/s40168-017-0237-y

Xiao, W., Ge, X., Zeng, L., Huang, Z., Lei, J., Zhou, B., et al. (2014). Rates of litter decomposition and soil respiration in relation to soil temperature and water in different-aged pinus massoniana forests in the three gorges reservoir area, China. *PLoS ONE* 9: e101890. doi: 10.1371/journal.pone.0101890

Yarwood, S. A., Myrold, D. D., and Högberg, M. N. (2009). Termination of belowground C allocation by trees alters soil fungal and bacterial communities in a boreal forest. *FEMS Microbiol. Ecol.* 70, 151–162. doi: 10.1111/j.1574-6941.2009.00733.x

Zak, D. R., Pellitier, P. T., Argiroff, W., Castillo, B., James, T. Y., Nave, L. E., et al. (2019). Exploring the role of ectomycorrhizal fungi in soil carbon dynamics. *New Phytol.* 223, 33–39. doi: 10.1111/nph.15679

Zelles, L. (1999). Fatty acid patterns of phospholipids and lipopolysaccharides in the characterisation of microbial communities in soil: a review. *Biol. Fertil. Soils* 29, 111–129. doi: 10.1007/s003740050533

Zhu, W., and Ehrenfeld, J. G. (1996). The effects of mycorrhizal roots on litter decomposition, soil biota, and nutrients in a spodosolic soil. *Plant Soil* 179, 109–118. doi: 10.1007/BF00011648

Conflict of Interest: The authors declare that the research was conducted in the absence of any commercial or financial relationships that could be construed as a potential conflict of interest.

frontiers
in Plant Science

ORIGINAL RESEARCH
published: 30 July 2021
doi: 10.3389/fpls.2021.704000

Enhanced Iron Uptake in Plants by Volatile Emissions of *Rahnella aquatilis* JZ-GX1

Wei-Liang Kong[1,2], Ya-Hui Wang[1,2] and Xiao-Qin Wu[1,2]*

[1] Co-Innovation Center for Sustainable Forestry in Southern China, College of Forestry, Nanjing Forestry University, Nanjing, China, [2] Jiangsu Key Laboratory for Prevention and Management of Invasive Species, Nanjing Forestry University, Nanjing, China

Iron deficiency in soil has crucially restricted agricultural and forestry production. Volatile organic compounds (VOCs) produced by beneficial microorganisms have been proven to play an important role in inducing abiotic stress tolerance in plants. We investigated the effects of VOCs released by the rhizobacterium *Rahnella aquatilis* JZ-GX1 on the growth and root parameters of *Arabidopsis thaliana* under iron deficiency. The effect of the rhizobacterial VOCs on the gene expression in iron uptake and hormone signaling pathways were detected by RT-qPCR. Finally, the VOCs of the JZ-GX1 strain that could promote plant growth under iron deficiency stress were screened. The results showed that the JZ-GX1 strain could induce *A. thaliana* tolerance to iron deficiency stress by promoting the development of lateral roots and root hairs and increasing the activities of H^+ ATPase and Fe^{3+} reductase. In addition, the *AHA2*, *FRO2*, and *IRT1* genes of *A. thaliana* exposed to JZ-GX1-emitted VOCs were upregulated 25-, 1. 81-, and 1.35-fold, respectively, and expression of the abscisic acid (ABA) synthesis gene *NCED3* was upregulated on both the 3rd and 5th days. Organic compounds were analyzed in the headspace of JZ-GX1 cultures, 2-undecanone and 3-methyl-1-butanol were found to promote *Medicago sativa* and *A. thaliana* growth under iron-limited conditions. These results demonstrated that the VOCs of *R. aquatilis* JZ-GX1 have good potential in promoting iron absorption in plants.

Keywords: iron deficiency, *Rahnella aquatilis*, volatile organic compounds, ABA, *Arabidopsis thaliana*, *Medicago sativa*

Edited by:
Erik Verbruggen,
University of Antwerp, Belgium

Reviewed by:
Kris Vissenberg,
University of Antwerp, Belgium
Ma. del Carmen
Orozco-Mosqueda,
Michoacan University of Saint
Nicholas of Hidalgo, Mexico

***Correspondence:**
Xiao-Qin Wu
xqwu@njfu.edu.cn

Specialty section:
This article was submitted to
Plant Symbiotic Interactions,
a section of the journal
Frontiers in Plant Science

Received: 14 May 2021
Accepted: 25 June 2021
Published: 30 July 2021

Citation:
Kong W-L, Wang Y-H and
Wu X-Q (2021) Enhanced Iron Uptake
in Plants by Volatile Emissions
of Rahnella aquatilis JZ-GX1.
Front. Plant Sci. 12:704000.
doi: 10.3389/fpls.2021.704000

INTRODUCTION

In contrast to animals, plants are fixed organisms, and their growth and development occur in the soil; thus, plants can suffer from a variety of biotic or abiotic stresses from the soil throughout their life cycle (Zhou et al., 2016a, 2019). As one of the essential micronutrients in plants, iron (Fe) plays a very important role in the electron transport chain and enzymatic reaction pathways in many physiological metabolic processes, such as photosynthesis, respiration, nitrogen fixation, protein, and nucleic acid synthesis (Zhou et al., 2016b). Although iron is abundant in most soils, its bioavailability is relatively low in alkaline or calcareous soils (Arikan et al., 2018). Iron forms extremely difficult-to-dissolve iron hydroxide, which is not easily utilized by plants (Freitas et al., 2015). It has been reported that calcareous soil covers approximately 1/3 of the Earth's crust, and many plants growing on such soils often show chlorosis and yield loss related to iron deficiency (Tsai and Schmidt, 2017).

To cope with iron deficiency, non-gramineous monocotyledons and dicotyledons mainly use reduction-based strategies (strategy I), while gramineous monocotyledons use chelation-based strategies (strategy II), although it is known that there are plants that can use both (Flores-Cortez et al., 2019). In strategy I, iron uptake by plants consists of three steps: (1) release of protons into the plant rhizosphere to reduce pH and increase the solubility of insoluble iron oxide by H^+ ATPase (*AHA2*), (2) reduction of Fe^{3+} to ferrous form by plasma membrane-bound chelating iron reductase (*FRO2*), and (3) transport of reduced Fe^{2+} to the root epidermis through divalent metal transport protein IRT1 across the plasma membrane (Del Carmen Orozco-Mosqueda et al., 2013). *FRO2* and *IRT1* are finely regulated by iron deficiency-induced transcription factors (*FIT1*), and *FIT1* plays a central role in iron homeostasis (Montejano-Ramirez et al., 2018). However, neither gramineous nor non-gramineous monocotyledons can obtain enough iron in alkaline or calcareous soils by strategy I or strategy II (Castulo-Rubio et al., 2015). Thus, for the sustainable development of agriculture, there is an urgent need to improve the ability of plants to absorb iron from low-iron available soils.

The use of plant growth promoting rhizobacteria (PGPR) to help plants obtain available iron is considered to be environmentally friendly (Masalha et al., 2000; Rroco and Kosegarten, 2003; Montejano-Ramirez et al., 2015). It is known that several beneficial microorganisms can promote iron uptake by plants based on the mechanisms of chelation, reduction, acidification and induction, among which the induction of plant systemic resistance mediated by volatile organic compounds (VOCs) has attracted wide attention in recent years (Back et al., 2020). Compared with soluble compounds, the VOCs released by rhizosphere microorganisms have two advantages in the interaction of microbial communities: first, volatile compounds with low molecular weights (<300 Da) can evaporate and migrate freely via soil pores over long distances (Sharifi and Ryu, 2018a,b); second, these gaseous substances act as signal molecules and can activate or enhance plant defense responses (Fincheira and Quiroz, 2018; Netzker et al., 2020). Some studies showed that *Bacillus subtilis* GB03 directly and indirectly promoted the growth of *Arabidopsis thaliana* under iron deficiency through the emission of acetoin and 2,3-butanediol (Zhang et al., 2009). *Arthrobacter agilis* UMCV2 induced iron acquisition in *Medicago sativa in vitro* via dimethyl hexadecylamine (Elizabeth Aviles-Garcia et al., 2016; Ramirez-Ordorica et al., 2020). The airborne signals from *Trichoderma asperellum* T-34 increased the expression of the iron uptake genes *LeFER*, *LeFRO*, and *LeIRT* in tomato roots (Martinez-Medina et al., 2017). The transcription factor MYB72, which is related to induced systemic resistance (ISR) and iron uptake in *A. thaliana* roots, is activated by VOCs released by *Pseudomonas simiae* WCS417 and enhances the iron acquisition and systemic immunity of *A. thaliana* roots at the same time (Zamioudis et al., 2015).

A previous study by our laboratory showed that *Rahnella aquatilis* JZ-GX1 could promote iron absorption in *Cinnamomum camphora* by producing siderophores and organic acids, thus alleviating iron deficiency-induced chlorosis (Kong et al., 2020b). However, it is not clear whether the tested strain can further induce the systemic tolerance of plants to iron deficiency stress by producing VOCs. For this reason, in this study, *A. thaliana* and *M. sativa* model plants were used in a two-grid Petri dish system to: (1) explore the effects of VOCs produced by *R. aquatilis* JZ-GX1 on the growth of *A. thaliana* under iron-deficient conditions; (2) clarify the signaling pathway of resistance to iron deficiency stress induced by the JZ-GX1 strain in *A. thaliana*; and (3) identify one or more VOCs produced by the JZ-GX1 strain that act as elicitors.

MATERIALS AND METHODS

Plant Preparation

In this study, we used *A. thaliana* wild-type accession Col-0 and *M. sativa* as our test subjects. First, the seeds of these two plants were treated with 70% ethanol for 5 min and 2.6% NaClO for 1 min and then rinsed with sterile water 7–8 times for surface sterilization. The seeds were poured into 1/2 Murashige and Skoog (MS) agar-solidified medium with sterile water; a pipette was used to remove the sterile water, and the seeds were spread evenly and as far apart as possible. The Petri dish was placed on a super-clean table and blown dry with a fan, sealed with parafilm, and vernalized in a refrigerator at 4°C for 2 days. The Petri dish was placed vertically in a light incubator for 5 days to raise seedlings. The conditions of the light incubator were as follows: 16 h of light, 8 h of dark, 70% relative humidity, a light intensity of 4000 lux and a temperature of 25°C (Zhou et al., 2017).

Bacterial Cultures

Rahnella aquatilis JZ-GX1 is a plant growth-promoting bacterium isolated from the rhizosphere soil of a 28-year-old *Pinus massoniana* in Nanning, Guangxi. It is now stored in the typical Culture Preservation Center of China (CCTCC, NO: M2012439). This strain was inoculated on Luria-Bertani (LB) medium for activation, and then a single colony was selected and transferred into a shake flask containing LB liquid medium and then incubated at 28°C and 180 rpm. The bacterial liquid was diluted to 1×10^7 CFU/mL with phosphate buffer at pH 7.8.

Co-culture of Plants and Bacteria

To study the effect of VOCs released by the JZ-GX1 strain on the growth of *A. thaliana* under iron-limited conditions, I-plates (90 mm in diameter) were used in this experiment. Each petri dish was divided into two chambers such that the non-gaseous metabolites produced by bacteria could not reach *A. thaliana*, which was inoculated in a separate chamber; thus, the bacteria could only affect *A. thaliana* through VOC signals over the plate. One chamber of the Petri dish contained 1/2 MS medium, and

TABLE 1 | Primers used in RT-qPCR analysis.

Gene name	Gene function	Primers
AHA2	Plasma membrane H^+ ATPase	GAGAATGTGCATGTGCCAAA TGACTGATCTTCGATCCTCTCA
FRO2	Fe^{3+} reductase	TGCCACAAAGATTCGTCATGTGCG TGTGGCTCTTCTTCTCTGGTGCTT
IRT1	Fe^{2+} transporter	TCCCGGAGGCGAAACACTTAATGA ACCCGTGCGTCAACAAAGCTAAAG
FIT	Iron deficiency-induced transcription factors	TTCATCTTCTTCACCACCGGCTCT ACCTCTTCGACGAATTGCCTGACT
PDF1	Jasmonic acid biosynthesis	CAACGGGAAAATAAACATTAAAACAG CTGTTACGTCCCATGTTAAATCTACC
NPR1	Salicylic acid biosynthesis	AACCGTGGAACTCGGGAAACGA GTCTTCTCCGCAAGCCAGTTGA
ERF1	Ethylene biosynthesis	TCCCGAGCCAAACCCTAATAC CCTTCCGATCAAATCCGTAAG
NCED3	Abscisic acid biosynthesis	TTAGCTCCGTTGCGCACATA ATCTGCGCTTCACACTCCTC
YUC1	Auxin biosynthesis	CAAAGAAAGGAGCAAAGTTTATGG CTGAAGCCAAGTAGGCACGTT
YUC8	Auxin biosynthesis	TGTATGCGGTTGGGTTTACG CAGAGCCTATGTCTTGTGCGAT
Actin	Endogenous control, Reference gene	GAAATCACAGCACTTGCA AGCCTTTGATCTTGAGAG
MsAHA2	Plasma membrane H^+ ATPase	TCATGGGTCATGGAAATG CTCCTGGGACAAGAATAGC
MsIRT1	Fe^{2+} transporter	CCCTAGCTGATTGTGAAAGT TCCCAAGAATAATACCAGCC
MsBHLH1	Iron deficiency-induced transcription factors	TTATCCTTCATTCGGCTTCG TGATCCTACTTCTTCACTTGGTTC
MsActin	Endogenous control, Reference gene	CTCTCAAGTACCCCATTGAGC TATTGGCCTTTGGGTTAAGTG

the other contained LB medium. 1 M KOH (containing 6 mM $NaHCO_3$) was added to the 1/2 MS medium on which the *A. thaliana* side was placed to a final pH of 8.0 as iron deficiency treatment. Seven-day-old *A. thaliana* seedlings were transplanted into the chamber containing 1/2 MS medium, five seedlings were transplanted into each dish, and the distance between seedlings was the same. Seedlings with good and consistent growth were selected when transplanting. The hypocotyl part of the seedling was gently clamped with sterilized tweezers and then transplanted into the upper part of the Petri dish. 10 μL of bacterial solution was added to the other compartment, and LB medium without bacterial solution was used as the control. After the bacterial solution was homogeneously distributed in the culture medium, the Petri dish was sealed with parafilm and cultured vertically in a light incubator for 14 days (Wang et al., 2017). The culture conditions were the same as described in plant preparation.

Determination of Plant Root Parameters

After the bacterium was co-cultured with *A. thaliana* for 14 days, the Petri dish was removed to observe the overall effect of VOCs produced by the bacterium on *A. thaliana*, and the root tips of *A. thaliana* were photographed with a Zeiss stereomicroscope (Zeiss Microscope System Standard 16; Carl Zeiss Ltd., Germany). Measurements were determined using Image J Tool software; pixel areas were calibrated based on a known distance. Root hairs length were measured in a region of 500 μm at approximately 1 cm from the primary root tip. The *A. thaliana* seedlings were removed and weighed with a 1/10000 balance; the length of the main root of *A. thaliana* was measured and recorded with a Vernier caliper. Then, the seedlings were placed in a Petri dish filled with clear water so that the roots could be fully elongated, and the number of lateral roots was counted and recorded (Perez-Flores et al., 2017).

Leaf Chlorophyll

Leaves (500 mg) were combined with a small amount of 80% acetone and quartz sand were then ground into a homogenate. Then, additional 80% acetone was added, the homogenate was transferred to a centrifuge tube, the volume was brought to 10 mL, and the tube was centrifuged at 12000 *g* and 4°C for 15 min. The absorbance of the supernatant was detected at 645 and 663 nm, and the total chlorophyll content was calculated as follows: total chlorophyll = $(8.02A663 + 20.21A645) \times V/1000 \times W$, where V is the total extract volume and W is the sample weight (Castulo-Rubio et al., 2015).

Determination of Endogenous Iron Content

The leaves from the seedlings were chopped and placed in 1 mol/L HCl at a 1:10 ratio (v/v) for 24 h (Koseoglu and Acikgoz, 1995). The extract was filtered and assayed using an atomic absorption spectrophotometer (AA900T, Perkin Elmer).

Visualization of Rhizosphere Proton Release

The change in pH value in the rhizosphere was determined by the staining location method. A total of 1 g of agar, 13.6 mg of $CaSO_4$ and 6 mg of bromocresol violet were added to 100 mL of distilled water, heated to dissolve, mixed well, and cooled to approximately 50°C, and the pH was adjusted until the solution color was dark red. The liquid on the root surface was drained, the roots were placed flat on the bottom of a culture dish, and the prepared agar containing the indicator was evenly and quickly poured on the culture dish at a thickness of approximately 0.8–1 cm. After agar solidification, the dish was placed in the dark at room temperature for 24 h, and the change in indicator color was observed (Li et al., 2020).

Quantitative Real-Time PCR

Seven-day-old *A. thaliana* seedlings were co-cultured with bacterial VOCs for 3 and 5 days, frozen with liquid nitrogen and fully ground, and the total RNA of *A. thaliana* was extracted by a rapid plant RNA extraction kit (Beijing Zoman Biotechnology

Co., Ltd., Beijing, China). The relative expression levels of the *AHA2*, *FRO2*, *IRT1*, *FIT*, *PDF1*, *NPR1*, *ERF1*, and *NCED3* genes were determined, and the *Actin* gene was used as the internal control (Zhou et al., 2016c; Ines Dinolfo et al., 2017). The expression levels of related genes were calculated by ABI 7500 software (Applied Biosystems, United States) and the $2^{-\Delta\Delta CT}$ method (Kong et al., 2020a). The primers used to amplify these genes are listed in **Table 1**.

Determination of H^+ ATPase and Fe^{3+} Reductase Activities in Plants

To verify whether the expression of key iron absorption genes was consistent with enzyme activity, H^+ ATPase and Fe^{3+} reductase were extracted from plant roots according to the research of Zhang et al. (2009) and Arikan et al. (2018) and their activities were measured at 450 and 562 nm, respectively.

Verification of the Selected Synthetic VOCs on the Plant Growth Under Iron-Limited Medium

According to our previous research (Kong et al., 2020a), the authentic reference standard compounds detected by GC-MS were diluted with dimethyl sulfoxide to 10, 50, 100, and 200 μM and were added to one side of the Petri dish; no compounds were added to the Petri dish in the control test (Pinedo et al., 2015; Ledger et al., 2016). The plate was cultured vertically in a light incubator, and each compound at each concentration was tested as four parallel samples. The culture conditions were the same as detailed above. After 14 days of culture, the results were observed, and the growth indexes of the plants were determined.

Data Analysis and Processing

The data were subjected to analysis of variance and Duncan's multiple comparison test with SPSS 21.0 software (IBM Inc., Armonk, NY, United States), and the standard errors of all mean values were calculated ($p < 0.05$). Graphs were generated using GraphPad Prism 8.0 (GraphPad Software, Inc., United States).

RESULTS

R. aquatilis JZ-GX1 Promoted the Growth of *A. thaliana* Under Iron Deficiency Through the Emission of VOCs

Arabidopsis thaliana was cultured with 1/2 MS medium (pH = 8.0) on one side of a Petri dish, and the tested bacterium was cultured on the other side with LB medium. After 14 days, the interaction results were observed, and the fresh weight and chlorophyll and active iron contents of the plants were determined. The growth-promoting effect of the JZ-GX1 strain on *A. thaliana* was analyzed. These results showed that the growth of 14-day-old *A. thaliana* in an alkaline environment

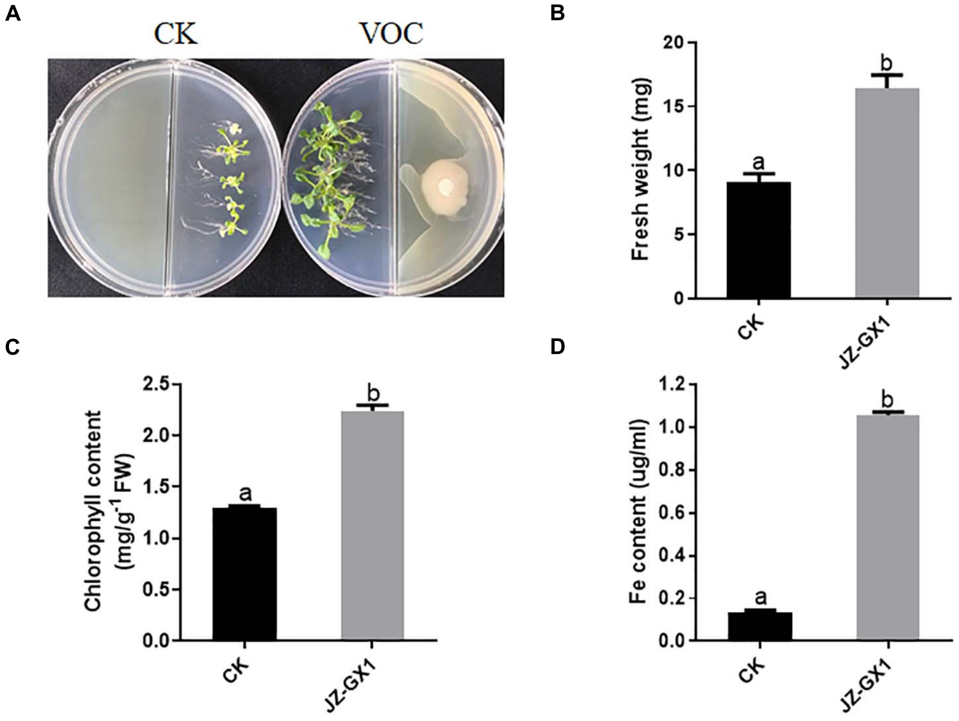

FIGURE 1 | Effects of VOCs of *Rahnella aquatilis* JZ-GX1 on the growth of *Arabidopsis thaliana* under iron limitation. **(A)** Plant phenotype, **(B)** plant fresh weight, **(C)** chlorophyll content, and **(D)** active iron content. CK: control. One-way ANOVA was performed, and Duncan's *post hoc* test was applied. Different letters indicate statistically significant differences ($p < 0.05$) among treatments.

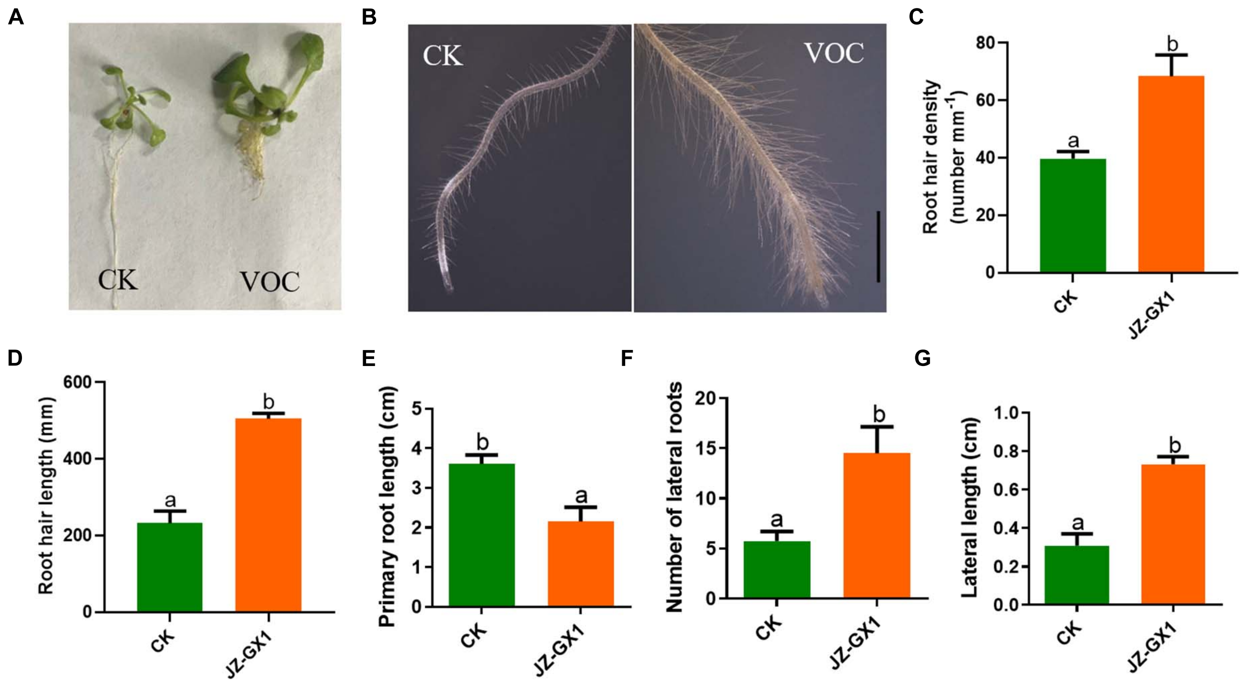

FIGURE 2 | Effect of *Rahnella aquatilis* JZ-GX1 VOCs on the root system architecture of *Arabidopsis thaliana* compared to the control (CK) under iron deficiency stress. **(A)** The overall structure of the root system, **(B)** root hair morphology, **(C)** root hair density, **(D)** root hair length, **(E)** primary root length, **(F)** lateral root number, and **(G)** lateral root length. The scale is 0.5 mm. One-way ANOVA was performed, and Duncan's post hoc test was applied. Different letters indicate statistically significant differences ($p < 0.05$) among treatments.

was significantly inhibited; the plants were thin and the leaves were yellowish, while the *A. thaliana* plants co-cultured with the JZ-GX1 strain under iron-limited conditions were healthy and had dark green leaves (**Figure 1A**); the fresh weight, chlorophyll content and active iron content of the co-cultured plants increased by 2.71%, 58.11%, and 7.84 times, respectively (**Figures 1B–D**).

R. aquatilis JZ-GX1 VOCs Changed the Root System Architecture of *A. thaliana* Under Iron Deficiency Stress

The development of the root system determines the ability of plants to absorb water and nutrients. In this experiment, the effects of VOCs produced by the tested strains on root hair production, primary root length, lateral root length, and number of lateral roots in *A. thaliana* were studied. From **Figures 2A,E**, it was observed that the elongation of the main root of *A. thaliana* seedlings exposed to JZ-GX1 VOCs was significantly inhibited, while the number of lateral roots increased by 2.53 times compared with that of the control (**Figure 2F**). At the same time, the length of the lateral root of the control was 0.309 cm, while that of *A. thaliana* treated with JZ-GX1 VOCs was 0.732 cm, which increased by 2.37 times (**Figure 2G**). Using stereomicroscopy, it was observed that the root hairs of *Arabidopsis* seedlings treated with VOCs were more developed and denser than those of the control seedlings (**Figures 2B–D**).

R. aquatilis JZ-GX1 VOCs Regulate the Expression of Genes Related to Iron Uptake in *A. thaliana*

To determine whether JZ-GX1 can regulate Fe^{3+} reductase and Fe^{2+} transporter genes in plants, we analyzed the transcript abundance of H^+ ATPase (*AHA2*), Fe^{3+} reductase (*FRO2*), and Fe^{2+} transporter (*IRT1*) genes in *A. thaliana* grown in iron-deficient medium. Compared with that in the control plants, the expression of *AHA2*, *FRO2,* and *IRT1* in the plants exposed to JZ-GX1 VOCs for 4 days was significantly upregulated and was 25, 1.81, and 1.357 times higher than that in the control plants, respectively. However, there was no significant difference in the iron transcriptional regulator *FIT* (**Figure 3**). The abundance and activity of iron-obtained transcripts increased in plants treated with VOCs produced by the JZ-GX1 strain, which indicated that the JZ-GX1 strain activated iron acquisition in plants by regulating the strategy I plant iron deficiency response.

R. aquatilis JZ-GX1 VOCs Activated Iron Absorption in *A. thaliana*

H^+ ATPase and ferrate reductase are key enzymes in the process of iron uptake by plants. To test whether the JZ-GX1 strain affected the ability of plants to acidify the rhizosphere, bromocresol purple, an indicator of pH, was added to the medium for chromogenic acidification. Plants were initially grown in iron-deficient media for 14 days (including treatments exposed to JZ-GX1 and control treatments) and then transferred

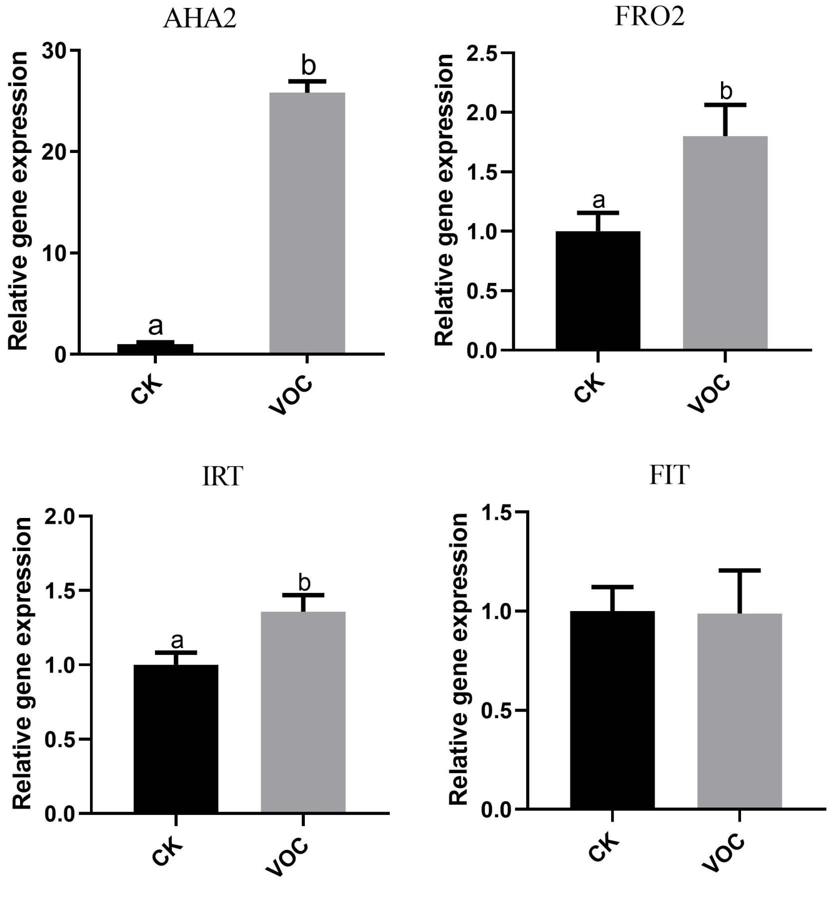

FIGURE 3 | Effects of VOCs from *Rahnella aquatilis* JZ-GX1 on the expression of the *AHA2*, *FRO2*, *IRT1*, and *FIT* genes in *Arabidopsis thaliana*. One-way ANOVA was performed, and Duncan's *post hoc* test was applied. Different letters indicate statistically significant differences ($p < 0.05$) among treatments.

to the medium containing pH indicator, which turned yellow when the pH decreased to below 5.0. The results showed that within 24 h of transfer to the indicator medium, plants exposed to JZ-GX1 showed significant rhizosphere acidification compared with the control plants (**Figure 4A**). Accordingly, the enzyme activity of H^+ ATPase was 4.51 times higher than that of the control (**Figure 4B**). In addition, the iron reductase activity of the plants exposed to JZ-GX1 VOCs was 2.32 times higher than that of the control (**Figures 4C,D**). The above experiments show that the JZ-GX1 strain can not only effectively reduce the pH value of the rhizosphere by inducing root proton release but also trigger *Arabidopsis* roots to secrete more ferrate reductase, thus transforming insoluble Fe^{3+} into Fe^{2+} for plant absorption and utilization.

Changes in the Iron Deficiency Resistance Pathway in *A. thaliana* Induced by *R. aquatilis* JZ-GX1 VOCs

To explore the signaling pathway of *A. thaliana* tolerance to low iron induced by the JZ-GX1 strain, the key genes in the biosynthesis pathways of jasmonic acid (JA), salicylic acid (SA), ethylene (ET), auxin, and abscisic acid (ABA) were detected by qPCR. Compared with that in the control plants, the expression of *NCED3* in the ABA signaling pathway of the plants treated with JZ-GX1 was upregulated 3 days after exposure to VOCs and was approximately 1.223 times higher than that in the control plants; this pathway was still upregulated on the 5th day, and the expression was approximately 1.654 times higher than that of the control plants. However, the expression of *NPR* in the SA signaling pathway, *ERF1* in the ET pathway, *PDF1* in the JA signaling pathway and YUC1, YUC8 in the auxin signaling pathway were downregulated on the third and 5th day (**Figure 5**). It was suggested that the VOCs produced by the JZ-GX1 strain induced *A. thaliana* resistance to iron deficiency stress through the ABA-mediated signaling pathway.

R. aquatilis JZ-GX1 Promoted the Growth of *M. sativa* Under Iron Deficiency

To investigate whether we could reproduce the effect of bacterial VOCs also in other plant species than *Arabidopsis*, we investigated the impact of JZ-GX1 VOCs on the Fe deficiency response in *M. sativa* seedlings. At 14 days, *M. sativa* exposed to VOCs of the JZ-GX1 strain showed better development and

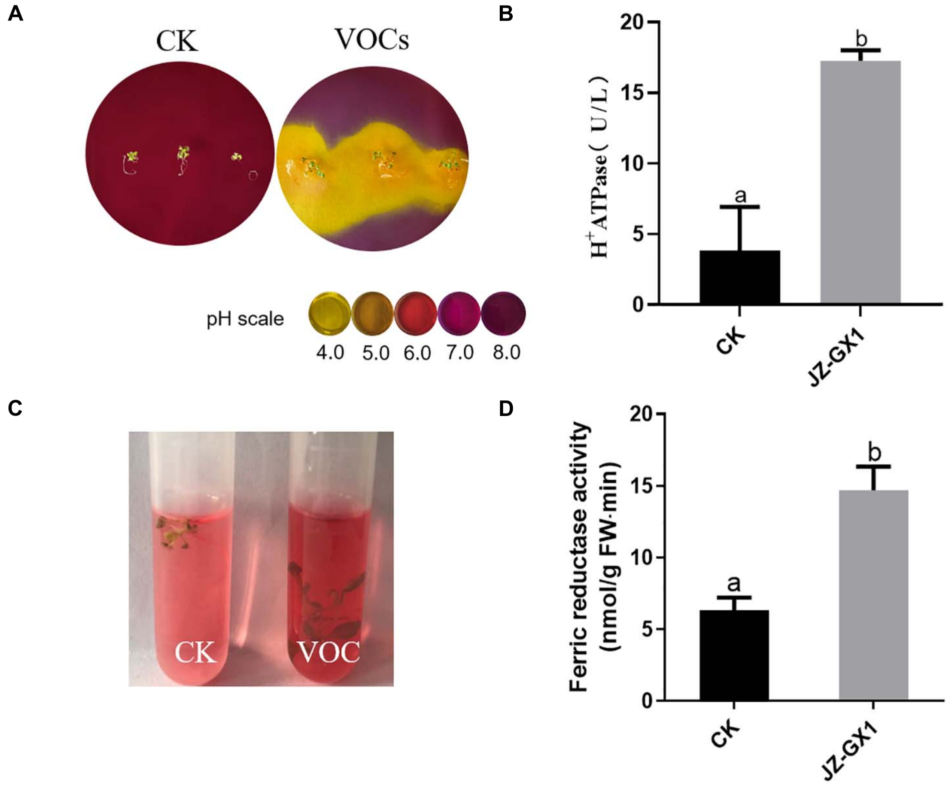

FIGURE 4 | Effects of VOCs from *Rahnella aquatilis* JZ-GX1 on H^+ ATPase and ferrate reductase activities in *Arabidopsis thaliana*. **(A)** H^+ secretion, **(B)** H^+ ATPase enzyme activity, **(C)** ferrate reductase reaction, and **(D)** quantitative analysis. CK: control. One-way ANOVA was performed, and Duncan's *post hoc* test was applied. Different letters indicate statistically significant differences ($p < 0.05$) among treatments.

growth than the control plants (**Figure 6A**), resulting in a significant increase in plant fresh weight and chlorophyll content (**Figures 6B,C**). The root system of the seedlings treated with bacterial VOCs was more developed than that of untreated control seedlings, and the number and length of lateral roots increased by 1.68 and 6.41 times, respectively (**Figures 6D,E**). In addition, bacterial VOCs up-regulated the expression of *MsBHLH1*, *MsAHA2,* and *MsIRT1* (**Figure 6F**). These results showed a very clear promotional effect is demonstrated both in *A. thaliana* and *M. sativa*.

Effect of Specific VOCs Released by *R. aquatilis* JZ-GX1 on the Growth of *M. sativa* Under Iron-Deficient Conditions

According to the VOC profile of the JZ-GX1 strain obtained from previous experiments (Kong et al., 2020a), we tested the growth-promoting effects of eight VOCs on plants. **Figure 7** shows that 2-undecanone and 3-methyl-1-butanol could promote the growth of *M. sativa* under iron deficiency stress. When 10–200 μM 2-undecanone solutions were added, the fresh weight of *M. sativa* increased, and there is no significant difference among different concentrations ($p < 0.05$). Similarly, these two compounds significantly promoted the growth of *A. thaliana* under iron deficiency. The plant fresh weight reached the maximum when a small amount (10 μM) of 2-undecanone was added, and when 100 μM of 3-methyl-1-butanol was added, the effect was the best ($p < 0.05$). The six other compounds had no significant effect on plant growth.

DISCUSSION

To maintain normal growth and development, most plants form robust roots to obtain water and mineral nutrients from the soil (Dahmani et al., 2020). Root system architecture (RSA) integrates the topological structure of the root system, the spatial distribution of the main root and lateral roots, and the number and length of various types of root systems (Thanh et al., 2020). Some abiotic and biological factors, including plant growth-promoting rhizobacteria (PGPR), can affect the RSA. The most common effect of PGPR is to inhibit the growth of primary roots, increase the proliferation of lateral roots and root hairs, and lead to an increase in aboveground biomass. The other effect is that the increase in plant biomass is accompanied by an increase in primary root growth (Zhou et al., 2016a; Sun et al., 2020). In this study, the VOCs of *R. aquatilis* JZ-GX1 increased the length and number of lateral roots in *A. thaliana* and *M. sativa* under iron deficiency stress, which not only

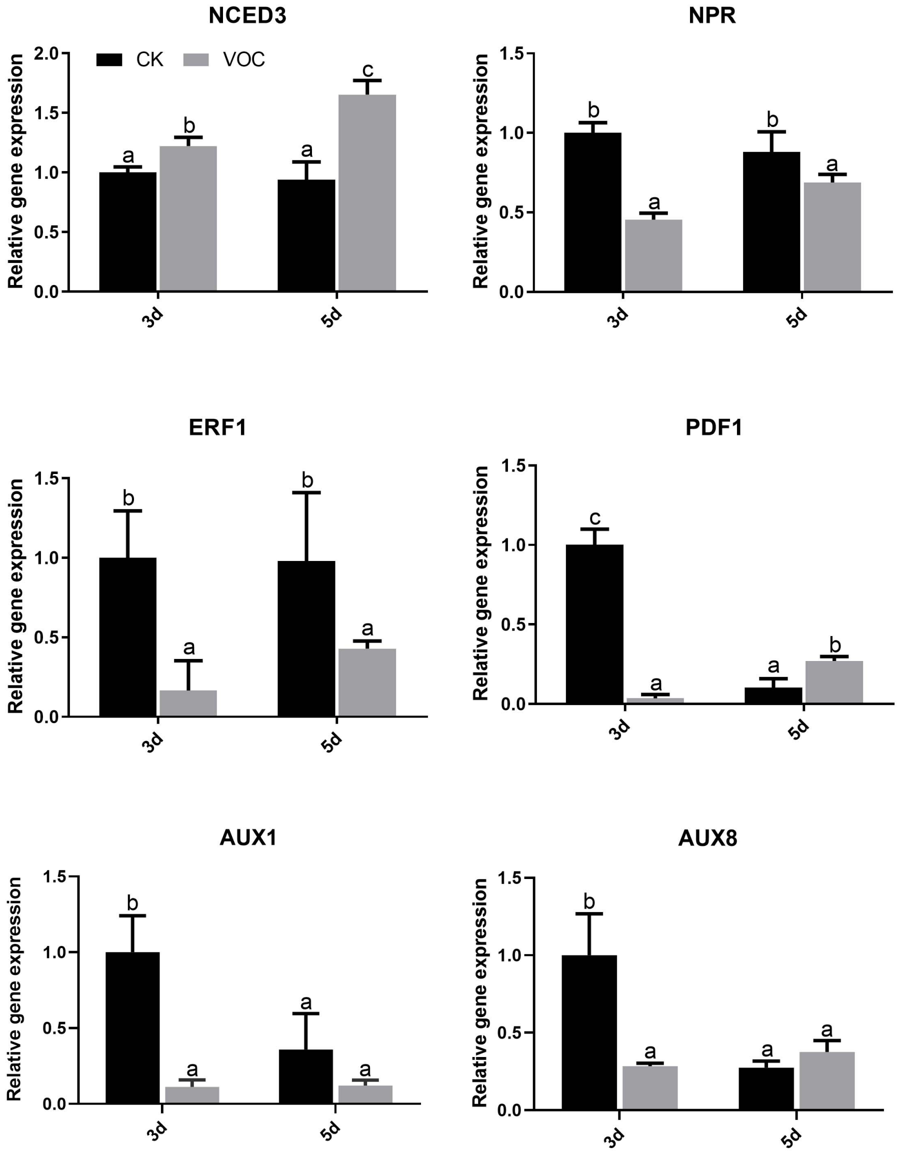

FIGURE 5 | Effects of VOCs from *Rahnella aquatilis* JZ-GX1 on the transcriptional expression of genes related to hormone biosynthesis in *Arabidopsis thaliana.* One-way ANOVA was performed, and Duncan's *post hoc* test was applied. Different letters indicate statistically significant differences ($p < 0.05$) among treatments.

increased the distribution sites of Fe^{3+} reductase in roots but also increased the area of iron nutrition absorbed by roots. Accordingly, these observations suggest that the VOCs released by *R. aquatilis* JZ-GX1 enhance the capacity of the host root to access Fe by modulating morphological adaptive responses to iron-deficient conditions.

Rhizosphere acidification is very important for plants to absorb iron. Studies have shown that when the soil pH increases by 1.0, the solubility of iron decreases 1000 times (Zhou et al., 2018). Previous researchers used MS medium to remove iron salt when studying the effect of microbial volatiles on the growth of *A. thaliana* under iron deficiency (Castulo-Rubio et al., 2015; Wang et al., 2017; Montejano-Ramirez et al., 2018), but in this experiment, the total nutrient MS medium pH was directly adjusted to 8.0. The growth environment of *A. thaliana* was relatively close to environmentally relevant alkaline soil conditions; that is, the soil was not free of iron, but the high-pH environment led to a decrease in iron availability (Pii et al., 2015; Aras et al., 2018). In the dichotomous dish culture experiment, the roots of *A. thaliana* seedlings treated with JZ-GX1 VOCs changed from purple to yellow, indicating that the acidification ability of *A. thaliana* seedlings was significantly enhanced, and the significant increase in H^+ ATPase activity in *A. thaliana* seedlings treated with JZ-GX1 VOCs could explain this acidification effect. Thus, the rapid decrease in pH value was beneficial to the dissolution of iron in the rhizosphere. Second, the *Arabidopsis* root iron reductase gene was highly expressed, and a higher iron reductase activity was detected in *A. thaliana* roots exposed

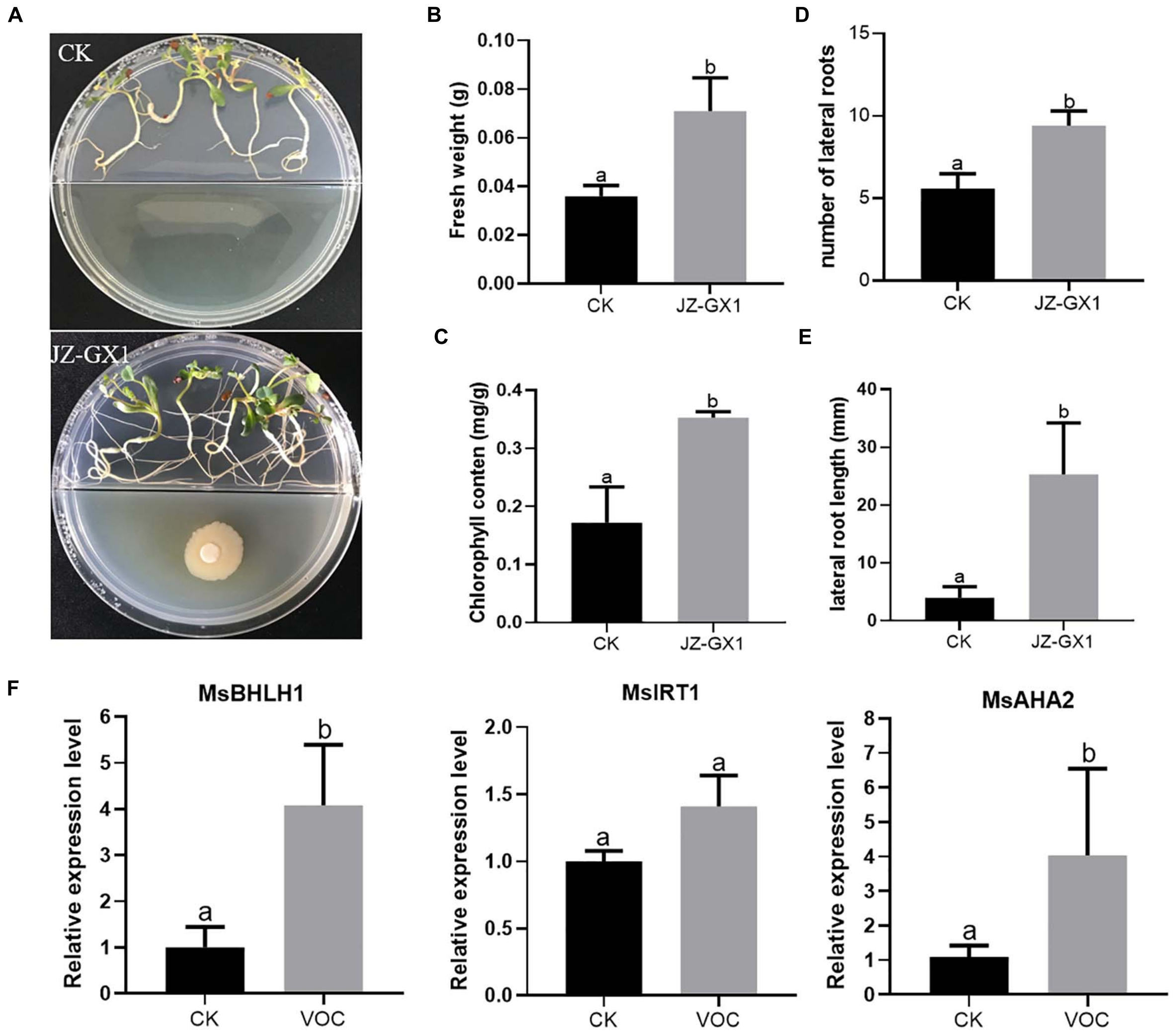

FIGURE 6 | Effect of VOCs from *Rahnella aquatilis* JZ-GX1 on the growth of *Medicago sativa* under iron-deficient conditions. **(A)** Plant phenotype, **(B)** fresh weight, **(C)** chlorophyll content, **(D)** lateral root number, **(E)** lateral root length, and **(F)** relative expression of *MsBHLH1*, *MsIRT1*, and *MsAHA2* in roots of *M. sativa* seedlings that were CK (control) or treated with VOCs from *R. aquatilis* JZ-GX1 (VOC). One-way ANOVA was performed, and Duncan's *post hoc* test was applied. Different letters indicate statistically significant differences ($p < 0.05$) among treatments.

to JZ-GX1 VOCs than in control seedling roots. Studies have shown that the optimum pH environment for Fe^{3+} reductase is 5.6 (Arikan et al., 2018). Although plants in alkaline soils initiate their own adaptive response to iron deficiency stress, they are quickly buffered by high pH values, which explains why some iron deficiency-sensitive plants are prone to yellowing in calcareous soils (Zhou et al., 2016b). Therefore, the VOCs released by *R. aquatilis* JZ-GX1 can enhance the ability of *A. thaliana* to absorb iron by activating the physiological response of the plant itself.

Although it has been reported that microorganisms induce plant iron uptake by releasing VOCs, there are few studies on the related signaling pathways. It is well known that the phytohormones auxin, ET, JA, and SA are involved in the regulation of resistance to abiotic stresses. But it seems that this four pathways had no effect on the induction of iron deficiency in plants conferred by JZ-GX1 VOCs, because JZ-GX1 VOCs significantly suppressed the expression of *YUC1*, *YUC8*, *NPR*, *ERF1*, *PDF1* that involved in auxin, ET, JA, and SA synthesis in plants under iron deficiency condition. Only *NCED3* in the ABA synthesis pathway was induced and expressed in large quantities on the 3rd and 5th days. *NCED3* is an enzyme that encodes ABA biosynthesis, namely, 9-cis-epoxide dioxygenase (Xing et al., 2019). Zhang et al. (2020) reported that the addition of exogenous ABA can alleviate iron deficiency in apples and promote long-distance iron transport in plants by regulating the distribution of iron in roots and stems. Under iron-deficient conditions, exogenous ABA can also promote the activation of apoplast iron by promoting an increase in phenols secreted by *Arabidopsis* roots and lead to an increase in citric acid concentration and iron concentration in xylem sap, thus increasing the available iron content in the aboveground parts

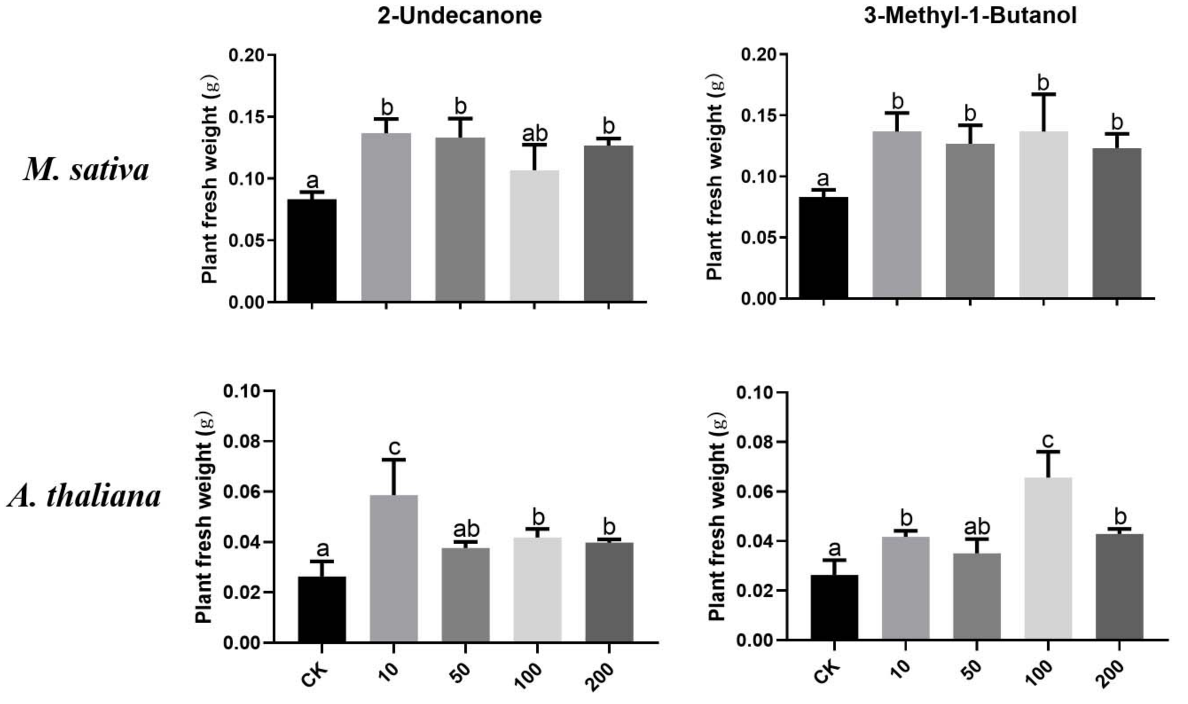

FIGURE 7 | Effects of pure compounds at different concentrations on the growth of *M. sativa* and *A. thaliana* under iron deficiency. CK: control. One-way ANOVA was performed, and Duncan's *post hoc* test was applied. Different letters indicate statistically significant differences ($p < 0.05$) among treatments.

of plants (Lei et al., 2014). In addition, ABA can promote the hydrolytic activity and proton transport of H^+ ATPase (Olaetxea et al., 2019). In our experimental results, the expression of *AHA2* in *A. thaliana* exposed to JZ-GX1 VOCs for 5 days was upregulated 25-fold, which may be due to the increase in endogenous ABA content in *A. thaliana*. However, different results were obtained in other studies. Liu et al. (2020b) found that in addition to ABA signaling, JA signaling also played important roles in mediating systemic salt stress tolerance after inoculating FZB42 on the roots. Chen et al. (2016) found that the expression of NCED was down-regulated with the inoculation of SQR9 under salt stress condition. In addition, Bhattacharyya et al. (2015) showed that VOCs emitted by *Alcaligenes faecalis* JBCS1294 induced salt tolerance in *Arabidopsis* by modulating the auxin and gibberellin pathways. These different results might be explained by different stress environments of plants or differences in chemical signaling by PGPR VOCs.

To identify the compounds involved in the regulation of plant iron absorption in the VOCs of *R. aquatilis* JZ-GX1, we analyzed the present VOCs by gas chromatography-mass spectrometry in a preliminary experiment (Kong et al., 2020a). In this study, after concentration screening, we finally identified two bioactive substances among the eight VOCs obtained. The addition of low concentrations of 2-undecanone and 3-methyl-1-butanol could improve the growth of *M. sativa* and *A. thaliana* under iron deficiency stress. In one study, these two substances were reported to be produced by *Paraburkholderia phytofirmans* PsJN and could also induce the growth of *A. thaliana* under salt stress (Ledger et al., 2016). The plant fresh weight measured in this study were significantly increased with exposure to these two compounds, but the enhancement effect was not as good as that of the JZ-GX1 strain treatment group. This is a common phenomenon observed in other studies (Liu et al., 2020b); that is,compared with commercially available, pure 2-undecanone or 3-methyl-1-butanol, the mixture of JZ-GX1 VOCs was more effective. This can be explained by the concentration of these two substances in the VOC mixture. In the plant-bacteria interaction system, the concentration of 2-undecanone or 3-methyl-1-butanol was unknown, so we could not determine the true concentration of these two substances after the interaction between bacteria and plants. Another possible explanation is that the JZ-GX1 strain produced VOCs other than 2-undecanone or 3-methyl-1-butanol and that one or more of these VOCs contributed to stress tolerance induction, or there are probably other volatile compounds that work in synergy and were not detected.

Plant growth promoting rhizobacteria have great potential in helping plants cope with adversity (Pinedo et al., 2015; Yang et al., 2020). An increasing number of studies have realized that microbial VOCs play an important ecological role in mediating interspecies and intraspecific interactions (Vaishnav et al., 2016; Del Rosario Cappellari and Banchio, 2020; Rivera-Mendez et al., 2020). In this study, it is reported for the first time that VOCs produced by *R. aquatilis* can promote plant growth under iron-deficient conditions. In view of the fact that salt stress and alkali stress occur simultaneously under natural conditions

(Liu et al., 2020b; Liang and Shi, 2021), it is necessary to explore whether VOCs from the JZ-GX1 strain can promote plant growth under salt stress. Second, the molecular mechanism of how plants sense gas signals emitted by bacteria should be further revealed.

DATA AVAILABILITY STATEMENT

The raw data supporting the conclusions of this article will be made available by the authors, without undue reservation.

AUTHOR CONTRIBUTIONS

W-LK completed the experimental research and the first draft of the manuscript. Y-HW participated in the experimental result analysis. X-QW directed the experimental design, data analysis, and manuscript writing and revision. All authors read and agreed on the final text.

FUNDING

This work was supported by the National Key Research and Development Program of China (2017YFD0600104) and the Priority Academic Program Development of the Jiangsu Higher Education Institutions (PAPD). Postgraduate Research and Practice Innovation Program of Jiangsu Province (KYCX20_0872).

SUPPLEMENTARY MATERIAL

The Supplementary Material for this article can be found online at: https://www.frontiersin.org/articles/10.3389/fpls.2021.704000/full#supplementary-material

REFERENCES

Aras, S., Arikan, S., Ipek, M., Esitken, A., Pirlak, L., Donmez, M. F., et al. (2018). Plant growth promoting rhizobacteria enhanced leaf organic acids, FC-R activity and Fe nutrition of apple under lime soil conditions. *Acta Physiol. Plant.* 40, 2693–2699.

Arikan, S., Esitken, A., Ipek, M., Aras, S., Sahin, M., Pirlak, L., et al. (2018). Effect of Plant Growth Promoting Rhizobacteria on Fe Acquisition in Peach (*Prunus Persica* L) Under Calcareous Soil Conditions. *J. Plant Nutrit.* 41, 2141–2150. doi: 10.1080/01904167.2018.1482910

Back, D., Rokibuzzaman, M., Khan, A., Kim, M. C., Park, H. J., Yun, D., et al. (2020). Plant-Growth Promoting *Bacillus oryzicola* YC7007 Modulates Stress-Response Gene Expression and Provides Protection From Salt Stress. *Front. Plant Sci.* 10:1646. doi: 10.3389/fpls.2019.01646

Bhattacharyya, D., Yu, S. M., and Lee, Y. H. (2015). Volatile compounds from *Alcaligenes faecalis* JBCS1294 confer salt tolerance in Arabidopsis thaliana through the auxin and gibberellin pathways and differential modulation of gene expression in root and shoot tissues. *J. Plant Growth Regulat*. 75, 297–306.

Castulo-Rubio, D. Y., Alejandre-Ramirez, N. A., Castulo-Rubio, D. Y., Alejandre-Ramirez, N. A., Orozco-Mosqueda, M. D. C., Santoyo, G., et al. (2015). Volatile organic compounds produced by the rhizobacterium *Arthrobacter agilis* UMCV2 modulate sorghum bicolor (Strategy II Plant) morphogenesis and SbFRO1 transcription in vitro. *J. Plant Growth Regulat.* 34, 611–623.

Chen, L., Liu, Y., Wu, G., Njeri, K. V., Shen, Q., Zhang, N., et al. (2016). Induced maize salt tolerance by rhizosphere inoculation of *Bacillus amyloliquefaciens* SQR9. *Plant Physiol*. 158, 34–44.

Dahmani, M. A., Desrut, A., Moumen, B., Verdon, J., Mermouri, L., Kacem, M., et al. (2020). Unearthing the Plant Growth-Promoting Traits of *Bacillus megaterium* RmBm31, an Endophytic Bacterium Isolated From Root Nodules of Retama monosperma. *Front. Plant Sci.* 11:124. doi: 10.3389/fpls.2020.00124

Del Carmen Orozco-Mosqueda, M., Velazquez-Becerra, C., Macias-Rodriguez, L. I., Santoyo, G., Flores-Cortez, I., et al. (2013). *Arthrobacter agilis* UMCV2 induces iron acquisition in Medicago truncatula (strategy I plant) *in vitro* via dimethylhexadecylamine emission. *Plant Soil* 362, 51–66. doi: 10.1007/s11104-012-1263-y

Del Rosario Cappellari, L., and Banchio, E. (2020). Microbial Volatile Organic Compounds Produced by *Bacillus amyloliquefaciens* GB03 Ameliorate the Effects of Salt Stress in *Mentha piperita* Principally Through Acetoin Emission. *J. Plant Growth Regulat.* 39, 764–775. doi: 10.1007/s00344-019-10020-3

Elizabeth Aviles-Garcia, M., Flores-Cortez, I., Hernandez-Soberano, C., Santoyo, G., and Valencia-Cantero, E. (2016). The plant growth-promoting rhizobacterium *Arthrobacter agilis* UMCV2 endophytically colonizes *Medicago truncatula*. *Rev. Argent. Microbiol.* 48, 342–346. doi: 10.1016/j.ram.2016.07.004

Fincheira, P., and Quiroz, A. (2018). Microbial volatiles as plant growth inducers. *Microbiol. Res.* 208, 63–75. doi: 10.1016/j.micres.2018.01.002

Flores-Cortez, I., Winkler, R., Ramirez-Ordorica, A., Cristina Elizarraraz-Anaya, M. I., Teresa Carrillo-Rayas, M., Valencia-Cantero, E., et al. (2019). A Mass Spectrometry-Based Study Shows that Volatiles Emitted by *Arthrobacter agilis* UMCV2 Increase the Content of Brassinosteroids in *Medicago truncatula* in Response to Iron Deficiency Stress. *Molecules* 24:301116.

Freitas, M. A., Medeiros, F. H. V., Carvalho, S. P., Guilherme, L. R. G., Teixeira, W. D., Zhang, H., et al. (2015). Augmenting iron accumulation in cassava by the beneficial soil bacterium *Bacillus subtilis* (GBO3). *Front. Plant Sci.* 6:00596. doi: 10.3389/fpls.2015.00596

Ines Dinolfo, M., Castanares, E., and Stenglein, S. A. (2017). Resistance of *Fusarium poae* in Arabidopsis leaves requires mainly functional JA and ET signaling pathways. *Fungal Biol.* 121, 841–848. doi: 10.1016/j.funbio.2017.06.001

Kong, W. L., Rui, L., Ni, H., and Wu, X. Q. (2020a). Antifungal Effects of Volatile Organic Compounds Produced by *Rahnella aquatilis* JZ-GX1 Against *Colletotrichum gloeosporioides* in *Liriodendron chinense* x *tulipifera*. *Front. Microbiol.* 11:1114. doi: 10.3389/fmicb.2020.01114

Kong, W. L., Wu, X. Q., and Zhao, Y. J. (2020b). Effects of *Rahnella aquatilis* JZ-GX1 on Treat Chlorosis Induced by Iron Deficiency in *Cinnamomum camphora*. *J. Plant Growth Regulat.* 39, 877–887. doi: 10.1007/s00344-019-10029-8

Koseoglu, A. T., and Acikgoz, V. (1995). Determination of iron chlorosis with extractable iron analysis in peach leaves. *J. Plant Nutrit.* 18, 153–161. doi: 10.1080/01904169509364892

Ledger, T., Rojas, S., Timmermann, T., Pinedo, I., Poupin, M. J., Garrido, T., et al. (2016). Volatile-Mediated Effects Predominate in *Paraburkholderia phytofirmans* Growth Promotion and Salt Stress Tolerance of *Arabidopsis thaliana*. *Front. Microbiol.* 7:1838. doi: 10.3389/fmicb.2016.01838

Lei, G. J., Zhu, X. F., Wang, Z. W., Dong, F., Dong, N. Y., and Zheng, S. J. (2014). Abscisic acid alleviates iron deficiency by promoting root iron reutilization and transport from root to shoot in Arabidopsis. *Plant Cell Environ.* 37, 852–863. doi: 10.1111/pce.12203

Li, F., Shi, T., Tang, X., Tang, M., Gong, J., and Yi, Y. (2020). *Bacillus amyloliquefaciens* PDR1 from root of karst adaptive plant enhances *Arabidopsis thaliana* resistance to alkaline stress through modulation of plasma membrane H^+-ATPase activity. *Plant Physiol. Biochem.* 155, 472–482. doi: 10.1016/j.plaphy.2020.08.019

Liang, J., and Shi, W. (2021). Cotton/halophytes intercropping decreases salt accumulation and improves soil physicochemical properties and crop productivity in saline-alkali soils under mulched drip irrigation: A three-year field experiment. *Field Crops Res.* 262:108027. doi: 10.1016/j.fcr.2020.108027

Liu, M., Wang, C., Liu, X., Lu, Y., and Wang, Y. (2020a). Saline-alkali soil applied with vermicompost and humic acid fertilizer improved macroaggregate microstructure to enhance salt leaching and inhibit nitrogen losses. *Appl. Soil Ecol.* 156:103705. doi: 10.1016/j.apsoil.2020.103705

Liu, S., Tian, Y., Jia, M., Lu, X., Yue, L., Zhao, X., et al. (2020b). Induction of Salt Tolerance in *Arabidopsis thaliana* by Volatiles From *Bacillus amyloliquefaciens* FZB42 via the Jasmonic Acid Signaling Pathway. *Front. Microbiol.* 11:562934. doi: 10.3389/fmicb.2020.562934

Martinez-Medina, A., Van Wees, S. C. M., and Pieterse, C. M. J. (2017). Airborne signals from Trichoderma fungi stimulate iron uptake responses in roots resulting in priming of jasmonic acid-dependent defences in shoots of *Arabidopsis thaliana* and *Solanum lycopersicum*. *Plant Cell Environ.* 40, 2691–2705. doi: 10.1111/pce.13016

Masalha, J., Kosegarten, H., Elmaci, O., and Mengel, K. (2000). The central role of microbial activity for iron acquisition in maize and sunflower. *Biol. Fertil. Soils* 30, 433–439. doi: 10.1007/s003740050021

Montejano-Ramirez, V., Martinez-Camara, R., Garcia-Pineda, E., and Valencia-Cantero, E. (2015). Volatile Organic Compounds Produced by the Rhizobacterium *Arthrobacter agilis* UMCV2 Modulate *Sorghum bicolor* (Strategy II Plant) Morphogenesis and SbFRO1 Transcription *In Vitro*. *J. Plant Growth Regulat.* 34, 611–623. doi: 10.1007/s00344-015-9495-8

Montejano-Ramirez, V., Martinez-Camara, R., Garcia-Pineda, E., and Valencia-Cantero, E. (2018). Rhizobacterium *Arthrobacter agilis* UMCV2 increases organ-specific expression of FRO genes in conjunction with genes associated with the systemic resistance pathways of *Medicago truncatula*. *Acta Physiol. Plant.* 40:2712–x.

Netzker, T., Shepherdson, E., Zambri, M. P., and Elliot, M. A. (2020). Bacterial Volatile Compounds: Functions in Communication, Cooperation, and Competition. *Annu. Rev. Microbiol.* 74, 409–430. doi: 10.1146/annurev-micro-011320-015542

Olaetxea, M., Mora, V., Bacaicoa, E., Baigorri, R., Garnica, M., Fuentes, M., et al. (2019). Root ABA and H^+-ATPase are key players in the root and shoot growth-promoting action of humic acids. *Plant Direct* 3:e00175.

Perez-Flores, P., Valencia-Cantero, E., Altamirano-Hernandez, J., Pelagio-Flores, R., Lopez-Bucio, J., Garcia-Juarez, P., et al. (2017). *Bacillus methylotrophicus* M4-96 isolated from maize (Zea mays) rhizoplane increases growth and auxin content in *Arabidopsis thaliana* via emission of volatiles. *Protoplasma* 254, 2201–2213. doi: 10.1007/s00709-017-1109-9

Pii, Y., Penn, A., Terzano, R., Crecchio, C., Mimmo, T., and Cesco, S. (2015). Plant-microorganism-soil interactions influence the Fe availability in the rhizosphere of cucumber plants. *Plant Physiol. Biochem.* 87, 45–52. doi: 10.1016/j.plaphy.2014.12.014

Pinedo, I., Ledger, T., Greve, M., and Poupin, M. J. (2015). *Burkholderia phytofirmans* PsJN induces long-term metabolic and transcriptional changes involved in *Arabidopsis thaliana* salt tolerance. *Front. Plant Sci.* 6:466. doi: 10.3389/fpls.2015.00466

Ramirez-Ordorica, A., Valencia-Cantero, E., Flores-Cortez, I., Teresa Carrillo-Rayas, M., Cristina Elizarraraz-Anaya, I., Montero-Vargas, J., et al. (2020). Metabolomic effects of the colonization of *Medicago truncatula* by the facultative endophyte *Arthrobacter agilis* UMCV2 in a foliar inoculation system. *Sci. Rep.* 10:84261.

Rivera-Mendez, W., Obregon, M., Moran-Diez, M. E., Hermosa, R., and Monte, E. (2020). *Trichoderma asperellum* biocontrol activity and induction of systemic defenses against *Sclerotium cepivorum* in onion plants under tropical climate conditions. *Biol. Control* 141:104145. doi: 10.1016/j.biocontrol.2019.104145

Rroco, E., and Kosegarten, H. (2003). The importance of soil microbial activity for the supply of iron to sorghum and rape. *Eur. J. Agronomy* 19, 487–493. doi: 10.1016/s1161-0301(02)00185-5

Sharifi, R., and Ryu, C. (2018a). Revisiting bacterial volatile-mediated plant growth promotion: lessons from the past and objectives for the future. *Ann. Bot.* 122, 349–358. doi: 10.1093/aob/mcy108

Sharifi, R., and Ryu, C. (2018b). Sniffing bacterial volatile compounds for healthier plants. *Curr. Opin. Plant Biol.* 44, 88–97. doi: 10.1016/j.pbi.2018.03.004

Sun, L., Cao, M., Liu, F., Wang, Y., Wan, J., Wang, R., et al. (2020). The volatile organic compounds of *Floccularia luteovirens* modulate plant growth and metabolism in *Arabidopsis thaliana*. *Plant Soil* 456, 207–221. doi: 10.1007/s11104-020-04709-8

Thanh, N. C., Le Van, B., and Minh, T. T. H. (2020). *Pseudomonas* PS01 Isolated from Maize Rhizosphere Alters Root System Architecture and Promotes Plant Growth. *Microorganisms* 8:8040471.

Tsai, H. H., and Schmidt, W. (2017). Mobilization of Iron by Plant-Borne Coumarins. *Trends Plant Sci.* 22, 538–548. doi: 10.1016/j.tplants.2017.03.008

Vaishnav, A., Kumari, S., Jain, S., Varma, A., Tuteja, N., and Choudhary, D. K. (2016). PGPR-mediated expression of salt tolerance gene in soybean through volatiles under sodium nitroprusside. *J. Basic Microbiol.* 56, 1274–1288. doi: 10.1002/jobm.201600188

Wang, J., Zhou, C., Xiao, X., Xie, Y., Zhu, L., and Ma, Z. (2017). Enhanced Iron and Selenium Uptake in Plants by Volatile Emissions of *Bacillus amyloliquefaciens* (BF06). *Appl. Sci. Basel* 7:851.

Xing, Q., Zhang, X., Li, Y., Shao, Q., Cao, S., Wang, F., et al. (2019). The lipoxygenase CmLOX13 from oriental melon enhanced severe drought tolerance via regulating ABA accumulation and stomatal closure in Arabidopsis. *Environ. Exp. Bot.* 167:103815. doi: 10.1016/j.envexpbot.2019.103815

Yang, A., Akhtar, S. S., Fu, Q., Naveed, M., Iqbal, S., Roitsch, T., et al. (2020). *Burkholderia Phytofirmans* PsJN Stimulate Growth and Yield of Quinoa under Salinity Stress. *Plants Basel* 9:6726.

Zamioudis, C., Korteland, J., Van Pelt, J. A., van Hamersveld, M., Dombrowski, N., Bai, Y., et al. (2015). Rhizobacterial volatiles and photosynthesis-related signals coordinate MYB72 expression in Arabidopsis roots during onset of induced systemic resistance and iron-deficiency responses. *Plant J.* 84, 309–322. doi: 10.1111/tpj.12995

Zhang, H., Sun, Y., Xie, X., Kim, M., Dowd, S. E., and Paré, P. W. (2009). A soil bacterium regulates plant acquisition of iron via deficiency-inducible mechanisms. *Plant J.* 58, 568–577. doi: 10.1111/j.1365-313x.2009.03803.x

Zhang, J., Wang, X., Wang, X., Wang, F., Ji, X. L., An, J., et al. (2020). Abscisic acid alleviates iron deficiency by regulating iron distribution in roots and shoots of apple. *Sci. Horticult.* 262:109018. doi: 10.1016/j.scienta.2019.109018

Zhou, C., Guo, J., Zhu, L., Xiao, X., Xie, Y., Zhu, J., et al. (2016a). *Paenibacillus polymyxa* BFKC01 enhances plant iron absorption via improved root systems and activated iron acquisition mechanisms. *Plant Physiol. Biochem.* 105, 162–173. doi: 10.1016/j.plaphy.2016.04.025

Zhou, C., Liu, Z., Zhu, L., Ma, Z., Wang, J., and Zhu, J. (2016b). Exogenous Melatonin Improves Plant Iron Deficiency Tolerance via Increased Accumulation of Polyamine-Mediated Nitric Oxide. *Int. J. Mol. Sci.* 17:177711.

Zhou, C., Ma, Z., Zhu, L., Xiao, X., Xie, Y., Zhu, J., et al. (2016c). Rhizobacterial Strain *Bacillus megaterium* BOFC15 Induces Cellular Polyamine Changes that Improve Plant Growth and Drought Resistance. *Int. J. Mol. Sci.* 17:9766.

Zhou, C., Zhu, L., Guo, J., Xiao, X., Ma, Z., and Wang, J. (2019). *Bacillus subtilis* STU6 Ameliorates Iron Deficiency in Tomato by Enhancement of Polyamine-Mediated Iron Remobilization. *J. Agricult. Food Chem.* 67, 320–330. doi: 10.1021/acs.jafc.8b05851

Zhou, C., Zhu, L., Ma, Z., and Wang, J. (2017). *Bacillus amyloliquefaciens* SAY09 Increases Cadmium Resistance in Plants by Activation of Auxin-Mediated Signaling Pathways. *Genes* 8:1737.

Zhou, C., Zhu, L., Ma, Z., and Wang, J. (2018). Improved iron acquisition of *Astragalus sinicus* under low iron-availability conditions by soil-borne bacteria *Burkholderia cepacia*. *J. Plant Interact.* 13, 9–20.doi: 10.1080/17429145.2017.1407000

Conflict of Interest: The authors declare that the research was conducted in the absence of any commercial or financial relationships that could be construed as a potential conflict of interest.

Advantages of publishing in Frontiers

OPEN ACCESS
Articles are free to read
for greatest visibility
and readership

FAST PUBLICATION
Around 90 days
from submission
to decision

HIGH QUALITY PEER-REVIEW
Rigorous, collaborative,
and constructive
peer-review

TRANSPARENT PEER-REVIEW
Editors and reviewers
acknowledged by name
on published articles

Frontiers
Avenue du Tribunal-Fédéral 34
1005 Lausanne | Switzerland

Visit us: www.frontiersin.org
Contact us: frontiersin.org/about/contact

REPRODUCIBILITY OF RESEARCH
Support open data
and methods to enhance
research reproducibility

DIGITAL PUBLISHING
Articles designed
for optimal readership
across devices

FOLLOW US
@frontiersin

IMPACT METRICS
Advanced article metrics
track visibility across
digital media

EXTENSIVE PROMOTION
Marketing
and promotion
of impactful research

LOOP RESEARCH NETWORK
Our network
increases your
article's readership